Development of an intrabody capable of activating interferon regulatory factor-1 (IRF-1) and identification of IRF-1-binding peptide motifs

Angeli Möller

Doctor of Philosophy

The University of Edinburgh **2011**

i. Declaration

I confirm that I have composed this thesis. The majority of the work is my own and contributions by other members of my research group have been clearly indicated. This work has not been submitted for any degree or professional qualification other this PhD.

Angeli Möller

Signature ……..

Date ……..

ii. Acknowledgements

This thesis is dedicated to my family: my parents Niru and Kishor who always taught me to value my education, my brother Ashish and sister Asha for their love and support and most especially my husband Ulrich who waited for me.

Special thanks are owed to my supervisor Professor Kathryn Ball. She has always been available and given me lots of excellent advice. I have also received helpful support throughout my post-graduate studies from my PhD committee members Dr Elizabeth Patton and Dr Maura Wallace.

In addition I would like to thank Dr Emma Pion, Vikram Narayan and Lucy Malin for their invaluable work on IRF-1; and all the members of the Hupp/Ball lab, who have made the Edinburgh Cancer Research Centre a great place to work.

Finally, I would like to thank Cancer Research UK for providing the funding for this PhD.

iii. Abstract

Interferon regulatory factor 1 (IRF-1) is a tumour suppressor protein and transcription factor. It has been shown to modulate target gene expression in response to stimuli, which include viral infection and DNA damage, and to be down-regulated in several forms of cancer. This thesis details the development of an intrabody, an intracellular antibody, that binds specifically to endogenous IRF-1. The binding of the intrabody to IRF-1 enhanced transcription from IRF-1-responsive reporter gene constructs and endogenous promoters, thus it was shown to activate IRF-1. Intrabody binding also increased the rate at which IRF-1 was degraded, suggesting that the intrabody epitope may be regulating both IRF-1 activity and turnover. These results were supported point mutation within the intrabody epitope (P325 to A) as the resultant mutant also displayed both a higher transcriptional activity and increased rate of degradation.

In an effort to understand the mechanisms which regulate IRF-1 activity a search for novel IRF-1-interacting proteins was carried out using phage peptide display. This *in vitro* technique enables the identification of peptides able to bind a specific target protein. The sequence of these peptides can then be used to search protein databases for homologous, full-length proteins that could also bind the target protein. This led to the identification of an IRF-1-binding peptide that held sequence similar to a region of Zinc Finger 350 (ZNF350), a transcription factor involved in regulating the DNA damage response. Subsequently, endogenous ZNF350 and IRF-1 were co-immunoprecipitated from a human cancer cell line. The extreme C-terminus of IRF-1 was shown to be sufficient for an interaction with ZNF350, although a second, more N-terminal site was also shown to be essential for a stable intracellular interaction.

This data sheds new light on the role of the extreme C-terminus of IRF-1 in modulating the protein's activity. This study also provides new and IRF-1-specific molecular tools, in the form of intrabodies and IRF-1-binding peptides, which could be used in the future to further characterise the activity and regulation of this tumour suppressor protein.

iv. Abbreviations

BSA	Bovine serum albumin
CDR	Complementarity determining region
cfu	Colony forming units
C.V.	Column volumes
DBD	DNA binding domain
DMEM	Dulbecco's minimal essential media
DMSO	Dimethyl sulfoxide
DNA	Deoxyribonucleic acid
DSP	Dithiobis [succinimidyl propionate]
E.coli	*Escherichia coli* bacterium
EDTA	Ethylenediaminetetraacetic acid
ER	Endoplasmic reticulum
g3p	Minor phage coat protein encoded by gIII gene
GFP	Green fluorescent protein
GST	Glutathione-S-transferase
His	Histidine
HRP	Horseradish peroxidise
IPTG	Isopropyl β-D-1-thiogalactopyranoside
IRF-1	Interferon regulatory factor 1
LB	Luria Bertani
Luc	Luciferase
Ni^{+}-NTA	Nickel-nitrilotriacetic acid
NLS	Nuclear localisation signal
O.D. 600	Optical density at (absorbance at a wavelength of 600 nm)
PBS	Phosphate buffered saline
PCR	Polymerase chain reaction

iv. Abbreviations continued

PEG	Polyethylene glycol
pfu	Plaque forming units
RBA	Relative binding affinity
scFv	Single chain variable fragment antibody
SDS	Sodium Dodecyl Sulphate
SGSG	Amino acid sequence: Serine Glycine Serine Glycine
TAE	Tris acetate-EDTA
TE	Tris, EDTA buffer (provided by QIAGEN)
$t_{0.5}$	Half life
Tris	Tris(hydroxymethyl)aminomethane
VH	Variable heavy antibody domain
VL	Variable light antibody domain

v. Contents

1 Introduction

The work reported in this thesis is aimed at increasing current understanding of the mechanisms through which IRF-1 (interferon regulatory factor 1) is regulated. This introduction is split into two parts; the first describes the disease types associated with dysfunctional IRF-1, mechanisms of IRF-1 induction, its functions and structure. The second part of this introduction focuses upon phage display technology as this thesis details the use of both antibody and peptide phage display in the study of IRF-1.

1.1 IRFs (Interferon regulatory factors)

There are currently nine known human IRFs (interferon regulatory factors), identified through a highly conserved DNA-binding domain. IRF-1 was the first to be identified and was initially characterised as a transcription factor able to bind enhancer elements in the promoter of the IFN-β gene [1, 2]. A transcription factor is a DNA-binding protein that attaches to only specific sequences within the promoter regions of its target genes [3]. This binding is a rate-limiting step regulating transcription of DNA to mRNA, with transcription factors able to both repress and activate this process by controlling the recruitment of RNA polymerase [4].

IRF-2, an inhibitor of IRF-1's transcriptional activity that possessed a similar DNA-binding domain structure was described soon after IRF-1 [5]. Mechanisms through which IRF-2 may regulate IRF-1 are detailed in section 1.2.3.2. Both bind and compete for a common DNA motif, which was found in other promoters regulated by the interferon signalling pathway [6]. This IRF-binding motif was therefore named the IFN-stimulated response element (ISRE) [7, 8]. IRF-1 targeted ISRE have been found in a large number of genes which can be either induced or repressed by IRF-1 [9-11]. These genes are involved in diverse pathways including the immune-response, anti-proliferation, apoptosis and tumour suppression.

1.2 IRF-1

1.2.1 Association with cancer

Upregulation of *IRF-1* is associated with growth inhibition in several cancer cell lines [12-14] and reversion of c-myc- or fosB-induced transformation [15]. Although *IRF-1* null mice do not spontaneously develop tumours, unlike those lacking the tumour suppressor *p53*, embryonic fibroblasts (EFs) from *IRF-/-* mice can be transformed by activated c-Ha-ras expression [16, 17]. It is again possible to reverse the transformed phenotype through concomitant expression of exogenous IRF-1. In addition IRF-/- cells are protected from the c-Ha-ras oncogene triggered apoptosis that can be observed in wild type cells under conditions of low serum concentration, high cell density or following treatment by anticancer drugs or ionizing radiation [17].

IRF-1 mutations have been observed in a variety of human cancers. Chromosomal loci 5q31 is the smallest, most commonly deleted region in leukemia and myelodysplasia (MDS), and *IRF-1* has been identified as the most frequently deleted gene at this loci in patients with these diseases and 5q31 aberrations [18]. Strikingly, *IRF-1* mRNA is undetectable in approximately 20% of patients with MDS or overt leukemia from MDS [18]. Furthermore, skipping of exon 2 of the *IRF-1* gene, which contains the AUG translation initiation codon [18], has also been linked to the development of leukaemia and MDS [6, 19, 20].

IRF-1 has been reported to be reduced in 53% of human hepatocellular carcinomas (although this study involved a limited sample size of only 13 tissue samples) [21]. Additionally, during mutational analysis of gastric genes implicated in adenocarcinoma, a tumour-specific point mutation was identified in exon 2 (ATG to TTG) [22], which resulted in a substitution of IRF-1 amino acid 8 from methionine to leucine. This mutant was found to bind to DNA with a similar affinity to the wild type protein, but unlike wild type IRF-1, was unable to activate the IFN-β p125-luciferase promoter or inhibit cell growth when over expressed [22]. Other exon deletions, which would cause truncated forms of the protein to be produced, have also been identified in chronic myeloid leukaemia [23] and cervical cancer patients [24].

Taken together the data described in this section have identified IRF-1 as a tumour suppressor protein i.e. one that protects the cell from cancer.

1.2.2 Induction of IRF-1

Although expressed at low levels by most types of resting cells [2, 25-27], IRF-1 can be upregulated by a wide range of agents including: viruses, concanavalin A (conA), lipopolysaccharide (LPS), interleukin-1 (IL-1), IL-12, IFN-β, IFN-γ and tumour-necrosis factor (TNF) [2, 5, 25, 27, 28]. These factors are part of a signalling network that indicates the presence of an infection and their induction of IRF-1 is an important part of host defence. Furthermore, it has been shown that IRF-1 can be induced in response to DNA damage [29] or in a cell-cycle-dependent manner to inhibit proliferation prior to DNA synthesis [6]. *IRF-1* has been well characterised as a downstream target of the interferon-stimulated JAK/STAT-signalling pathway in virus-infected cells [28, 30, 31]. This signalling pathway is initially stimulated by interferons released by lymphocytes in response to infection. Interferons belong to a class of glycoproteins known as cytokines, which signal locally between cells to stimulate an immune response. Interferons (IFNs) play key roles in both innate (IFN-α and IFN-β) and adaptive (IFN-γ) immunity. The two most studied type I interferons are IFN-α and IFN-β, both of which can be expressed in all cell types. The type II interferon, IFN-γ, is produced only in activated T lymphocytes (T-cells) and natural killer (NK) cells.

Type 1 interferons bind a heterodimer of IFNARs (IFN-α receptor) 1 and 2. The type II interferon, IFN-γ binds to a tetramer of two IFNGR2 (IFN-γ receptor 2) chains and two IFNGR1 chains. By binding to their receptors IFNs activate JAK (Janus Kinase) phosphotyrosine kinases, which phosphorylate tyrosine residues on the interferon receptors. This allows STATs (Signalling Transducers and Activators of Transcription) to bind the receptors via a phosphotyrosine-binding SH2 domain [32]. STAT dimers can then move into the nucleus and bind to the IFN-activated palindromic GAS (gamma activated site) sequence within the *IRF-1* promoter [33].

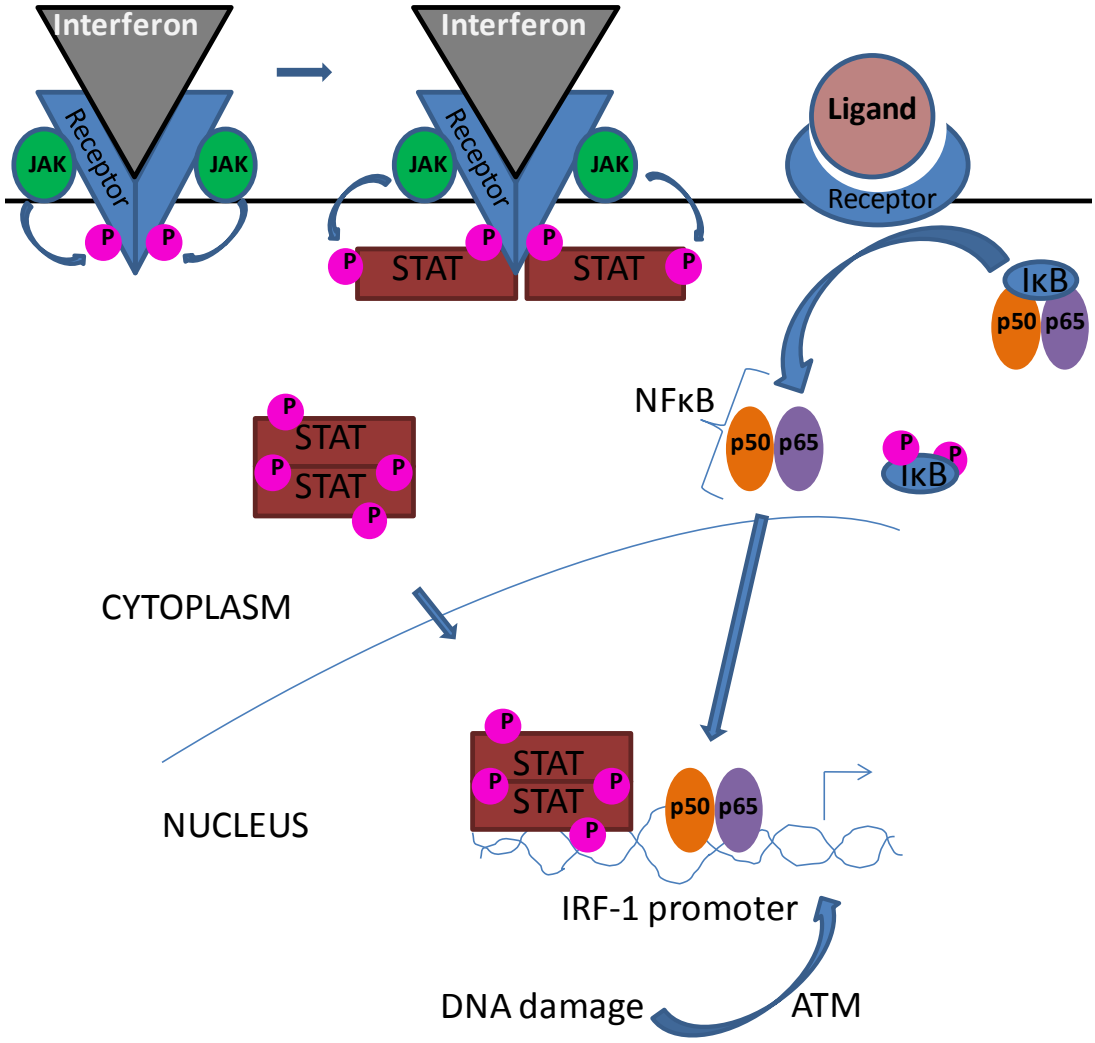

Figure 1.1: Synergistic induction of IRF-1 gene expression by STAT dimers and NF-κB. Based upon the following publication [33].

Other pathways have also been shown to induce IRF-1 expression. Overlapping the GAS element targeted by the JAK/STAT pathway is a binding site for NF-κB (Nuclear Factor kappa B). Binding of the p50/p65 heterodimer form of NF-κB to this region has been shown to stimulate IRF-1 expression and allow it to act in concert with NF-κB to stimulate other downstream targets [33, 34]. Whereas the JAK/STAT cascade is an essential element of an anti-microbial response, IRF-1 is also stimulated in DNA damaged cells, this time by the ATM (ataxia telangiectasia, mutated) -signalling pathway [29]. In cells in which ATM was knocked down *IRF-1* could still be induced as part of a viral response, but only when ATM was present could *IRF-1* be induced by DNA damage [29], indicating that *IRF-1* is a downstream target of distinct pathways. IRF-1's ability to respond to a range of stimuli helps

explain its involvement in diverse cellular functions, which are discussed in section 1.2.3.

1.2.3 Functions of IRF-1

First recognised for its role in viral response, IRF-1 later became characterised as a tumour suppressor molecule. To understand how these two functions are intertwined it is important to first understand the "tumour surveillance" hypothesis [35], which suggests that as tumour cells have an abnormal physiology the immune system should be able to recognise them and attempt their eradication. This theory has been supported by experiments showing that mice lacking factors essential for immune development, such as perforin (a cytolytic protein released by natural killer and cytotoxic T-cells) or IFN-γ, show impaired tumour resistance [36, 37]. It has also been shown that cells involved in immuno-surveillance can recognise tumour-specific antigens [38, 39]. For example, DNA damage has been shown to lead to the upregulation of ligands for the NKG2-D receptor [40], which is expressed on the surface of natural killer cells, cytotoxic T-cells and macrophages and which recognises specific "non-self" antigens. These ligands have been shown to be upregulated on the surface of numerous tumour cells [38] and their ectopic over expression has been shown to target cells for destruction [39].

This section details IRF-1's role in the immune system, cell growth and apoptosis (also known as programmed cell death), however these functions are not really separate but together help explain IRF-1's tumour suppressor activities. As part of the immune system IRF-1 can be activated following the detection of tumour or DNA damaged cells [29], and then elicit the appropriate response; either halting progression of the cell cycle (section 1.2.3.2) or triggering a signalling cascade ending in cell death (section 1.2.3.3).

1.2.3.1 Immune-response

Following microbial infection, interferons are able to swiftly induce IRF-1 expression through the JAK/STAT signalling pathway [2]. IRF-1 is then able to regulate the induction of IFN-response genes involved in the host's defence response. For instance, IFN-induced IRF-1 has been shown to form a complex with

IRF-8 and bind ISRE elements in the nitric oxide synthase (iNOS) promoter [41]. This results in the production of nitric oxide (NO), which is used by macrophages to destroy intracellular infectious agents [42]. IFN-induced IRF-1 also mediates the transcriptional activation of the p35 subunit of interleukin-12 (IL-12) [43], which is essential for phagocytic cell activation and inflammation following infection [44] and which stimulates further IRF-1 expression in natural killer and T-cells [27].

IRF-1 also plays an important role in the adaptive immune system, specifically in the activation of cytotoxic T-lymphocytes (also known as $CD8^+$ T-cells) which are able to induce the death of infected or tumour cells [45]. These T-cells are activated when their cell surface receptor binds to "non-self" antigens [46]. These antigens are peptides released following the degradation of invading pathogen by the immunoproteosome in antigen-presenting cells (APCs). Peptides are then presented as part of the major histocompatibility complex (MHC) on the surface of APCs [46]**.** IRF-1 has been shown to regulate expression of TAP1 (Transporter for Antigen Processing 1) [9]. This transmembrane pump transports peptides from the cytoplasm of antigen-presenting cells into the lumen of the endoplasmic reticulum where they bind nascent MHC class I molecules and the immunoproteasome components LMP2 and MECL1 in response to IFN-γ [9, 47, 48], thereby influencing the presentation of viral and tumour antigens to $CD8^+$ T-cells. IRF-1 also regulates antigen display following induction by the CD40 receptor on antigen-presenting cells by the CD40 ligand (CD40L) on the surface of T-cells. CD40L can induce IRF-1 via recruitment of NF-κB to a promoter element proximal to the *IRF-1* gene transcription start site [34]. *De novo*-synthesized IRF-1 then acts in concert with NF-κB to regulate the expression of genes responsible for antigen processing and transport such as the *TAP1*, *TAP2*, *tapasin*, *LMP2*, and *LMP10* genes.

It has also been shown that IRF-1 regulates genes involved in differentiation of T-helper 1 (T_H1) cells [43], which in turn activate cytotoxic T-cells and macrophages. In antigen-presenting cells (APCs), IRF-1 activates the transcription of p35 and p40, components of the T_H1-cell-inducing cytokines IL-12 and IL-23 [43]. Furthermore, IRF-1 binds three different sites in the IL-4 promoter and represses IL-4 transcription, thereby inhibiting differentiation into T_H2 cells [11]. In bone marrow,

IRF-1-mediated IL-15 production promotes the maturation of natural killer (NK)-cell precursors [49]. Mature NK cells then produce IFN-γ, which induces APCs and TH1 cells to synthesize IRF-1. In a positive-feedback loop, the IRF-1 that is produced by T_H1 cells further increases the activity of APCs and differentiation into T_H1 cells (see figure 1.2).

Additionally, IRF-1 has been implicated in the initial induction of type I interferons α and β. Overexpression of IRF-1 enhances virus-stimulated IFN-β expression in human fibroblasts [50], and IRF-1 has been described as part of an autoregulatory loop in which it is both a target and a transcriptional activator of IFN-β [51-53]. It has also been demonstrated that transient expression of IRF-1 can upregulate the *IFN-α* promoter, but did not increase endogenous IFN-α expression [54].

More recently, studies in *IRF-1* null cell lines and mice have indicated that an IRF-1-independent mechanism for *IFN-α/β* induction exists [55, 56]. *IRF-1 -/-* mouse embryonic fibroblasts showed unimpaired *IFN-β* induction following infection with Newcastle Disease Virus (NDV), but three to ten-fold reduction in poly(I):poly(C)-mediated *IFN-β* induction [55]. Poly(I):poly(C) is a synthetic analogue of double-stranded RNA that simulates viral-infection [57]. *IFN- β* induction by poly(I):poly(C) could be restored by pre-treating the cells with IFN-β (a process referred to as priming), thus triggering a positive feedback-loop [55]. This result indicated that IFN-stimulated factors were responsible for the IRF-1-independent induction of *IRF-β*. A separate study confirmed that *IFN-β* could be induced in *IRF-1* null mouse embryonic stem cells (following 4 or 8 days of differentiation), although this induction was 1.3 to 6.6 fold lower than that observed in the presence of IRF-1 [58]. It was subsequently shown *in vivo* that *IFN-β* could be induced by both NDV and poly(I):poly(C) in mice lacking IRF-1 [56]. The authors of this paper report no significant difference *IFN-β* induction between the control and IRF-1 null mice, but did point out that considerable variation was seen between the individuals in each treatment group.

Taken together the data suggests that although IRF-1 can enhance *IFN-β* induction, it is not essential for expression of this gene. Chromatin immunoprecipitation has verified that IRF-1 (and IRF-2) bind to the *IFN-β* promoter in HeLa cells following

viral infection [59], but the importance of IRF-1 in *IFN-α/β* gene stimulation is still unclear. IRF-3 and IRF-7 have also been shown to bind the *IFN- β* promoter [60] and IFN- β expression is completely disrupted in *IRF-3/7* double knockout mouse embryonic fibroblasts [61]. It has therefore been proposed that, unlike IRF-1, the IRF-3:IRF-7 complex plays an essential role in *IRF- β* expression [61].

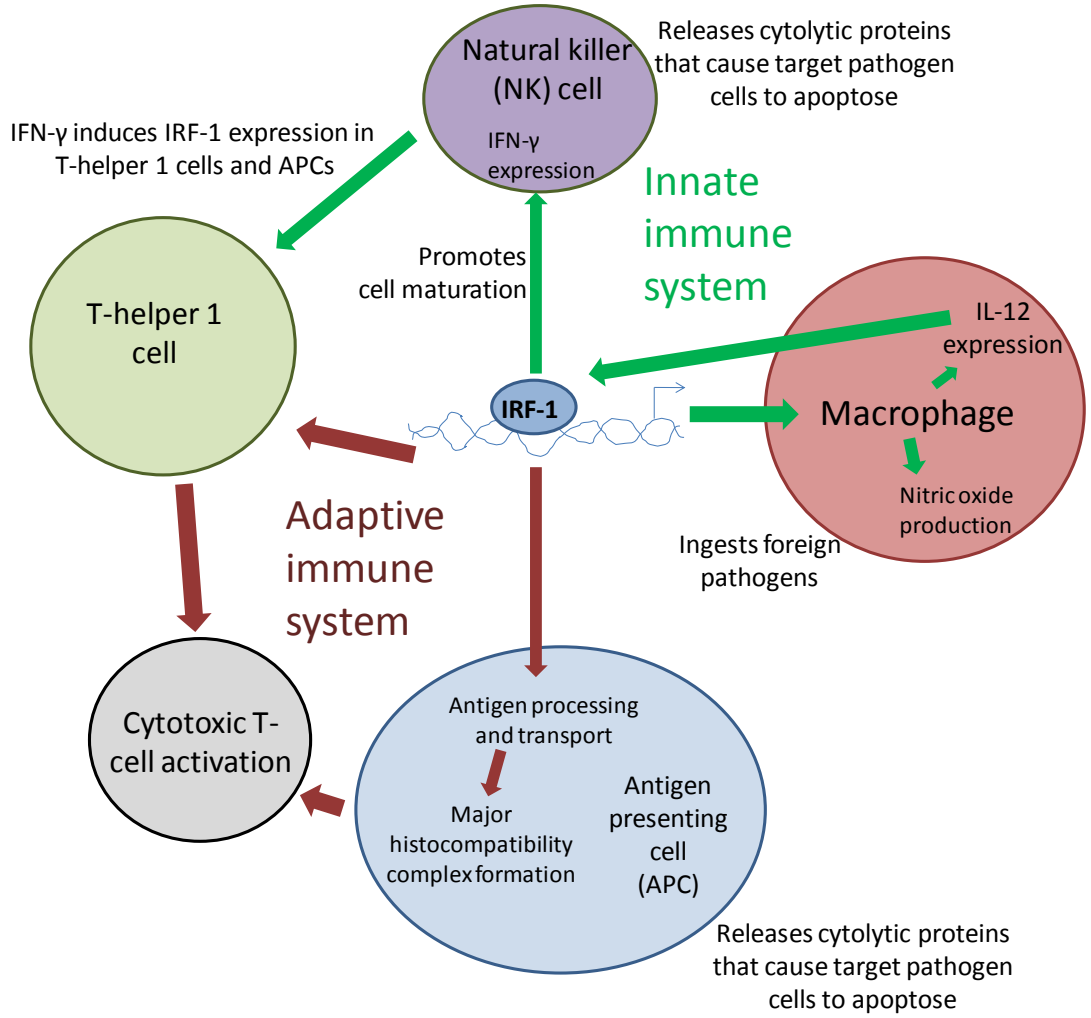

Figure 1.2: IRF-1 expression in T-helper 1, antigen presenting, macrophage and natural killer cells has been linked to the activation of the innate and adaptive immune responses. Furthermore, positive feedback loops continue to stimulate IRF-1 expression during the immune response. Specifically, IRF-1 induces IL-12 expression in macrophages and causes natural killer cells to mature, which enables them to produce IFN-γ; these cytokines then signal to T-helper 1 and antigen presenting cells producing an increase in the expression of IRF-1 in these cells.

1.2.3.2 Inhibition of cell proliferation

IRF-1 regulates interferon-responsive genes involved in negative growth control [1, 62] and is involved in G_1 cell cycle arrest [63]. Its overexpression leads to a pronounced reduction in cell growth [64], whereas knockdown of endogeneous IRF-1 stimulates cell proliferation [65]. Modulation of the IRF-2:IRF-1 ratio appears to be a critical mechanism in regulation of cell growth; for instance it has been shown that IRF-1-induced growth inhibition in human breast cancer cell lines can be overcome through the induction of IRF-2 [6, 66]. IRF-1 expression peaks in cells arrested by serum starvation (G_1 arrest), rapidly declines following serum stimulation, then once more gradually increases prior to the onset of DNA synthesis [6]. In contrast, IRF-2 mRNA expression remains essentially constant throughout the cell cycle [6].

In further support of the importance of the IRF-2:IRF-1 ratio, exogenous IRF-1 expression was able to revert IRF-2-induced cellular transformation and enhanced tumorigenicity in nude mice [6]. There are currently two models to explain the mechanism through which IRF-2 suppresses interferon-induced gene expression: that it is able to out-compete IRF-1 for promoter binding owing to its longer half life (8 hours compared to 30 minutes) [67], or alternatively that it induces changes in chromatin structure that silence gene expression through the inhibition of core histone acetlylation by p300 [68]. In correspondence with the effects seen following its knockdown and overexpression, IRF-1's target genes are known to include a large number of those involved in cell cycle regulation. Some examples are outlined below:

IRF-1 was observed to induce cell cycle arrest in coronary artery smooth muscle cells in the G0/G1 phase [63]. The cyclin A/CDK2 kinase complex is activated in late G_1 at the G_1/S transition [69] and can be inhibited by cycle dependent kinase inhibitors of the cip/kip family such as p21 [70]. IRF-1 has been shown to repress CDK2 expression, lowering endogeneous protein levels and repressing transcription of a CDK2 promoter luciferase construct [62]. IRF-1 has also been shown to induce expression of firefly luciferase encoding gene under the control of the *p21* promoter sequence [63] and to upregulate p21 expression in cooperation with the tumour

suppressor protein p53 following DNA damage [71]. It was subsequently shown that *p21* stimulation by IRF-1 is independent of IRF-1 binding DNA and instead involves IRF-1 binding to the p53 coactivator p300, which stimulates p53 acetylation [72], thus up-regulating p53-dependent *p21* activation (which is extensively described elsewhere [73, 74]). Additionally, IRF-1 has been shown to mediate IFN-γ-induced upregulation of *p27* [75], a cyclin-dependent kinase inhibitor that causes cell cycle arrest by binding to CDK2 and thus suppressing the formation of cyclin E/CDK2 complexes essential for cell cycle progression [76, 77]. Exogenous expression of IRF-1 stimulated p27 expression and IFN-γ stimulation of p27 was abrogated in *IRF-1-/-* mouse embryonic fibroblasts [75].

Thus IRF-1 represses CDK2 on two levels: by directly binding to its promoter to decrease its expression or by promoting the expression of its inhibitor p21 and p27.

Cyclin D1 is a regulatory subunit of the CDK4 holoenzyme that phosphorylates and inactivates the tumour suppressor pRb, this is a critical event in the G_1 cell cycle checkpoint [78]. In *myc/ras*-transformed mouse EFs, IRF-1 expression resulted in a marked decrease in cyclin D1 protein and mRNA levels and was able to decrease expression from a luciferase construct under the control of the *cyclin D1* promoter [79]. In agreement with this observation, pRb's phosphorylation was also reduced following IRF-1 activation. Concomitant Cyclin D1 overexpression was able to overcome the growth inhibitory effects of IRF-1 [79].

IRF-1 is also involved in the regulation of cell cycle progression genes that do not directly block Cyclin/CDK complex formation. For instance, IRF-1 functionally interacts with and activates the *histone 4* promoter cell cycle element (CCE), 5′-CTTTCGGTTTT-3′, which controls transcription at the G1/S phase transition [80]. An increase in histone transcription is coupled to DNA synthesis during S phase of the cell cycle [81]. Regulation of histone transcription may therefore be linked to the gradual increase in IRF-1 expression seen prior to the onset of DNA synthesis [6].

1.2.3.3 Apoptosis

Apoptosis is the process of programmed cell death, and misregulation of apoptosis is associated with tumour development and autoimmune disease [82, 83]. In IFN-

gamma-sensitive ovarian cancer cells, IFN-γ-induced apoptosis was reduced through the knockdown of *IRF-1* or overexpression of IRF-2. Furthermore, apoptosis could be strongly induced through IRF-1 transient expression without IFN-γ treatment. This effect was repressed when IRF-1 was co-expressed with its antagonist IRF-2 [84].

IRF-1 has been shown to bind directly to the promoters of several pro-apoptotic genes, thus inducing their expression and triggering a signalling cascade ending in cell death. Such targets include: *caspase 1, PUMA, TRAIL, XAF1* and the *Angiotensin II type 2 (AT_2) receptor.*

Caspases are aspartate-specific cysteine proteases, and their activation leads to the proteolysis of proteins essential for cell survival, thereby ultimately causing cell death [85]. IRF-1-induced apoptosis is also inhibited when cells are treated with caspase 1-inhibitors [84], and an IRF-1 binding site has been identified within the caspase 1 promoter [86], the mutation of which reduced IFN-γ-stimulated caspase 1 expression [87]. Another apoptosis-related target of IRF-1 transcriptional activation is *PUMA* (p53 upregulated modulator of apoptosis) [88]. Characterised as a critical mediator of p53-dependent and -independent apoptosis, PUMA functions by inducing mitochondrial dysfunction and caspase activation [89].

One target of IRF-1 of particular interest, given IRF's tumour suppressor function, is *TRAIL* (tumour necrosis factor-related apoptosis-inducing ligand) [90]. TRAIL is a potent inducer of death of cancer but not normal cells [91], which also functions through activation of the caspase signalling pathway (reviewed in [92]). *XAF1* (X-linked inhibitor of apoptosis protein (XIAP)-associated factor 1) is also an IRF-1 stimulated gene involved in the caspase signalling pathway. IFN-α induction of *XAF1* was shown to be mediated by IRF-1 and abrogated by mutation of the IRF-1 binding site (ISRE) in the *XAF1* promoter [93, 94]. XAF1 promotes apoptosis by associating with and antagonising XIAP, an inhibitor of caspase catalytic function [95].

Finally, stimulation by IRF-1 has been shown to enhance apoptosis mediated by the angiotensin II type 2 (AT_2) receptor [96]. Expression of this receptor was shown to be regulated by IRF-1/IRF-2 competition for an ISRE motif within its promoter [97].

1.2.4 Structure/function mapping of IRF-1

The IRF-1 gene consists of 10 exons. Mutant forms of the protein with impaired tumour suppressor activity have been identified in gastric adenocarcinoma [22], chronic myeloid leukaemia [23] and cervical cancer [24]. In some cases only specific functions of IRF-1 are abrogated by mutation. For example an exon 2 missense mutation (A22T) in human gastric adenocarcinoma produced an IRF-1 protein with unimpaired DNA binding ability but reduced transcriptional activity [22]. Another mutant protein, identified in cervical cancer patients, that lacked the C-terminal transactivation domains of IRF-1 (splicing variants involving exons 7, 8 and 9) was shown to compete with wild type IRF-1 for DNA binding, have a longer half life and, unlike the wild type protein, be expressed in a cell cycle independent manner [24]. Understanding the function of discrete domains in the wild type IRF-1 protein could increase current understanding of the role these mutants play in tumour progression.

A series of studies based on deletion mutants have already provided broad mapping of IRF-1 domains. These studies were carried out on either human (325 amino acids) or murine IRF-1 (329 amino acids). Comparison of mouse and human IRF-1 has shown the two proteins are highly homologous (84% identity: determined using the BLAST (Basic Local Alignment Search Tool) sequence comparison program [98]) and that both can activate transcription of the target genes *IFN-β, iNOS*, and *COX-2* [99], therefore studies describing structural mapping of both mouse and human IRF-1 are included here. Studies involving murine IRF-1 are indicated by an "^{m}" after the reference, all other studies are based on human IRF-1.

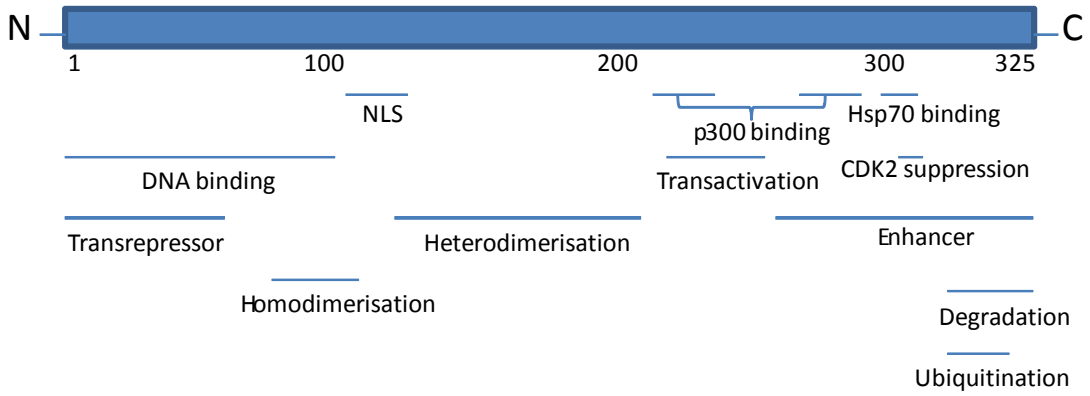

Figure 1.3: Mapping of human IRF-1 functions and regulation. NLS: nuclear localisation signal.

1.2.4.1 The DNA binding domain

The N-terminal DNA binding domain of IRF-1 (defined as amino acids 1-124) shares significant homology with other members of the IRF family (see figure 1.4) and is characterized by five conserved tryptophan repeats, each of which are separated by 10-18 amino acids. These tryptophan residues mediate the specific binding of IRF-1 to the IFN-stimulated response element (ISRE) in target promoters [5]. The first 113 amino acids of IRF-1 have been crystallised bound to a 13 base-pair IFN-stimulated response element [100].

1.2.4.2 N-terminal transrepressor

The N-terminal 60 amino acids of IRF-1 were shown to act as an internal repressor of IRF-1 activity [101]^{m}. In this study truncated sections of IRF-1 were fused to the DNA binding domain (DBD) of the transcription factor Gal4, and the ability of these IRF-1 regions to modulate activation of a promoter bound by the Gal4 DBD was assessed. In this way the enhancer domain (see section 1.2.4.7) of IRF-1 was identified; and a "GAL4 DBD-IRF-1 transactivation and enhancer domain" fusion protein was shown to have a reduced ability to activate transcription when combined to the N-terminal 60 amino acids of IRF-1[101]^{m}.

Figure 1.4: Sequence alignment of IRF family DNA binding domain (DBD). The N-terminal 124 amino acids of human IRF-1 were compared to IRF-2 to 9, (excluding IRF-5) using the BLAST program [98]. IRF-5 was excluded as it has low primary sequence homology to the IRF-1 DBD, although it still retains the 5 highly conserved tryptophan repeats that characterise the IRF DBD (highlighted in blue for the other IRFs) [102] and 36% sequence identity to a C-terminal region of IRF-1 (amino acids 291-315) (noted during BLAST analysis: data not shown). Only the sequence of isoform-a of IRF-7 was used in this analysis, other isoforms of this protein were excluded to simplify analysis.

1.2.4.3 Homodimerisation domain

Amino acids 90-115 were shown to be essential for an intracellular interaction between two recombinant IRF-1 proteins [103] [m]. The crystal structure of IRF-1's DNA binding domain indicates that a monomeric IRF-1 binds to the core GAAA sequence within the ISRE, however, the authors of this study speculate that as some ISRE contain two GAAA core sequence they could accommodate two IRF-1 molecules [100].

1.2.4.4 Nuclear localisation signal

The nuclear localisation signal of IRF-1 has been mapped to amino acids 117-141 [104] [m]. When fused to GFP, this discrete domain was able to re-localise the fluorescent protein to the nucleus.

1.2.4.5 Heterodimerisation domain

A region of IRF-1 overlapping the NLS, spanning amino acids 125-219, was shown to be necessary but not sufficient for heterodimerisation with IRF-8 (an IRF-1 co-factor) [104] [m]. This association is further discussed in section 1.2.5.4.3.

1.2.4.6 Transactivation domain

Fusion to fragments containing IRF-1 amino acids 185-220 or 220-256, enabled the DNA binding domain to induce transcription thus defining the transactivation domain (amino acids 185-256) [101, 104] [m]. This domain was further reduced to amino acids 233-257 in human IRF-1 and was able to transactivate the DNA binding domains of other transcription factors as part of fusion proteins [105]. Deletion of this region interfered with wild type IRF-1's ability to stimulate IFN-β expression, inhibit growth and induce apoptosis, possibly through formation of an inactive homodimer or by competing for target promoters [105]. Following identification of the transactivation domain it was demonstrated that this region of IRF-1 could mediate downstream signalling in a manner independent of DNA binding activity. p53 and IRF-1 can act synergistically to promote p21 expression [71] and p300-dependent acetylation was previously shown to increase p53 transcriptional activity [106-108]. It was revealed that specific regions of IRF-1 (amino acids 226-245 known as CT3, and amino acids 271-290 known as CT2) could bind directly to the acetyl transferase p300, promote p300 binding to p53 and the acetylation of DNA-bound p53 at the p21 promoter [72].

The transactivation domain also appears to be involved in post-translational modification, as the deletion of IRF-1 amino acids 219-231 blocked *in vitro* phosphorylation of IRF-1. Additionally, mutation of four putative phosphoaceptor residues in the transactivation domain significantly decreased transactivation mediated by IRF-1. Interestingly, in this same study casein kinase II was co-purified from cell lysate with exogenous His-tagged IRF-1 and shown to bind to it directly, indicating that it may be involved in the regulation of IRF-1 function [109] [m].

1.2.4.7 Enhancer domain

Unlike the transactivation domain, a more C-terminal region of IRF-1 spanning amino acids 257-329 could not independently increase transcriptional activity of a

GAL4 DNA binding domain [101] [m]. However, the inclusion of this region increased transcriptional activation compared to that generated by the Gal4 DBD-transactivation domain alone. This extreme C-terminal region was therefore identified as an enhancer domain [101] [m].

As a link between the C-terminus of IRF-1 and its ability to activate transcription had been established, it was possible that this trans-acting region could influence IRF-1 repressor functions. IRF-1 has been shown to repress certain genes including *SLPI* (secretory leukocyte protease inhibitor) and *CDK2* (cyclin-dependent kinase 2*)* [10, 62]. Deletion of the C-terminal 25 amino acids increased IRF-1-dependent induction of *IFN-β*, but mitigated *CDK2* repression. Smaller deletion mutants and alanine substitutions revealed that amino acids 311-317 act as an internal suppressor of IRF-1's transcriptional activator function. Thus, mutation of these residues increases *IFN-β* induction. Furthermore, amino acids 306-310 were shown to be essential for *CDK2* suppression [64]. These C-terminal mutants did not affect IRF-1's DNA binding suggesting that they may modulate IRF-1's association with as yet unidentified co-factors.

The extreme C-terminus was also shown to play a role in the stability of IRF-1. IRF-1 has an extremely short half life of 20-40 min [110] [m] and [111]. Truncations of more than 39 C-terminal amino acids generated a degradation resistant form of IRF-1 [110] [m]. It has also been shown that the protein is capable of being polyubiquitinated and degraded by the 26S proteosome [110] [m]. Inhibition of the proteosome leads to an increase in polyubiquitinated forms of IRF-1 [110] [m], indicating that IRF-1's ubiquitination is linked to its degradation. During a more detailed mapping of this function it was seen that deletion of the last 70 amino acids of IRF-1 prevented both polyubiquitination and degradation, whereas deletion of the last 25 amino acids did not prevent ubiquitination, but did inhibit degradation [111]. Furthermore, exogenous expression of the C-terminal 70 amino acids was shown to reduce ubiquination of endogenous wild type IRF-1. This suggests that the C-terminus may act as a docking region for ubiquitin-promoting co-factors (e.g. E3 ligases) and compete *in trans* with full-length IRF-1 for binding to these proteins. An increase in the half life of IRF-1 has previously been linked to its upregulation during ATM-dependent DNA damage

response [29], highlighting the physiological importance of IRF-1's degradation in its regulation.

An LXXLL motif residing between amino acids 306 and 318 in the C-terminus of IRF-1 has been shown to be of particular significance in regulation of IRF-1 turnover, as an Hsp90-dependent increase in half life and protein levels of nuclear IRF-1 was shown to be reliant on direct binding of Hsp70 to this motif [112].

1.2.5 Post-translational regulation of IRF-1

IRF-1 expression is tightly regulated during the cell cycle and in response to infection. However, several lines of evidence also indicate that it is regulated post-translationally. Its phosphorylation state has been linked to its ability to form heterodimers [113], ubiquitination and SUMOylation seem to affect its degradation and activity [110, 114] and the exchange of co-factors enables it to respond to a range of stimuli including DNA-damage, interferon stimulation and toll-like receptor activation (detailed in section 1.2.5.4). The repression or activation of diverse sets of genes by IRF-1 in response to specific stimuli appears to be dependent on the co-factor associated with IRF-1. Thus these post-translational associations may determine which of a range of possible responses will be induced following IRF-1 expression.

1.2.5.1 Phosphorylation

IRF-1 was shown to bind directly to the alpha catalytic subunit of CKII (casein kinase II), a tetrameric serine/threonine protein kinase, through its N-terminal 120 amino acids [109]. Alanine substitution of potential CKII phosphoacceptor sites in the C-terminus of IRF-1 (amino acids 219–231) blocked *in vitro* phosphorylation and reduced the IRF-1 dependent activation of the interferon β promoter [109]. IRF-1 has also been shown to be tyrosine phosphorylated following IFN-γ stimulation [113], supporting the possibility that phosphorylation is a means through which IRF-1 is regulated.

1.2.5.2 Ubiquitination

Covalent attachment of small (8.5KDa) ubiquitin moieties to lysine residues in a target protein has been linked to directing proteins for degradation or altering

localisation and activity [115]. Figure 1.5 summarises the attachment of ubiquitin to a target protein. Inhibition of the proteasome, a multi-protein complex responsible for protein degradation, causes an increase in polyubiquitinated forms of IRF-1 [110], indicating that ubiquitination of IRF-1 mediates its degradation. Deletion of the last 25 amino acids of IRF-1 does not prevent its ubiquitination, but does inhibit degradation [111], suggesting that following ubiquination the C-terminus of IRF-1 is involved in a further regulatory step that enables degradation. An Hsp70 binding site has been identified in this region and this interaction was shown to be essential for an Hsp90-dependent increase in IRF-1 stability [112], it is therefore possible that abrogation of Hsp70 binding may mediate IRF-1 degradation. Reduced degradation of IRF-1 has also been linked to its upregulation during the ATM-dependent DNA damage response [29] highlighting the physiological importance of this form of regulation. The E3 ubiquitin ligases that facilitate IRF-1 degradation have not yet been identified.

1.2.5.3 SUMOylation

The attachment of a SUMO protein (Small Ubiquitin-like Modifier) to lysine residues is a post-translational modification similar to ubiquitination and can also affect target protein activity [117]. Ubc9, a SUMO E2-conjugating enzyme and SUMO-1 were shown to directly interact with IRF-1 and, when overexpressed, to decrease IRF-1-dependent transcription [118]. Furthermore, co-expression of SUMO-1 and IRF-1 was seen to increase the half life of IRF-1 suggesting SUMOylation may stabilise the protein [114]. This data suggests that SUMOylation may hold IRF-1 in a less active form with a lower rate of degradation. Additionally, SUMOylated IRF-1 has been reported to be elevated in cancer cells lines [114], indicating that this modification has physiological relevance.

One drawback of co-expressing SUMO-1 is that it can bind to a wide range of cellular proteins [117]; thus changes in IRF-1 activity observed may not have been caused by its SUMOylation, but rather as a product of SUMO-1's off-target effects. Another study into this post-translational modification demonstrated that IRF-1 fused C-terminally to a SUMO moiety, thus mimicking SUMOylated IRF-1, was able to transform mouse embryonic fibroblast-cells and down-regulate IRF-1-dependent

transcription [119]. Covalent attachment of a SUMO moiety has been used in functional studies of other proteins, together with untagged mutant proteins that could not be SUMOylated as controls [120, 121], however in the SUMO-IRF-1 study no such mutants were used, and it is not clear that this fusion accurately mimicked the functions of a SUMOylated IRF-1.

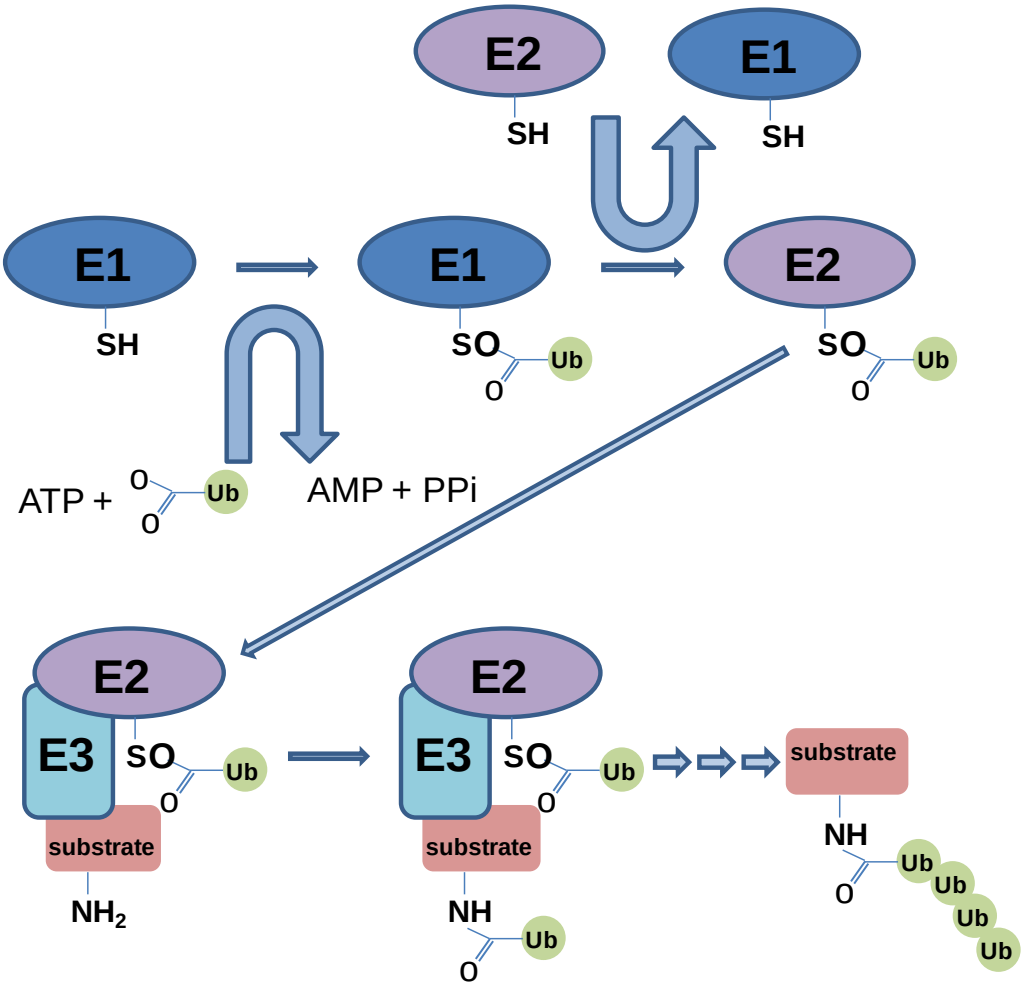

Figure 1.5: Flow diagram showing ubiquitination of a target protein substrate by the E1 ubiquitin-activating enzyme, E2: ubiquitin-conjugating enzyme and E3: ubiquitin ligase. Based on the following reference [116].

The SUMO E3 ligase PIAS3 (Protein inhibitor of activated STAT3) was identified as an IRF-1 interacting protein in a yeast-2-hybrid screen [122]. It was further shown that a point mutation in the ring finger domain of PIAS3 (C334S), which is required for its SUMO-ligase activity, prevented SUMOylation of IRF-1 without interfering with IRF-1:Pias3 binding. Co-transfection of wild type PIAS3 also inhibited

expression from an IRF-1 reporter gene 30% more than the C334S mutant, supporting the idea that IRF-1 is negatively regulated by SUMOylation.

1.2.5.4 IRF-1 co-factors

1.2.5.4.1 NF-κB

EMSA and co-immunoprecipitation assays involving cell lysates or nuclear extracts have been used in the past to show IRF-1 and NF-κB form complexes able to enhance or suppress transcription from target promoters [123-125]. For example, IRF-1 was co-immunoprecipitated in complex with HDAC-1 (histone deacetylase 1) and p65 (an NF-κB subunit) at the *PDGF -D* (platelet-derived growth factor-D) promoter following stimulation by the proinflammatory cytokine interleukin (IL)-1β [126]. This complex was abrogated by HDAC-1 knockout; but when intact mediated silencing of its target promoter. A direct interaction between purified IRF-1, HDAC-1 and/or the p65 subunit of NF-κB was not validated, meaning that other proteins may also form integral parts of the complex and mediate its association. Another study demonstrated that IRF-1 can bind directly to the p50 NF-κB subunit [127]. In the same study IRF-1 was also shown to bind HMGI(Y) (High mobility group I (Y)), a non-histone chromatin protein [128]. HMGI(Y) and p50 were shown to stabilise IRF-1 binding to a promoter targeted by both IRF-1 and NF-κB (*VCAM-1*), and co-transfection with IRF-1 and NF-κB was seen to enhance transcription to a greater extent than was generated by overexpressing either transcription factor alone [127], indicating that the two acted synergistically. Subsequently the NF-κB/IRF-1/HMGI(Y) complex was shown to activate other promoters (*IFN-β*) and was described as an enhanceosome [129]. The enhanceosome formed on the *IFN-β* promoter was also shown to recruit the co-activator protein p300 which bound directly to both IRF-1 and the NF-κB subunit p65 [130]. p300 is an intrinsic acetyltransferase and ubiquitin ligase involved in transcriptional regulation [131, 132]. The contribution of IRF-1 to the enhanceosome is debated [133], as IRF-1 null mice still show IFN-β expression [56] (discussed in section 1.2.3.1). However, these studies still suggest a process of co-factor exchange may exist that determines whether the IRF-1:NF-κB complex functions as a transcriptional activator as on the *IFN-β* promoter, or repressor as on the *PDGF-D* promoter.

1.2.5.4.2 STAT1

IRF-1 has also been shown to directly interact with the transcription factor STAT1 (signal transduction and transcription 1) [134]. This interaction was shown to mediate transcription from a gene targeted by both transcription factors: *LMP2* (low molecular mass polypeptide 2). His-tagged STAT1 immobilised on an oligonucleotide based on the *LMP2* promoter could bind to both purified and endogenous IRF-1. The minimal region of IRF-1 required for STAT1 binding was mapped to amino acids 170-200. Additionally, the adenovirus E1A protein was able to block the STAT1:IRF-1 interaction and thereby inhibit expression from the LMP2 promoter [134], indicating that disruption of this association is one of the mechanisms employed by the virus to overcome the host's immune response.

1.2.5.4.3 IRF-8

Another transcription factor capable of interacting with IRF-1 is IRF-8. IRF-1 and IRF-8 have been shown to compete for interferon response elements (ISRE) in target promoters, thus IRF-8 has been described as a repressor of IRF-1 [135]. IRF-8 has also been shown to repress IRF-1-induced activity by directly binding to IRF-1 and disrupting its interaction with other co-factors such as the HIV protein Tat (Trans-Activator of Transcription) [136]. However, the IRF-1: IRF-8 complex has also been described as activating transcription. It was initially demonstrated that IRF-1 binding could enhance IRF-8's affinity for the ISRE [137]; and that the IRF-1:IRF-8 complex can bind and thereby activate transcription from the *IL (interleukin)-12 p35* [138] and *RANTES* (Regulated on Activation, Normal T-cell Expressed and Secreted) [139] genes. More recently IRF-1 and IRF-8 have been shown to bind overlapping regions of the *IL-27 p28* promoter *in vivo* following stimulation by IFN-γ [140]. siRNA knockdown of IRF-8 was also shown to reduce IRF-1 binding to the *IL-27 p28* promoter, in agreement with the observation that expression of this gene was defective in IRF-8 deficient cells [140]. Furthermore, IRF-1 and IRF-8 synergistically activated IL-27 p28 expression when co-expressed [140].

It has also been demonstrated that the interaction between IRF-1 and IRF-8 can be blocked by tyrosine kinase inhibitors [113]. However, as both IRF-1 and IRF-8 are

tyrosine phosphorylated, the mechanism through which this post-translational modification facilitates this interaction requires further investigation.

1.2.5.4.4 p300

Induction of *the IL (interleukin)-12p40* promoter by the IRF-1:IRF-8 complex was enhanced by co-transfection of another IRF-1-binding protein: p300 [141]. In a separate study IRF-1 binding to p300 was shown to stimulate p53 acetylation, thereby up-regulating p53-dependent p21 activation [72], but the exact role of p300 in the IRF-1:IRF-8 complex still requires elucidation.

1.2.5.4.5 PCAF

Histone acetylases associated with transcription factors have been found to generally enhance transcription [142, 143]; a finding consistent with reports that transcriptionally active chromatin is composed of highly acetylated histones [144, 145] and that a histone acetylase is one of the components of the TATA binding protein (TBP)-associated factor [146]. Histone deacetylases on the other hand have been linked to transcriptional repression [147-149]. IRF-1 was shown to recruit the histone acetylase PCAF (P300/CBP-associated factor) to an interferon-stimulated response element (ISRE) [150]. PCAF was seen to increase IRF-1 induction of an ISRE-reporter gene in a dose-dependent manner. Taken together with the previously discussed finding that the histone deacetylase HDAC forms a silencing complex with IRF-1 and p65 [126], this data suggests that switching between histone acetylase and deacetylase co-factors may be a mechanism through which IRF-1 mediates activation or repression of a target gene.

This system can also be utilised by pathogens to deactivate IRF-1. For instance, the human papillomavirus oncoprotein E7 is implicated in the malignant phenotype of cervical cancer and has been shown to directly interact with the C-terminus of IRF-1 (amino acids 217–325) [151]. This interaction inhibits IRF-1-directed stimulation of an IFN-β reporter gene construct, but does not affect IRF-1 degradation. E7 repression of IRF-1 activity was shown to be alleviated by a HDAC (histone deacetylase) inhibitor or by deletion of the carboxyl-terminal zinc finger domain of E7 which was previously shown to associate with HDAC [151], indicating that IRF-1 repression is mediated by E7 recruitment of HDAC.

1.2.5.4.6 NPM

Other non-transcription factor proteins have also been shown to modify IRF-1 activity. For example, IRF-1 has been shown to bind directly to NPM (nucleophosmin) [144], a multifunctional protein that shuttles between the nucleus and cytoplasm and regulates rRNA export from the ribosome [152] and the activity of tumour suppressor proteins ARF and p53 [153, 154]. Association with NPM negates IRF-1's ability to bind DNA and thus reduces IRF-1 dependent transcription [144]. NPM has been characterised as an oncogene; it is present at elevated levels in several leukaemia cell lines, and its exogenous overexpression can transform mouse embryonic fibroblasts [144]. It is therefore possible that suppression of IRF-1 is one of the mechanisms through which the oncogenic effects of NPM are mediated.

1.2.5.4.7 GRIP-1

GRIP-1 (Glucocorticoid receptor-interacting protein 1) is able to bind IRF-1 directly, but unlike NPM, GRIP-1 enhances transcription of IRF-1's downstream targets; with siRNA targeting GRIP-1 reducing IRF-1-dependent reporter gene activity by more than 57% [155]. The *CD38* (cluster of differentiation 38) gene which is expressed in an IRF-1-dependent manner also showed reduced expression following knockdown of GRIP-1, suggesting that this interaction can modulate IRF-1 activity *in vivo* [155].

1.2.5.4.8 MyD88

Another IRF-1 co-activator is MyD88 (Myeloid differentiation primary response gene 88), an adapter protein recruited by TLRs (Toll-like receptors) upon pathogen recognition that then interacts with and activates down-stream mediators of the TLR signalling pathway, such as IRF-5 or IRF-7, to induce an immune response [156, 157]. MyD88 can bind directly to IRF-1. Additionally co-expression with MyD88 increases the rate at which IRF-1 was translocated to the nucleus and enhances expression from an IRF-1 dependent reporter gene [158]. Controlling transcription factor sub-cellular localisation has been described as an efficient way of regulating their activity [159].

1.2.5.4.9 KPNA2

IRF-1 is also translocated into the nucleus by KPNA2 (karyopherin α2, also known as importin α) [160], a cytosolic receptor that docks nuclear localisation signal

(NLS)-containing proteins at the nuclear pore complex on the nuclear membrane [161]. Like IRF-1, KPNA2 is expressed following stimulation with IFN-γ, which suggests KPNA2 may be induced to facilitate downstream IFN-γ signalling by promoting IRF-1 nuclear localisation [160]. However, the effect of KPNA2 expression on IRF-1-dependent promoters was not investigated nor was its binding to the previously identified IRF-1 NLS [104].

These studies indicate that IRF-1 can function as part of a complex of transcription factors and that facilitation or disruption of such complexes could be a means through which IRF-1 activity is regulated. They also show that viral proteins like Tat or E1A hijack IRF-1 by competing against its normal co-factors to limit the IRF-1-dependent immune response.

The studies described here support the idea that post-translational modification and protein:protein interactions play an important role in controlling IRF-1 activity. However these experiements necessarily relied on transfected IRF-1 for most of their findings, and it would be interesting to see if these interactions are rate-limiting for the activity of the endogenous protein. Furthermore, it is clear that important IRF-1 interactions remain unidentified. What is/are the E3 ubiquitin ligase(s) that target IRF-1? Do other kinases beside CKII phosphorylate IRF-1? Are other proteins important components of its activating or silencing complexes? The identification of novel IRF-1 interacting proteins will hopefully begin to answer some of these questions. Phage display has been used in this study to both isolate antibodies that bind to specific regions of IRF-1 and to identify IRF-1 binding peptides. The antibodies were subsequently developed into intrabodies able to modulate the activities of endogenous IRF-1 and the phage display peptide sequences have been used to select potential IRF-1-interacting proteins for future characterisation. Section 1.3 describes the phage display techniques that are central to the work described in this thesis.

1.3 Phage display

A bacteriophage (usually shortened to phage) is any virus capable of infecting bacteria [162]. Filamentous phage M13 [163] and fd [164] are the most commonly

used carriers in phage display, but lytic bacteriophage, such as T4 [165], T7[166], and λ [167] phage have also been used.

Phage display technology relies on a physical linkage between phenotype and genotype; a polypeptide displayed on the surface of a phage virion is also encoded within the phage genome. Extremely diverse libraries ($>10^{10}$) of DNA-encoded peptides or proteins can be generated and cloned into phage [168]. These polypeptides are then expressed as fusions to phage coat proteins and selected for binding to immobilised ligands [169]. In this way the phage library becomes enriched for those that bind specific ligands. Phage that do not bind the target ligand are simply washed away before high affinity phage are eluted. The newly generated pool of high affinity phage can be amplified in host bacteria and used again in another selection round [169]. Finally, and most importantly, the amino acid sequence of any protein or peptide displayed can be easily determined by sequencing the DNA inside the phage particles.

Several factors influence the choice of phage carrier. The exposed end of most coat proteins differs between the filamentous (N-terminal) and lytic (C-terminal) phage. The presented peptide can therefore be affixed to the carboxy (filamentous) or amino (lytic) termini of a coat protein, making it possible to choose which end of a peptide should be left most exposed for interaction with the bait protein [166], although N-terminal fusion is still possible in filamentous phage via the g6p coat protein [170]. Capsids of lytic phages such as T7 and lambda phages are assembled in the cytoplasm, whereas filamentous phage capsids are formed in the periplasm [171]. The biological constraints for folding the displayed protein are therefore different. Additionally, use of lytic phage involves time-consuming purification steps between selection rounds to avoid panning amplified phage in the presence of cellular proteins from the lysed bacterial host (including proteases), whereas non-lytic phage are secreted through the bacterial membrane and can be purified by a simple PEG (poly[ethylene glycol]) precipitation step [172].

The methods described in this thesis utilise M13 bacteriophage; a filamentous, *Escherichia coli*-specific virus consisting of a circular, single-stranded DNA (ssDNA) core surrounded by a protein coat [173]. In this study the displayed peptide

or antibody fragment is fused to the g3p minor coat protein (~ 3 copies per phage) [174].

Phage display libraries can be created in two ways [175], by cloning the polypeptide: 1) into the phage genome (phage vector) in frame with a coat protein, in which case the number of displayed polypeptides corresponds to the number of coat proteins, or 2) into a modified phage genome known as a phagemid, in which most viral genes have been deleted, but which still carries the gene encoding the coat protein. When a cell harbouring a phagemid is infected by helper phage (which supply the deleted phage genes), virions that display a mixture of recombinant coat proteins, encoded by the phagemid, and the corresponding wild type proteins, encoded by the helper phage genome, are produced [176]. Phagemid cloning enables the display of longer polypeptides than is possible with a phage vector [176]. In this thesis a library based on cloning into a phage genome was used for peptide phage display (chapter 6), and one based on phagemid cloning for antibody phage display (chapters 4 and 5).

Other display surfaces can also be used to select for high affinity antibody or peptide interactions including: surface expression on bacterial, yeast or mammalian cells, or cell-free systems such as ribosome display [177].

1.3.1 Antibody phage display

Unlike standard hybridoma technology, the generation of antigen-specific antibody fragments can be performed within a couple of weeks though antibody phage display [178]. Performed *in vitro*, phage display circumvents the need for immunogenicity and is therefore particularly well suited to generating antibodies against self, low-immunogenic (like IRF-1) or toxic proteins [178]. Additionally human antibody fragments can be generated, which would present a lower risk of immune response in subsequent therapeutic studies [179]. Once an antibody has been selected, the phage can continue to act as a genetically stable source of the antibody, which can be stored over a long period. The antibody genes can be easily sequenced, mutated and then screened again for improved specificity [180].

Antibody phage display relies on large (10^{10} clones) naive or immune antibody libraries [178]. Following two to three rounds of selection, this population becomes

enriched for antibody fragments specific for the target antigen. In order to generate the antibody library, antibody fragments are cloned into a phagemid upstream of a phage coat protein (usually g3p or g8p) and expression is controlled by the use of a promoter such as lacZ. Phagemids also carry an antibiotic resistance marker. The relatively small size of phagemid plasmids (~ 4.6 Kb) means that they have higher transformation efficiencies than phage vectors, enabling the construction of large libraries [181]. Incorporation of an amber stop codon between the antibody fragment and phage coat protein results in their expression as a fusion protein in suppressor strains of *E.coli* (e.g. TG1) or as an isolated antibody fragment in non-suppressor strains (e.g. HB2151).

The phagemid alone is insufficient for the production of infective phage particles in bacteria as it does not contain all the genes needed for phage replication and assembly. These are provided by helper phage [182]. During the amplification step, bacterial cells already containing the phagemid vector are co-infected with the helper phage. The growth media is supplemented with glucose, which suppresses the lacZ promoter and therefore expression of the antibody-coat protein fusion. Once helper phage infection is complete, the glucose is removed and production of antibody-displaying phage particles can commence [182].

1.3.1.1 Different types of antibody fragments

Multivalent naturally occurring human antibodies (IgG, IgM, IgA, IgE) are highly specific targeting reagents and provide our key defence against pathogenic organisms and toxins. IgG is most often developed for use as a molecular tool and therapeutic [183]. It is a Y-shaped, bivalent protein with two antigen-binding sites located within Fab domains and an Fc domain that mediates recruitment of cytotoxic effectors [184]. The constituent domains of IgGs can be expressed as soluble antibody fragments, which retain the specific binding properties of a complete IgG, either as monovalent (Fab, scFv, single variable V_H and V_L domains) or multivalent fragments generated through fusions of these moieties [185, 186]. Restricting antibody size allows fragments to be displayed by fusion to phage coat proteins and expressed in cells.

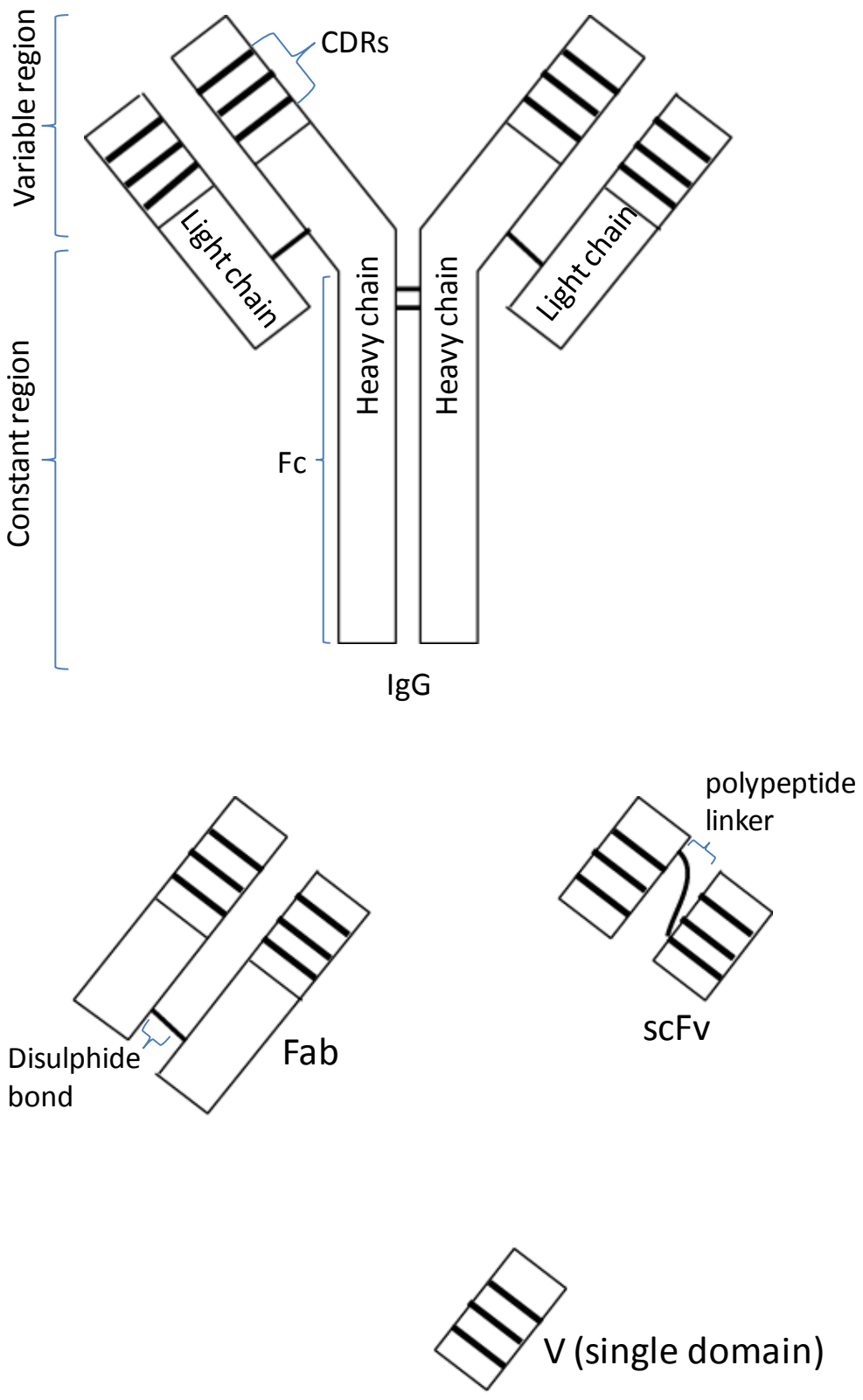

Figure 1.6: Structure of immunoglobulin G (IgG), Fab, scFv and single domain antibody fragments.

1.3.1.1.1 Fab

Fab (fragment antigen-binding) are composed of both the constant and variable regions of the antibody heavy and light chain (unlike scFv which are made up of only the variable regions) [187]. Within the N-terminal variable (V) domain of each chain are Complementarity Determining Regions (CDRs, also called hypervariable loops) which form the antigen binding site.

1.3.1.1.2 scFv

The two phage display libraries used in this thesis, the Tomlinson and ETH-2-gold libraries [188, 189], both involve the display of single chain variable fragments (scFv) attached to the phage coat protein. scFv consist of the variable regions of the heavy ($V_{H)}$ and light (V_L) chains connected by a flexible polypeptide linker to prevent dissociation [190, 191].

1.3.1.1.3 Single domain (V) antibodies (nanobodies)

Naturally occurring antibodies, consisting of only a heavy chain, have been identified in camelids (camels and llamas) [192] and cartilaginous fish (wobbegong and nurse sharks) [193] and were shown to play an important role in the immune system of these organisms. These heavy chain domains (known as VhH in Camelids and IgNAR in sharks) display longer hypervariable loops than murine and human antibodies and are therefore better at penetrating cavities in target antigens such as enzyme active sites [194, 195].

Mouse single variable (V) domains were shown to be functional [196] at an early stage of antibody engineering. It was subsequently established that antibodies based on human heavy chain and light chain variable domains (V_H and V_L) selected by phage display also have good antigen recognition and affinity [197, 198]. It has been proposed that, because of their smaller size, single domain antibodies could potentially target cryptic epitopes [199].

1.3.1.1.4 Multivalent antibody fragments

For many applications, it is desirable to engineer the monovalent Fab, scFv fragments or V-domain molecules into multivalent molecules, which show increased functional affinity (termed avidity) and slower dissociation rates. Fab fragments have

been chemically cross-linked into bi- or trivalent multimers [200, 201]. Shortening the scFv linker induces self-assembly into either bivalent [202, 203], trivalent [204, 205], or tetravalent [206] multimers.

Multivalent antibody fragments are not only able to possess increased avidity (the number of identical binding sites) but can also be converted into bispecific antibodies with two different binding specificities fused into a single molecule. Such antibodies can bind either two adjacent epitopes on a single antigen, thereby increasing both avidity and specificity, or two different antigens. Multivalent antibodies targeting more than one antigen have numerous potential uses and have already been utilised in recruitment of cytotoxic T- and natural killer (NK) cells [207, 208] and targeting of toxins [209, 210], radionuclides [211] or cytotoxic drugs [212, 213] for cancer treatment.

1.3.1.2 Different types of library

There are several different types of antibody phage display library available. The key differences between available antibody phage display libraries are 1) the source, 2) the level of antibody diversity and 3) the type of antibody fragment displayed (fab, scFv etc.).

The genomic information coding for antibody variable domain can come from B cells of various animals, but are typically murine [13], human [214], cammelid [215, 216] or from cartilaginous fish [217]. The donor can additionally be naive (non–immunised) or immunised. Immune libraries provide an antibody repertoire enriched against the antigen that caused the original immunogenic response in the donor. Such a library can be generated from immunised animals [164] or diseased humans [218]. For example, a human Fab phage display library produced from lymphocytes of an individual still asymptomatic 10 years after infection with human immunodeficiency virus type-1 (HIV-1) was used to generate single chain antibodies targeting HIV Rev and Tat regulatory proteins [218].

Antibody fragment library construction involves: reverse transcription of the B-cell derived mRNA, PCR to amplify the VH and VL gene segments from the cDNA and restriction-based cloning to insert the VH and VL encoding DNA into a phagemid

vector to be expressed as a fusion with the g3p phage coat protein [164]. scFv are thus expressed as single chains [164]. Additional synthetic diversity can be added to the antibody library through the random reassortment of VH and VL gene segments and by introducing artificial sequence diversity into the complementarity determining region (CDRs) using degenerate oligonucleotide primers [189]. To create a library of Fab fragments the complete heavy and light chains (conserved and variable regions) are amplified, and cloned into a phagemid vector under the control of two separate LacZ promoters or with an intervening ribosomal binding site [219]. One chain is expressed as a coat protein fusion and the other independently directed to periplasm by a signal sequence (pelB). During phage assembly the coat proteins are exported into the bacterial periplasm. Thus, an antibody chain fused to a coat protein will also be carried into the periplasm where it can be non-covalently attached to a pelB-antibody chain [174, 219].

The phagemid vectors are transformed into *E.coli* cells to generate the antibody library. These phagemids can then replicate as normal plasmids. Then, upon infection with helper phage, which provide all the genes required for phage assembly, the phagemid is packaged into a phage particle and secreted into the culture medium [220]. These antibody-displaying phage particles can easily be recovered through PEG precipitation [172].

The pre-constructed antibody phage display libraries used in the experiments described in this thesis are the Tomlinson (I and J) [188] and ETH-2-Gold libraries [189], both of which are human, non-immune and predominantly encode scFv.

1.3.1.3 Antibody selection strategies

The standard antibody selection protocol consists of five stages: 1) immobilisation of the antigen, 2) a blocking stage to limit non-specific binding, 3) incubation of antibody-displaying phage with the antigen, 4) washing to remove unbound phage and 5) elution of phage displaying specific high-affinity antibodies [181]. Several antibody selection strategies are available and primarily differ in whether or not the antigen is predetermined and if it is selected *in vivo* or *in vitro*. Phage display is an *in vitro* technique which limits the possibility of selecting indirect binders. The antigen can be coated onto a plastic surface (as described in this thesis), displayed on cell

surfaces [221-223] or as protein bands on nitrocellulose membranes following electrophoresis [224, 225]. Recently, phage-independent *in vivo* screening methods based on the yeast-two-hybrid system have been developed to screen for antibody fragments that are functional within the reducing environment of the cell cytoplasm [226, 227].

The antibody epitope is not always chosen in advance. Antibody phage display has been used to identify novel protein markers by selecting antibodies that show differential binding between diseased and healthy tissues [228, 229]. The disease-specific antigens can later be identified through their antibody-binding specificity [126]. Alternatively, as described in this thesis, the antigen can be pre-determined in order to study a specific protein or pathway. Additionally, when a target protein has already been partially characterised, specific protein functions can be targeted by using the relevant protein sub-domains or amino-acid motif as an antigen. For example, by using a GST fusion of the kinase domain of Etk as an antigen, intracellular scFv were developed that could block the endogeneous protein's ability to phosphorylate downstream substrates [230].

A range of options are now available to anyone wishing to develop a functional antibody fragment, including a choice of: library, antigen, selection technique and subsequent screening procedure. Additionally, in cases where a high affinity monoclonal already exists, it can be engineered to give a functional single chain antibody, thus eliminating the need for library generation altogether [231].

1.3.1.4 Intracellular antibodies (intrabodies)

1.3.1.4.1 Stable intracellular expression of antibodies

Single chain antibodies are stabilised by inter- and intra-chain disulphide bonds, which are inefficiently formed or absent under the reducing conditions of the cell cytoplasm [232]. This can lead to misfolding, which (as with any other protein) is linked to reduced solubility, a shorter half life and tendency to aggregate triggering proteosomal degradation [233]. Yet numerous intracellularly expressed antibody fragments have been shown to remain active and specific to their target antigen (detailed in section 1.3.1.4.2). To explain the functionality of intrabodies in reducing

environments, it has been proposed that intrinsically stable amino acid sequences could fold properly in the absence of disulfide bond formation [233, 234].

1.3.1.4.2 Modes of action

Intracellularly expressed antibody fragments have been successfully used to modulate the activity of their target proteins through a wide range of mechanisms, including: altering intracellular localisation [231, 235-237], blocking enzyme activity [230], triggering target protein degradation [238], inducing a transactivating conformational change [239, 240] and disrupting normal protein-protein [227, 240-242] or DNA-protein [227] interactions.

By relocating specific proteins away from their natural site of action, intrabodies can disrupt specific signalling pathways. This can be achieved by fusing a specific sub-cellular localisation signal to the scFv. Previous work has shown that intracellular antibodies targeted to the endoplasmic reticulum (ER) can be used to capture specific proteins as they enter the ER, preventing their transport to the cell surface. For example ER retention motifs added to intrabodies have previously been used to: trap the viral protein gp 160 in the ER thus blocking HIV-1 replication [236], to prevent localisation of cell surface receptors like the transferrin receptor (TfR), the knockdown of which leads to a reduction of cellular iron uptake and inhibition of tumour cell proliferation [243] or block transit of the oncogene ErbB-2 through the ER, thereby rendering the receptor inactive and reverting the ErbB-2-transformation phenotype [235]. scFv intrabodies that re-directed the ErbB-2 receptor to the ER have subsequently been shown to have *in vivo* antitumor activity in erbB-2-overexpressing ovarian cancer animal models [244] and ovarian cancer patients [245].

scFv carrying nuclear localisation signals have also been shown to effectively modulate the activity of their target proteins. For example, a nuclear-targeting intrabody against the NF-κB subunit p65 caused the downregulation of NF-κB target genes and inhibition of glioblastoma cell angiogenesis, invasion, and intracranial tumour growth [237]. Additionally, single chain intrabodies expressed without any additional localisation signal have been shown to sequester their target protein. A scFv derived from a monoclonal antibody previously mapped to the DNA-binding

domain of ATF-1 [246], a transcription factor overexpressed in melanoma cells, was shown to reduce melanoma tumour growth and metastasis [247]. The anti-ATF-1 intrabody functioned by retaining its target protein within the cytoplasm, thus inhibiting its transcription activation function [231]. Finally, intrabodies against cytosolic caspase-7, a protein activated upon cell death stimuli to induce apoptosis, successfully retargeted the protein to the nuclei, thus inhibiting apoptosis [248].

Another mechanism through which the activity of a target protein can be disrupted is by triggering its degradation. This can be an unplanned function of an antibody, observed following its intracellular expression. This was true for an intrabody targeting the interleukin 2 receptor IL-2Rα, which was seen to induce rapid degradation of its target protein within the ER [249]. Alternatively the ability to direct a target molecule down a degradation pathway can be explicitly engineered into an intrabody by adding a proteasome-targeting sequence [238].

Re-localisation and degradation of a target protein are effective means of disrupting all of its normal cellular activities. However, several studies have been carried out to develop intrabodies that target specific sub-domains and therefore specific activities or interactions of their target antigens. In such cases a single domain of the target protein is used as the target for antibody selection. A single domain (light chain only) intrabody was used by Paz et al. (2005) to efficiently block the autophosphorylation of the Etk and its tyrosine kinase function, by binding specifically to its kinase domain [230]. Intrabodies selected against an N-terminal region of hCyclinT1 that participates in Tat transactivation, an interaction essential for HIV-1 replication, were able to disrupt the hCyclinT1-Tat interaction without inhibiting basal transcription or inducing apoptosis and thereby inhibit viral replication [242].

Although disruption of normal antigen activity has proven a useful tool, activation of some proteins by intrabodies has also been recorded. An anti-p53 scFv that only localised to the nucleus in p53-positive cells was able to restore transcriptional activity to a His273 mutant [239]. In another study p53 was targeted to a synthetic promoter containing tetracycline-operator sequences by an anti-p53 scFv fused to a tetracycline DNA binding domain [250]. Gene expression from the synthetic promoter was lost in *p53* null cells and enhanced in tumour cells harbouring mutant

p53 [250], illustrating a novel mechanism through which antibody fragments targeting disease-related proteins can be used as small molecule therapeutics.

1.3.2 Peptide phage display

Peptide phage display technology is technically very similar to antibody phage display. The biopanning procedure is much the same, consisting of incubation of the target with the peptide library, washing away of unbound phage, elution of binding phage and amplification in a bacterial host for further selection. It differs in that peptides and not antibody fragments are displayed.

1.3.2.1 Different types of library

As with phage display of antibody fragments, the peptide is normally fused to the minor coat protein g3p of filamentous phage. Peptides are generally cloned into a phage, rather than phagemid, vector which means that the number of displayed peptides correlates with the number of coat proteins. In the case of coat protein g3p that means 3-5 per virion. Cloning a peptide into the phage genome rather than a phagemid relinquishes the need for helper phage, but limits the size of the insert. The g3p minor coat protein has been shown to tolerate peptides of up to 36 residues in length [251], whereas the major coat protein g8p, of which there are ~2500 copies per virion, can display a peptide of only 6 amino acids in length before coat assembly is affected [252]. In designing a phage peptide library a choice must be made between a longer peptide or one displayed at a higher frequency. Peptides displayed on the end of coat proteins gp3 and gp8 are tethered by their C-terminus, with their N-termini exposed. However, by using the minor coat protein g6p, peptides can be displayed with an exposed C-termini, which may alter binding of some epitopes [170]. This format is used less frequently, as g6p fusions are incorporated into the phage capsid less efficiently than g3p fusions [170]. The D coat protein of lytic bacteriophage λ can also been used as a peptide scaffold [172]. Peptides can be fused to the D-protein N or C terminus as both ends are exposed on the surface of the phage head. However, bacterial lysis following lytic phage replication makes the subsequent phage purification step more complicated than for filamentous phage, which are secreted from the bacterial cell membrane [172].

Other considerations include the length of peptide displayed. Short peptides (~7-mer) are useful for identifying binding motifs concentrated in a short stretch of amino acids. Longer peptides (~12-mer) are useful for identifying motifs that are more spread out, i.e. have more intervening amino acids. For example, the binding motif LLXXHHXXAL has only 6 essential residues, but could not be detected in a 7-mer library. Using a longer randomised peptide also increases the chances of identifying a peptide that interacts through multiple weak interactions, rather than a few strong ones. As longer peptides have the ability to fold into short structural elements, like alpha-helices, they can be useful for identifying structured ligands [253]. Constrained peptides, which shaped into a loop by a disulphide bond, can also be used for this purpose [254]. Constraining the conformational freedom and thus decreasing the entropy of unbound peptides in a library can result in the isolation of higher-affinity ligands [255]. However, constraining a peptide could also trap it in a conformation unable to bind a given target protein. In the end it is impossible to predict in advance which library is suitable for a given target.

The most commonly used peptide phage display libraries are made up of random peptides of a defined length. The peptide encoding DNA inserts are derived from "degenerate" oligonucleotides usually comprising of the sequence NNKNNKNNK…etc. where N is an equal mixture of A, G, C, and T, and K is an equal mixture of G and T, so that each of the 32 nucleotide triplets that encode all 20 natural amino acids are represented [256]. However, a library may also be generated using peptides with limited variation, for example that all display some homology to a known ligand of the target protein [257].

The library used in the experiments described in chapter 6 of this thesis involves the display of random 12-mer peptides fused to coat protein g3p of M13 filamentous phage.

1.3.2.2 Peptide selection strategies

Like antibody phage display, peptide phage display can be used to identify novel disease markers for diagnosis or future therapeutic development. In such cases peptide libraries are pre-cleared for phage capable of binding to healthy cells/tissues and then selected against: the surface of cultured diseased cells [139, 258, 259],

biopsy tissues [260], *in vivo* in diseased animals [261] or humans [262]. The last of these is a particularly interesting strategy aimed at developing patient-specific therapies. Selection of tumour-specific phage in patients involves serial infusions of phage libraries, recovery of tumour binding phage through biopsy and reinfusion of tumour-binding phage.

Identification of the disease specific markers through binding assays and/or genome-wide database searches using the peptide sequence (binding motif) can contribute to a greater understanding of a disease phenotype [114, 259, 263]. For example, a peptide associated with human atheroma tissues was found to be homologous to residues within IL-4 that were critical for binding to its receptor. The same study then went on to demonstrate that the IL-4 receptor was upregulated in atherosclerotic tissues [114]. Such disease-specific peptides can also be used for the targeted drug delivery [264].

Alternatively, by first identifying a particular target against which binding peptides are to be selected, phage peptide display can be used to identify peptide motifs that have a high affinity for the target protein. Following selection of a high-affinity peptide, its amino acid composition can be determined by sequencing the phage vector. This supplies a binding motif which can then be used to: develop peptide aptamers that can modulate specific molecular interactions [265], identify novel interacting proteins which harbour the same motif [264-272] or map residues crucial for a known interaction, such as an antibody epitope [266, 267], protease cleavage site [142, 268] or ligand-receptor docking [269]. It should also be noted that peptide motifs can be identified that mimic the interactions of a known sub-domain, without bearing any sequence similarity [270, 271]. For example, the TNF family receptor BCMA binds its ligand through a conserved six residue DXL motif ((F/Y/W)-D-X-L-(V/T)-(R/G)); out of 10 novel peptides identified through phage display able to bind the ligand and disrupt this interaction only one contained the DXL motif [270].

As previously described for antibody fragments, peptides can be selected for binding to specific domains of proteins to target localised functions. For example peptides selected as binding to the SH3 domain (expressed as a GST fusion) of the protein-

tyrosine kinase Src were able to accelerate Src-mediated oocyte maturation and block co-precipitation of previously identified Src binding partners [251].

Peptides have also been selected against non-protein targets such as oligonucleotides [272], lipopolysaccharides [273] and inorganic materials [274, 275].

1.3.2.3 Bioactive peptides

Phage display peptides have been used extensively to develop reagents against a range of human disease types including: cancer [139, 276], HIV [277, 278], other viral infections [279], atherosclerosis (thickening of artery walls) [280], obesity [281], bacterial infection [282, 283], parasitic infection [284], autoimmune disorders [285], thrombosis and inflammation [269, 286] and neurodegenerative diseases [287]. The technology has also been utilised to increase vaccine efficacy using peptides that mimic epitopes on the disease-causing organism; such peptides are identified through binding to an antibody that targets the infectious agent [288, 289].

Biologically active peptides can function through a variety of mechanisms, including: blocking the activity of enzymes (for example proteases [290] and isomerases [291]), disrupting ligand receptor docking [270], preventing nuclear-localisation of transcription factors [292], inhibiting polyglutamine protein aggregation associated with neurodegenerative diseases [287] and mimicking ligands, thereby acting as receptor antagonists [293-296].

The mechanisms listed above all involve the "knock-out" of a protein's function. However, peptides have also been identified that can activate a target protein upon binding. Such peptides can function by mimicking receptor ligands and acting as agonists [43, 257]. Phage display-derived peptides have also been used to activate non-receptor proteins, possibly through a conformational change or by mimicking a co-activator interaction [271].

In summation, both peptide and antibody phage display technologies are able to generate reagents that can map or modulate a protein's function.

2 Aims

As the introduction to this thesis reveals, the post-translational mechanisms through which IRF-1 is regulated are poorly understood. The research conducted in this thesis is primarily aimed at the development of IRF-1-specific molecular tools that can be used to study regulation of the endogenous protein. Two approaches are taken to meet this goal. First, antibody phage display is used to develop single chain antibodies targeting IRF-1 (chapters 4 and 5). Second, peptide phage display is used to identify IRF-1-binding peptides (chapter 6). Another goal of the research detailed in this thesis is the identification of novel IRF-1-binding partners; this is also described as part of chapter 6.

3 Methods

3.1 Chemical reagents

Cycloheximide (Supelco) was dissolved in H_2O to 5 mg/ml and used at a concentration of 30 µg/ml in cell culture medium. MG-132 (Calbiochem) was dissolved in DMSO to 10 mM and used as indicated. DSP Dithiobis[succinimidyl propionate] (Thermo Scientific Pierce) was used at 2 mM. Trypsin T-1426 Type XIII from Bovine Pancreas (Sigma) was prepared as a 10 mg/ml stock solution in 50 mM Tris-HCl pH 7.4, 1 mM $CaCl_2$ and stored at -20°C, this stock solution was then diluted 1/10 with PBS before use. The HRP substrate TMB (3,3´,5,5´-tetramethylbenzidine) was supplied by Thermo Scientific Pierce, and used as indicated. Peptides (Chiron Mimotopes) were synthesised with a SGSG spacer and N-terminal biotin tag. Oligonucleotide primers were provided by Sigma and used as described. HRP-conjugated protein A (BD Biosciences) was used at a 1/1000 dilution for detection of single chain antibodies as described.

3.2 Mammalian cell culture and transfection

Cell line	Source	Growth conditions
A375	**Human, skin, malignant melanoma**	**10% CO_2, 37°C, DMEM* media**
HeLa	**Human, cervix, epithelial adenocarcinoma**	**5% CO_2, 37°C, DMEM* media**

* DMEM: Dulbecco's minimal essential media (GIBCO-BRL)

A375 and HeLa cells were cultured in DMEM (Invitrogen), supplemented with 10% (v/v) fetal bovine serum and 1% penicillin/streptomycin at 37 °C and 10% or 5% CO_2, respectively. For protein half life determination and accumulation assays, cells were transfected at 80% confluence using Attractene (QIAGEN) as described in the manufacturer's handbook.

3.3 DNA constructs

Following plasmids were a kind gift from Dr Mirjam Eckert and were described in Dr Mirjam Eckert PhD thesis and publication [64]: pcDNA3 IRF-1 wild type, pcDNA3 IRF-1 P325A, pcDNA3 IRF-1 ΔC25, pcDNA3 IRF-1 ΔC70, TLR3-Luc, mTLR3-Luc, IFN-β-Luc, mIFN-β-Luc, CDK2-Luc. The pTrcHis B, Gateway pDONR 221, pDEST 14, pDEST 15 and pcDNA-DEST53 vectors were supplied by Invitrogen. The TRAIL-luc, mTRAIL-luc, IL-7-luc and mIL-7 luc reporter gene constructs were described previously [90, 297].

3.4 Cloning

IRF-1 domains were cloned into the pTrcHis B vector (Invitrogen) and scFv antibodies were cloned into the Gateway system (Invitrogen). In this system genes are first cloned into the Gateway donor vector pDONR 221, from which they can be transferred into the appropriate destination vector (pDEST 14, pDEST15 or pcDNA-DEST53) through homologous recombination.

3.4.1 PCR primers

3.4.1.1 Cloning of IRF-1 domains into the pTrcHis B vector

3.4.1.1.1 IRF-1 domain amino acids 1-140

Forward Primer 5'-TTCTCGAGCCCATCACTCGGATGCGCATG-3'

Reverse Primer 5'-TTGAATTCCTATGGAATCCCCACATGACTTCC-3'

3.4.1.1.2 IRF-1 domain amino acids 60-124

Forward Primer 5'-TTCTCGAGCACACAGGCCGATACAAAGCAGGG-3'

Reverse Primer 5'-TTGAATTACTACTTTCTTTCTTTTCTCTGGTTCTT-3'

3.4.1.1.3 IRF-1 domain amino acids 117-184

Forward Primer 5'-TTCTCGAGAACCAGAGAAAAGAAAGAAAG -3'

Reverse Primer 5'-TTGAATTCCTACGACAGTGCTGGAGTCAGGGC-3'

3.4.1.1.4 IRF-1 domain amino acids 117-256

Forward primer 5'-TTCTCGAGAACCAGAGAAAAGAAAGAAAG -3'

Reverse Primer 5'-TTGAATTCCTAGTACCCCTTCCCATCCACGTT-3'

3.4.1.1.5 IRF-1 domain amino acids 256-325

Forward primer 5'-TTCTCGAGAGGGGTACCTACTCAATGAAC-3'

Reverse Primer 5'-TTGAATTCCTACGGTGCACAGGGAATGGC-3'

3.4.1.2 scFv cloning into the Gateway system

3.4.1.3 pDEST14 vector (untagged *E.coli* expression)

Forward 5'-
GGGGACAAGTTTGTACAAAAAAGCAGGCTTCGAAGGAGATAGAACCATG
AAATACCTATTGCCTACGGCA-3'

Reverse 5'-
GGGGACCACTTTGTACAAGAAAGCTGGGTCCTATGCGGCCCCATTCAGAT
CCTC-3'

3.4.1.4 pDEST15 vector (N-terminally GST tagged *E.coli* expression)

(In N-terminally tagged scFv gateway constructs the Shine-Dalgarno and Kozak sequences lie within the vector and is therefore not included in these primers)

Forward 5'-GGGGACAAGTTTGTACAAA
AAAGCAGGCTTCATGAAATACCTATTGCCTACGGCA-3'

Reverse 5'-
GGGGACCACTTTGTACAAGAAAGCTGGGTCCTATGCGGCCCCATTCAGAT
CCTC-3'

3.4.1.5 pcDNA-DEST53 vector (N-terminally GFP tagged mammalian cell expression)

Forward 5'-GGGGACAAGTTTGTACAAA AAAGCAGGCTTCATGAAATACCTATTGCCTACGGCA-3'

Reverse 5'-GGGGACCACTTTGTACAAGAAAGCTGGGTCCTATGCGGCCCCATTCAGATCCTC-3'

3.4.1.6 PCR mix

The following PCR mix was made up in thin-walled sterile tubes (BD Biosciences) and heated in a thermocycler.

Distilled water 34.1 µl
$MgCl_2$ (0.1 M) 1.0 µl
10 x cloned pfu reaction buffer 5.0 µl
DNA template (100 ng/µl) 1 µl
Forward primer (10 µM) 0.2 µl
Reverse primer (10 µM) 0.2 µl
Pfu turbo DNA polymerase (2.5 U/µl) 1 µl
Total reaction volume 50 µl

3.4.1.7 PCR Programme

15 min 95°C
35 cycles { 1 min 94°C; 1 min 72°C; 1 min 50-70°C }
10 min 72°C

3.4.1.8 Purification of PCR product

QIAGEN PCR product purification kit used as described in the manufacturer's handbook

3.4.1.9 Detection of DNA

Tris-acetate (TAE) buffer	**5 x DNA loading buffer**
40mM Tris	15 % (w/v) Ficol
20mM Boric acid	0.25 % (w/v) Bromophenol blue
1mM EDTA (pH 8.0)	0.25 % (w/v) Xylene cyonol
Stored at room temperature	

DNA samples were mixed with 5 x DNA gel loading buffer, and resolved on 1% (w/v) agarose gel. Agarose gels were prepared by adding 1g agarose into 100 ml 1 x TAE buffer and heating in a microwave until the agarose powder dissolved. Ethidium bromide was added to the final concentration of 0.5 µg/ml. Once the gel had set samples were loaded and run for 1 hour at 100 V in 400 ml of 1 x TAE buffer. DNA was visualised using the Genesnap program Syngene under a UV transilluminator.

3.4.1.10 Cloning of IRF-1 domains into pTrcHis B

Digestion of pTrcHisB vector and IRF-1 domain PCR products was performed using the protocol described below. Buffers and enzymes were supplied by New England Biolabs, Inc.

Digestion reaction

30 µl of purified PCR product (concentration not determined)
or 3 µl of vector (100 ng/µl)
1 µl of EcoRI (20 units/ µl)
1 µl of XhoI (20 units/ µl)
4µl 10 X EcoRI buffer (100 mM Tris-HCl, 50 mM NaCl, 10 mM $MgCl_2$,
0.025 % Triton X-100, pH 7.5 at 25°C)
100 µg/ml Bovine Serum Albumin (BSA)
Made up to 40 µl with nuclease free distilled H_2O

Each digestion mixture (containing PCR product or vector) was incubated separately at 37 °C for 2 hours and inactivated by heating to 65°C for 20 minutes. Digestion products were run on a 1% (w/v) agarose gel (see section 3.4.1.9) and purified using the QIAGEN gel purification kit.

Ligation of the cleaved pTrcHis vector and IRF-1 domain PCR products was performed according to the protocol below. Buffers and enzymes supplied by New England Biolabs.

Ligation reaction

3 µl gel purified insert (digested PCR product)

1 µl gel purified digested vector

0.33 µl T4 DNA ligase (2,000 cohesive end units/µl)

1 µl 10 x T4 DNA ligase buffer (10 mM $MgCl_2$, 1 mM ATP, 10 mM DTT, pH 7.5 at 25°C)

Made up to 10 µl with nuclease free distilled H_2O

Each ligation mixture was incubated separately at 4 °C overnight and inactivated by heating at 65°C for 10 minutes. 5 µl of each ligation reaction was then transformed (see section 3.4.2) into *E.coli*.

3.4.1.11 Gateway cloning of scFv

Anti-IRF-1 scFv were cloned into pDEST15, pDEST14 and pDEST53 for expression in bacterial and mammalian systems using Gateway technology (Invitrogen). The Gateway system involves homologous recombination of a PCR product into a holding pDONR vector (pDONR 221) and then into a pDEST (14, 15 or 53) vector for expression. Reagents were supplied by Invitrogen.

Gateway cloning BP reaction (PCR product into pDONR)

BP™ Clonase reaction buffer 4 µl

attB PCR product 5 µl (concentration not determined)

Donor vector (pDONR 221™) 300 ng

BP Clonase enzyme mix 4 µl

Total reaction volume made up to 20 µl with distilled water.

The reaction mix was incubated for 1 hour at 25 °C and terminated by the addition of 1 µl of 2 µg/µl proteinase K solution and incubation for 10 minutes at 37 °C. 5 µl of the reaction mix was then transformed into *E.coli* via heatshock (see section 3.4.2).

Bacteria containing positive clones were grown selectively on LB/Kanamycin (50 μg/ml) plates.

Gateway cloning LR reaction (pDONR into pDEST)

LR™ Clonase reaction buffer 5 μl
Entry clone 100 ng
Destination vector (pDEST™) 300 ng
LR Clonase enzyme mix 4 μl
Total reaction volume made up to 20 μl with distilled water.

The reaction mix was incubated for 1 hour at 25 °C and terminated by the addition of 1 μl of 2 μg/μl proteinase K solution and incubation for 10 minutes at 37 °C. 5 μl of the reaction mix was then transformed into *E.coli* cells via heatshock (see section 3.4.2). Bacteria containing positive clones were grown selectively on LB/Ampicillin (100 μg/ml) plates.

3.4.2 Heatshock transformation

Luria Bertani (LB) media

1% (w/v) Tryptone
0.5% (w/v) Yeast Extract
1% (w/v) NaCl
Sterilised by autoclaving at 121°C for 20 minutes.

LB agar

1 % (w/v) Tryptone
0.5 % (w/v) Yeast extract
1 % (w/v) Agar, granulated
Sterilised by autoclaving at 121°C for 20 minutes.

3.4.2.1 Preparation of competent cells

Buffer A

1.2% (w/v) RbCl
0.99% (w/v) $MgCl_2.4H_2O$
0.59% (w/v) potassium acetate
1.5% (w/v) $CaCl_2.2H_2O$
15% (w/v) glycerol
pH adjusted to 5.8 with acetic acid

Buffer B

10 mM MOPS pH6.8
0.12% (w/v) RbCl
1.1% (w/v) $CaCl_2.2H_2O$
15% (w/v) glycerol
pH adjusted to 5.8 with NaOH

A bacterial culture was grown in 50 ml LB media until the O.D. 600 nm reached 0.4. The cells were then centrifuged at 3,200 x g for 15 minutes at 4°C. The following steps were all performed at 4°C. The bacterial pellet was re-suspended in ice-cold buffer A (16 ml buffer A per 50 ml of original bacterial culture). This mix was incubated on ice for 10 minutes. The cells were pelleted again via centrifugation at 3,200 x g (15 minutes at 4°C), resuspended in buffer B (2 ml buffer B per 50 ml of original bacterial culture) and incubated once more on ice for 10 minutes. The cells were then aliquoted into pre-chilled tubes, snap frozen and stored at -80°C.

3.4.2.2 Heatshock protocol

DH5α or BL21 DE3 (50 µl) competent bacteria cells were mixed with 0.5 µg of plasmid or 5 µl of ligation, BP or LR reaction product. Cells were then incubated on ice for 45 minutes and heatshocked through incubation at 42°C for 2 minutes. This was followed by 5 minutes of incubation on ice. LB media (1 ml) was added to the transformed cells and the culture was incubated at 37°C with shaking (225 rpm) for 30 minutes. Transformed bacteria were then spread on LB/agar plates (50 µg/ml ampicillin). These plates were incubated at 37°C overnight to allow colony formation to occur. The colonies were then picked and grown separately overnight in 5 ml LB (50 µg/ml ampicillin) to enable DNA plasmid amplification (see section 3.4.3).

3.4.3 DNA plasmid amplification

QIAGEN Maxiprep or Miniprep kits were used as described in the manufacturer's handbook.

3.4.4 Sequencing

All sequencing was out-sourced to: DNA Sequencing & Services, Medical Research Council Protein Phosphorylation Unit, Dundee.

3.4.4.1 Sequencing primers

IRF-1 domains pTrcHis forward 5' of multiple cloning site:

5´- GAGGTATATATTAATGTATCG–3´

IRF-1 domains pTrcHis reverse 3' of multiple cloning site:

5´- GATTTAATCTGTATCAGG–3´

scFv phagemid (pIT2) LMB3:

5´- CAG GAA ACA GCT ATG AC–3´

scFv phagemid (pIT2) pHEN seq:

5´- CTA TGC GGC CCC ATT CA–3´

scFv pDEST53/15/14 T7 promoter forward:

5´-TAATACGACTCACTATAGGG–3´

Peptide phage display -96 gIII sequencing primer:

5´- CCC TCA TAG TTA GCG TAA CG –3´

Peptide phage display -28 gIII sequencing primer

5´- GTA TGG GAT TTT GCT AAA CAA C –3´

3.5 Protein purification from *E.coli*

Transformed BL21 DE3 *E.coli* cells were grown in 1L LB until the culture had an optical density at 600 nm (O.D. 600) of 0.4. Protein expression was then induced by the addition of 0.5 mM IPTG until the O.D. reached 1 (approximately 3 hours later). Cells were centrifuged (3,200 x g, 10 mins, 4°C), the supernatant discarded and the pellet snap frozen in liquid nitrogen. The pelleted cells were thawed in 2 ml bacterial lysis buffer and sonicated for 2 x 10 seconds (samples kept on ice between bursts of sonication).

Bacterial lysis buffer

50 mM HEPES pH 7.6

150 mM NaCl

1 mM EDTA*

1 x protease inhibitor mix[§] (see below)

1 mg/ml lysozyme

Protease inhibitor mix[§]

- 1 µg/ml leupeptin
- 0.4 µg/ml aprotinin,
- 0.2 µg/ml pepstatin,
- 10 µg/ml soya bean trypsin inhibitor
- 40 µg/ml Pefabloc
- 0.12mM Benzamidine

*** EDTA excluded if proteins were to be purified on a Ni^{2+} column (see section 3.5.1)**

Triton X-100 was added to make up 1% of the lysate. The lysate was then incubated on ice for 20 min and centrifuged at 16,800 x g for 10 minutes at 4˚C. The resultant supernatant made up the detergent soluble fraction of lysate and the remaining pellet formed the insoluble fraction.

3.5.1 His tagged protein purification

EDTA was excluded from the bacterial lysis buffer described above.

Approximately 2 ml of the detergent soluble fraction of lysate was mixed with an equal volume of IMAC 5. The Lysate/IMAC5 mix was then filtered with a 0.45 µm filter (Milipore™).

Loading Buffer IMAC5	**Wash with detergent IMAC25**
20 mM Tris/HCl pH 7.5-8	20 mM Tris/HCl pH 7.5-8
0.5 mM NaCl	0.5 mM NaCl
5 mM imidazole	25 mM imidazole
	0.5% Triton X-100
	0.5% Tween 20

Wash without detergent IMAC25	**Elution Buffer IMAC150**
20 mM Tris/HCl pH 7.5-8	20 mM Tris/HCl, pH 7.5-8
0.5 mM NaCl	0.5 M NaCl
25 mM imidazole	150 mM imidazole

Ni^{2+}-NTA resin (QIAGEN) (250 µl) was washed thoroughly with IMAC5 and then kept in an equal amount of IMAC 5. Ni^{2+}-NTA/IMAC5 and lysate/IMAC5 were combined and rotated for 1 hour at 4°C. The mix was poured into a column jacket (MoBiTec) and washed with 5 column volumes (C.V.) of IMAC5, 20 C.V. of IMAC25 with detergent and 5 C.V. of IMAC25 without detergent. His-tagged protein was then eluted with 10 C.V. of IMAC150 and collected in 1 ml fractions. The fractions were analysed by SDS-PAGE to determine which contained the purified protein.

3.5.2 GST tagged protein purification

TNEN buffer	**Elution buffer**
20 mM Tris/HCl pH 8.0	100 mM Tris/HCl pH 8
100 mM NaCl	20 mM glutathione reduced
1 mM EDTA	NaCl 120 mM
0.5% NP40	

Glutathione Sepharose beads (150 µl, Amersham) were added to an equal amount of TNEN buffer, plus 4% (w/v) BSA and approximately 2 ml of detergent soluble lysate. The mix was incubated at 4 °C on a rotating wheel for 30 minutes and then washed 3 x with TNEN/100 mM NaCl. After the final wash the beads were resuspended in 5 ml elution buffer and eluted overnight at 4 °C on a rotating wheel.

3.6 Detection of protein: SDS-PAGE

Resolving gel – 12%	**Stacking gel**
40% (v/v) 30% Acrylamide mix	16.7 (v/v) 30% Acrylamide mix
0.375 M tris pH 8.8	0.19 M tris pH 8.8
0.1 % (v/v) SDS	1% (w/v) SDS
0.04% (v/v) TEMED (Sigma)	0.1% (v/v) TEMED (Sigma)
0.1% (w/v) Ammonium peroxidisulphate	10 % (w/v) Ammonium peroxidisulphate

Running buffer	**SDS-PAGE Sample buffer**
129 mM glycine	5% (w/v) SDS
25 mM Tris pH 8.8	25% (v/v) Glycerol
0.1% (w/v) SDS	0.24 M Tris pH6.8
	400 mM DTT
	0.1% (w/v) Bromophenol blue

The polyacrylamide electrophoresis gels were prepared using the MiniProtean3™ (Bio-Rad) system as described by manufacturers. Each protein sample was mixed 1:1 with SDS-PAGE sample buffer and heated for 2 minutes at 90°C. The samples were then loaded onto a gel and run at 100 V until the bromophenol blue dye front reached

the bottom of the gel. The separated proteins were then analysed by immunoblot as described in section 3.8, or using Colloidal blue staining kit (Invitogen) according to the manufacturer's guidelines.

3.7 Protein quantification

Protein was quantified by the Bradford assay (reagent provided by Biorad, manufacturer's guidelines followed).

3.8 Immunoblot

Mammalian lysis buffer

50 mM HEPES

150 mM NaCl

0.1 mM EDTA

2 mM DTT

1 x protease inhibitor mix[§] (see section 3.5)

10 mM NaF

0.1mM EDTA

Mammalian cells were lysed in the lysis buffer detailed above or 5 x reporter lysis buffer (Promega) (as part of IRF-1 transcriptional activity assays) and incubated on ice for 20 or 10 minutes respectively. Following centrifugation at 16,800 x g for 2 minutes the supernatant (detergent soluble fraction) or pellet (detergent insoluble fraction) were analysed by SDS-PAGE and transferred to a nitrocellulose membrane (PROTRAN™) electrophoretically at 100 V for 1 hour. Purified GST-IRF-1 (0.3 µg/lane) was analysed by SDS-PAGE and transferred to nitrocellulose in the same way. The membranes were blocked in 5% MPBS-0.1% Tween (5% Marvel milk powder in PBS containing 01% Tween) for 1 hour at room temperature and incubated with the appropriate primary antibody (see section 3.9) diluted in 5% MPBS-0.1% Tween overnight at 4˚C, followed by the secondary antibody for 1 hour at room temperature. The immunoblots were washed extensively between each step with PBS 0.1% Tween and antibody binding was detected with enhanced chemiluminescence (see section 3.10).

3.9 Antibodies

Primary antibodies			
Target protein	**Supplier**	**Product/ catalogue number**	**Dilution**
Caspase 3	Santa Cruz Biotechnology	sc-7272	1/1000
CDK2	Santa Cruz Biotechnology	sc-53220	1/1000
GFP	Clonetech	632375	1/2000
GST	Sigma	G1160	1/2000
GAPDH	Abcam	ab8245	1/1000
His	Novagen	70796	1/2000
HP1α	Millipore	MAB3446	1/1000
IRF-1	BD Biosciences	612046	1/1000
IRF-1	Santa Cruz Biotechnology (C20)	sc-497	1/1000
IRF-2	Abcam	ab55331	1/1000
ISG20	Abnova	H00003669-M01	1/1000
g3p (pIII) M13 coat protein	New England Biolab (NEB) (HRP-conjugated)	27-9421-01	1/1000
PKR	Santa Cruz Biotechnology	sc-707	1/1000
ZNF350	Abcam	ab67881	1/1000

Secondary antibodies were purchased from Dako Cytomation.

3.10 ECL for enhanced chemiluminescence

ECL solution 1	**ECL solution 2**
2.50 mM luminol	0.02% H_2O_2
4 mM p-coumaric acid	100 mM Tris pH 8.5
100 mM Tris pH 8.5	

ECL solutions 1 and 2 were combined in a 1:1 ratio and used immediately to cover an immunoblot/dot blot (1-2 ml) or fill an ELISA well (100 µl) and thus induce enhanced chemiluminescence.

3.11 ELISA

For peptide binding assays 96-well microtitre plates were incubated with 20 µg/ml streptavidin for overnight at 37°C. The streptavidin solution was then discarded and the plates washed with PBS containing 01% Tween. Biotin-labelled peptides were diluted in PBS (quantities described in figure legends) and incubated with the pre-coated streptavidin plates for 1 hour at room temperature. Non-reactive sites were blocked using PBS containing 3% BSA and the peptides incubated with scFv, GST or GST-IRF-1 (1 µg/ml) in PBS-0.1% BSA for 1 hour at room temperature. The plates were washed extensively with PBS-0.1% Tween and scFv binding was detected using the appropriate primary antibodies (as indicated in the figure legends) and enhanced chemiluminescence.

The protein binding assays were performed by coating 96-well microtitre plates with the protein of interest (quantities detailed in the figure legends) in 0.1 M $NaHCO_3$. Non-reactive sites were blocked using PBS containing 3% BSA and the wells were incubated with empirically determined amounts (see section 3.7) of IRF-1 or scFv protein in PBS-0.1% BSA for 1 hour at room temperature. Binding was detected using the appropriate primary antibodies (as indicated in the figure legends) and enhanced chemiluminescence (see section 3.9)

3.12 Antibody phage display: Selection and monoclonal screening

2 x TY media

1.6% (w/v) Tryptone

10% (w/v) Yeast Extract

5% (w/v) NaCl

TYE plates

15% (w/v) Agar

8% (w/v) NaCl

10% (w/v) Tryptone

5% (w/v) Yeast Extract

3.12.1 Anti-C-terminus scFv

Single chain antibodies (scFv) against the C-terminal 20 amino acids of IRF-1 (LDSLLTPVRLPSIQAIPCAP) were selected from the Tomlinson I and J human scFv library (Geneservice). The two library stocks (I and J) provided were used separately during selection, i.e. against the same peptide in two separate immunotubes. The selection strategy was identical for both stocks. Stocks of the scFv library and helper phage were maintained according to guidelines provided by Geneservice.

3.12.1.1 Selection

Immunotubes (Nunc), with a volume of 4 ml, were pre-coated with 20 µg/ml steptavidin (4 ml) for 2 hours at room temperature and then washed 3 x with PBS. An excess of biotinylated peptide (50 µg/ml) diluted in PBS (4 ml) was then added to each steptavidin-coated immunotube and incubated at 4°C overnight. The immunotubes were then washed 3 x with PBS and blocked with 2% MPBS (2% Marvel milk powder in PBS) for 2 hours at room temperature. The immunotubes were then again washed 3 x with PBS before being filled with 10^{13} cfu (colony forming units) of phage in 2% MPBS. The immobilised peptides were incubated with the phage for 1 hour on a rotating wheel and 1 hour standing; all at room temperature. The supernatant was then discarded and the tubes washed 10 (round 1) or 20 (rounds 2 and 3) x with PBS 0.1% Tween. Bound phage were eluted with 50 µl of a 10 mg/ml trypsin stock solution (made up in 50 mM Tris-HCl pH 7.4, 1 mM $CaCl_2$) in 450 µl of PBS.

3.12.1.2 Amplification of selected phage

The eluted phage (250 µl) was added to a 1.75 ml culture of TG1 bacteria (O.D. 600 of 0.4) and incubated at 30 °C in a water bath. The resultant phage-infected bacterial culture was pelleted by centrifugation at 11,600 g for 5 minutes and resuspended in 50 µl of 2 x TY, before being plated on TYE plates (100 µg/ml ampicillin and 1% glucose) and grown overnight at 37 °C. The overnight bacterial growth was then loosened from the plate with a glass spreader into 2 ml of 2 x TY containing 15% glycerol. 50 µl of the cell suspension was added to 50 ml of 2 x TY containing 100 µg/ml ampicillin and 1 % glucose and grown at 37 °C, shaking (250 rpm), until the O.D. 600 was 0.4. At this point 5 x 10^{10} cfu of helper phage were incubated with 10 ml of the bacterial culture in a water bath at 37 °C for 30 minutes. The culture was then centrifuged at 3,000 g for 10 minutes, resuspended in 50 ml 2 x TY (100 µg/ml ampicillin, 50 µg/ml kanamycin and 0.1% glucose) and incubated overnight (30 °C and shaking at 250 rpm). The helper phage allowed mature phage particles to form inside the bacteria, which were then secreted into the media. The overnight culture was centrifuged at 3,300 g for 15 minutes before 10 ml of PEG/NaCl (20 % Polyethylene glycol 6000, 2.5 M NaCl) was added to 40 ml of the supernatant. The supernatant/PEG/NaCl mix was kept on ice for 1 hour causing the phage particles secreted by the bacteria to precipitate. The precipitated phage was then collected by centrifugation at 3,300 g for 30 minutes. Any remaining supernatant was removed by aspiration. The phage pellet was resuspended in 2 ml of PBS and centrifuged again, this time at 11,600 g for 10 minutes, to remove any remaining bacterial debris. 1 ml of the supernatant, made up of phage suspended in PBS, was then used in the next selection round. 3 selection rounds were carried out in total.

3.12.1.3 Phage titering

This step allowed the number of phage particles to be determined following each selection round and separated individual phage clones prior to sequencing. LB media (10 ml) was inoculated with the TG1 bacteria stock provided by Geneservice and grown at 37 °C with 250 rpm shaking until the O.D. 600 reached 0.4. A phage solution (unamplified phage eluates) was prepared for titration by being serially diluted (10^{1}-10^{3}) into 100 µl PBS. The TG1 (900 µl) at an OD 600 of 0.4 was added to each phage dilution and incubated at 37°C for 30 minutes. Each dilution (10 µl)

was then spotted onto a TYE plate containing 100 μg/ml ampicillin and 1 % glucose and grown overnight at 37°C. Following overnight incubation at 37 °C phage-infected bacteria form white colonies. The number of colonies on a plate was then multiplied by the dilution factor to give the number of colony forming units (cfu) in 10 μl of the original phage solutions.

3.12.1.4 Production of monoclonal scFv:

Eluted 3rd round phage (10 μl) were used to infect 200 μl exponentially growing HB2151 bacteria (O.D. 600 of 0.4) for 30 min at 37°C in a water bath. The phage-infected bacteria (50 μl) was spread onto TYE plates (100 μg/ml ampicillin and 1 % glucose) and grown overnight at 37°C. The following day 100 μl of 2 x TY (100 μg/ml ampicillin and 1 % glucose) was added to each well of a 96-well plate, then one colony of the overnight bacterial growth was transferred to each of these wells and again grown overnight (37 °C, shaking 250 rpm). 96 colonies were picked in total, comprising of 48 colonies from selection with Tomlinson library stock I and 48 from selection with stock J. The overnight cultures (2 μl) were then transferred to a second 96-well plate, each well of which already held 200 μl 2 x TY (100 μg/ml ampicillin and 0.1 % glucose). These cultures were allowed to grow for 3 hours (37 °C, shaking 250 rpm) before 25 μl of 2 x TY (100 μg/ml ampicillin and 9 mM IPTG (isopropyl β-D-thiogalactoside) was added (final concentration 1 mM IPTG). The IPTG induced expression of soluble scFv while the culture continued to be grown at 30°C overnight with shaking (250 rpm). The 96-well plate was then centrifuged at 3,200 x g for 15 minutes to pellet the bacteria and leaving the soluble scFv in solution.

3.12.1.5 Dot Blot for screening soluble monoclonal scFv

A nitrocellulose membrane, marked with a grid was incubated with 0.3 μg/μl GST-IRF-1 and blocked for 30 min in 5% MPBS-1% Tween. Each monoclonal scFv (2 μl of the soluble scFv generated in section 3.11.1.4) was dotted onto the membrane and incubated for 1 hour at room temperature in a humidified container. The membrane was then incubated with 1/1000 protein A-HRP in 5% MPBS-1% Tween for 1 hour at room temperature. Between each step the membrane was washed extensively with

PBS-0.1% Tween and scFv binding was detected using enhanced chemiluminescence (see section 3.9).

3.12.1.6 Preparation for sequencing

Pelleted bacteria from wells that produced IRF-1-specific scFv (that gave a positive signal in the dot blot) were re-suspended in 50 µl of LB and added to 50 ml of 2 x TY containing 100 µg/ml ampicillin and 1 % glucose and grown at 37 °C, shaking (250 rpm), until the O.D. 600 was 0.4. Amplification and phage precipitation was then carried out as previously described (section 3.11.1.2). Phage DNA was extracted as described in section 3.13.

3.12.2 Anti-IRF-1 N-terminus scFv

scFv against the IRF-1 amino acids 60-124 were selected from the ETH-2-gold scFv library provided by Prof. Dario Neri [189]. A His-tagged domain made up of IRF-1 amino acids 60-124 (60 µg/ml) diluted in PBS was immobilised on an Immunotube (Nunc). 2 rounds of selection were carried out as described in section 3.11.1.1. Monoclonal scFv were expressed from HB2151 *E. coli* infected with 2nd round scFv-displaying phage. As with the anti-IRF-1 C-terminus, scFv expression was induced in 225 µl cultures in a 96-well plate inoculated with individual bacterial colonies, with 1 mM IPTG and shaking at 30°C overnight (see section 3.11.1.4). The 96-well plate was then centrifuged 3,200 x g for 15 minutes to pellet the bacteria and leaving the soluble scFv in solution. Phage stocks were titred as previously described (see section 3.11.1.3).

3.12.2.1 Colorimetric ELISA for screening of soluble monoclonal scFv

Purified His-tagged IRF-1 domain amino acids 60-124 (60 µg/ml) was incubated in a 96-well microtitre plate overnight at 4°C. The wells were then washed 3 x with PBS-1% Tween and blocked with 5% MPBS for 1 hour at room temperature. 90 µl of PBS was added to each well, followed by 10 µl of soluble scFv-containing supernatant. The scFv were incubated with the immobilised IRF-1 domain for 1 hour at room temperature, before each well was washed 3 x with PBS-1% Tween. Bound scFv were then detected with 100 µl of 1/1000 HRP-protein A in 5% MPBS, which was incubated in each well for 1 hour at room temperature. The microtitre plate was again

washed (3 x with PBS 1% Tween) before 100 µl of the HRP substrate TMB (3,3´,5,5´-tetramethylbenzidine supplied by Thermo scientific) was added, followed by 100 µl 0.16 M sulphuric acid. The TMB gave a blue colour change, which turned yellow following the addition of sulphuric acid. The absorbance was then measured at 450 nm on a spectrophotometer.

3.12.2.2 Preparation for sequencing

As for anti-IRF-1 C-terminus scFv.

3.13 Peptide phage display

IPTG/Xgal stock

5% (w/v) IPTG

4% (w/v) Xgal (5-Bromo-4-chloro-3-indolyl-β-D-galactoside)

100% (v/v) dimethyl formamide

(stored at -20 °C)

LB/IPTG/Xgal plates

99.9% (v/v) LB agar

(prepared as described under section 3.4.2 of methods)

0.1% (v/v) IPTG/Xgal stock

Top Agar

1% (w/v) Tryptone

0.5% (w/v) yeast extract

0.5% NaCl

0.7% agar

Sterilised by autoclaving at 121°C for 20 minutes.

Phage displayed peptides were selected for binding to His-tagged IRF-1 domains spanning amino acids 1-140, 1-124, 60-124, 117-184, 117-256, 256-325.

3.13.1.1 Selection

A stock solution of 50 µg/ml was prepared of each domain target in 0.1 M NaHCO3, pH 8.6. Each diluted domain (150 µl) was then incubated in separate well of a 96-

well microtitre plate overnight at 4°C in a humidified container. This coating solution was then poured away and the wells were blocked (blocking buffer: 0.1 M $NaHCO_3$ (pH 8.6) and 5 mg/ml BSA) for 1 hour at 4°C. The blocking solution was discarded and the wells washed 6 x with PBS 1% Tween. The phage library (2 x 10^{11} pfu) was added to each well in 100 µl of PBS 1% Tween, and then incubated for 1 hour with gentle rocking at room temperature. The phage solution was discarded, and the plate washed 10 x with PBS 1% Tween. Bound phage were then eluted with 100 µl of 0.2 M Glycine-HCl (pH 2.2) containing 1 mg/ml BSA over 10 minutes (with rocking), the eluates were then transferred to sterile microcentrifuge tubes and neutralised with 15 µl of 1 M Tris-HCl, pH 9.1.

3.13.1.2 Amplification of selected phage

The phage selected by each domain were amplified simultaneously but separately according to the following protocol. 20 µl of the ER2738 bacteria stock provided by NEB with the phage library was used to inoculate 20 ml of LB (15 µg/ml tetracycline) and grown at 37 °C with shaking (250 rpm) until an O.D. 600 of 0.01 was reached. At this point, the phage eluate was added to the bacterial culture and amplified by continued incubation at 37 °C with shaking (250 rpm). The culture was centrifuged for 10 minutes at 12,000 g at 4 °C. The supernatant was transferred to a fresh centrifuge tube and centrifuged again to remove bacteria. The resultant supernatant (16 ml) was then combined with 2.67 ml of 20% PEG/2.5 M NaCl, after which the phage was allowed to precipitate overnight at 4°C. The precipitated phage were collected through centrifugation at 12,000 g for 15 minutes at 4°C and then resuspended in 1 ml of TBS (50 mM Tris-HCl pH 7.5 and 150 mM NaCl). The suspension was transferred to a microcentrifuge tube and centrifuged at 16,800 g for 5 minutes at 4°C to pellet and remove residual bacterial cells. The phage was then again precipitated (to reduce bacterial contamination) by adding 167 µl of 20% PEG/2.5 M NaCl and incubating for one ice for 1 hour, before centrifuging at 16,800 g for 10 minutes at 4°C. The supernatant was discarded and the phage pellet resuspended in 200 µl of TBS. 100 µl of amplified phage (~10^{12} pfu) was then used in the next round. In total, three selection rounds were performed for each IRF-1 domain.

3.13.1.3 Phage titering

This step allowed the number of phage particles to be determined following each selection round and separated individual phage clones prior to sequencing. LB media (10 ml) was inoculated with the ER2738 bacteria stock provided by NEB and grown at 37 °C with 250 rpm shaking until the O.D. 600 reached 0.5. A phage solution (unamplified phage eluates) was prepared for titration by being serially diluted (10^1-10^3) in LB, 10 µl of each phage dilution was added to 200 µl of the bacterial culture, briefly vortexed and incubated at room temperature for 5 minutes. The infected cells were then added to tubes containing 3 ml of Top Agar, which had been pre-warmed to 45 °C. Following another brief vortex, this Top Agar was then poured onto an LB/IPTG/Xgal plate and equally distributed. Following overnight incubation at 37 °C phage-infected bacteria formed blue plaques. The number of plaques on a plate was then multiplied by the dilution factor to give the number of plaque forming units (pfu) in 10 µl of the original phage solutions.

3.13.1.4 Preparation for sequencing

10 plaques per IRF-1 domain were picked for sequencing from the titre plates generated with unamplified eluted phage from the 3rd selection round. Each plaque was transferred to 20 ml of LB (15 µg/ml tetracycline) and precipitation of phage was carried out as previously described (see section 3.13.1.2).

3.14 Phage DNA extraction

Precipitated phage was pelleted (16,800 x g for 10 min at 4°C) and re-suspended in 100 µl of Iodide Buffer (10 mM Tris-HCl pH 8.0, 1 mM EDTA, 4 M NaI). The suspension was incubated with ethanol (250 µl) for 10–20 minutes at room temperature. Precipitated phage DNA was then collected by centrifugation (16,800 x g for 10 minutes at 4°C) washed with 0.5 ml of 70% (v/v) ethanol, re-centrifuged and dried briefly under a vacuum. For subsequent sequencing and PCR reactions the DNA was suspended in TE buffer and quantified using a spectrophotometer (Nanodrop ND-1000). Phage DNA sequencing was out-sourced and the sequencing primers used are described in section 3.4.4.1.

3.15 EMSA (electrophoretic mobility shift assay)

C1 probe sense
5'-
AGCGGATCCTCTAGAGTCTCACTTTCACTTTCACTTTCACTTCGACCGATG
CCC-3'

C1 probe anti-sense

5'-

GGGCATCGGTCGAAGTGAAAGTGAAAGTGAAAGTGAGACTCTAGAGGAT

CCGCT-3'

3.15.1 Labelling the probe

The following reaction mixture was prepared and incubated for 2 hours at 37°C.

0.6 µg C1 probe sense DNA

0.6 µg C1 probe antisense DNA

10% (v/v) T4 DNA kinase buffer

4% (v/v) T4 DNA kinase

0.004 mCi γ-^{32} ATP

After this 52% (v/v) of TE buffer (QIAGEN) was added and the mixture heated to 92°C for 2 minutes, then allowed to cool to room temperature. The “hot” probe was then purified through a Chroma Spin STE 10 column (Clontech) by briefly spinning in a tabletop centrifuge, before being collected into a 1.5 ml microcentrifuge tube for storage.

3.15.2 Assay protocol

6 X EMSA buffer

120 mM HEPES pH 7.5

300 mM KCl

30% (v/v) glycerol

2.4 mM DTT

0.6 mg/ml BSA

3% (v/v) Triton X-100

GST-IRF-1 (quantities detailed in figure legends), 2 µl of 6 X EMSA buffer, 1.5 µl non-specific DNA (1 µl of 1µg/µl p[d(I:C)] and 0.5 µl of 1µg/µl salmon sperm DNA) plus or minus 0.5 µl of an anti-IRF-1antibody (1/1000 dilution, BD biosciences) or 200 ng scFv were pre-incubated for 30 min on ice prior to the addition of the ^{32}P-labelled C1 probe (1 µl, from section 3.15.1). Following further incubation for 30 min at room temperature the reactions were analysed on a 5% polyacrylamide gel and radiolabelled bands were detected using a phosphoimager.

3.16 Reporter assay

For luciferase reporter assays, cells were cultured in 24-well plates and transiently transfected with pCMV-Renilla/Luc (60 ng) together with 120 ng of either p125-luc IFN-β (wild type or mutant −ISRE), TLR3-Luc (wild type or mutant −ISRE), -683CDK2-Luc, TRAIL-Luc (wild type or mutant −ISRE), or IL-7-Luc (wild type or mutant −ISRE) reporter gene constructs. Luciferase assays were performed 24 hours post-transfection using the Dual Luciferase® reporter assay system (Promega) according to the manufacturer's instructions. Luminescence was quantified using a Fluoroskan Ascent F1 luminometer (Labsystems). Signals were normalised using the internal control (*Renilla* luciferase signal).

3.17 Sub-cellular localisation

As described in the manufacturer's handbook using the Thermo Scientific subcellular fractionation kit. Fractions (20 µl) were analysed through SDS-PAGE and immunoblotting as described in the figure legends.

3.18 IRF-1 turnover

For half life determination cells were transfected at 80% confluence using Attractene (Qiagen) according to the manufacturer's handbook and as indicated in the figure legends; for endogenous IRF-1 half life determination, the cells were left untransfected. 24 hours post-transfection cells were treated with cycloheximide (30 µg/ml) and harvested at time points 0, 15, 30, 45, 60, 90 and 120 min after treatment. For accumulation assays cells were also transfected at 80% confluence using Attractene (Qiagen) as described in the manufacturer's handbook this time with

either wild type or mutant IRF-1 P325A. They were then treated with the proteosomal inhibitor MG132 (50 µM) and harvested at time points 0, 15, 30, 45, 60, 90 and 120 min after treatment. Detergent soluble cell lysate (mammalian cell lysis described under section 3.8) and the detergent insoluble pellet (solubilised via re-suspension in 100 µl SDS-sample buffer and heating to 85°C for 10 minutes) were analysed by SDS-PAGE/immunoblotting as described in figure legends.

3.19 scFv co-immunoprecipitation

Purified scFv (1 µg) in buffer A (20 mM Tris-HCl pH 7.5, 0.5 M NaCl) was incubated with Ni^{2+}-NTA agarose (15 µl) for 1 hour at 4˚C then washed 2 x 5 min with buffer A plus 5 mM imidazole. The beads were subsequently incubated with detergent soluble HeLa cell lysate (500 µg), and mixed at 4˚C for 2 hours. Unbound proteins were removed by washing 3 x with buffer A plus 25 mM imidazole, 0.5% Triton X-100 and 0.5% Tween 20, followed by 3 x with buffer A plus 25 mM imidazole. The beads were heated to 85˚C for 10 minutes in SDS-sample buffer (100 µl) to elute bound proteins. This eluate was analysed via SDS-PAGE and immunoblot as described in figure legends.

3.20 One-STrEP pull down

0.2% Triton X-100 lysis buffer without DTT

50 mM Hepes pH 8
0.2% (v/v) Triton X-100
150 mM NaCl
10 mM NaF
0.1 mM EDTA
protease inhibitors:
- 20 µg/ml leupeptin
- 1µg/ml aprotinin
- 2µg/ml pepstatin

One-STrEP-tagged IRF-1 wild type, ΔC25 or ΔC70 (4 µg) were transfected into A375 cells grown in 10 cm plates. After 24 hours intracellular protein complexes were cross-linked by incubating the cells with 2 mM DSP (Dithiobis [succinimidyl propionate]) for 30 min at room temperature, this reaction was then stopped through

the addition of 20 mM Tris pH 7.5 for 15 min at room temperature. Cells were washed with cold PBS and harvested by scraping in the presence of 1 ml 0.2% Triton X-100 lysis buffer. This lysis buffer contained no DTT as DSP is cleaved by reducing agents. The scraped cells were incubated on ice for 20 min followed by centrifugation at 16,800 x g for 15 min at 4°C. This lysate (0.5 mg) was added to a 50% suspension (40µl) of streptactin macroprep (IBA) and rotated for 1 hour at room temperature. Beads were washed 1 x with wash buffer, (100 mM Tris pH 8, 150 mM NaCl, EDTA), 4 x with PBS containing 0.2% Triton X-100 and then again 1 x with the same wash buffer as before. One-STrEP-tagged complexes were eluted in 50 µl of SDS sample buffer by heating to 95°C for 5 min. After further centrifugation at 1,600 x g for 5 min, 25 µl of the eluted samples were analysed by SDS-PAGE/immunoblot using anti-ZNF350 and anti-IRF-1 antibodies.

3.21 Peptide pull-down

A375 cells were washed with cold PBS then harvested by scraping in the presence of 1 ml 0.2% Triton lysis buffer (described under One-STrEP pull down, section 3.20) supplemented with 2 mM DTT. Avidin (40 µg/ml) was added to the lysates and they were incubated on ice for 30 min before being pre-cleared on Sepharose beads (100 µl of beads/1 ml of lysate) for 1 hour at 4°C. Cleared mammalian lysate (0.5 mg) was then added to 100 µl (50% suspension) of streptavidin-agarose (Sigma), which had previously been washed 3 x in wash buffer A (100 mM Tris pH 8, 150 mM NaCl, 1 mM EDTA) and incubated for 1-2 hours with 50 µg/ml of biotinylated peptide. The lysate and streptavidin-agarose bound peptides were incubated for 1 hour at room temperature then washed 1 x with wash buffer B (PBS containing with 0.2% Triton X-100, 20 µg/ml leupeptin, 1µg/ml aprotinin, 2µg/ml pepstatin), 4 x with wash buffer C (PBS containing 0.2% Triton X-100) and then again with wash buffer B. The samples were centrifuged at 1,600 x g for 5 min at 4°C and excess liquid was removed. Bound proteins were eluted in 50 µl of SDS sample buffer by heating to 95°C for 5 min. 25 µl of eluate was then analysed through SDS-PAGE and immunoblot using anti-ZNF350 and anti-IRF-1 antibodies.

4 *In vitro* selection and characterisation of anti-IRF-1 scFv

4.1 Introduction

This chapter describes the use of antibody phage display to select single chain antibodies (scFv) capable of binding to specific regions of IRF-1. A peptide consisting of the C-terminal 20 amino acids of IRF-1 was used as an antigen in the phage biopanning procedure. Antibody selection by phage display and the importance of the C-terminus of IRF-1 in regulating its activities are outlined in this thesis.

4.1.1 Antibody phage display technology

Phage display technology relies on four principle features: genotypic diversity, selection pressure, amplification and genotype/phenotype coupling [298]. First, a hugely diverse library of genes encoding full length proteins or peptides is cloned into phage DNA. This generates a large population of phage, each displaying a variable protein or peptide fused to an external coat protein. This initial phage population is brought into contact with a target antigen, non-binding phage are discarded and only those able to bind are selected. The now reduced population of phage, displaying only high-affinity binders fused to their coat proteins, is amplified in a host bacterial culture. The amplified phage are again subjected to the same biopanning selection procedure until a sufficient enrichment of strong binders is achieved. The phage DNA from this final population can be extracted and sequenced to allow identification of the antigen-binding proteins/peptides. Thus, phage display provides a selection platform through which specific, high-affinity interactions can be identified [169].

Antibody phage display involves the selection of antibody fragments displayed on the surface of phage [299]. The basic functional unit of an antibody, the immunoglobulin domain (IgG), consists of four polypeptide chains: two heavy and two light chains connected by disulphide bonds. Both the heavy and light chains house variable domains, which each contain three variable loops, termed

Complementarity Determining Regions (CDRs), that are responsible for antigen binding. Recombination of antibody variable (V) genes, encoding the heavy (VH) and light (VL) variable domains, transfers the antibody-antigen binding capacity to a single chain polypeptide. Thus, large diverse sets of VH and VL genes are amplified from lymphocytes [196, 300] and randomly paired to provide diverse libraries of antibody single chain variable fragments, scFv [301]. Sequence variability in the CDRs is increased by PCR using partially degenerate primers [189].

The following chapter will describe the selection and characterisation of single-chain antibodies selected from the Tomlinson (I and J) [188] or ETH-2-gold [189] libraries using phage display. In both libraries the single-chain Fv antibody fragments are fused to the minor coat protein g3p of filamentous phage and tagged with His and Myc.

4.1.2 C-terminal antigen

The ratio of the tumour suppressor IRF-1 and its homologous repressor IRF-2 oscillates during the cell cycle, falling following growth stimulation and reaching its highest point in growth-arrested cells [67, 302]. Ectopic overexpression of IRF-1 results in strong inhibition of cell growth, and abrogation of this activity is linked to tumour progression [302]. This ability to inhibit cell growth is lost following deletion of the C-terminal 70 amino acids and reduced by loss of the last 25 amino acids of IRF-1 [64].

Mutant IRF-1 protein, lacking the C-terminal transactivation domain (splicing variants involving exons 7, 8 and 9), has been identified in cervical cancer patients [24] and shown to: compete with wild type IRF-1 for DNA binding, have a longer half life and be expressed in a cell cycle independent manner [24]. Understanding the function of IRF-1 discrete sub-domains in the wild type protein could increase current understanding of the role these mutants play in tumour progression.

Further study of IRF-1's C-terminus has revealed that it plays a role in modulating target gene expression [101] and regulating degradation [111]. The extreme C-terminal 70 amino acids of IRF-1 have been characterised as an enhancer domain [101]. Unlike the more N-terminal transactivation domain (amino acids 184-256), the

enhancer cannot independently increase transcriptional activity of a GAL4 DNA binding domain. However, in cooperation with the transactivation domain, this region can further enhance transcriptional activation [101]. The mechanism through which this domain increases transcription is not fully understood, but it has been shown to house one of two sites bound to by the transcriptional co-activator p300 [72]. As yet no link has been found between IRF-1's ability to bind p300 and its transcriptional activities.

IRF-1 can function both as a transcriptional activator and repressor. Earlier studies have described its ability to repress CDK2 [10, 62] and induce IFN-β expression [51]. The establishment of a link between the extreme C-terminus of IRF-1 and enhanced induction of transcription [101] prompted investigation of this region's ability to influence IRF-1's repressor functions. Deletion of the last 70 amino acids, loss of the enhancer domain, dramatically reduced IFN-β induction and CDK2 repression [64]. However, more detailed mapping revealed a C-terminal deletion of the last 25 amino acids could increase IRF-1 induction of IFN-β and mitigate CDK2 repression. Smaller deletion mutants and alanine substitutions revealed that amino acids 311-317 acted as an internal suppressor of IRF-1's transcriptional activator function, i.e. mutation of these residues increases IFN-β induction. Furthermore, residues 306-310 were shown to be essential for CDK2 suppression [64]. Although the transcriptional activities of IRF-1 were modulated, the C-terminal mutants of IRF-1 used in this study retained the ability to bind DNA.

The extreme C-terminus was also shown to play a role in the stability of IRF-1. IRF-1 has an extremely short half life of 20-40 minutes [110, 111]. Removal of the C-terminal 39 amino acids of IRF-1 generated a degradation resistant form of the protein and addition of these residues to GFP reduced its half life [110]. Polyubiquitination of full-length IRF-1 has also been demonstrated [110]. Inhibition of the proteosome leads to an increase in polyubiquitinated forms of IRF-1, supporting the connection between IRF-1's ubiquitination and its degradation [110, 111]. However, these two processes were uncoupled by a series of C-terminal deletions. Loss of the last 70 amino acids of IRF-1 prevented both polyubiquitination and degradation, whereas removal of the last 25 amino acids did not prevent

ubiquitination, but did inhibit degradation [111], indicating that a further regulatory step is required before the protein can be broken down. Expression of the C-terminal 70 amino acids as a truncated protein was shown to reduce ubiquitination of wild type IRF-1. One possible explanation for this observation is that the C-terminus may act as a docking region for ubiquitin-promoting co-factors (e.g. E3 ligases) and compete with full-length IRF-1 for these binding proteins.

To date, very little is known about IRF-1 interactions that influence degradation. Further evidence that these map to the extreme C-terminus of IRF-1 was provided by a study of chaperone interactions within this region [112]. The Hsp90 inhibitor 17AAG caused a decrease in intracellular IRF-1 levels after 12 hours. This decrease was lessened by proteasomal inhibition with MG123, indicating that Hsp90 can protect IRF-1 from proteosomal degradation. Additionally, the ability of an Hsp90 inhibitor to decrease IRF-1 protein levels was shown to be dependent on Hsp70 binding to IRF-1 between amino acids 306 and 318, specifically to an LXXLL motif [112]. Prior to the decrease in IRF-1 protein levels (0-12 hours after treatment), 17AGG inhibited IRF-1's transcriptional activity thus implying that this may be enhanced by Hsp90. Furthermore, Hsp90 was shown to increase the half life and protein levels of nuclear IRF-1.

An increase in the half life of IRF-1 has previously been linked to its upregulation during ATM-dependent DNA damage response [29]. Tight control over IRF-1's degradation pathway could enable a speedy response to DNA damage, followed by a quick return to normal IRF-1 levels. Taken together the studies described here reveal the importance of the extreme C-terminus of IRF-1 in regulating its protein turnover and the expression of downstream target genes. However, out of necessity these studies rely on exogenously expressed mutant proteins and it is not yet known if these regions of IRF-1 are rate-limiting for the activity and turnover of the endogenous protein.

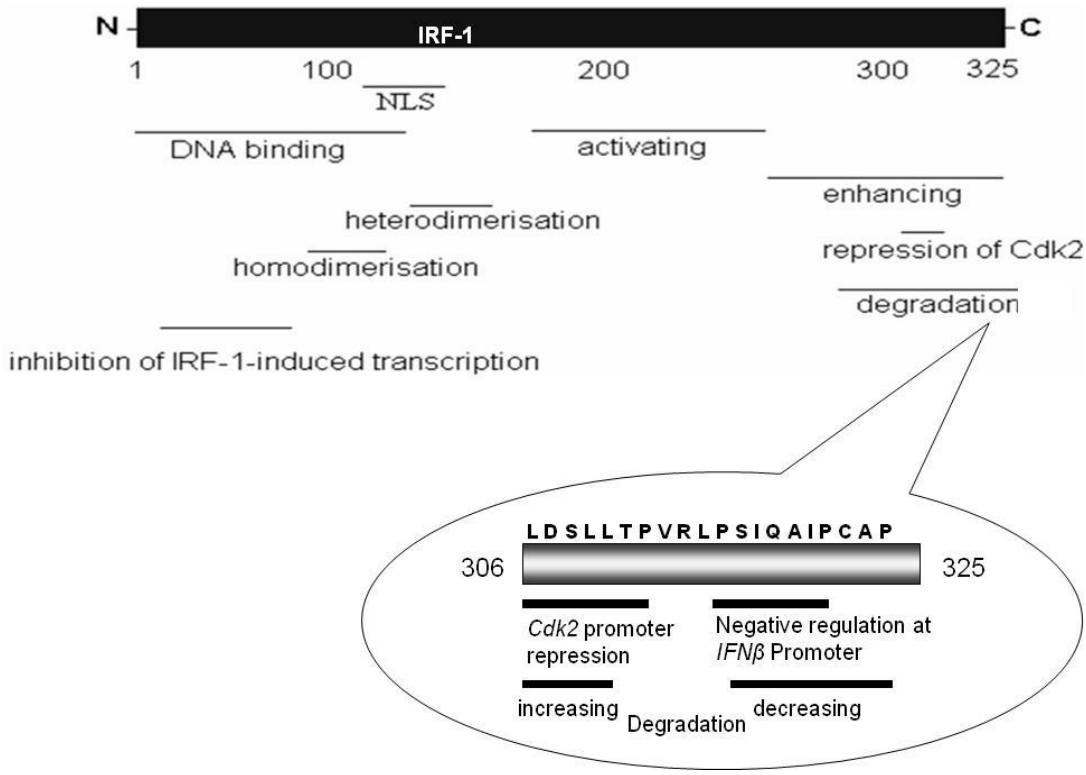

Figure 4.1: Functional mapping of the C-terminus of IRF-1. Adapted from [303]

4.2 Results

This chapter details the validation of phage display as a technique through which IRF-1 targeting monoclonal antibodies can be derived. The activity of these monoclonal antibodies was examined in a series of *in vitro* assays. Monoclonals were selected on the basis of relative affinity and specificity following cytoplasmic expression so that they could subsequently be developed as intracellular antibodies (the topic of chapter 2).

4.2.1 Polyclonal phage-scFv

To generate single chain antibodies (scFv) against the extreme C-terminus of IRF-1, a biotinylated peptide covering the last 20 amino acids of IRF-1 (amino acids 306-325) was used as the target antigen. Peptide-specific antibodies were selected from the Tomlinson phage display library [188] in which diverse single chain antibody fragments (scFv) carrying His and Myc tags are expressed on the surface on phage

particles as fusions to the minor coat protein g3p. Each scFv consists of antibody heavy and light chain variable domains connected by a flexible glycine serine linker.

The biotinylated peptide antigen (C2: LDSLLTPVRLPSIQAIPCAP) was captured onto streptavidin-coated immunotubes (Nunc), blocked with 2% MPBS to reduce selection of plastic-binding antibodies and washed with PBS to remove excess peptide. Two stocks of phage (I and J) are supplied with the Tomlinson antibody phage display library, which possess a diversity of 1.47×10^8 pfu and 1.37×10^8 pfu respectively. Therefore, for each round of selection, two plastic immunotubes were coated with the target antigen and each incubated with a separate phage stock (either I or J). To each of the antigen-coated immunotubes 10^{13} pfu (plaque forming units) of phage were added. This equated to incubation with ~ 68000 (stock I) or ~73000 (stock J) copies of each different phage-expressed antibody. Having each scFv-displaying phage represented at high frequency prior to selection increased the chances of detecting an antigen-binding clone. Phage were quantified (titred) based on colony growth of infected bacteria on ampicillin plates, as the scFv encoding phagemid vector contained an antibiotic resistance gene. The scFv displaying phage were incubated with the peptide antigen for 2 hours, 1 hour on a rotating turntable and 1 hour standing, both at room temperature. Unbound phage was then discarded following rigorous washing with phosphate buffered saline (PBS), and bound phage eluted with trypsin in PBS (see figure 4.2)

In order to produce new phage particles in the amplification step that follows selection, a bacterial host must be infected with both phagemid-carrying phage and helper phage. The resultant phage virions display the g3p coat proteins encoded in either the phagemid (which are fused to scFv) or the helper phage (which have no scFv attached). The insertion of a trypsin cleavage site in the helper phage g3p coat protein renders them incapable of infecting bacteria following trypsin-elution, whereas the trypsin cleavage site in the phagemid encoding scFv is inserted inbetween the coat protein-scFv fusion, so that phage carrying antibody fragments can be eluted and still infect a bacterial host in subsequent amplification steps [304]. This ensures all phage particles taken forward for further selection present antibody fragments.

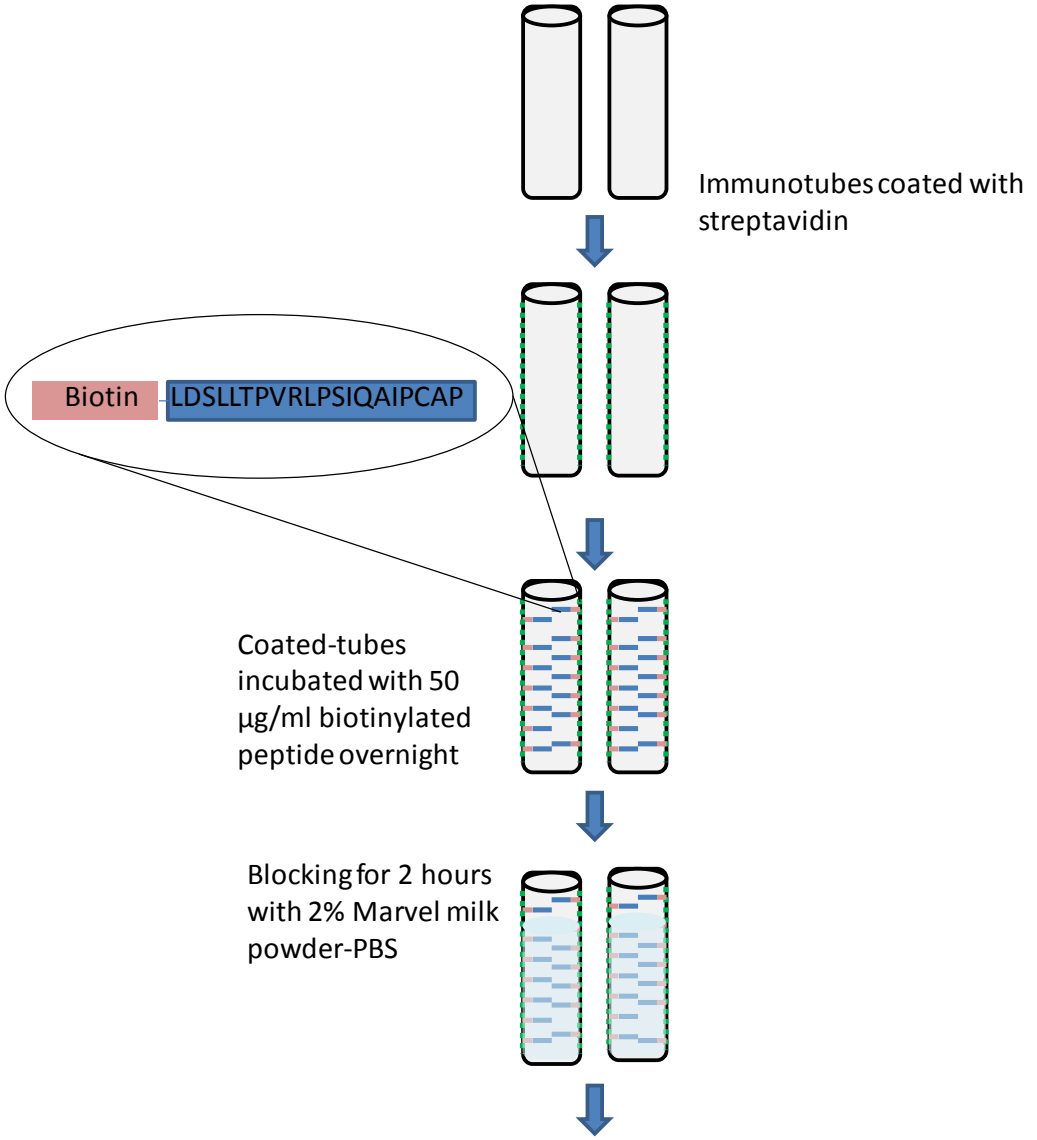

Figure 4.2: protocol for selection of scFv-displaying phage targeting the C-terminal 20 amino acids of IRF-1. Continued on next page.

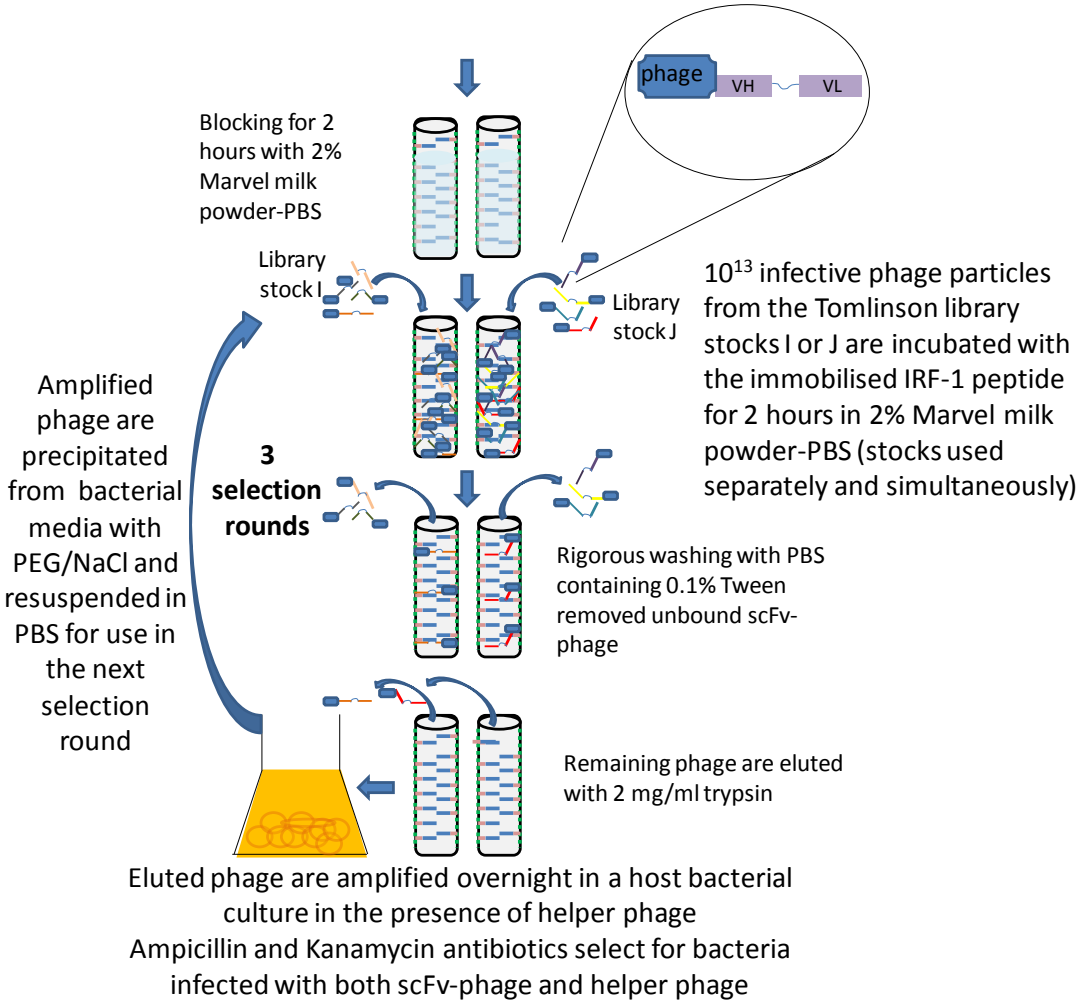

Figure 4.2: protocol for selection of scFv-displaying phage targeting the C-terminal 20 amino acids of IRF-1 (figure continued from previous page). The selection procedure is based on that supplied with the Tomlinson phage display library, but adapted for use against biotinylated peptides rather than full length protein.

Following selection and amplification the polyclonal pool of IRF-1 binding phage was precipitated from the bacterial culture medium with PEG/NaCl and re-suspended in PBS. The polyclonal phage-scFv from each of the 3 selection rounds was resuspended in PBS and tested for its relative affinity to IRF-1 in an ELISA. The biotinylated peptide used as a target during phage display was immobilised on a plastic microtitre plate and separately incubated with the polyclonal scFv-displaying phage from each of the 3 selection rounds. Following rigorous washing, the phage able to bind the peptide antigen were quantified using a HRP-conjugated antibody against the phage g3p coat protein, which emitted a measurable fluorescent signal following the addition of enzymatic chemiluminescence (ECL) solution (see methods section 3.10). It can be seen in figure 4.3 that with each successive round the polyclonal pool of phage was successfully enriched for IRF-1 binding activity. The polyclonal pools consist of a phage derived from both Tomlinson stocks I and J combined for analysis.

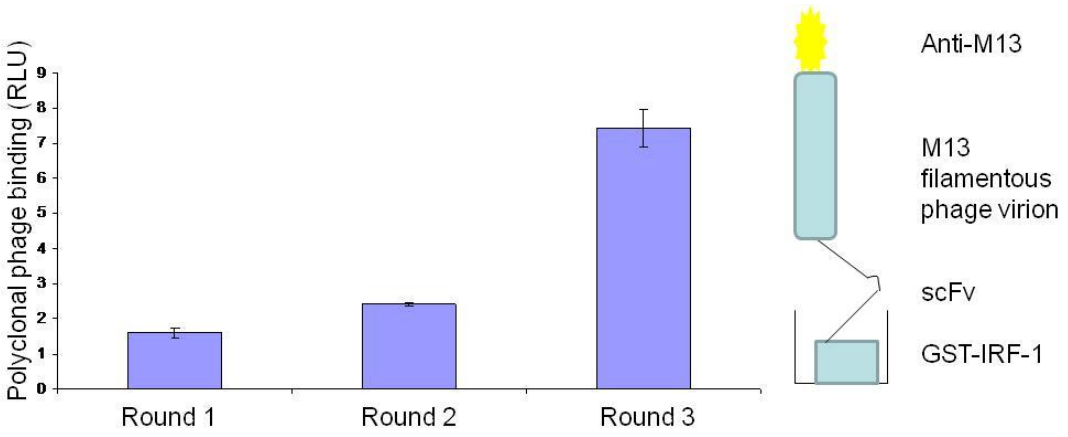

Figure 4.3: (Left panel) Polyclonal phage from each selection round were amplified in TG1 bacteria precipitated from the bacterial culture medium and resuspended in PBS. Phage titre following amplification was ~10^{13} pfu (plaque forming units). A 1/10 dilution of phage from each round was incubated with 200 ng of immobilised GST-IRF-1. Binding was detected using an anti-M13 antibody, which targets the minor phage coat protein g3p, and enhanced chemiluminescence. RLU:relative light units. (Right panel) diagram of scFv-displaying phage binding to full-length IRF-1 in an ELISA format.

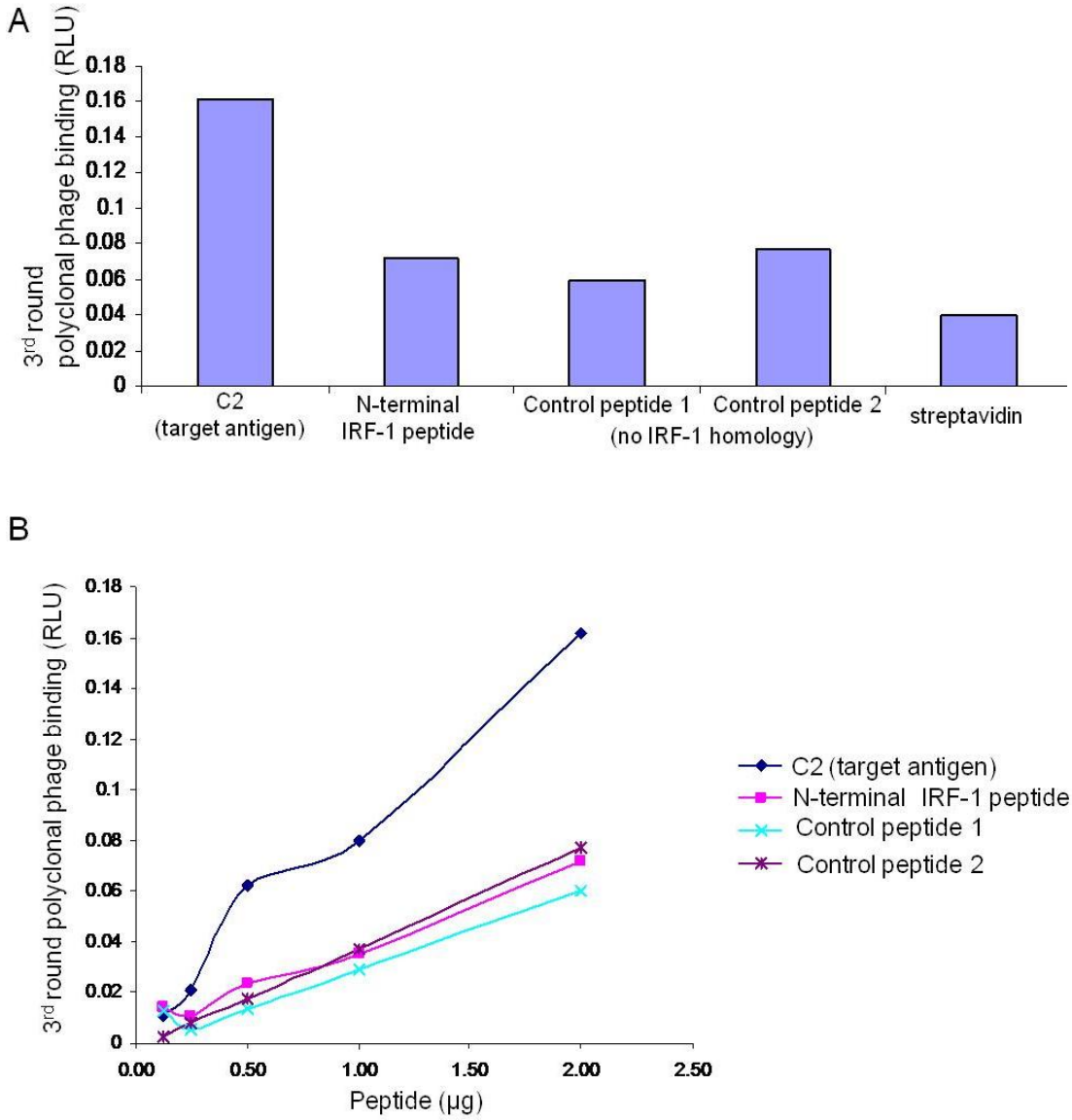

Figure 4.4: (A) Polyclonal phage from the third and final selection round were amplified in TG1 bacteria, precipitated out of the bacterial culture medium and resuspended PBS. Phage titre following amplification was ~10^{13} pfu (plaque forming units). A 1/10 dilution of phage from each round was incubated with 200 ng of: C2 the C-terminal 20 amino acids of IRF-1 (LDSLLTPVRLPSIQAIPCAP), an N-terminal IRF-1 peptide with no homology to C2 and control peptides 1 and 2 which show no homology to IRF-1. As each peptide was biotinylated, relative binding affinity was also evaluated for the streptavidin background. (B) Polyclonal 3rd round scFv-phage assessed for binding to increasing levels (0-2 µg) of immobilised target peptide in an ELISA format. Biotinylated peptides were as described for figure 7A. Binding was detected by anti-M13, which targets the minor phage coat protein g3p, and enhanced chemiluminescence. RLU: relative light units.

Next the specificity with which the 3rd round polyclonal pool could bind the target antigen was determined. This polyclonal pool was seen to bind with greater stability to the C-terminal IRF-1 peptide (C2) than to the three control peptides (figure 4.4). This stable interaction suggests that the scFv-phage selected have a higher affinity for C2 than for the control peptides, but this experiment does not measure affinity (*Kd*) directly. Furthermore, negligible background binding to streptavidin was observed.

4.2.2 Monoclonal scFv screening

The phage displayed antibody fragments present in the 3rd round polyclonal pool could prove useful reagents in some *in vitro* assays, but to extend their use to intracellular assays (as described in chapter 5), it was important to select antibodies that exhibit target specificity when expressed as soluble proteins without a phage scaffold. For this reason, the soluble monoclonal antibody fragments were screened for IRF-1 specificity.

All subsequent experiments described in this chapter and chapter 5 involve monoclonal scFv. By screening numerous monoclonal antibodies, rather than simply using the polyclonal antibody pool, interesting epitope specificities can be selected and antibodies against a wider range of antigenic determinants identified for further analysis.

Soluble antibody fragments are secreted by phage-infected bacteria following induction with IPTG (Isopropyl β-D-1-thiogalactopyranoside). To produce monoclonal antibodies, the polyclonal phage-scFv were used to infect HB2151 bacteria. Between the previously described antibody phage display selection rounds the TG1 bacterial strain was used for phage amplification. However, TG1 is a suppressor strain and would introduce a glutamate residue at the amber stop codon (TAG) between the scFv and gIII gene (which encodes the phage coat protein g3p), causing a scFv-g3p fusion to be expressed. In the non-suppressor strain HB2151, TAG will be read as a stop codon. As the intention of the study is to transfer the minimal scFv required for binding out of the phagemid expression system, it was advantageous to select for scFv that did not require the gp3 coat protein scaffold.

However, expression from HB2151 has the disadvantage that any scFv carrying a premature amber stop codon would now be truncated and therefore at a selective disadvantage, even if they had exhibited a high relative affinity when expressed full-length during phage display. Additionally, some full-length scFv lose their antigen affinity when expressed without g3p, and only re-introduction of the coat protein can restore binding activity [305, 306]. Should no high affinity binders have appeared following expression of isolated antibody fragments from HB2151 bacteria, monoclonal screening would have been repeated, this time following TG1 expression.

Following infection of HB2151 bacteria with the 3rd round polyclonal phage pool, 48 individual colonies were picked for each library (96 colonies in total). Production of scFv for screening was performed on a small scale in 225 µl cultures. Monoclonal scFv were secreted from HB2151 phage-infected bacteria into the culture medium following induction. As the scFv were selected for binding against only the last 20 amino acids of IRF-1, the first characterisation step was to verify binding to full-length IRF-1. The dot blot method allows simultaneous and fast testing of numerous antibodies against the same antigen. A nitrocellulose membrane was coated with IRF-1, blocked and then spotted with each antibody. Following incubation with the antibodies, the membrane was washed and antibody binding detected with HRP-conjugated protein A (figure 4.5).

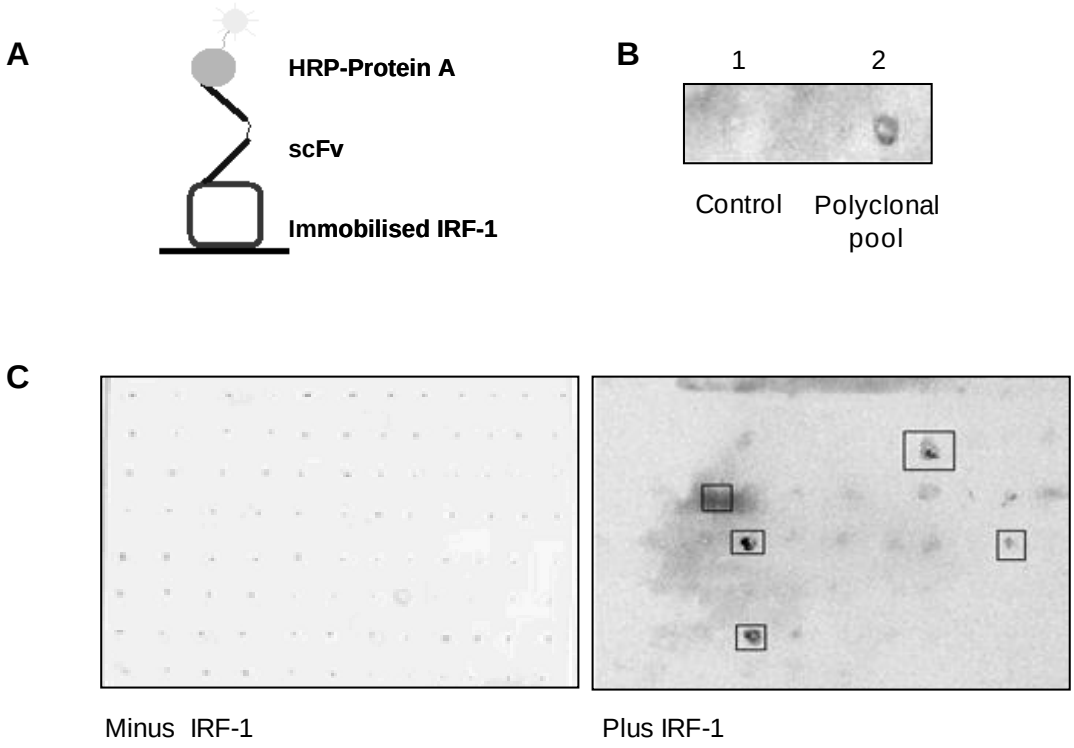

Figure 4.5 Screening for monoclonal anti-IRF-1 scFv antibodies. **(A)** Diagram of scFv binding to full-length IRF-1 in a dot blot format. **(B)** Media from an uninfected bacterial culture ("control"), or one infected with 3rd round polyclonal scFv-displaying phage and thus secreting soluble polyclonal scFv ("polyclonal pool"), was spotted onto a nitrocellulose membrane coated with 0.3 µg/ml GST-IRF-1. After extensive washing, bound scFv were detected using protein A-HRP and enhanced chemiluminescence. **(C)** As in B except soluble scFv were secreted from individual monoclonal phage-infected colonies.

The results suggests that the polyclonal pool of 3rd round scFv contained clones able to bind the C-terminal 20 amino acids in the context of full length IRF-1 (figure 4.3 and 4.5B) and allow the identification of five monoclonal scFv capable of binding stably to the full-length protein. The relative affinities detected by the dot blot method are affected by several factors. scFv expressed from phage-infected bacteria may have low solubility or fold differently without the scaffold of a phage coat protein. Additionally, protein stability and secretion levels may have varied. However, the dot blot does create conditions appropriate for identifying stable, soluble antibodies that are likely to work in similar *in vitro* immunoblots, one of the uses for which novel anti-IRF-1 antibodies could be employed. One limitation of the dot blot is that the antigen was not first separated by chromatography. Therefore,

even though purified GST-IRF-1 was used as the target antigen, scFv may have bound low level contaminants, a possibility which is tested for in subsequent characterisation steps, as is the possibility that the selected scFv targeted the GST tag.

4.2.3 Selected scFv sequence

Sequencing of the five positive clones selected in the dot blot revealed that each consisted of only a light chain variable domain (VL). This was surprising, as the primary protein A epitope has been mapped to the heavy chain [307], and the entire Tomlinson phage display library was screened by its manufacturers so that it would only contain active protein A binders [188]. The restriction sites SfiI/NcoI and XhoI, between which the heavy chain should have been cloned, were intact, as was the intervening pIT2 phagemid sequence present in the unrestricted vector (Figure 4.6).

In agreement with the sequencing data, the library provider Geneservice reported that "There are clones in the library with no insert or with only light chain" and that they "have seen specific binders from the library that only have a VH or VL" [308]. They go on to point out that "Not all the clones in the library contain inserts, and with growth passage the number without inserts does increase, because clones that express no or low levels of scFv-pIII fusion grow better and produce more phage." [308]. The selection of light chain-only antibody fragments from the Tomlinson I and J library has been reported elsewhere, and these short fragments were shown to remain active binders [309, 310].

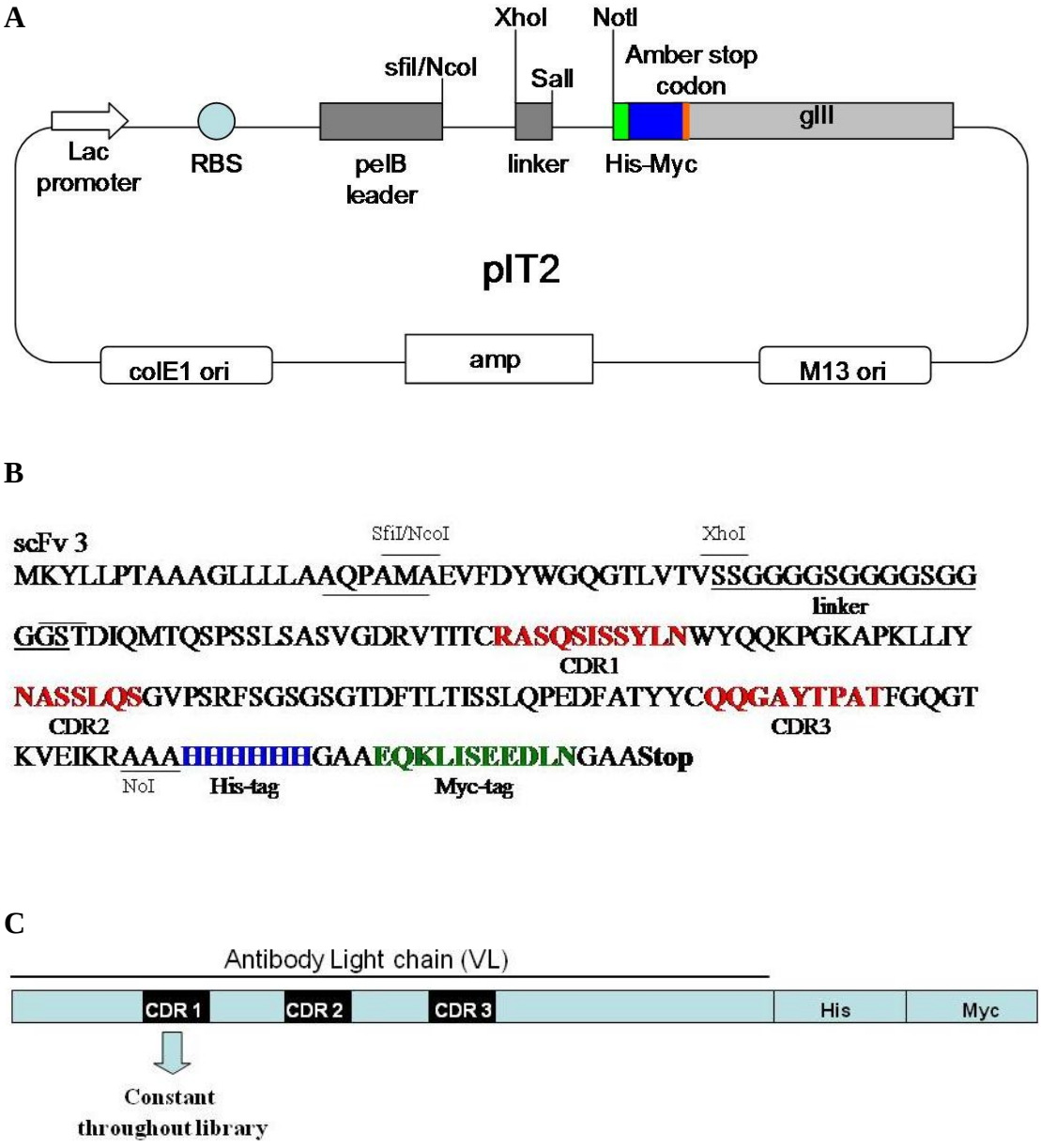

Figure 4.6: (A) Map of PIT2 vector adapted from Tomlinson (I+J) library manual. **(B)** Annotated sequence of scFv 3, one of the 5 anti-IRF-1-C terminus antibodies chosen following dot blot screening. Sequence is identical to the other anti-IRF-1 single chain antibodies apart from CDR2 and 3. **(C)** Diagrammatic representation of antibody fragement expressed from phage infected HB2151, a non-suppressor strain of *E.coli* that recognises the amber stop codon.

4.2.4 Cytoplasmic expression

The next stage in selection was to generate antibody fragments that could be expressed stably within cells. Cytoplasmic bacterial expression has been reported to increase protein yield [311]. Additionally intracellular antibodies (intrabodies) have previously been used to modulate the activities of their target antigen. Selecting antibody fragments that function following cytoplasmic expression at this stage will increase the chance of successfully developing active intrabodies later. Such antibodies could be used to study the function of endogenous IRF-1 within the cell. The five monoclonal light-chain antibody fragments that bound stably to IRF-1 contain intradomain stabilising disulphide bonds, which may not form *in vivo* due to the reducing environment of the cytoplasm. It has previously been shown that scFv disulphide bonds do not form in the cytoplasm [232]. However, some scFv have been shown to tolerate the absence of this bond and maintain their binding activity in *in vitro* assays [234, 312]. One previously described method for selecting antibodies stable in reducing environments is to test antigen binding following *E.coli* [313, 314] or mammalian cell [315, 316] cytoplasmic expression. With this aim in mind the single domain antibodies were cloned into the Gateway vector system (Invitogen) for cytoplasmic expression. Once cloned into this system, a DNA insert can easily be transferred between different destination vectors through homologous recombination, enabling expression with additional tags, or in completely different cell systems. This broadened the range of assays in which antibody activity could be characterised. As the sequencing revealed that none of the antibody fragments selected contained premature amber stop codons, they could be expressed in any *E.coli* non-suppressor strain, and for this study were produced in the BL21 strain.

Following bacterial cytoplasmic expression, the antibody fragments were purified via a His tag, which along with the scFv and Myc tag was cloned from the origin phagemid into the Gateway system, or through an additional GST tag. The GST tag was added through the Gateway system, as an available commercial anti-GST antibody gave very low background binding on immunoblots compared to the accessible anti-His or anti-Myc antibodies. However, in all experiments assessing binding to GST-IRF-1, anti-His was used for detection.

Tagged scFv extracted from lysate following bacterial cytoplasmic expression have previously been shown to specifically bind to their target antigen without a re-folding or oxidising step to regenerate the intradomain disulphide bonds [296, 317]. Although the location of the tag (C or N terminal) has been known to interfere with antigen binding [318], such interference is difficult to predict prior to experimental validation, particularly in the case of the antibody light chain variable domains in which the primary binding regions (CDRs) are located throughout the protein. The GST tag was N-terminal and the His-Myc tags C-terminal.

Purified scFv were used as primary antibodies in a series of binding assays aimed at establishing their specificity for the target antigen, IRF-1. By first purifying the scFv, their concentrations could be normalised to allow for better comparison of their relative affinities. The scFv were initially tested for binding to denatured protein. Purified His-tagged IRF-1 and IRF-2 were run on an SDS-polyacrylamide gel, transferred to nitrocellulose, blocked and probed for binding to commercial anti-His, anti-IRF-1 and anti-IRF-2 antibodies, or the five monoclonal scFv (figure 4.7A). Each of the scFv showed a similar level of binding to His-IRF-1, but did not detect any purified IRF-2. Next, scFv specificity for untagged intracellular IRF-1 was assessed. IRF-1 or IRF-2 were transfected into A375 cells, which were harvested and lysed after 24 hours. The lysate was separated by SDS-PAGE, transferred to a nitrocellulose membrane and probed with commercial anti-IRF-1 and anti-IRF-2, or each of the purified scFv. All five cytoplasmically expressed scFv were able to detect denatured full-length IRF-1 in crude lysate, but not IRF-2 (figure 4.7B).

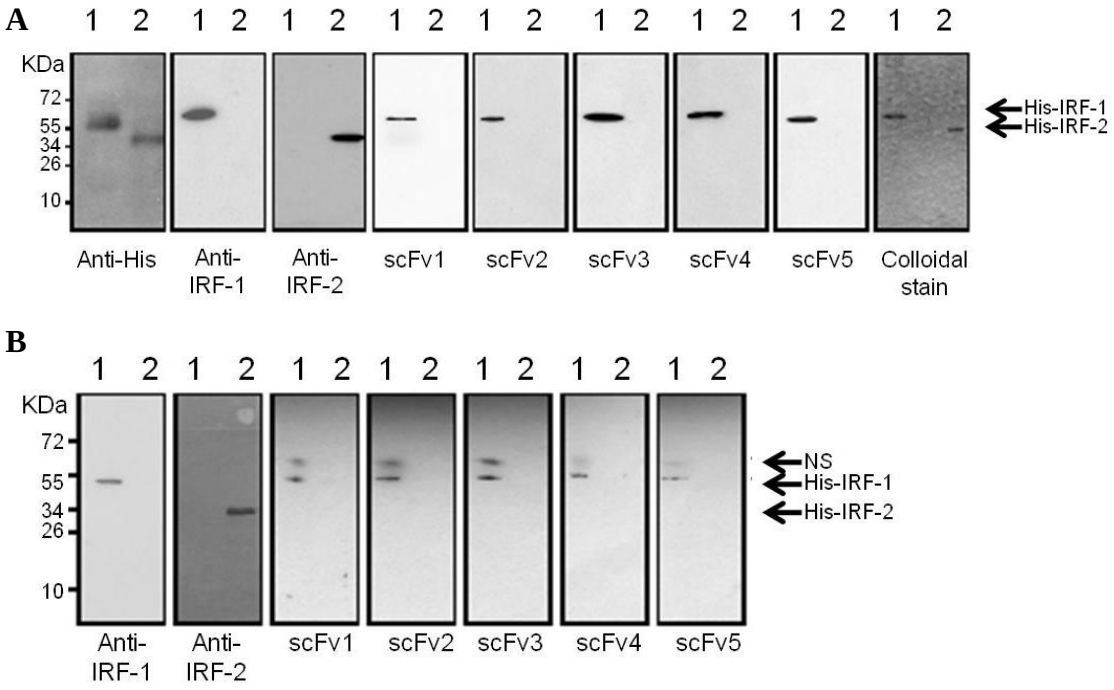

Figure 4.7: (A) Purified His-IRF-1 (lane 1) and His-IRF-2 (lane 2) (0.3 µg/lane) were analysed on a 12% SDS-PAGE/immunoblot and probed with anti-His, anti-IRF-1, anti IRF-2 and the scFv antibodies (1 µg/ml). scFv binding was detected using anti-GST monoclonal antibody and enhanced chemiluminescence A colloidal stain shows the purity of His-IRF-1 and His-IRF-2. (B) Lysate from HeLa cells transfected with 1 µg of pcDNA3 IRF-1 or pcDNA3 IRF-2 were analysed by 12% SDS-PAGE/immunoblot and probed with the antibodies listed for A excluding the anti-His antibody. NS: non-specific band detected by antibodies. The data are representative of at least 2 independent experiments.

A non-specific band was detected by all 5 scFv in lysate containing exogenously expressed IRF-1, but not in lysate from cells transfected with IRF-2 (figure 4.7B). It is therefore possible that this band may represent a modified form of exogenous IRF-1 that cannot be detected by the commercial anti-IRF-antibody, although further analysis of the "NS" protein band would be required to test this hypothesis.

The single chain antibodies were all originally selected for binding to the last 20 amino acids of IRF-1. This region of IRF-1 has been implicated in the regulation of degradation and transcription (see section 4.1.2), therefore antibodies that specifically target this epitope would be especially useful for studying IRF-1 function. Figure 4.4 already established that the polyclonal pool of phage produced by 3 rounds of phage display could specifically bind the IRF-1 C-terminal peptide,

however it was important to verify binding of the monoclonal scFv to the same antigen. Therefore, all five scFv were tested for binding to the C-terminal IRF-1 peptide (labelled C2) and other overlapping peptides spanning the complete length of IRF-1 (figure 4.4). The peptides were also incubated separately with a commercial polyclonal antibody to the C-terminal 20 amino acids of IRF-1 (Santa Cruz Biotchnology) or with streptavidin-HRP (to check that equal amounts of biotin-labelled peptide had been captured per well). All five scFv showed stable binding to peptide C2, and in four out of five cases (scFv 1,3,4 and 5) binding to C1, a peptide that overlapped C2 by 15 amino acids (see figure 4.8B). This suggests that the scFv may have slightly different epitope specificities. For example, whereas scFv2 has a requirement for the IPCAP sequence at the C-terminus of the C2 peptide, these residues are dispensable for scFv1 binding. Very low binding was observed to all other IRF-1 peptides. The commercial antibody confirmed that peptides C1 and C2 represented the C-terminus of IRF-1; however, the relative affinity of the commercial antibody cannot be compared to that of the monovalent scFv, as it is a polyclonal sera made up of bivalent IgG.

Detection of the peptide antigen and denatured full length protein are both useful ways to validate antibodies. However, the C-terminal 20 amino acids of IRF-1 may not be available for binding in the protein's native conformation. An ELISA has the advantage over an immunoblot that the protein is not first fully denatured. Therefore a titration of GST-IRF-1 immobilised on a microtitre plate was probed with either the scFv or anti-GST in the mobile phase (Figure 4.9A top panel). This showed that all 5 of the scFv antibodies were able to bind IRF-1, although there were differences in their ability to form stable complexes. For example scFv3 and 4 bound better to IRF-1 in this assay than scFv2. Next the scFv were tested for their ability to specifically target the extreme C-terminus of IRF-1 by comparing binding to full length IRF-1 and a C-terminal truncation (ΔC25) (figure 4.9A top panel versus bottom panel). As expected, scFv1, 2, 3 and 5 were no longer able to detect the protein, however it was revealed that scFv 4 can bind IRF-1 outside of the C-terminal 20 amino acids under the conditions of the assay. This lack of specificity was not previously detected in the peptide ELISA. It may be that this off-target binding is dependent on conformational changes within the longer protein.

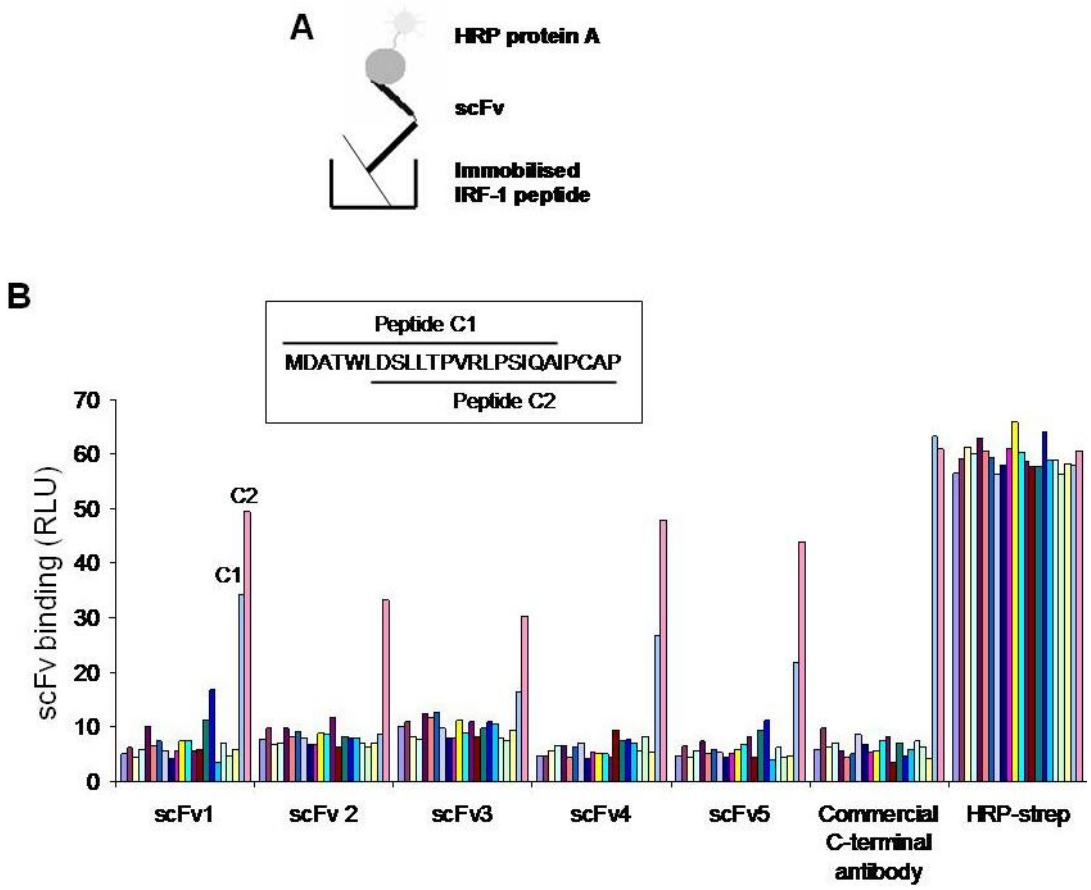

Figure 4.8: scFv binding to IRF-1 peptides. Continued on next page.

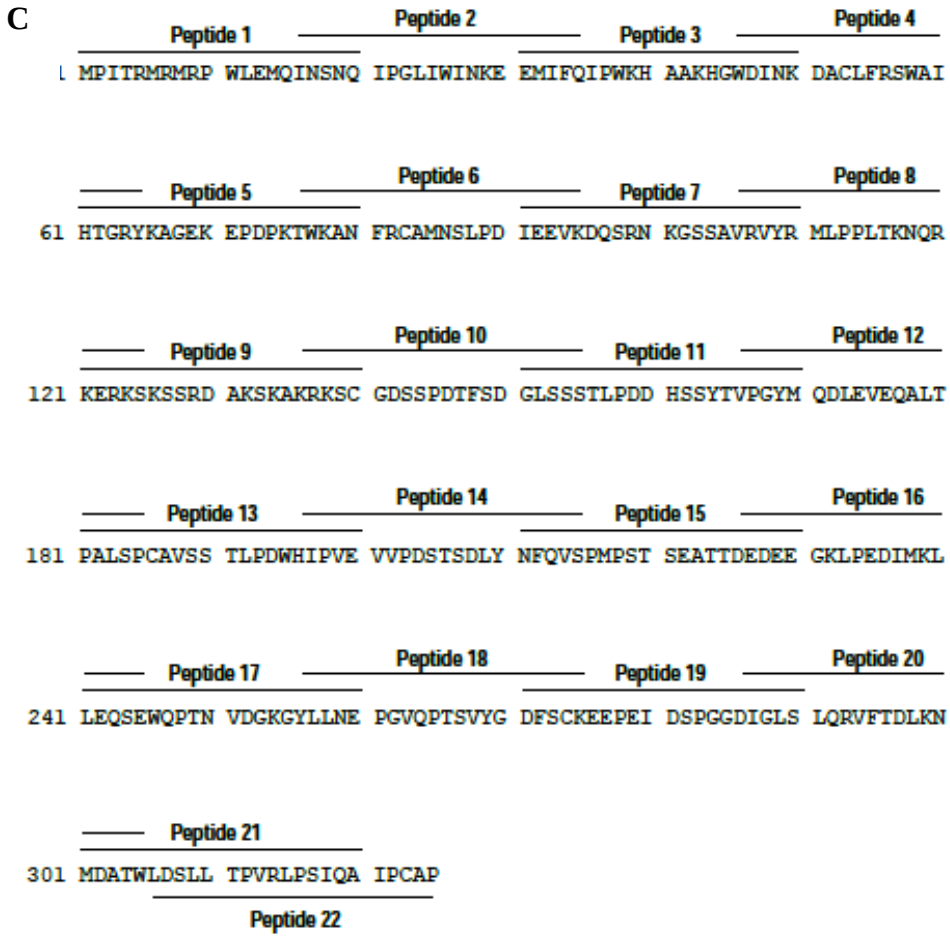

Figure 4.8: scFv binding to IRF-1 peptides (figure continued from previous page). (A) Schematic of scFv binding to biotinylated peptides in a peptide binding assay. (B) Immobilised overlapping peptides covering the whole length of IRF-1 were incubated with each scFv (1µg/ml). Following extensive washing scFv binding was detected with an anti-His monoclonal antibody and enhanced chemiluminescence. A commercial anti-IRF-1 C-terminus antibody was used as a control, and peptide normalisation was demonstrated using HRP-streptavidin. The sequences of two overlapping peptides (C1 and C2) are shown in the inset. (C) Sequence of overlapping peptides covering the full length of IRF-1, kindly provided by Vikram Narayan.

ELISA results can be affected by immobilised proteins partially unfolding to reveal more hydrophobic residues to the plastic surface of a microtitre plate [319]. To control for unfolding of either IRF-1 or the antibody upon immobilisation, the assay was performed in the alternative orientation, with the scFv immobilised on the plate and IRF-1 in the mobile phase (figure 4.9B). Under these conditions a more pronounced difference in stable binding was detected. In this case, scFv3 bound significantly better than the other scFv antibodies, with the exception of the non-specific monoclonal scFv4. Again this suggests that the epitope specificities of each scFv may differ and that some antibodies, for example scFv3, preferentially bind their epitope when IRF-1 is in a native conformation.The experiments described confirm that antibody phage display can be used to develop soluble monoclonal antibody fragments that can retain antigen specificity following cytoplasmic expression and subsequent purification. It also shows that peptide antigens can be used to develop antibodies that can bind their target epitope within the context of a full-length protein.

4.2.5 N-terminal IRF-1 antibody

In a parallel effort to find IRF-1 antibodies that bound to the N-terminus of IRF-1, the ETH-2-gold scFv library [189] was used to select antibody fragments that bound stably to an N-terminal domain of IRF-1 spanning amino acids 60-124 (figure 4.10B). This region of IRF-1 has been described as a homodimerisation domain, essential for an interaction between two molecules of IRF-1 *in vivo* [103]; however, this interaction has not been validated as direct or functionally significant. This region of IRF-1 was also shown to be highly disordered (have high entropy), see figure 4.10A. Such flexible unstructured protein regions have been shown to be important for regulatory interactions [320]. Development of the anti-N terminal antibody (scFvN) was as described for the five anti-C-terminal scFv, except in that only two rounds of biopanning were performed, and the antigen was a His-tagged recombinant protein domain. The ETH-2-Gold library, like the Tomlinson library, consists of filamentous M13 phage with diverse scFv antibodies (36×10^9 clones) displayed as fusions to the minor coat protein g3p. Again each scFv carries a His and Myc tag.

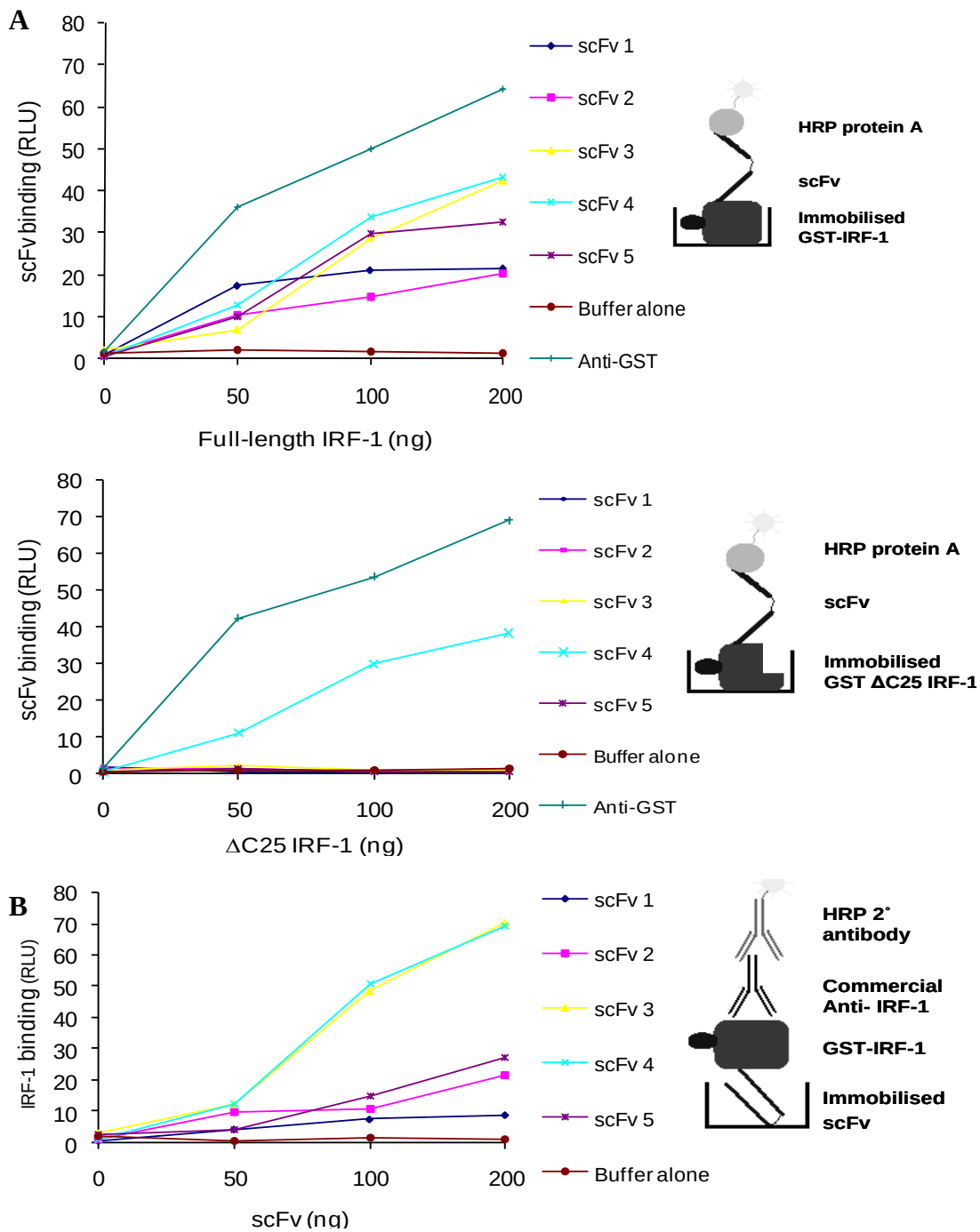

Figure 4.9: Binding of the scFv to IRF-1 under non-denaturing conditions. (A) A titration (0-200 ng) of immobilised GST-IRF-1 wild type or GST-IRF-1ΔC25 was incubated with the scFv antibodies (1µg/ml). scFv binding was detected with an anti-His antibody and enhanced chemiluminescence. An anti-GST antibody was used to confirm a titration of GST-IRF-1 (wild type or ΔC25) had been immobilised to the microtitre plate. The results are given as relative light units (RLU) for scFv binding plotted against IRF-1 amount and are representative of 2 separate experiments. (B) As in A except that the scFv were immobilised and GST-IRF-1 was in the mobile phase; binding was detected using anti-GST.

Following two selection rounds, one domain-binding clone was identified from the monoclonal screen (outlined in red: figure 4.11A). Monoclonals were this time screened in a colorimetric ELISA, in which scFv binding is still detected with HRP-protein A, but instead of using chemiluminescence, HRP was quantified with its substrate TMB (3,3',5,5'-tetramethylbenzidine) which yields a coloured product. The N-terminal targeting antibody fragment was sequenced and also shown to only consist of a light chain, suggesting that the phage amplification procedure used in this study favours only short inserts. An ELISA against overlapping peptides encompassing the entire length of IRF-1 mapped the epitope of scFvN to amino acids 91 to 110 (encompassed by peptide 7), confirming its N-terminal specificity (figure 4.11B). Limited binding was also seen to peptide 18, which is more C-terminal (amino acids 256-275) and unrelated in sequence, but this was much less stable than that displayed for the N-terminal antigen. The scFvN was also shown to bind specifically to full-length IRF-1 in an ELISA, either when the antibody or IRF-1 was immobilised (figure 4.12).

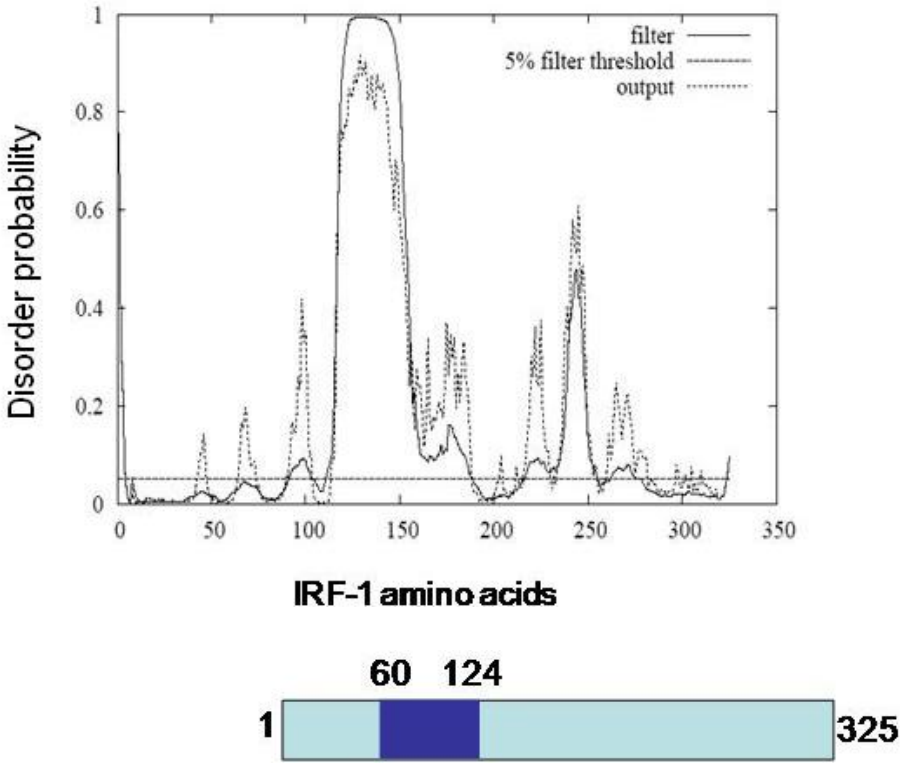

Figure 4.10: (A) Graphical representation of entropy predicted along the length of IRF-1. Created by Prof. Kathryn Ball using The DISOPRED server for the prediction of protein disorder [321]. **(B)** Diagrammatic representation of the N-terminal antigen, which spans IRF-1 amino acids 60-124.

A

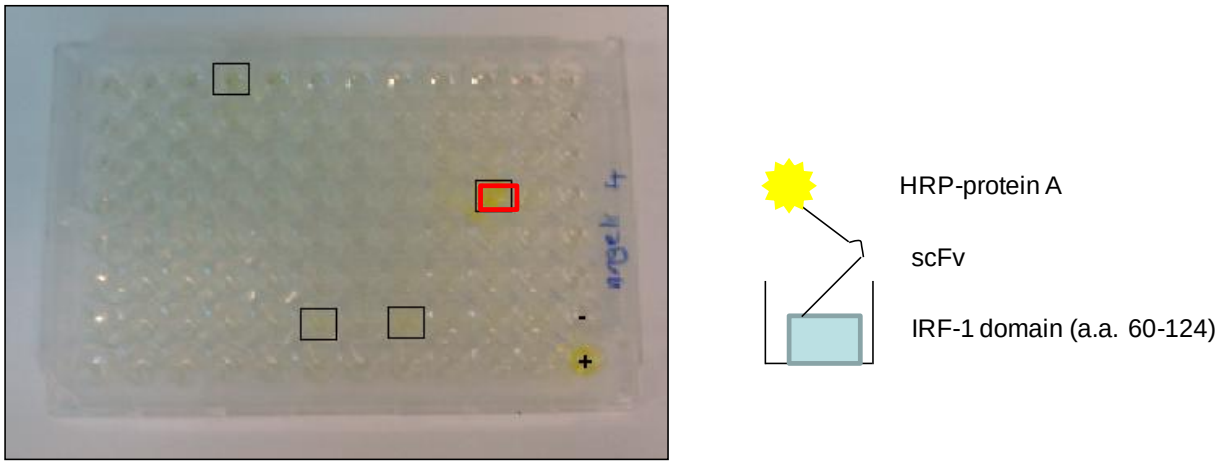

B

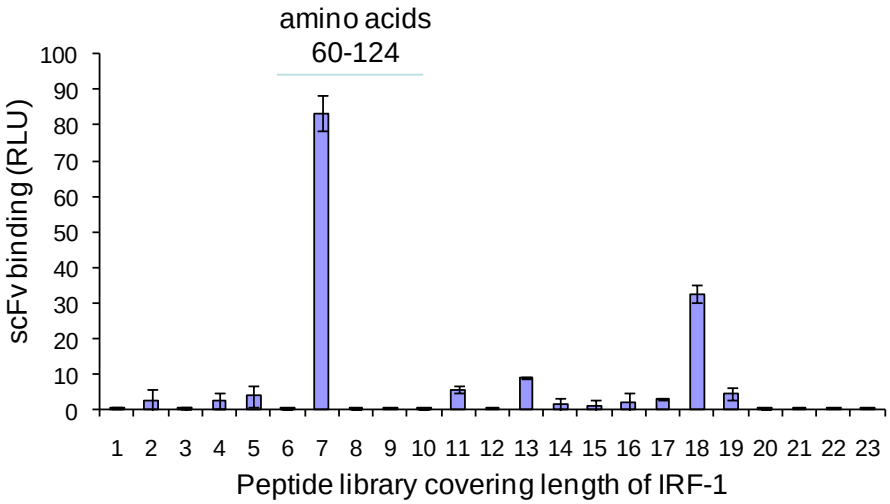

Peptide 7: IEEVKDQSRNKGSSAVRVYR

Peptide 18: YLLNEPEVQPTSVYGDFSCK

Figure 4.11: (A) (Left panel) Monoclonal scFv's secreted by phage-infected bacteria into culture media were incubated with GST-IRF-1. After extensive washing, bound scFv were detected using protein A-HRP and the coloured HRP substrate TMB. The clone selected for further analysis scFvN is outlined in red. Soluble scFv from 2nd round polyclonal phage and media from a culture in which scFv expression was not induced are used as controls in the bottom right wells; indicated with "+" and "-" symbols respectively. (Right panel) Schematic of scFv binding to full-length IRF-1 in an ELISA format. **(B)** Immobilised overlapping peptides covering the entire length of IRF-1 were incubated with scFvN (1µg/ml). Following extensive washing, scFv binding was detected with an anti-His monoclonal antibody and enhanced chemiluminescence. Sequence of peptides 7 and 18 shown in lower panel.

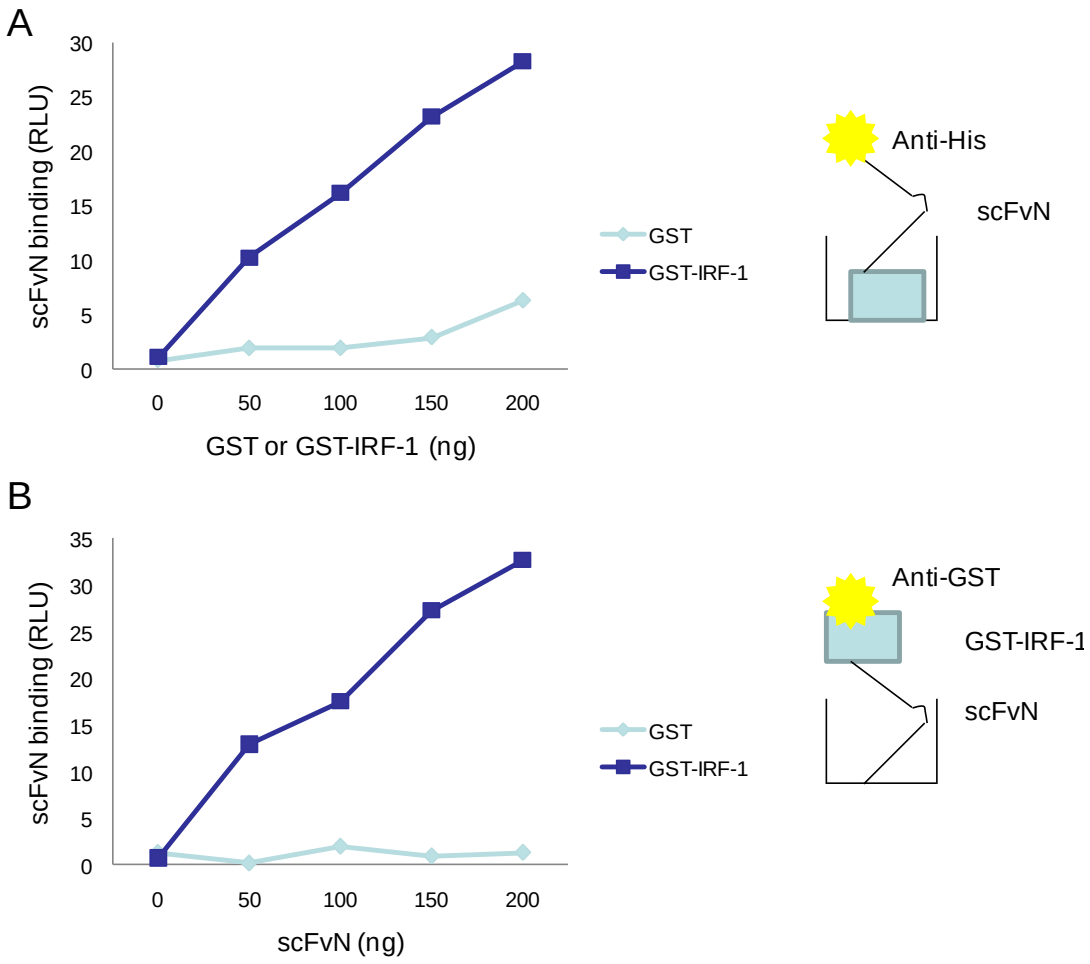

Figure 4.12: Binding of scFvN to IRF-1 under non-denaturing conditions. **(A)** A titration (0-200 ng) of immobilised GST-IRF-1 or GST was incubated with the scFvN antibody (1µg/ml). Binding was detected with anti-His/enhanced chemiluminescence. The results are given as relative light units (RLU) for scFv binding plotted against IRF-1 amount and are representative of 2 separate experiments. **(B)** As in A except that the scFv was immobilised and GST-IRF-1 or GST were in the mobile phase; binding was detected using anti-GST.

Owing to time limitations, no functional studies were carried out on the N-terminus of IRF-1; however scFvN remains a highly specific reagent available for future research into the activities of its target domain. In the experiments outlined in this thesis it has provided a useful control against which the anti-C terminal scFv could be compared.

4.2.6 Immunoprecipitation of IRF-1

The ability to precipitate IRF-1 from cell lysate would enable purification of the protein for further *in vitro* analysis and identification of co-precipitated binding partners. Therefore, to expand on the functionality of the scFv antibodies, their binding to IRF-1 in cell lysates was investigated. Each of the scFv (1 to 5 and N) were immobilised on Ni^{+} beads via their His tag. Lysate from HeLa cells transfected with either full length or ΔC25 IRF-1 was incubated with the scFv. Following several washing steps, scFv-bound protein was eluted by boiling the beads in SDS sample buffer and analysed on an SDS-PAGE gel (figure 4.13A). scFvN was able to co-precipitate both the full-length and truncated IRF-1. scFv 2, 3 and 5 specifically purified only the full-length protein which carried their C-terminal epitope. scFv 4 was able to bind both full-length and truncated IRF-1, supporting earlier indications that it can bind outside of the C-terminal 20 amino acids of IRF-1.

The numerous structure-function studies outlined in the introduction are based on purified or transfected protein. However, antibodies that bind the endogenous protein could eliminate the need for transfection. Therefore, untransfected HeLa cell lysate was incubated with each of the immobilised scFv and analysed as before (figure 4.13B). Under these conditions, scFv 1 could also immunoprecipitate IRF-1, as could scFv 3, 4, 5 and N, but scFv2 binding was lost. This suggests that epitope availability may vary between transfected and endogenous protein, highlighting the need for reagents that can target the endogenous form. scFv4 again exhibited low specificity, as it also co-precipitated the housekeeping protein GAPDH, which none of the other scFv bound.

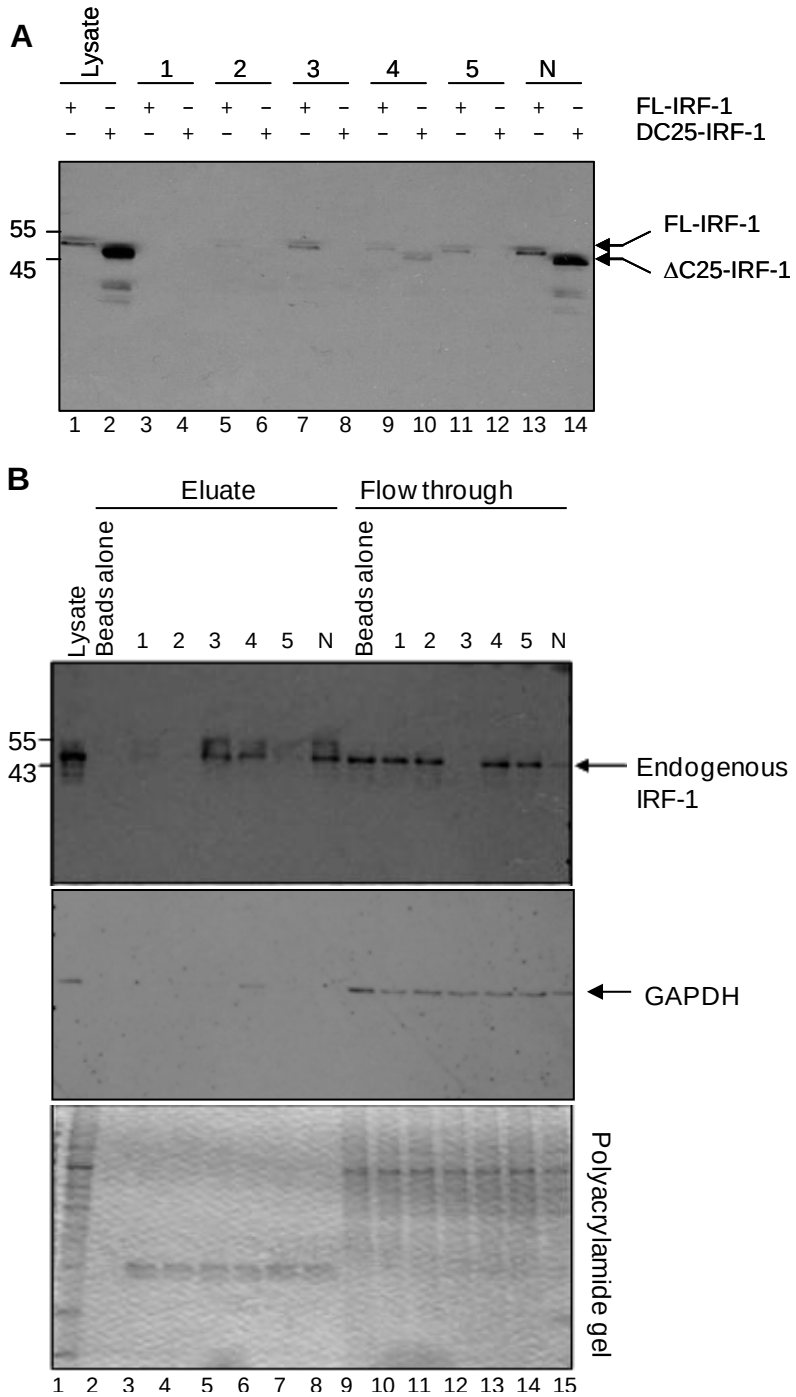

Figure 4.13: (A) scFv antibodies immobilised on Ni^{+}-NTA agarose beads were incubated with lysate (500 µg) from HeLa cells transfected with either WT or ΔC25 IRF-1 24 hours earlier. Bound proteins were analysed by SDS-PAGE/immunoblot and developed using anti-IRF-1 monoclonal antibody and enhanced chemiluminescence. **(B)** scFv antibodies immobilised on Ni^{+}-NTA agarose beads were incubated with lysate (500 µg) from untransfected HeLa cells. Following extensive washing, bound proteins were analysed by SDS-PAGE/immunoblot developed with either anti-IRF-1 or anti-GAPDH. Alternatively the gel was stained with colloidal blue (bottom panel). The results are representative of 2 independent experiments.

4.2.7 EMSA

An electrophoretic mobility shift assay (EMSA) can be used to determine an antibody's ability to bind to its target protein in complex with DNA. As most of IRF-1 activities are mediated through DNA binding, a scFv that could attach to promoter-bound IRF-1 may be able to affect its intracellular function. As scFv3 could bind endogenous IRF-1 from cell lysates, it appeared to be the best candidate for cell based studies using the C-terminal intracellular antibodies. Levels of scFv and the P^{32}-labelled DNA probe, which consisted of four IRF-1 binding elements (ISRE), were kept constant, and IRF-1 was increased. The EMSA established that scFv3 could bind an IRF-1:DNA complex producing a 'supershift' (figure 4.14 lanes 12-14). Although scFvN had previously shown it was efficient at capture of endogenous IRF-1 from detergent soluble lysates (figure 4.13), it displayed no significant binding to the IRF-1:DNA (figure 4.14 lanes 4-6). Consistent with its low relative affinity for IRF-1 when compared to scFv3, the scFv2 antibody had only a weak band-shift activity in the EMSA (figure 4.14 lane 9). Importantly the for later development of IRF-1 specific intracellular antibodies, none of the three scFv tested bound DNA (figure 4.14 lanes 3, 7 and 11)

4.2.8 Epitope mapping

The data presented in the previous sections indicate that all five anti-C terminal IRF-1 single chain antibodies bind to denatured IRF-1 with a similar relative affinity, but show considerable variation in their ability to bind both recombinant and cellular IRF-1 under non-denaturing conditions. This implies that although all 5 C-terminal scFv target the last 20 amino acids of IRF-1, their precise epitope is reliant on different sequence specificities within this region. To map the amino acid residues essential for binding for scFv 1-5, a library of peptides based on the C-terminal 20 amino acids of IRF-1 was generated in which the amino acids were sequentially mutated to an alanine for use in an ELISA. In agreement with their varied performance in earlier assays, the results revealed no two scFv bound to precisely the same epitope (figure 4.15). However, scFv3 and scFv5, which both specifically captured cell-expressed full-length IRF-1 (figure 4.13), required the proline residues at positions 322 and 325 (figure 4.15C).

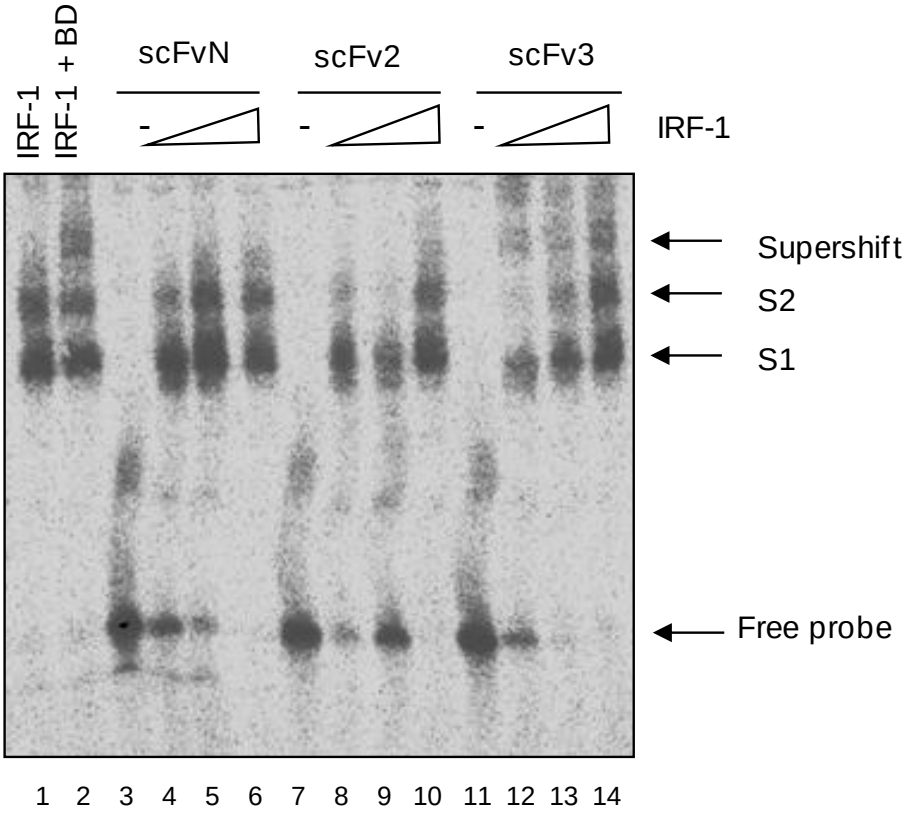

Figure 4.14: In this EMSA purified GST-IRF-1 (200 ng) bound a ^{32}P-labelled DNA probe (consisting of 4 x ISRE; Lane 1), to give a banding patterning consisting of two IRF-1:DNA complexes, labelled S1 and S2. DNA-bound IRF-1 is supershifted by a commercial anti-IRF-1 antibody (Lane 2). scFvN, 2 and 3 were used at 200 ng per reaction with a titration of IRF-1 (0, 50, 100 and 200 ng; lanes 3-6, 7-10 and 11-14). The data are representative of at least 3 independent experiments

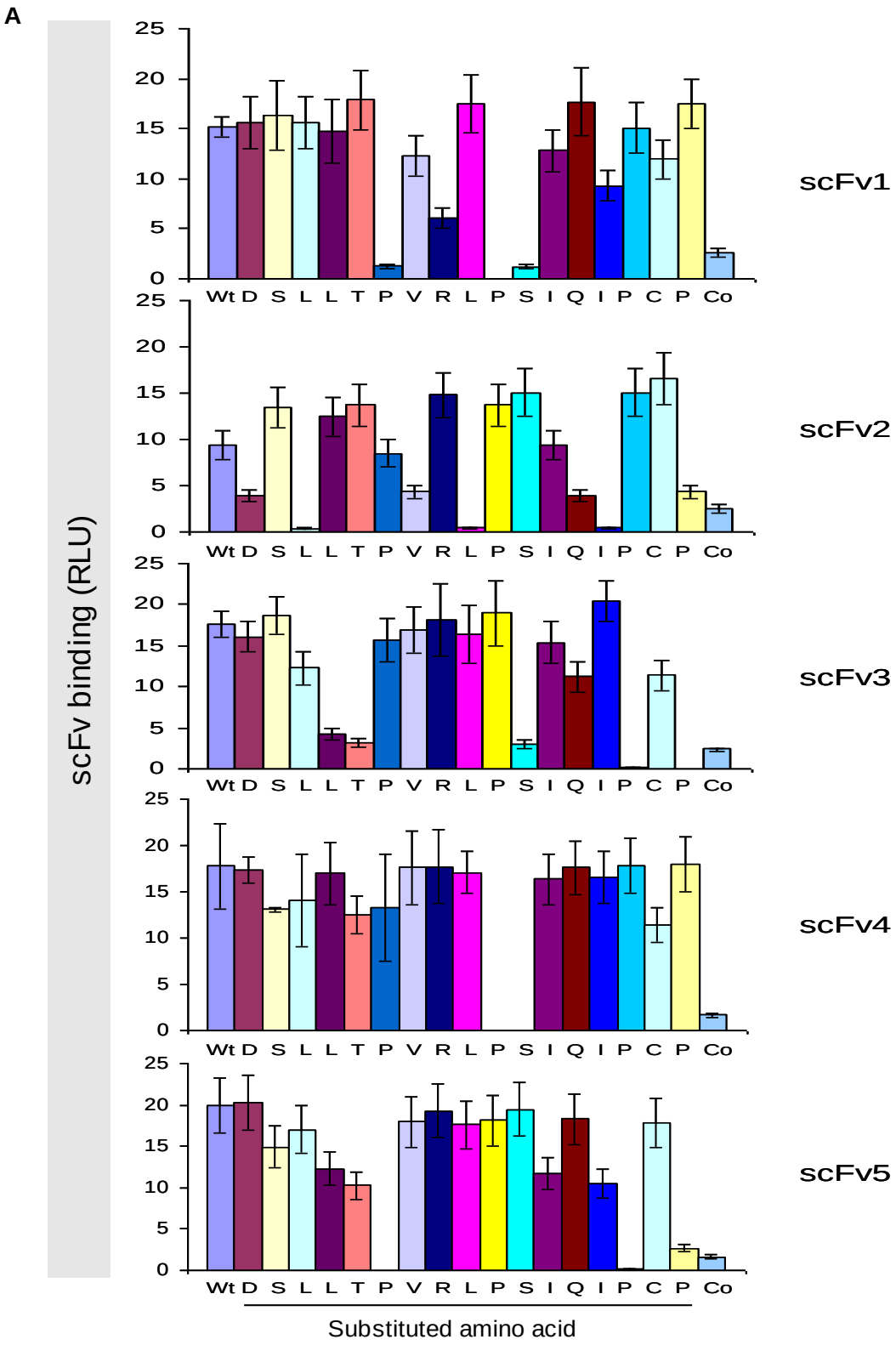

Figure 4.15: Continued and described on next page.

B

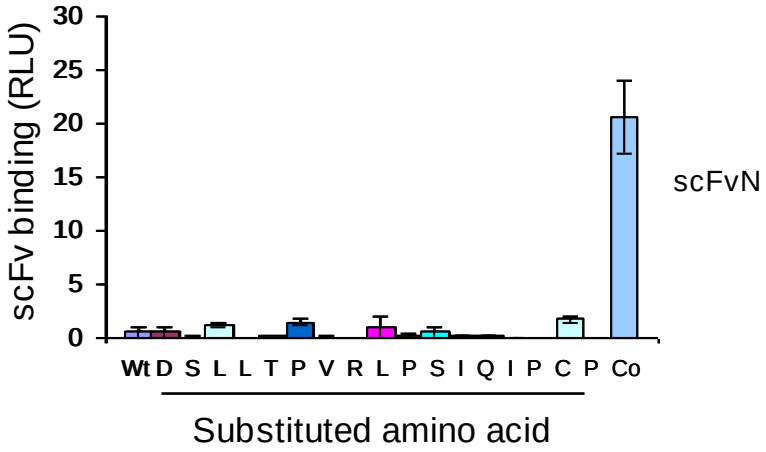

C

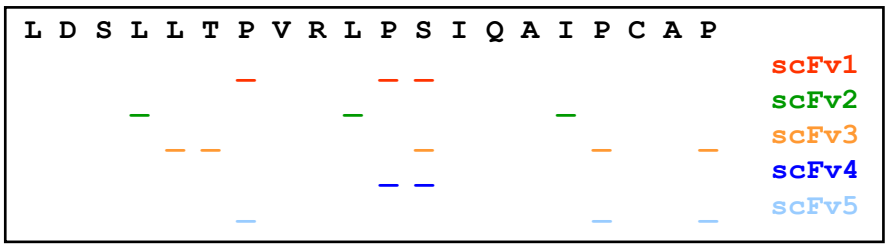

LDSLLTPVRLPSIQAIPCAP scFv1
LDSLLTPVRLPSIQAIPCAP scFv2
LDSLLTPVRLPSIQAIPCAP scFv3
LDSLLTPVRLPSIQAIPCAP scFv4
LDSLLTPVRLPSIQAIPCAP scFv5

Figure 4.15: Identification of scFv epitopes. **(A)** Immobilised biotinylated peptides, comprising of an alanine scan of the C-terminal 20 amino acids of IRF-1 (306 to 325) LDSLLTPVRLPSIQAIPCAP, were incubated with 1µg/ml of scFv 1 to 5. scFv binding was detected with anti-His. A peptide containing the epitope for scFvN is labelled as Co (for control, and is peptide 7 in figure 4.11B); the data are representative of 2 independent experiments. **(B)** As in A except using scFvN. **(C)** Diagrammatic representation of the amino acid motifs targeted by scFv 1 to 5.

scFv3's higher relative affinity for IRF-1 consistently observed in earlier experiments was supported by its requirement for three additional residues (Ser317, Leu310 and Thr311), compared to scFv5 requirement for only one other residue (Pro312). scFv4's non-specific nature was explained by its extremely limited epitope consisting of only two adjacent amino acids Pro316 and Ser317, a sequence found outside the C-terminus in the main body of IRF-1 and in GAPDH. As expected, scFvN did not bind to any of the C-terminal peptides but was specific for its epitope from the N-terminal domain of IRF-1 (Figure 4.15B).

Together, the characterisation of scFv antibodies selected against the C-terminal 20 amino acids of IRF-1 reveal differing specificities for binding to the full-length protein in non-denaturing conditions. In particular scFv3 was able to efficiently deplete endogenous IRF-1 from cell lysate and bind to an IRF-1:DNA complex.

4.3 Discussion

This chapter outlines the *in vitro* characterisation of 5 scFv targeting the extreme C-terminus of IRF-1. An N-terminus-targeting scFv (scFvN) is also described that can be used as a control in further anti-IRF-1 scFv analysis. Although scFvN is not used to study the N terminus of IRF-1 in this thesis, it provides a useful reagent for such studies in the future. This chapter also describes adaptation of the Tomlinson phage display library for use against peptide targets, and shows that scFv developed against peptides still have the potential to bind stably to their epitope in the context of a full-length protein. The ability of the scFv3 to supershift DNA-bound IRF-1 indicates that it could be used in the future to study the ability of IRF-1 to dimerise on target promoters. Furthermore, as it can deplete endogenous IRF-1 from cell lysate it could be used to immunoprecipitate protein complexes containing IRF-1 (see chapter 6).

Having selected only single domain antibodies has both advantages and disadvantages. These antibodies may have a lower affinity compared to scFv comprising of heavy and light chains. It has previously been shown that the cleft between these two domains can form an antigen binding pocket [322]. However numerous studies on functional single domain antibodies have shown that they can exhibit specific binding activity [323, 324] and that the light chain can prove to be a

highly active paratope [198, 325]. Additionally, single domain fragment stability is independent of the VH-VL interface and less reliant on the flexible glycine-serine linker that connects the heavy and light chain in a scFv.

Single domain antibodies consisting only of heavy domains are found naturally in some vertebrates [193, 215] and have are already extensively investigated for their technological and clinical applications [195, 217]. However, the potential of isolated light chains has only slowly gained recognition. Over the last 5 years free IgG light chains have been described as having a physiologically relevant role to play in mast cell activation during hypersensitivity responses [326-328] and have been detected at elevated levels in patients with autoimmune diseases [329]. The potential for light chains to be used as low molecular weight, high affinity, antigen binders is supported by biochemical studies, which demonstrate that isolated antibody light chains are capable of specifically binding target antigens [330-332]. The reduction of antibodies to minimal binding regions could increase their usefulness. Smaller proteins may be able to target binding pockets inaccessible to their larger parent antibodies. It has already been shown that single domains can be further reduced by the deletion of non-essential complementarity determining regions (CDRs) [333]. The affinity of such minimal binding domains will depend on their ability to fold correctly and maintain a stable structure, even when expressed cytoplasmically. The screen for scFv developed here, consisting of affinity testing in a range of platforms (based around immunoblot and ELISA assays) following cytoplasmic expression, has proven effective for detection of stable single domain antibodies with a high target specificity.

The selected monoclonal scFv characterised for binding to IRF-1 (1-5 and N) were derived from two different antibody phage display libraries, but the culture times between selection were the same. It is likely that the duration of the bacterial amplification step favoured selection of short clones, i.e. those that encoded only single domains. This may have added a selective pressure, not based on affinity, to the phage display system. In order to optimise this technique so that selection of clones is based solely on their affinity, shorter amplification times could be attempted in the future.

The development of a C-terminal antigen relied on a peptide antigen. However, there was no guarantee that the C-terminal 20 amino acids of IRF-1 would have a similar conformation in isolation to that displayed within the context of the full length protein. This may have reduced the number of clones that gave a positive signal in the dot blot screen. Another method for targeting the C-terminus would be to initially select scFv that can bind to the full length protein, and then from this reduced pool select for and discard those that bound a C-terminally truncated protein (IRF-1 ΔC20). This would mean keeping and amplifying phage that showed low affinity for the truncated protein and were thus eluted with PBS. However, the disadvantage of this strategy would be that all phage selected for binding to full-length IRF-1 may target particularly "sticky"/hydrophobic regions outside of the extreme C-terminus, so that the second screen for phage that cannot bind the truncated protein would reveal no positive clones. It appears in this study that the isolated C-terminal peptide does contain epitopes exposed in native, full-length IRF-1, and that screening of a sufficiently large number of antibody fragments enables identification of a small number of scFv able to target these epitopes.

5 Development of an activating anti-IRF-1 intrabody

5.1 Introduction

Following the publication of the human genome, investigation of gene function and regulation must now be systematically approached. There is a clear need for molecular tools that can act on a gene's functional products: proteins. Elucidation of the protein phenotype in intracellular complexes can be undertaken with the use of small molecules capable of specifically binding a target protein within the cell. Such small molecules can take the form of non-protein chemical compounds [334, 335], peptide or oligonucleotide aptamers [336] and proteins (such as intracellular antibodies, see below). This chapter details the characterisation of single chain intracellular antibodies (intrabodies) targeting the extreme C-terminus of IRF-1. It goes on to show that these intrabodies can modulate IRF-1's transcription factor function and stability.

5.1.1 Intrabodies

Single chain intrabodies have previously been used to modulate the functions of their target antigens: by altering intracellular localisation [231, 235-237], blocking enzyme activity, [230] inducing a transactivating conformational change [239, 240], disrupting normal protein-protein [227, 240-242] or DNA-protein interactions [227]. Such antibodies are expressed in the mammalian cell cytoplasm and screened for intracellular efficacy.

As discussed in the last chapter, expression of intrabodies in the reducing environment of the cytoplasm results in inefficient or absent disulphide bond formation [232]. Misfolded antibody fragments can have a reduced solubility, a shorter half life and tendency to aggregate triggering proteosomal degradation [233]. However, intrabodies fully functional under reducing conditions have been developed, and it has been proposed that antibodies fragments with an intrinsically stable amino acid sequence can fold properly in the absence of disulfide bond formation [233, 234, 337]. There are currently no consistent rules for predicting

intrabody folding and function [338], therefore identification of those able to modulate the activity of a target protein relies on screening numerous candidates.

Antibodies that do not show strong *in vitro* binding can still exhibit a specific, reproducible and strong modulating affect on their target antigen following intracellular expression [239, 339]. Preselection has allowed researchers to identify rare, stable scFvs from large scFv-phage libraries. Such strategies can involve selection of antibody fragments that are functional either: 1) following cytoplasmic bacterial expression [314, 315] (and as described in chapter 4), 2) within the yeast-two hybrid system [337, 340] or 3) under *in vitro* denaturating and reducing conditions [341]. However, such antibodies must still be screened again to validate their functionality within the mammalian cell. A long half life and high steady state levels of antibody accumulation have been described as critical for a functional intrabody [248], however this may not prove to be the case for target proteins with very short half lives, such as IRF-1. Furthermore low levels of antibody expression may decrease cellular toxicity caused by an exogenously expressed protein.

5.1.2 IRF-1 target genes

The functional studies described in this chapter examine the effect of intrabody binding on IRF-1's degradation and its regulation of target promoters. To study modulation of IRF-1's activities as a transcription factor, reporter constructs based on the *TLR3, IFN-β, CDK2, TRAIL* and *IL-7* promoters are used, and the effects on endogenous ISG20, PKR and CDK2 protein levels are observed.

5.1.2.1 TLR3

The TLR3 (Toll-like receptor 3) recognises double stranded RNA following viral infection and stimulates downstream regulators of the immune response, such as NF-κB and type I interferons [342, 343]. IRF-2 has been shown to be constitutively bound to ISRE (interferon response elements) within the *TLR3* promoter, whereas IRF-1 only binds in response to certain stimuli, such as ectopic IFN-β expression [344]. IRF-1 has shown to efficiently upregulate a luciferase reporter construct based on the *TLR3* promoter [344].

5.1.2.2 IFN-β

IFN-β (interferon-β) is a type I interferon that plays a role in anti-viral and anti-tumour response and was the first target gene of IRF-1 identified [1, 2]. Electromotility shift assays confirmed that IRF-1 could bind directly to the *IFN-β* promoter and helped define the interferon regulatory factor binding site: ISRE [1]. It was subsequently demonstrated that IRF-1 could increase transcription from *IFN-β*-reporter gene constructs [5]. *De novo* synthesis of IRF-1 has been shown to be necessary but insufficient for viral-mediated induction of *IFN-β* in certain cell lines, indicating that a further post-translational step is required [67].

5.1.2.3 CDK2

CDK2 (cyclin dependent kinase 2) is a serine/threonine kinase and a catalytic subunit of the cyclin-dependent protein kinase complex. CDK2 activity during the cell cycle is restricted to the S phase during which DNA replication occurs and the preceding G1 gap when the cell increases in size. This protein associates with cyclin E to regulate progression from G1 to S phase [345] and with cyclin A during DNA replication [346]. Cyclin association activates the CDK2 kinase, and in turn CDK2 phosphorylates target proteins involved in cell cycle progression. For example, CDK2/Cyclin E phosphorylates its own suppressor, p27, triggering p27 degradation by the proteasome [347]. Phosphorylation of another target, nucleophosmin, has been shown to be essential for centrosome duplication [348]. Interestingly, nucleophosmin is also involved in post-translational regulation of IRF-1 [144]. IRF-1 has been shown to inhibit *CDK2* promoter activity in a dose-dependent manner [62]. The region of the *CDK2* promoter required for IRF-1 repression was mapped, but did not display homology to the classic IRF binding site (ISRE). The authors did not therefore test for direct binding of IRF-1 to this site. However, the transcription factor Sp1, an activator of CDK2 expression, was shown to bind this region of the promoter. Exogenous expression of IRF-1 was shown to reduce Sp1-induced CDK2 expression, leading the authors to conclude that IRF-1 repressed CDK2 by interfering with SP1-mediated induction [62].

5.1.2.4 TRAIL

TRAIL (Tumor necrosis factor-Related Apoptosis-Inducing Ligand) is a cytokine that has been shown to induce apoptosis selectively in cancer cells, while normal cells remain insensitive to TRAIL-mediated apoptosis [349]. TRAIL homotrimers interact directly with four different cell surface receptors: death receptors DR4 and DR5 [19, 350] and decoy receptors DcR1 and DcR2 [19, 351, 352]. Activation of DR4 and 5 by TRAIL induces apoptosis [353] whereas the decoy receptors lack functional death domains and can therefore cannot stimulate cell death [19, 351, 352]. The decoy receptors are primarily expressed in normal tissues and absent from tumour cells [351]. Thus, it has been proposed that in these cells they compete with DR4 and DR5 for TRAIL binding, and in this way inhibit TRAIL-mediated apoptosis [349]. IRF-1 enhances TRAIL expression when exogenously expressed and has been shown to be recruited to the *TRAIL* promoter following exposure of cells to retinoic acid [90] or IFN-α [354]. Additionally, siRNA knockdown of IRF-1 reduces TRAIL expression and cell death in a human bladder cancer cell line [354], supporting TRAIL's role as a mediator of IRF-1 induced apoptosis.

5.1.2.5 IL-7

IL-7 (Interleukin-7) is a cytokine that plays a non-redundant role in lymphocyte development, proliferation and homeostasis [355-357]. *IL-7* and *IL-7 receptor* (*IL-7R*) null mice have been shown to have impaired B- and T-cell development [355, 356]. In support of these findings, injection into mice of an antibody able to block binding of IL-7 to its receptor was seen to cause a significant reduction in mature T- and B-cell numbers [358] and administration of human IL-7 to mice caused an increase in lymphocyte proliferation [359]. IL-7 also stimulates progenitor NK (natural killer) cell maturation [360] and protects NK cells from apoptosis [357]. Its proliferative effects have been linked to the down-regulation of the CDK2-repressor p27 [361]. IRF-1 is recruited to the *IL-7* promoter following IFN-γ treatment [297]. Additionally, exogenous expression of IRF-1 was able to induce expression from an IL-7-luciferase reporter construct, whereas siRNA knockdown of IRF-1 suppressed endogenous IL-7 expression [297]. Taken together, these results suggest IRF-1 could play a role in lymphocyte proliferation, in combination with its previously documented role in lymphocyte differentiation [43, 49].

5.1.2.6 ISG20

ISG20 (Interferon Stimulated exonuclease Gene 20kDa) has been characterised as a 3′-5′ exonuclease with a preference for RNA over DNA [362]. Its expression is induced by viral infection, and its overexpression has been show to trigger an anti-viral response [363, 364]. Overexpression of ISG20 conferred resistance to infection from three different RNA genomic viruses on HeLa cells [363]. This anti-viral activity was lost following mutation of the exonuclease domain of ISG20 [363], indicating that the protein's ability to degrade RNA was central to its anti-viral activity. Furthermore, ISG20 was seen to interfere with mRNA synthesis of Vesicular Stomatitis Virus (VSV) [363]. IRF-1 has been shown to mediate ISG20 induction in response to interferons (types I and II) and double stranded RNA [365, 366]. *ISG20* is therefore a well validated IRF-1 target gene that plays an important role in innate immunity.

5.1.2.7 PKR

PKR (Protein Kinase activated by double stranded RNA) is a serine/threonine kinase activated by binding of double stranded (ds) RNA to two N-terminal RNA binding domains [367], which causes dimerisation of the protein via its kinase domains [368]. Once activated, PKR phosphorylates the translation initiation factor eIF2, thus inhibiting protein synthesis [369]. During translation initiation, eIF2 binds the met-$tRNA_i$ in a GTP-dependent manner and recruits it to the 40S ribosomal subunit; this complex (which includes other eIFs) scans mRNA in a 5' to 3' direction until it reaches the AUG initiation codon [370]. At this point eIF2-bound GTP is hydrolysed, and GDP-eIF2 detaches from the 40S. The 40S can then associate with the 60S ribosomal subunit to form the 80S translation initiation complex which is able to form the first peptide bond [370]. The eIF2 guanine nucleotide exchange reaction is catalyzed by eIF2B and inhibited by phosphorylation of subunit α of eIF2 by PKR [371]. The phosphorylation of eIF2 by PKR therefore also inhibits translation initiation. Although the PKR promoter does contain an ISRE, an interaction between the promoter and IRF-1 has not been confirmed [372]. However, PKR protein levels have been shown to be reduced in IRF-1 deficient embryonic fibroblasts and increased following exogenous expression of IRF-1 [373].

These proteins are a small representation of IRF-1's role in mediating immune response and inhibition of cell growth. Excluding PKR, the ability of IRF-1 to modulate expression of these proteins has been well characterised, and they demonstrate IRF-1's ability to both activate and repress transcription.

5.2 Results

Three monoclonal scFv were brought forward for characterisation as intrabodies: scFv 2 and 3 against IRF-1's C-terminal 20 amino acids and scFvN which targets the N-terminal putative homodimerisation sub-domain (amino acids 60-124). During the *in vitro* characterisation of the scFv described in chapter 4, scFv3 formed the most stable interaction with native IRF-1 and was also able to supershift IRF-1 in complex with DNA. scFv2 was chosen to act as a control for scFv3 as they are highly similar in sequence (figure 5.1C), with only five variant amino acids through the CDR2 and CDR3 regions, but have differing affinities and antibody specificities within peptide C2 (figure 4.15A). scFvN was used as a second control antibody, in preference to a non specific scFv, as it again has good sequence conservation with scFv3 (Figure 5.1C) but binds outwith the IRF-1 C-terminal domain.

These scFv were amplified from their original phagemid vectors with primers that added a kozac consensus sequence for mammalian expression within the Gateway system (Invitrogen). A GFP tag was added to each scFv, as specific and high affinity antibodies targeting this tag were available. The scFv still carried the His-Myc tags that were attached to them during the initial phage display selection. Although no fluorescent microscopy studies are included in this thesis, the GFP-scFv provide reagents for such studies in the future.

5.2.1 The scFv3 intrabody enhances IRF-1-induced transcription

High level expression of intracellular scFv has previously been associated with misfolding, aggregation and localisation to inclusion bodies [374]. If the GFP-scFv had been misfolded in the mammalian cell cytoplasm, they would presumably have been rendered inactive and incapable of binding, and thereby modulating, intracellular IRF-1. IRF-1's best characterised function is that of a transcription

factor. Therefore, the ability of the intrabodies to modulate IRF-1 activity in a TLR3-luciferase reporter assay was investigated. The *TLR3* promoter has been shown to contain IRF-1 response elements and to be upregulated in response to IRF-1 binding [344]. Each of the scFv intrabodies were transfected with a TLR3-luciferase reporter construct in either an endogenous IRF-1 background or with a constant level of transfected IRF-1 (Figure 5.1A). In cells untransfected with IRF-1, low level stimulation of the TLR3 promoter was seen with increasing scFv3 expression. It may be that scFv3 expression alone can in some way directly modulate the activity of this reporter construct or that this stimulation was mediated by endogenous IRF-1. Transfection of IRF-1 alone stimulated the TLR3 promoter, in agreement with previous findings [344], and this stimulation was strongly enhanced by scFv3 co-expression. Although expressed at comparable levels, scFv2 and scFvN did not produce such a pronounced increase in IRF-1 activity. Consistent with its weak C-terminal binding activity, scFv2 only mildly enhanced IRF-1-dependent stimulation of TLR3, and scFvN caused a slight decrease in TLR3 induction. Figure 5.1B confirms the expression of each GFP-scFv in this experiment.

It appears in figure 5.1 that scFv3 is able to stimulate IRF-1-mediated induction of TLR3. However, this induction must be shown to be dependent on IRF-1 binding to the TLR3 promoter. Furthermore, before any biological relevance can be attached to the modulation of IRF-1 activity by C-terminus targeting-intrabodies, it would be helpful to know if this effect is limited to *TLR3* induction or if it applies to any other promoters regulated by IRF-1. Therefore scFv3 was co-transfected with IRF-1 in the presence of TLR3, IFN-β and CDK2 promoter-luciferase constructs. IRF-1 has previously been shown to induce *IFN-β* and repress *CDK2* at a transcriptional level [5, 62]. As IRF-1 directly binds interferon response elements in the *TLR3* and *IFN-β* promoters, mutated luciferase constructs in which the IRF-1 binding sites are absent were used as controls. No such control was used for CDK2, as IRF-1 is not thought to repress expression of this gene by binding directly to its promoter [62].

A

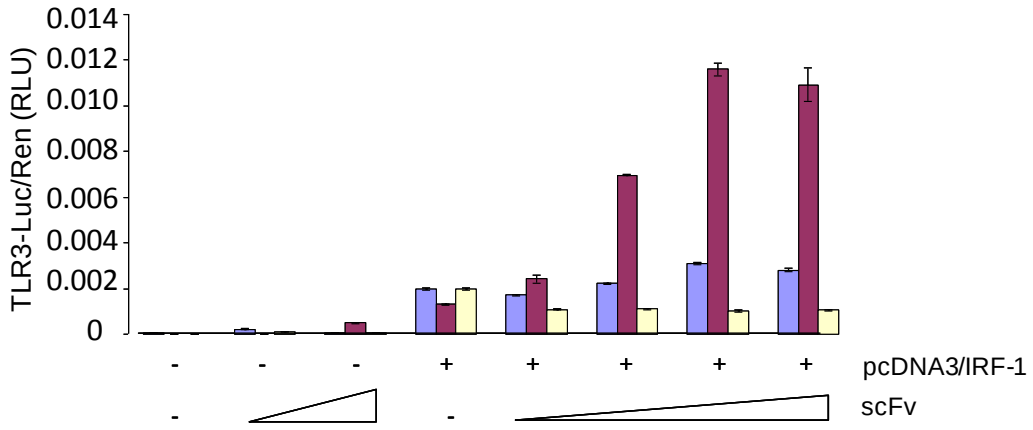

B

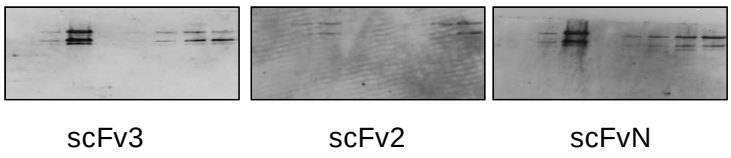

C

	CDR2	CDR3
scFv3	LIYNASSLQS	FATTYCQQGAYTPATFG
scFv2	LIYSASSLQS	FATTYCQQTASDPTTFG
scFvN	LIYAASGLQS	FATTYCQQSADSPSTFG

Figure 5.1: scFv3 intrabody activates IRF-1-dependent transcription. **(A)** A titration (0-250 ng) of GFP-tagged scFv2, scFv3 and scFvN were expressed in HeLa together with a TLR3(+ISRE)-luc reporter (120 ng), Rennila (60 ng) and IRF-1 (75 ng) as shown. DNA was normalised using an empty vector. Reporter gene activity was measured in relative light units (RLU) and is expressed as the ratio of Luc:Ren. The assays were carried out in duplicate; results are given as the mean ± half the range and are representative of at least 3 independent sets of experiments. **(B)** scFv protein levels were determined by SDS-PAGE/immunoblot and developed using an anti-GFP monoclonal antibody. **(C)** Sequence variation between scFv3, 2 and N. All variation was localised to CDRs 2 and 3.

In the presence of endogenous IRF-1 (figure 5.2 lanes 1 and 9), TLR3 and IFN-β reporter gene expression was reduced by mutating the IRF-1 binding site (ISRE) in these promoters (lanes 5 and 13), indicating that endogenous IRF-1 was able to bind and activate these promoters. scFv3 was seen to enhance this induction in the presence of the wild type but not the mutated promoters, supporting the hypothesis that scFv3 is acting in an endogenous-IRF-1 dependent manner in these cells. In the presence of transfected IRF-1, both the TLR3 and IFN-β promoters were induced and again this induction was reliant on IRF-1 binding directly to the promoter (i.e. it was abolished upon ISRE mutation) and enhanced by scFv3 co-transfection. Intrabody expression had no observable affect on IRF-1-mediated repression of the CDK2 reporter (lanes 17-20).

To confirm scFv3's C-terminal specificity, its ability to modulate the transcriptional activity of ΔC25 IRF-1 was investigated (figure 5.3). Stimulation of the TLR3 and IFN-β promoters in an endogenous IRF-1 background was again enhanced by scFv3 expression (figure 5.3: lanes 1 vs. 2 and 9 vs. 10). As has been previously observed, transfected ΔC25 IRF-1 was able to induce expression from these two promoters [303], but this stimulation was unaffected by scFv3 co-expression. It might be expected that a slight increase would be seen following scFv3 expression because endogenous IRF-1 is still present in the cell. However, as ΔC25 IRF-1 is expressed at a much higher level than endogenous IRF-1, it is likely that it can out-compete it for promoter binding. In agreement with published data, ΔC25 IRF-1 is unable to repress the CDK2 promoter [303], and this result was unaffected by scFv3.

The data given in chapter 4 indicate that *in vitro* scFv3 specifically targets the C-terminal 20 amino acids of IRF-1, binds stably to endogenous IRF-1 and can also bind IRF-1 in complex with DNA. Figures 5.1, 5.2 and 5.3 indicate that these characteristics are maintained following intracellular expression.

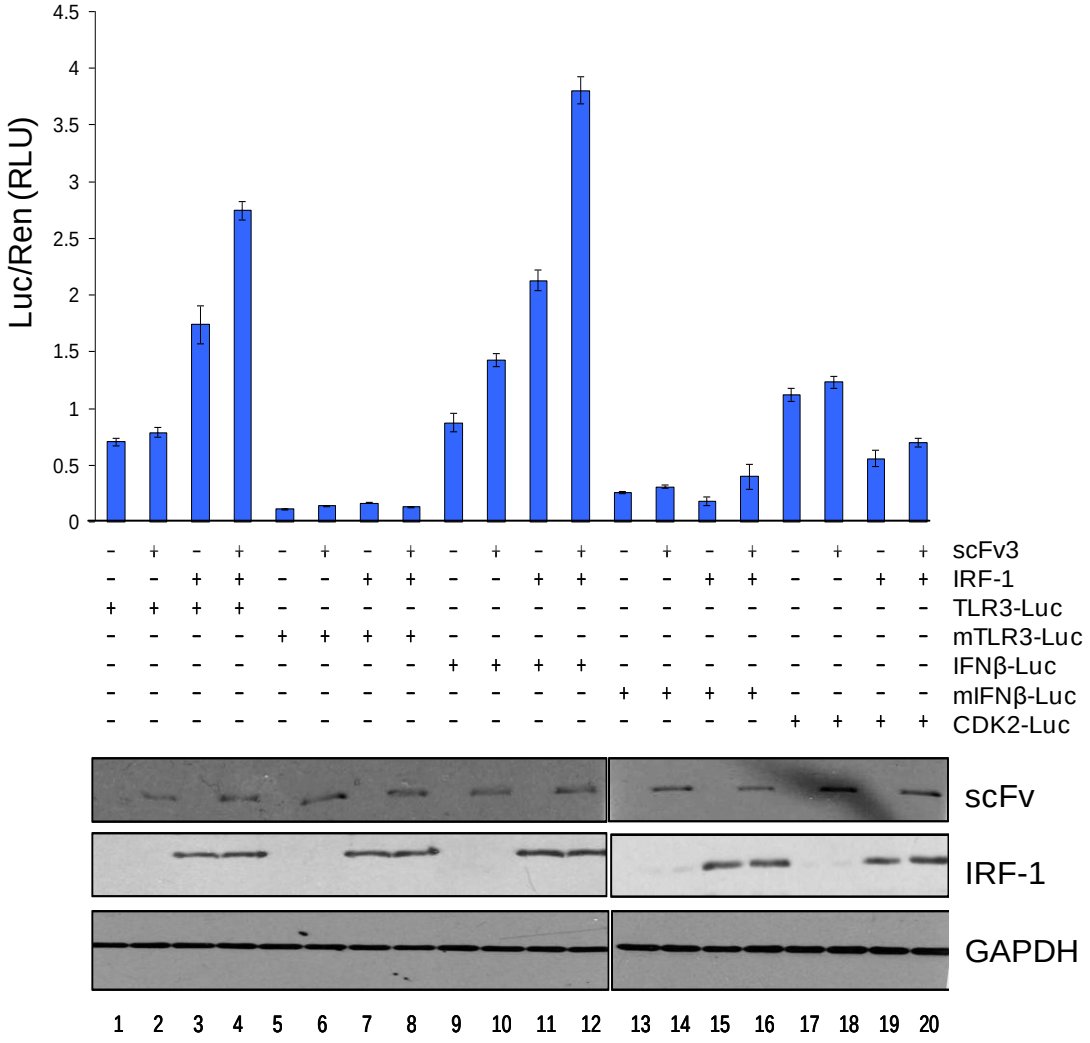

Figure 5.2: HeLa cells were transfected with Rennila (60 ng) and either TLR3(+ISRE), mTLR3(-ISRE), IFN-β(+ISRE), mIFN-β(-ISRE) or CDK2-luciferase reporter constructs (120 ng), plus IRF-1 (100 ng) and scFv3 (100 ng) as indicated. Reporter gene activity was measured in relative light units (RLU) and is expressed as the ratio of Luc:Ren. The assay was carried out in duplicate; results are given as mean ± half the range and are representative of at least 2 independent sets of experiments.

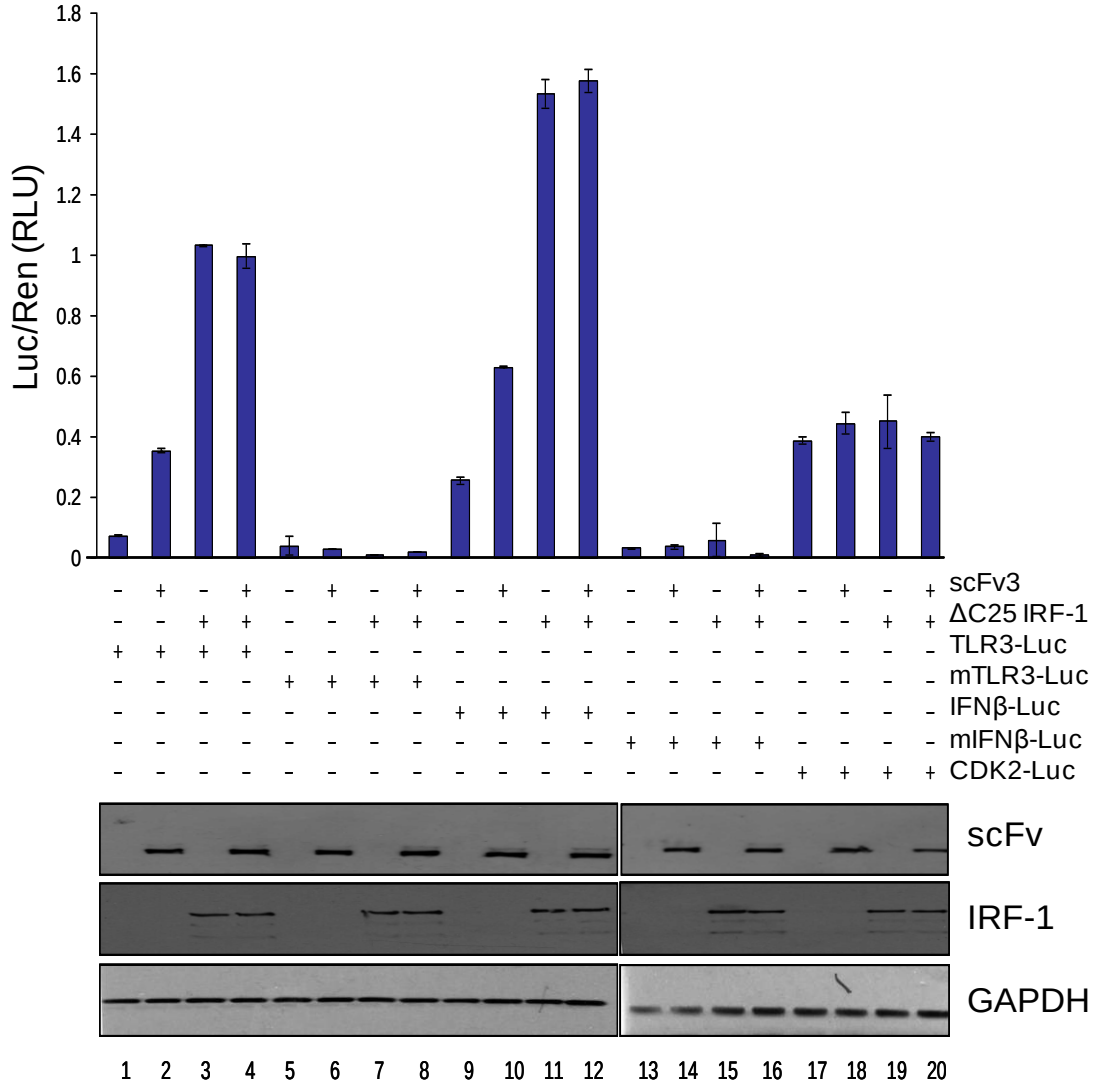

Figure 5.3: HeLa cells were transfected with Rennila (60 ng) and either TLR3(+ISRE), mTLR3(-ISRE), IFN-β(+ISRE), mIFN-β(-ISRE) or CDK2-luciferase reporter constructs (120 ng), plus ΔC25 IRF-1 (100 ng) and scFv3 (100 ng) as indicated. Reporter activity was determined as in figure 5.2. The assay was carried out in duplicate; results are given as mean ± half the range and are representative of at least 2 independent sets of experiments.

The data presented in figures 5.2 and 5.3 (lanes 2 and 10) suggest that scFv3 can regulate the transcriptional activity of endogenous as well as exogenous IRF-1. To verify the effect of scFv3 on promoter induction in the absence of exogenous IRF-1 and to investigate the dose-dependency of this effect, a titration of scFv3 and scFvN was co-transfected with either the TLR3 (figure 5.4) or IFN-β (figure 5.5) reporter. Under these conditions, scFv3 increased luciferase production from both the TLR3 and IFN-β promoters by 4-5 fold at the peak. In contrast, although expressed at similar levels to scFv3, scFvN had no significant effect on IRF-1 activity on either of the promoters used. scFv3's ability to activate endogenous IRF-1 was also confirmed for reporters constructs based on the IRF-1-responsive promoter regions of TRAIL and IL-7 (figure 5.6). scFv3 was able to activate the wild type reporters (+ISRE) but not mutant constructs (-ISRE) that were previously been shown to be defective in IRF-1 binding [90, 297]. As before, scFvN had no significant effect on reporter construct activation.

Next, the scFv's ability to enhance transcription of endogenous IRF-1 targets was investigated. This was done by observing the protein levels of endogenous ISG20, PKR and CDK2 following transfection of HeLa cells with a titration of scFv3, 2 or N (figure 5.7). An increase in the levels of ISG20 and PKR, which correlated with increasing amounts of scFv3, indicated that intrabody-activated IRF-1 can bind and induce transcription from endogenous target promoters. scFv2 and scFvN had no affect on ISG20 or PKR. Additionally, in agreement with data from the reporter assays (figure 5.2), CDK2 protein levels remained unaffected by any of the intrabodies (figure 5.7). Overall, the activity of scFv seen in these assays supports the conclusion that a sufficient quantity of the cytoplasmically-expressed scFv3 is correctly folding into a conformation capable of binding its intracellular target antigen. One interpretation of the data presented here, showing that the scFv3 intrabody can significantly increase IRF-1's transcriptional activity, is that the C-terminus of the endogenous proteins is rate-limiting for IRF-1-mediated gene activation and that the intrabody functions by relieving this intrinsic negative regulation.

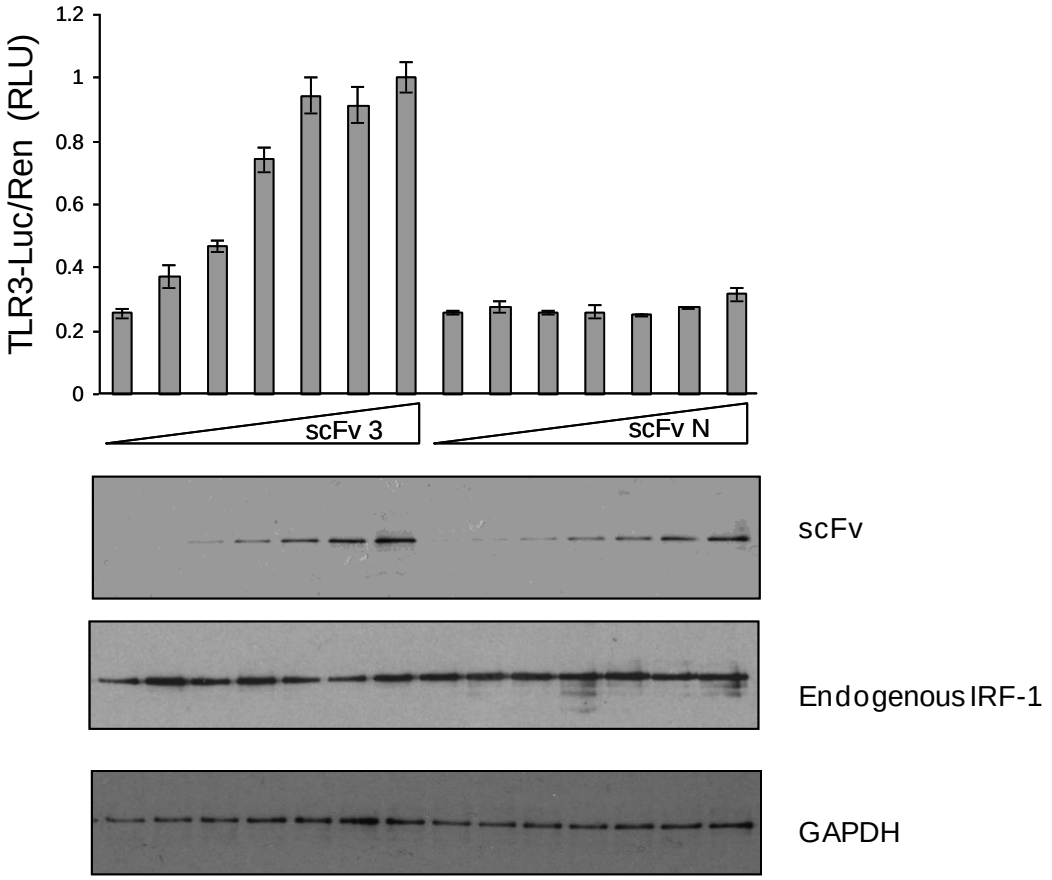

Figure 5.4: HeLa cells were transfected with a titration of scFv3 or scFvN (0-250 ng) plus Renilla (60 ng) and TLR3(+ISRE)-luc (120 ng). Reporter activity was determined as in figure 5.2. The assay was carried out in duplicate; results are given as mean ± half the range.

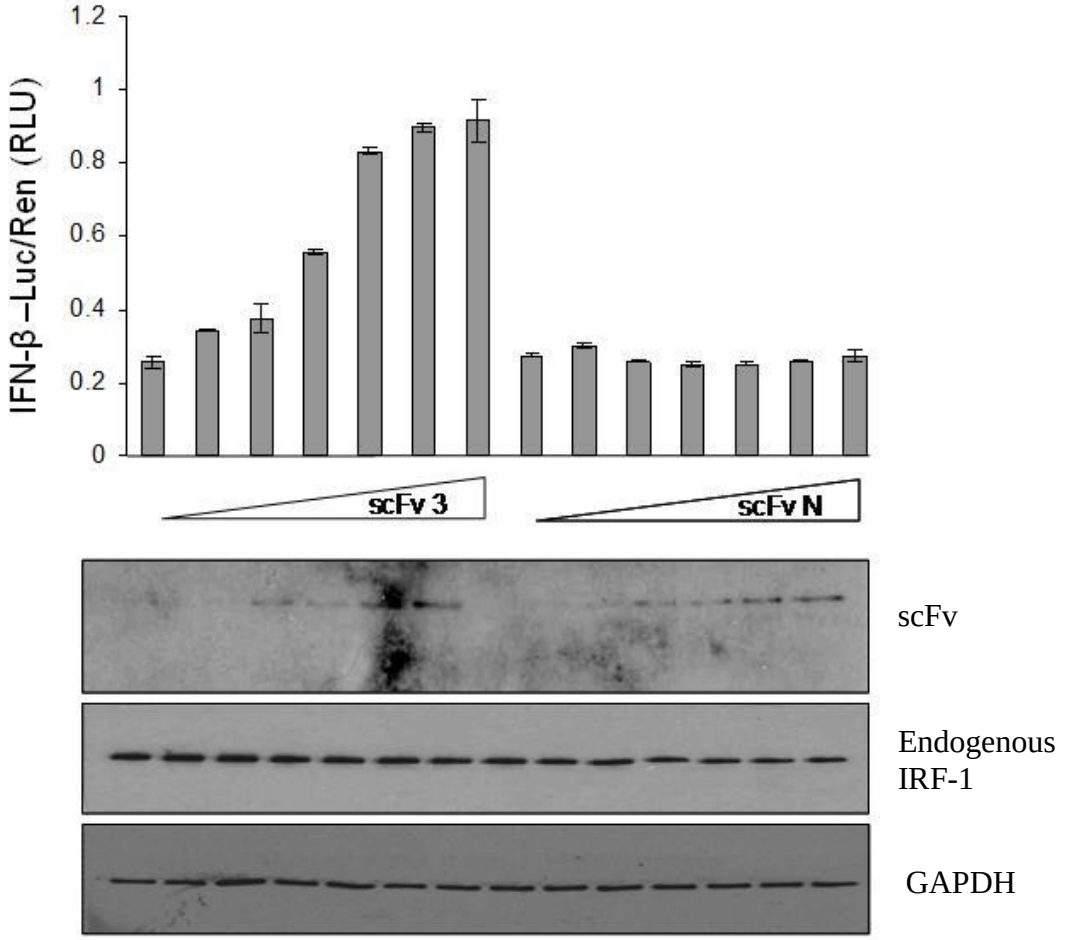

Figure 5.5: HeLa cells were transfected with a titration of scFv3 or scFvN (0-250 ng) plus Renilla (60 ng) and IFN-β(+ISRE)-luc (120 ng), and reporter activity was determined as in figure 5.2. The assay was carried out in duplicate; results are given as mean ± half the range.

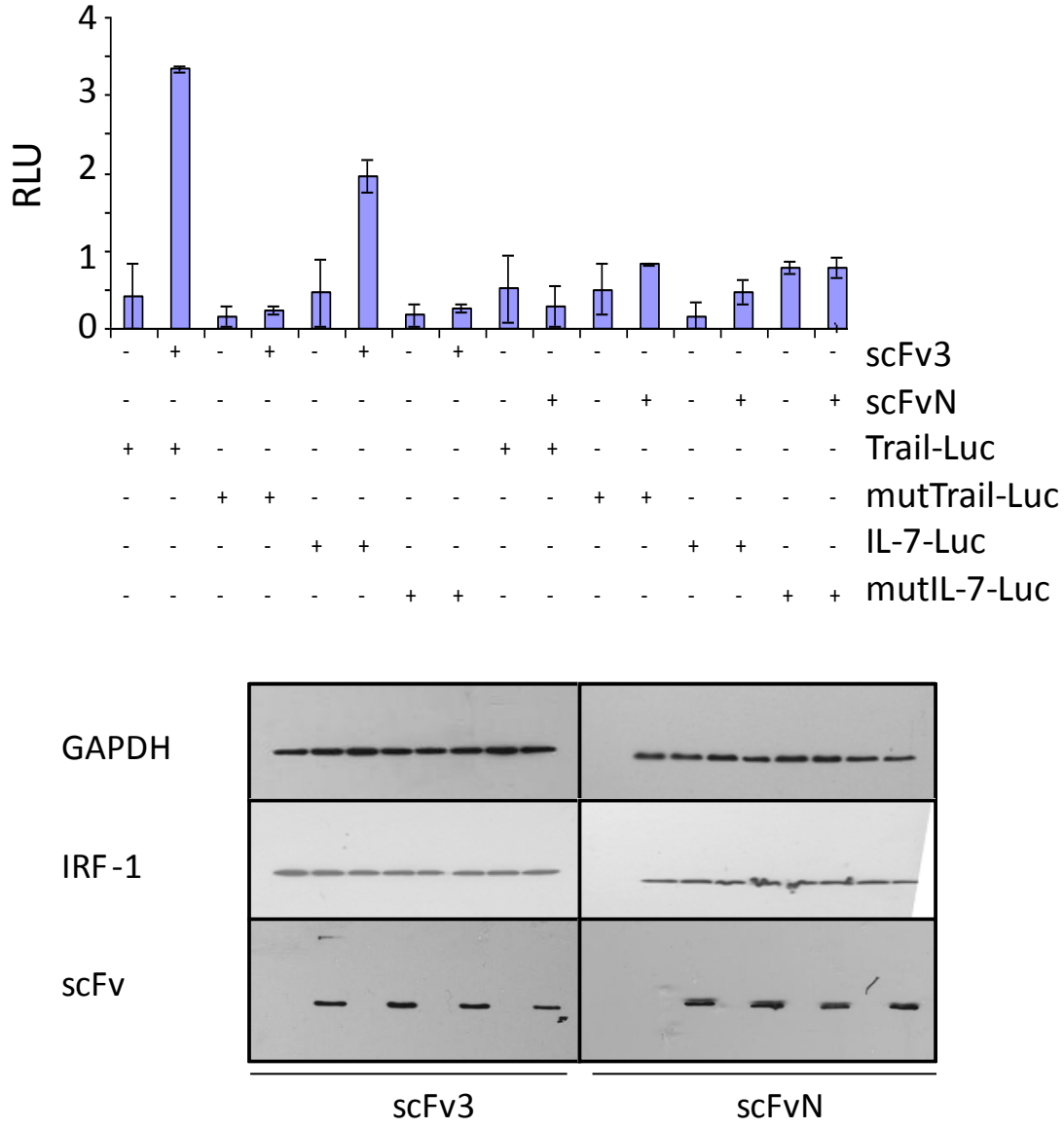

Figure 5.6: HeLa cells were transfected with of scFv3 or scFvN (250 ng), together with Renilla (60 ng) and either TRAIL (+ISRE), mTRAIL (-ISRE), IL7 (ISRE) or IL7 (-ISRE) luciferase reporter constructs. Reporter activity was determined as in figure 5.2. The assay was carried out in duplicate; results are given as mean ± half the range.

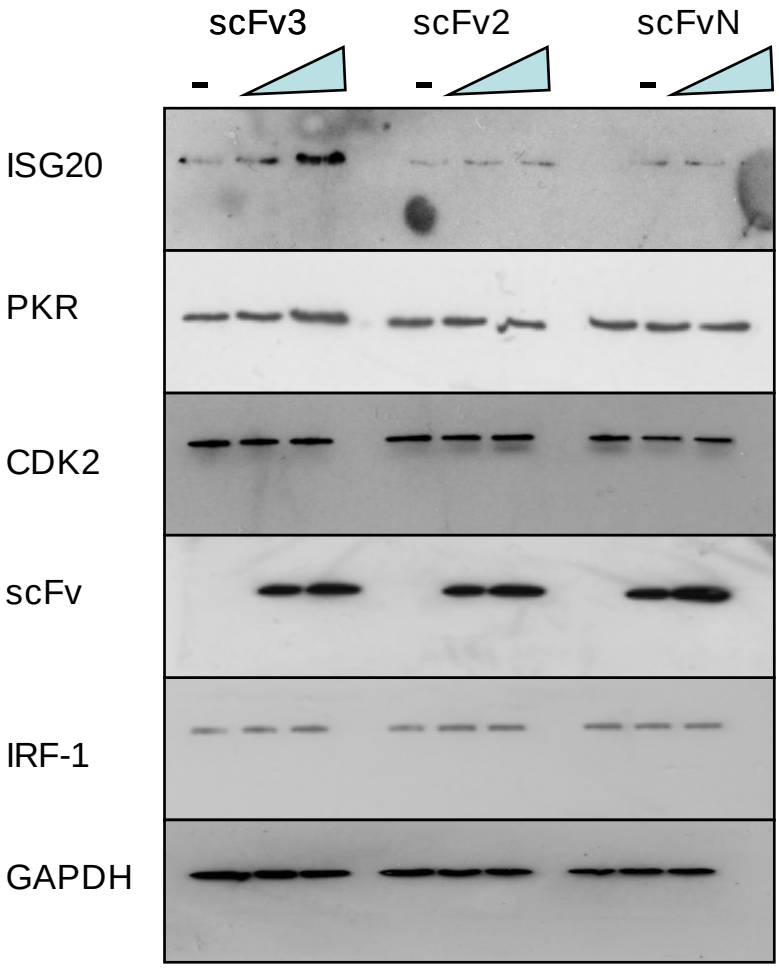

Figure 5.7: HeLa cells were transfected with 0, 0.5 or 1 µg of scFv3, 2 or N. After 24 hours the cells were lysed and the detergent soluble lysate was analysed by SDS-PAGE/immunoblot and developed with antibodies against ISG20, PKR, CDK2, GFP (to detect GFP-scFv), IRF-1 or GAPDH. The results given are representative of 2 independent experiments.

Alternatively, as the extreme C-terminus is involved in protein interactions which impact on IRF-1 localisation [112] and degradation [111], scFv3 may affect IRF-1-mediated transcription through an indirect mechanism. This possibility is investigated in the next section.

5.2.2 The scFv3 intrabody co-localises with IRF-1 and decreases its half life

Possible changes in the localisation of IRF-1 in response to scFv3 were investigated using subcellular fractionation. Figure 5.8 shows that in untransfected cells, IRF-1 is almost exclusively detected in the soluble nuclear compartment (fraction 3) and that this is not affected by the presence of either scFv3 or scFvN. The data also provide evidence that the intrabodies co-localise with IRF-1.

The C-terminus of IRF-1 has previously been shown to be required for efficient turnover [111], with truncation of the C-terminal 25 residues leading to enhanced steady state levels due to the generation of a relatively degradation-resistant protein [111]. The half life of soluble endogenous IRF-1 protein was therefore measured in cycloheximide-treated cells that had been transfected with scFv3 or scFvN, and this was compared to the half life in untransfected or GFP-expressing cells (Figure 5.9). Two independent experiments are shown which are representative of a total of 5 such experiments. In each case scFv3 caused a decrease in the half life of detergent extractable IRF-1 to around 17 min, from a value of 41 minutes in the GFP alone-expressing cells and 77 minutes in cells expressing scFvN.

Interestingly, the rate of degradation of scFv3 itself was similar to that of IRF-1 when the intrabody was present, suggesting that the scFv3:IRF-1 complex may be co-degraded. It is possible that binding of scFv3 to IRF-1 changes detergent solubility rather than the half life, therefore the $t_{0.5}$ for IRF-1 remaining in the detergent insoluble lysate was determined following extraction under denaturing conditions. As with the soluble fraction, the half life of IRF-1 in the insoluble fraction was reduced in the presence of scFv3 compared to the control (Figure 5.10).

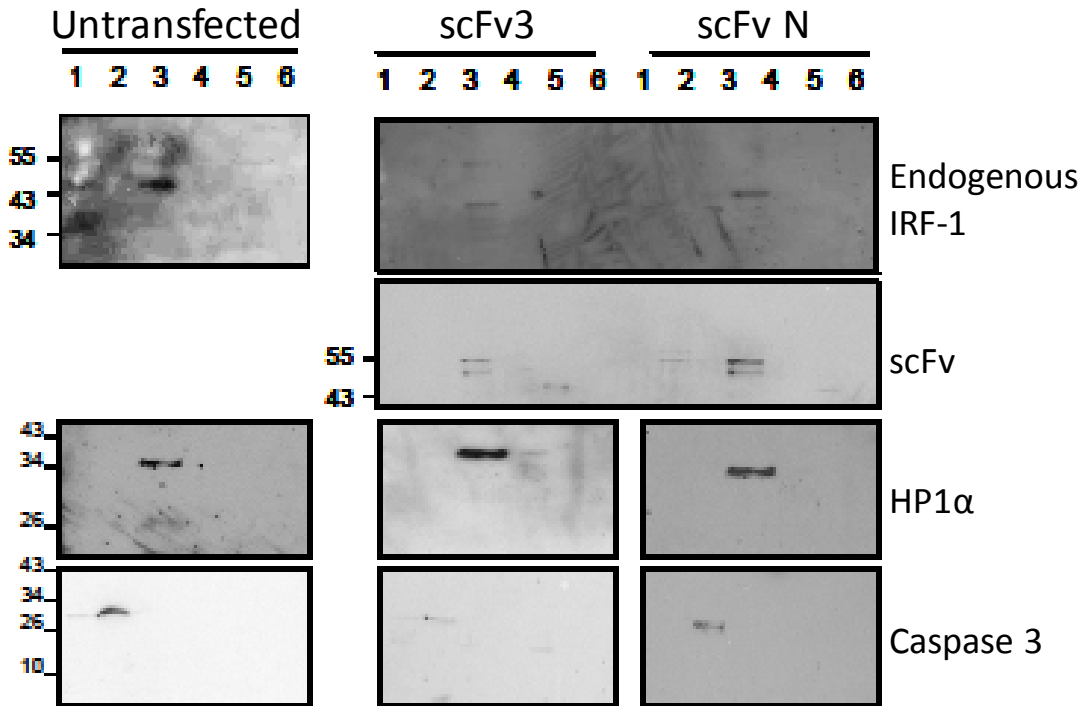

Figure 5.8: HeLa cells were transfected with scFv3 or scFvN (1.2 ug) and fractionated after 24 hours. Fraction 1: cytosol, 2: membrane/organelle, 3: soluble nuclear proteins, 4: chromatin bound nuclear proteins, 5: cytoskeletal proteins (as described by Thermo Scientific). Fraction 6 was created by re-suspending the residual pellet in SDS sample buffer. The fractions were analysed by SDS-PAGE/immunoblot and probed with anti-IRF-1, anti-GFP, anti-HP1α (a nuclear localisation marker) and anti-caspase 3 (a cytosolic localisation marker). 20 µl of sample were loaded per well. The data are representative of 2 independent experiments.

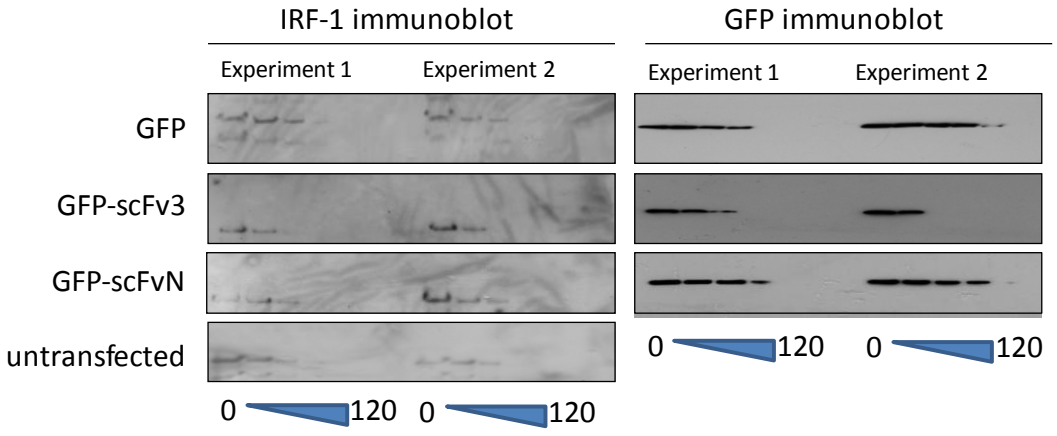

Figure 5.9: (A) $T_{0.5}$ of IRF-1 in detergent soluble mammalian cell lysate. Figure continued on the next page.

B

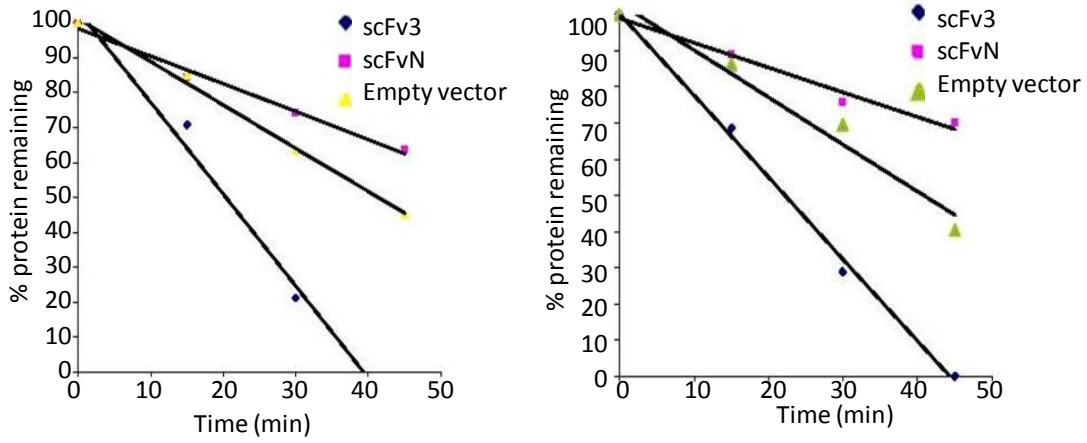

construct	Mean +/- half range
Vector	41+/-1
scFv3	17+/-1
scFvN	77+/-18

Figure 5.9: Continued from previous page. **(A)** $T_{0.5}$ of IRF-1 in detergent soluble mammalian cell lysate. HeLa cells were transfected with empty vector (pDEST53, which expresses GFP alone), scFvN or scFv3 (0.6 µg). Post-transfection (24 hours), the cells were treated with 30 µg/ml cycloheximide and harvested at 0, 15, 30, 45, 60, 90 and 120 minutes after treatment. Detergent soluble proteins were analysed by SDS-PAGE immunoblot developed using anti-GFP or anti-IRF-1 monoclonal antibody. The data shown here is for an experiment performed in duplicate, thus experiments 1 and 2, and is representative of 5 independent experiments. **(B)** Graphs showing the percentage of IRF-1 protein remaining since cycloheximide treatment, where protein level at time 0 is 100%. Relative protein levels are based on the density of the immunoblot bands shown in A and were determined using SynGene Imaging Systems. **(C)** Half life (in minutes) of endogenous IRF-1 in HeLa cells following transfections described in A. Calculated using the natural log of % protein remaining against time, thus $t_{0.5}$ occurs at y = ln(50). Half lives shown are an average for experiments 1 and 2 $\pm$ half the range.

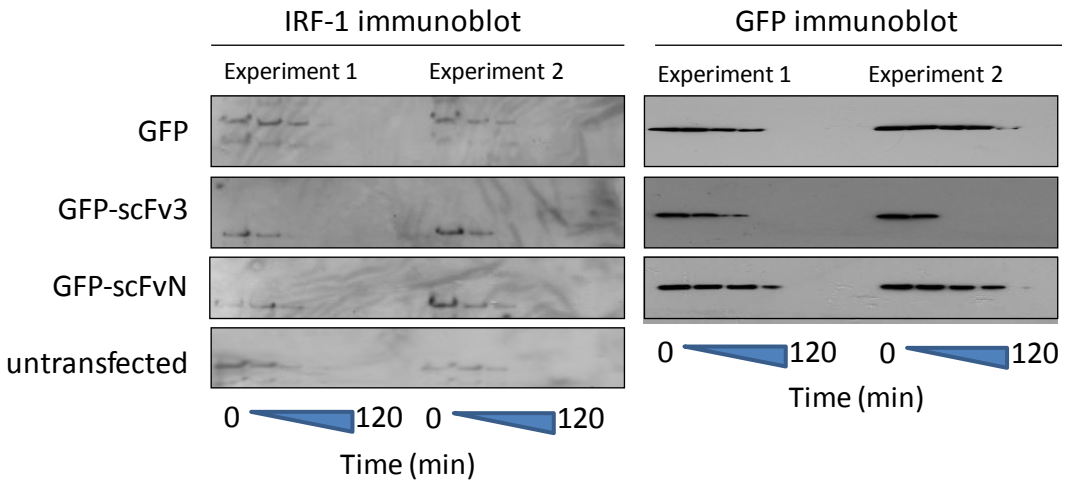

Figure 5.10: $T_{0.5}$ of IRF-1 in detergent soluble mammalian cell lysate. HeLa cells were transfected with with empty vector (pDEST53, which expresses GFP alone), scFvN or scFv3 (0.6 µg). Post-transfection (24 hours), the cells were treated with 30 µg/ml cycloheximide and harvested at 0, 15, 30, 45, 60, 90 and 120 minutes after treatment. Detergent insoluble proteins were analysed by SDS-PAGE immunoblot developed using anti-GFP or anti-IRF-1 monoclonal antibody. The data shown here is for an experiment performed in duplicate, thus experiments 1 and 2, and is representative of 5 independent experiments.

The results presented so far suggest that the observed increase in IRF-1 activity, caused by binding of scFv3 to the C-terminus of IRF-1, is not due to a change in its localisation or a decrease in the rate of degradation. It also suggests that, in addition to its previously documented role as a requirement for efficient degradation of IRF-1 [111], the extreme C-terminus of IRF-1 may also be involved in preventing IRF-1 from being degraded too rapidly.

5.2.3 A single point mutation at the C-terminus of IRF-1 mimics the effect of scFv3 intrabody binding

The observation that the increase in IRF-1 transcriptional activity seen in the presence of scFv3 was accompanied by a significant decrease in the protein's half life was unexpected, as deletion of the last 25 amino acids of IRF-1, which encompass scFv3's epitope, has previously been associated with a decrease in the rate of IRF-1 degradation [111]. Independent evidence was therefore sought that scFv3's epitope, as well as being required for efficient degradation of IRF-1 [110, 111], might also act as a 'brake' on IRF-1 turnover. During characterisation of C-

terminal truncation mutants, it was previously noted that a construct from which the four C-terminal residues had been deleted was expressed in cells at much lower levels than wild type IRF-1 [64]. Additionally, another researcher in the lab (Dr Emma Pion – unpublished observation) noticed a mutant form of IRF-1, in which the extreme C-terminal residue of IRF-1 Pro^{325} was substituted with an Ala (IRF-1P325A), had a very short half life; similar to that displayed by intrabody-bound IRF-1. Figure 5.11A shows that this mutant is expressed at very low levels, but accumulates in the presence of the proteasome inhibitor MG132, suggesting it is subject to rapid degradation. To investigate the difference in expression of wild type IRF-1 and the P325A mutant, their half-lives were determined in cycloheximide treated cells. The $t_{0.5}$ of wild type IRF-1 in HeLa cells was approximately 30 min, but less than 15 minutes for the P325A mutant protein (figure 5.11B, left panels). To ensure this apparent decrease in half life was not caused by a re-localisation of the mutant protein away from the detergent soluble fraction, the insoluble pellet was analysed following extraction under denaturing conditions. The half life of the IRF-1P325A mutant protein was seen to be reduced compared to the wild type protein in the pellet extract (figure 5.11B, right panel), confirming that the mutation had increased degradation and not simply changed the protein's solubility. In summation, mutation of Pro^{325} is sufficient to trigger an increase in the rate of IRF-1 degradation, suggesting that factors which bind to the extreme C-terminal residues of IRF-1 could modulate its degradation.

Having identified a mutation within the scFv3 epitope that could mimic the effect of intrabody binding on degradation, the next step was to investigate whether this mutant had a higher intrinsic transcriptional activity than the wild type protein. Figure 5.12 shows TLR3-luciferase expression following transfection with wild type IRF-1 or the P325A mutant. Protein levels were normalised (figure 5.12B) as the P325A mutant expressed at lower levels than the wild type protein. It was seen that the P325A mutant consistently displayed higher activity than the wild type protein (Figure 5.12A). Thus the P325A mutant provides intrabody-independent evidence that the C-terminus of IRF-1 can limit the rate at which the protein is degraded, and that changes in the rate of degradation correlate with increases in the activity of IRF-1 as an activator of gene expression.

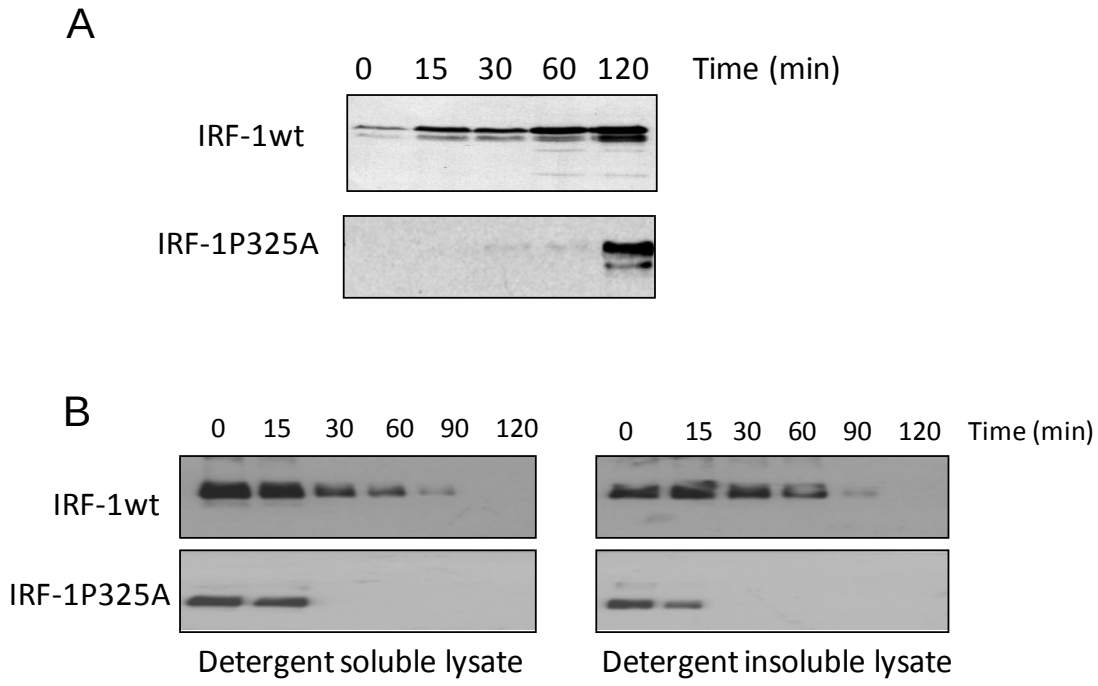

Figure 5.11: Mutation of Pro^{325} mimics scFv3 binding to IRF-1. **(A)** A375 cells were transfected with IRF-1 wild type and IRF-1P325A (0.5 µg); 24 hours later they were treated with MG132 (50 µM) and harvested at the times shown. IRF-1 was detected following analysis of the lysates by SDS-PAGE/immunoblot. The data are representative of 2 separate experiments, performed by Dr Emma Pion. **(B)** HeLa cells were transfected with wild type (wt) IRF-1 or P325A-mutant IRF-1 and treated 24 hours later with cycloheximide (30 µg/ml), before being harvested at the times shown. Detergent soluble (left panel) and insoluble (right panel) lysates were analysed by SDS-PAGE/immunoblot and developed using an anti-IRF-1 antibody, the data are representative of at least 3 experiments.

A

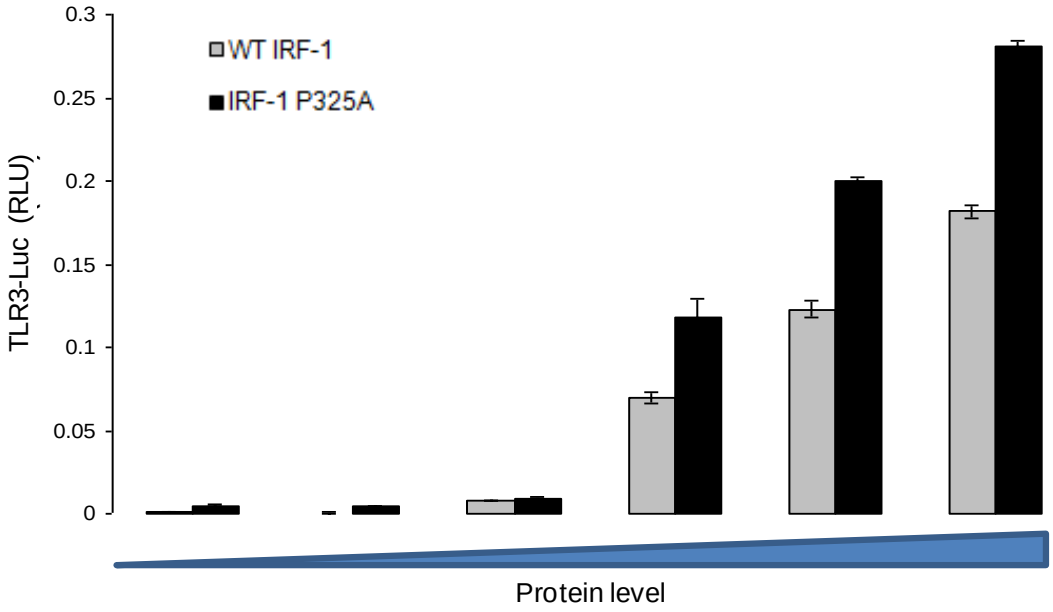

B

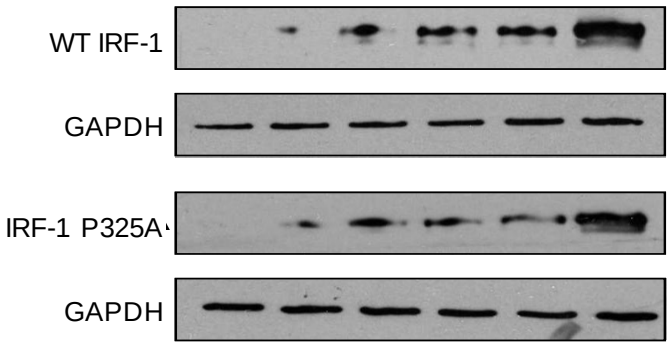

Figure 5.12: (A) HeLa cells grown in a 24-well plate were transiently transfected with TLR3(+)-luc (120 ng), Renilla (60 ng) and a titration of either of IRF-1 wild type (wt) (0-0.25 µg) or IRF-1P325A (0-0.5 µg). Reporter gene activity was measured in relative light units (RLU) and is expressed as the ratio of Luc:Ren. The assays were carried out in duplicate; results are given as mean ± half the range and are representative of at least 2 independent sets of experiments. **(B)** IRF-1 protein levels were determined by SDS-PAGE/immunoblot developed using anti-IRF-1 antibody.

5.3 Discussion

The data presented in this chapter indicate that the extreme C-terminal residues of IRF-1 inhibit its ability to activate transcription, and that this negative regulation can be relieved using an intrabody that binds to this region of endogenous IRF-1 or by mutating the C-terminal residue of the protein (P^{325}). In addition, the data highlight a possible role for the scFv3 epitope in coordinating a link between the rate of IRF-1 degradation and its transcriptional activity. Previous studies have suggested that IRF-1 activity is regulated primarily at the level of transcription, as IRF-1 steady state levels increase in response to agents such as interferon treatment and DNA damage which induce its transcriptional activity [2]. However, the data shown here suggests IRF-1 is also subject to post-translational regulation; that it is held in a latent or partially active state and that activity can be induced without an increase in its steady state levels.

As discussed in the introduction, single chain intrabodies have previously been used to modulate the function of their target antigens in a cellular environment. Mechanisms employed by intrabodies to produce changes in target protein activity have included: altering their intracellular localisation [231, 235-237], neutralising enzyme activity [230], disrupting normal protein–protein interactions [227, 240-242] or DNA-protein interactions [227]. Although most published intrabody studies involve the disruption of their target antigen's activities, some have been used to alleviate intrinsic negative regulation as shown in this study. For example, a domain within the carboxy terminus of another tumour suppressor, p53, has been shown to negatively regulate its transcriptional activity [375]. This inhibition could be relieved by C-terminal deletion of p53 or by binding of an anti-C-terminal monoclonal mouse IgG named PAb421 [375]. scFv intrabodies based on PAb421 and a second mouse IgG named 11D3 were shown to target the C-terminus of p53 and increase transcriptional activation of a p53 mutant His^{273} [239]. This mutant displayed 10% of the transcriptional activity of wild type p53 in a reporter gene assay, which was increased to ~25% following co-transfection with either of the anti-C-terminal scFv intrabodies [239]. These antibodies were shown to function by increasing the sequence specific DNA binding of p53 [239, 375].

In the current study, the scFv3 intrabody was able to activate endogenous IRF-1-induced transcription between four to six fold making it a powerful tool to study the normal intracellular functions of the IRF-1. However, there was no evidence that scFv3 could enhance IRF-1's ability to bind DNA. Additionally, the scFv3 intrabody clearly did not act through re-localisation of IRF-1, as both were detected only in the nuclear fraction and any re-localisation would presumably have reduced IRF-1 transcriptional activity. scFv3 binding may have switched the conformation and/or dynamics of endogenous IRF-1 to a more active form. At present, structural information is only available for the N-terminal DNA binding domain of IRF-1, and the contribution of the C-terminus to the protein's tertiary structure is unknown [100]. However, antibodies have previously been used to stabilise and help determine the structure of disordered proteins [376], and it may be possible to use scFv3 to determine the conformation of activated IRF-1 in future studies. Alternatively, the intrabody may function by disrupting or enhancing the binding of IRF-1 co-factors. To date very few proteins have been shown to directly interact with IRF-1, and even fewer with the extreme C-terminus. However, the scFv3 epitope mapped in chapter 4, contained within the last 20 amino acids of IRF-1 (amino acids 306 to 325 LDSL**LT**PVRLP**S**IQAI**P**CA**P**), overlaps with a previously determined co-factor binding motif (**L**DS**LL**TPVRLPSIQAIPCAP). Hsp70 binding to IRF-1's LXXLL motif has been shown to be essential for an Hsp90-induced increase in IRF-1's half life [112]. Additionally, deletion mutants of IRF-1 have previously indicated that amino acids 306-310, in which the LXLL motif is contained, are essential for IRF-1's ability to inhibit cell growth and mediated CDK-suppression [64]. However, the scFv3 intrabody did not affect CDK-suppression, which may mean it does not impinge upon LXLL co-factor binding.

Alanine scanning and deletion mutants have also been used to show that residues centred about amino acids 311-317 of IRF-1 house a negative-regulatory motif, the mutation of which enhances transcription from the IFN-β promoter [64]. The data shown in this thesis indicate that this negative regulatory domain is rate-limiting in the endogenous protein, and as scFv3 binding is dependent on amino acids T^{311} and S^{317}, it is possible that these residues are part of a novel co-factor binding element.

In the absence of small molecules capable of modulating IRF-1 activity, past studies relied on the use of transiently expressed IRF-1 mutant proteins. It was therefore not possible to determine the effect of the C-terminus on IRF-1 as a transcriptional activator under normal cellular conditions. By developing an intrabody that can bind to both endogenous and exogenous IRF-1, this study demonstrates that the last 20 amino acids of IRF-1 contain a regulatory element that is normally rate-limiting for IRF-1-mediated gene expression.

Previously published data has shown that the last 25 amino acids of IRF-1 are required for efficient degradation of IRF-1 [111]. The sharp decrease in half life caused by the scFv3 intrabody binding to this region seems to contradict this finding. However, fine mapping of the C-terminus has revealed that a P325A IRF-1 mutant protein (unpublished work by Dr Emma Pion), which mimics the affect of scFv3 binding, also reduces the protein's half life. The fact that both the intrabody and point mutation operate through the same residue, P^{325}, supports the idea that this change in half life is not an artefact and suggests that the two may be working through the same mechanism to increase the rate of IRF-1 degradation.

The combination of the results shown here (figures 5.9 and 5.10) and those of earlier studies that revealed ΔC25 mutants are degradation-resistant [111] indicate that the extreme C-terminus of IRF-1 contains elements that are required for efficient degradation and that act as a brake to prevent that degradation from being too rapid. The data indicates that this region may function in 'fine-tuning' IRF-1 turnover dependent on cellular conditions. IRF-1 polyubiquitination has been shown to be essential but not sufficient for proteosomal degradation of IRF-1, suggesting that a second step is needed [111]. Searching for proteins that interact with the extreme C-terminus of IRF-1 (the focus of chapter 6) could provide further insight into the tightly regulated turnover of IRF-1.

As both intrabody-bound IRF-1 and P325A IRF-1 have an increased transactivation activity and rate of degradation, it is possible that these two co-localised functions may be linked. It is increasingly clear that both the proteolytic and non-proteolytic functions of the proteasome are required for correct regulation of the transcriptional machinery, with evidence of both the 19S and 26S proteasomes being associated

with chromatin, components of the basal transcriptional machinery and/or various transcription factors [377-382]. The precise mechanism(s) linking transcriptional activation with protein degradation remain unclear. However, evidence suggests roles for proteasome-mediated degradation in establishing limits for transcription, promoting the exchange of transcription factors on chromatin and stimulating multiple rounds of transcription initiation [6, 301, 383-386]. As has been shown for other transcription factors, it is possible that binding of an activating co-factor to IRF-1 may also trigger degradation [248, 387].

Based on the results presented here, showing that significant enhancement of IRF-1 transcriptional activity can be achieved by post-translational mechanisms, it is interesting to speculate that therapeutic approaches may be designed which induce downstream targets of the IRF-1 tumour suppressor pathway in cancers which retain one or more IRF-1 allele. Conventional approaches, such as type I interferon therapy, that function, at least in part, by activating the IRF-1 pathway at the level of transcription [61, 388], are used sparingly as they are toxic and have severe side effects [389, 390]. The use of intrabodies to activate IRF-1 post-translationally, in the absence of increased IRF-1 transcription, could be a novel avenue for activating some of the downstream signalling pathways stimulated by type I interferons.

6 Selection of IRF-1-binding peptides and preliminary validation of ZNF350 as an IRF-1-interacting protein

6.1 Introduction

As discussed in chapter 5, scFv3 may be working by altering the IRF-1's structure and/or disrupting its co-factor interactions. The introduction to this thesis details the co-factors of IRF-1 that have previously been identified and shown to modulate its activity (section 1.2.5.4). However, the characterisation of additional co-factors could help explain the mechanics behind IRF-1's regulation and activation following cell stress and during the cell-cycle. In particular, its post-translational modification, which is not well understood (section 1.2.5 and [109, 111, 122]). This chapter describes the use of peptide phage display to identify IRF-1-binding peptides, the sequences of which were use to search human protein databases for putative IRF-1 interaction partners. The preliminary validation of one such binding partner, ZNF350, is also described.

6.1.1 Peptide phage display

Peptide phage display enables the identification of peptide motifs able to bind a specific target protein. This technique is summarised in figure 6.3; briefly short peptides (usually 6-20 residues) are expressed on the surface of filamentous phage virions and incubated with a target protein. Following rigorous washing, phage displaying peptides that bound the target protein are eluted and amplified in host bacteria. The amplified phage are secreted by the bacteria and can be purified to create a pool of phage that only display peptides with an affinity for the target protein. This pool can then be used in subsequent selection rounds against the target protein and thus becomes enriched for the highest affinity binders. Finally the phage DNA can be extracted and sequenced and the amino acid content of the binding peptides revealed.

Peptide phage display involves the fusion of a polypeptide to a phage coat protein. The peptide is thus displayed on the surface of the phage virion and encoded for

within the phage genome. Large libraries can be created that contain billions of phage, each displaying a different peptide. In this study the Ph.D. 12 (NEB) peptide phage display library was used. This library consists of linear 12-mer peptides fused to the minor phage coat protein g3p with an intervening flexible glycine-serine linker (Gly-Gly-Gly-Ser). The library contains 1.9×10^9 distinct clones. Unlike the previously described antibody phage display libraries (chapter 4), the phage particles in this library carry a complete phage genome and do not require additional genes provided by helper phage. Bacteria infected with these M13 phage form plaques caused by diminished cell growth when plated. As these plaques can be difficult to see, the phage vector also carries a *lacZα* gene. This results in blue plaques when an α-complementing *E.coli* strain such as ER2738 and Xgal/IPTG plates are used.

Since its initial development as a means of mapping of antibody epitopes [169], peptide phage display had been successfully applied in the identification of: bio-active molecules that can disrupt or activate target protein activities [43, 257, 292], disease or tissue specific bio-markers [139, 258, 259, 262], protein interactions with non-protein substances [273-275] and protein:protein interactions [268, 279]. In some cases intelligent modification of the basic peptide phage display protocol has increased its usefulness. For example, the addition of a streptavidin binding motif N-terminal to the displayed peptide has allowed the identification of protease cleavage sites [268, 391, 392]. In this case the phage are immobilised on a streptavidin surface, incubated with a protease and released into solution if their displayed peptide is cleaved. They can then be purified from solution and used again in successive selection rounds. Once the cleavage motif is identified, it can then be used to identify novel substrates of the protease. In this way a GenBank BLAST search of a motif derived from peptide phage display identified Matrilin-3, a cartilage component, as a substrate of ADAMTS-4, an aggrecanase responsible for the breakdown of cartilage aggrecan in osteoarthritis [268]. The BLAST search resulted in over 9056 “hits” but, by focusing on those involved in pathways in which ADAMTS-4 was known to play a crucial role, this study was able to characterise a physiologically relevant interaction.

In other studies recombinant domains of a protein have been used as the "bait" or target protein in peptide phage display [279, 393]. This approach has the advantage that functions/interactions can be mapped within the full-length protein, but has the disadvantage that interactions that rely on the tertiary structure of the full length protein will be excluded. However, several studies have highlighted the importance of contacts between short peptide motifs, particularly in transient regulatory interactions [394], and important interactions have been identified using isolated domains [279, 393]. For example, the PreS domain of the hepatitis B virus (HBV) large envelope is known to be involved in viral attachment to the membrane of hepatocytes during infection [395]; to identify binding partners of this domain it was recombinantly expressed, purified and used as a target protein in peptide phage display [279]. The resultant peptide consensus sequence was entered into a BLAST search, which gave a large number of "hits". The authors narrowed down this list to those in which the target-binding sequence was exposed on the outer surface of the membrane, discarding all intracellular hits. The group went on to eliminate new or hypothetical proteins for which information was limited. This led to only three potential interaction partners being investigated and one, lipoprotein lipase, being verified and shown to be physiologically relevant. In another study using isolated domains, the eukaryotic protein:protein interaction domain GYF (glycine-tyrosine-phenylalanine domain) was subjected to peptide phage display [393]. This provided a GYP-binding motif which was used to search the human and yeast proteome. Peptides were synthesised that contained the potential GYF-interaction sites from each protein hit. Proteins represented by peptides with the highest affinity for the GYF domain were carried forward for further analysis, and direct interactions between full-length proteins containing the GYF domain and GYF-binding sites validated through yeast-2-hybrid [393, 396].

The experiments described above show that peptide phage display can be used to detect physiologically relevant interactions; first by detecting a protein-binding peptide motif, then by searching for this motif in a protein database and finally by validating the interaction between two full-length proteins. Although such database searches can provide thousands of hits [268], filtering the proteins based on localisation and function can reduce those taken forward for future study to a level

that can be managed with the resources available to a particular research group and increases the chance of characterising an interaction important in a specific signalling pathway or disease. In this study, domains of IRF-1 are used as targets against which high affinity peptides are selected. The sequences of these peptides are then determined and used to search protein databases for potential IRF-1 binding partners. Such proteins are initially selected for homology to an IRF-1 binding peptide, but then subsequently for involvement in post-translational regulation, cancer progression and/or pathways in which IRF-1 is already known to participate.

6.1.2 Domains of IRF-1

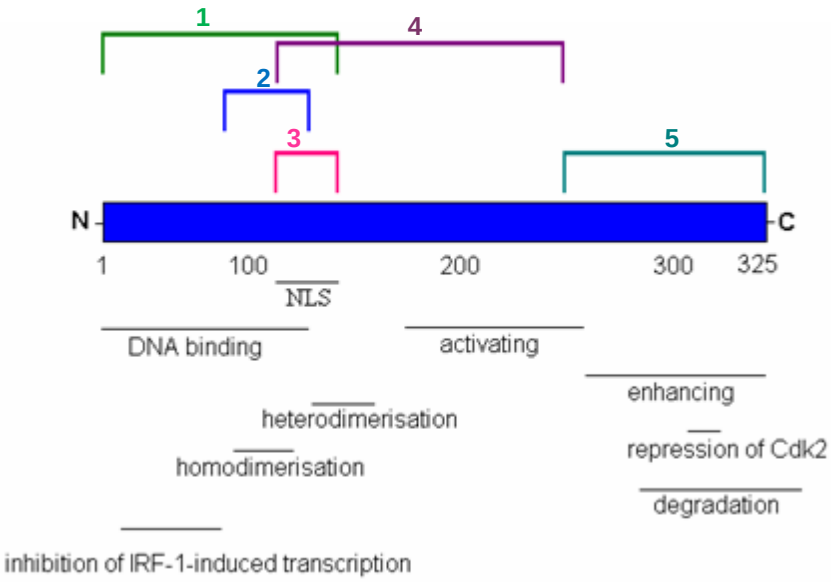

Figure 6.1: Diagram indicating mapped functions of IRF-1 (see thesis introduction) and the 5 domains used as targets in peptide phage display (indicated by coloured bars).

Five domains of IRF-1 were used as targets against which phage displayed peptides were selected. These domains spanned IRF-1 amino acids 1-140, 60-124, 117-184, 117-256 and 256-325 (see figure 6.1). Each was chosen based on previous functional mapping. Amino acids 1-140 encompass the DNA binding domain [5] and nuclear localisation signal (NLS) of IRF-1 [104]. Domain 60-124 contains residues shown to be essential for an *in vivo* interaction between two IRF-1 proteins, although this interaction has not yet been validated as direct [103]. Amino acid 117 signals the

start of the nuclear localisation domain; this region was mapped in mouse IRF-1 [104], but its sequence is almost identical to the human homologue (82.5/92.1 identity/similarity) [397]. Domain 117-184 includes the NLS and amino acids N-terminal to, but not including, the transactivation domain. The larger 117-256 domain includes both the NLS and transactivation domain. The transactivation domain (amino acids 185-256) is required for induction of the *IFN-β* promoter by murine [101, 104] and human [105] IRF-1. Additionally murine IRF-1 has been shown to be phosphorylated in a manner dependent on this region [109]. Finally domain 256-325 contains the C-terminal enhancer domain of IRF-1 [101]. This enhancer region also carries residues required for association with the p300 co-factor [72] and Hsp70 [112]. Furthermore, this region has not only been shown to enhance IRF-1 induced transcription [105], but also to regulate IRF-1 turnover ([111] and chapter 5 of this thesis), and CDK2 repression [64].

6.2 Results

6.2.1 Identification of IRF-1 binding peptides

Several studies reviewed in the introduction to this thesis (section 1.2.4) have mapped specific functions of IRF-1, such as transcriptional enhancement and DNA binding, to specific domains. However, little is known about the regulation of these functions. To discover potential IRF-1 co-factors that modify its activity, and to begin to isolate aptamers that could later be used in chemical genetic screens, phage display was used to identify peptides capable of binding IRF-1. This technique is summarised in figure 6.3 and described in the introduction. Five His-tagged domains encompassing the full-length of IRF-1 were used as targets in peptide phage display. These domains were chosen based on previously mapped IRF-1 functions (figure 6.1). The domains were cloned into the pTrcHis B vector, expressed in bacteria and purified on a nickel column (figure 6.2). A large and diverse library of peptide displaying phage was incubated with the immobilised domains. Specifically, a microtitre plate was coated with an excess (50 μg/ml) of His-tagged domain. This immobilised domain was then incubated for 1 hour with 2×10^{11} plaque forming units (i.e. infective phage particles) suspended in PBS-0.1% Tween. Phage that bound the domain with a low affinity were washed away, and high affinity phage

were eluted with 0.2 M Glycine-HCl (pH 2.2), 1 mg/ml BSA. After elution, this acidic buffer was neutralized with 1 M Tris-HCl (pH 9.1).

This new pool of phage, enriched for phage carrying peptides able to bind the IRF-1 domains, was amplified in an *E.coli* bacterial culture. The newly replicated phage particles were secreted into the culture medium by the bacteria from which they could be purified through PEG precipitation. These phage particles were then used in a further two selection rounds (3 rounds in total). The final polyclonal pool of phage was again used to infect bacteria, but this time individual plaques generated by infected bacteria were picked and phage DNA extracted. Sequencing of the phage genome revealed the amino acid composition of the displayed peptides. Although 10 plaques were picked per domain, the resultant phage DNA was not always sequenced successfully. 50 plaques were picked in total, but the sequence of only 41 was obtained. In total 24 different sequences were obtained from the five domains (see figure 5.4). Some sequences occurred with a high frequency, for example 50% (5) of the clones that were detected as binding the sub-domain spanning amino acids 117-256 had the same sequence "ALYKTSTATALL". In this chapter, the analysis of the 24 different peptides selected is described. However, in parallel with this analysis, alternative sequencing services were tested (all sequencing was necessarily out-sourced). In the end a more complete set of domain-binding peptide sequences was obtained and these are listed at the end of this chapter in figure 6.2.1 (new sequences shown in blue). However, owing to the time constraints of this PhD these sequences were not validated for their IRF-1 binding capacity, instead the possibility for future analysis is outlined in the discussion.

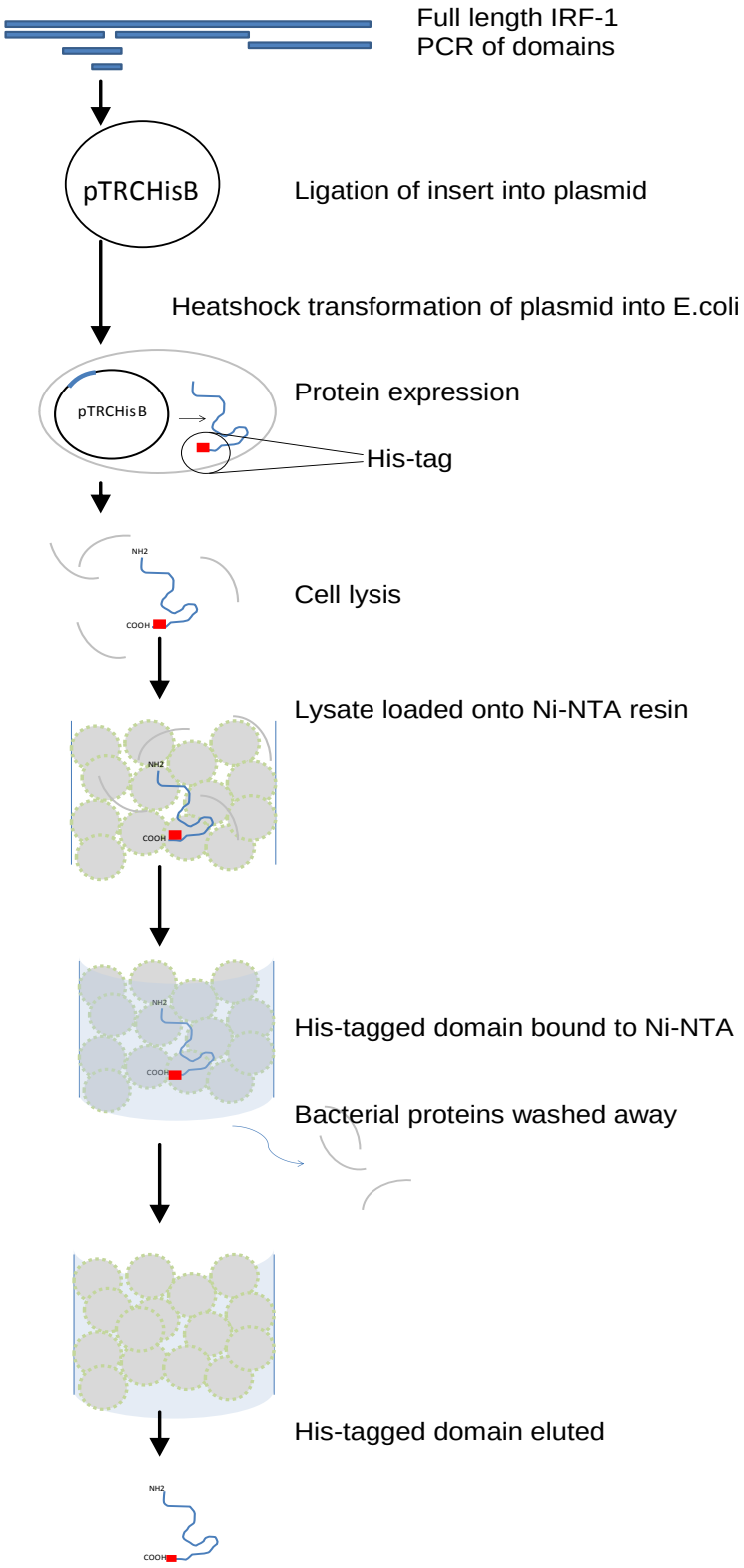

Figure 6.1: Five domains of IRF-1 were cloned in the pTRHis B vector for bacterial expression as His-tagged recombinant proteins. Following bacterial cell lysis the His-tagged domains were purified on a nickel column and used as targets in peptide phage selection.

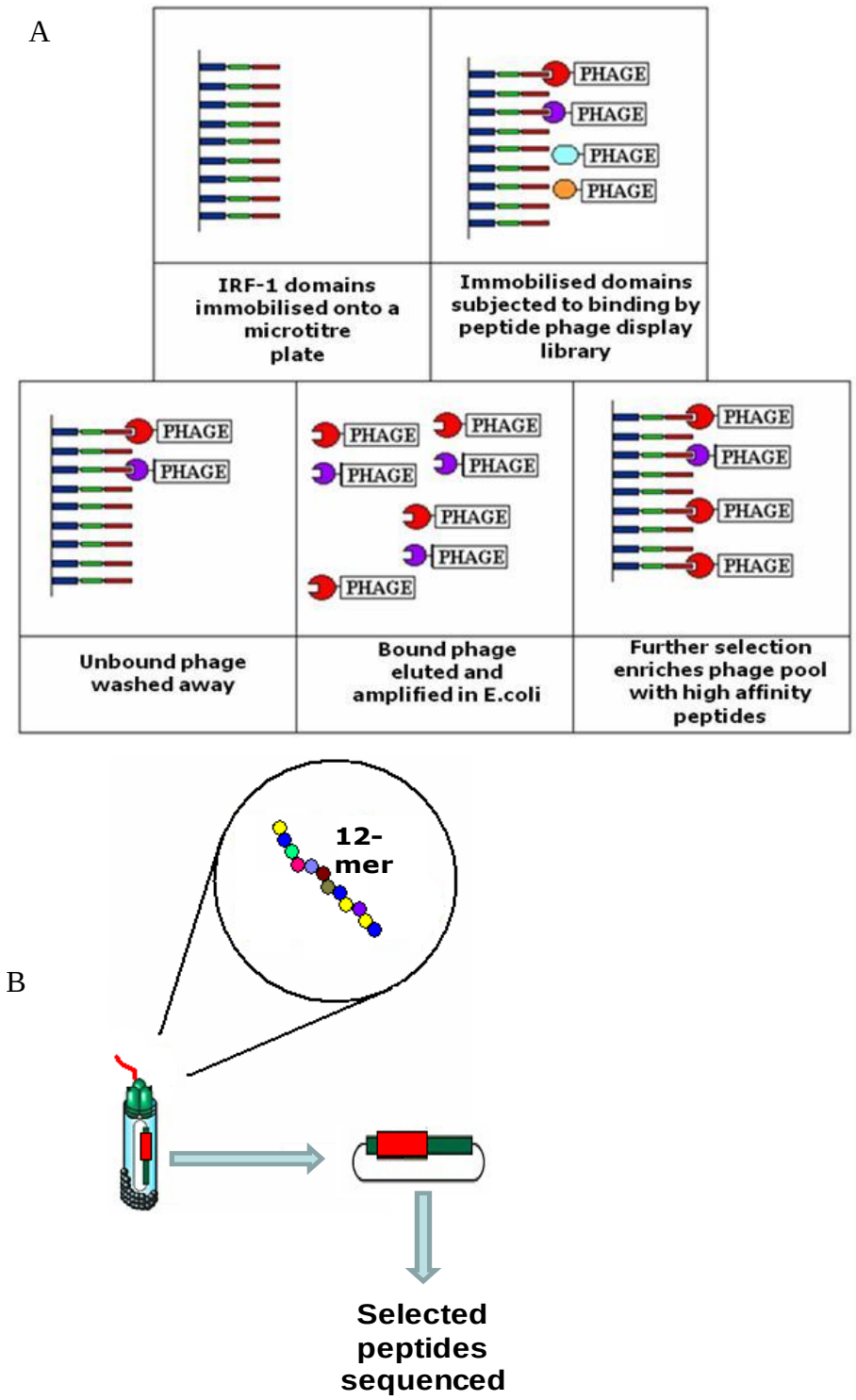

Figure 6.3: (A) Diagrammatic representation of the peptide phage display technique. In this study 3 selection rounds were performed. **(B)** A 12-mer peptide is encoded in the phage genome and expressed as a fusion to the minor phage coat protein g3p. Following selection phage DNA can be extracted and sequenced.

Peptide number	Sequence	Frequency	Domain selected with	Resultant Biotinylated peptide
1	SEWSYNSPPSLP	3	1-140	SEWSYNSPPSLP
2	HSKLNNRHHALL	1	1-140	HSKLNNRHHALL
3	ANPAWNADFSIF	1	1-140	ANPAWNADFSIF
4	NYSHLRVKLPTP	1	60-124	NYSHLRVKLPTP
5	ALYKTSTATALL	1	60-124	ALYKTSTATALL
6	HFHYPKKAGLPP	2	60-124	HFHYPKKAGLPP
7	SPFGMIAQQGLR	1	60-124	SPFGMIAQQGLR
8	NFMPSLPRLGMH	1	60-124	NFMPSLPRLGMH
9	SSYAPYVWQPIA	1	60-124	SSYAPYVWQPIA
10	NYXXDTTRPPSA	1	60-124	DTTRPPSA
11	TYHESQTSFTNT	1	60-124	TYHESQTSFTNT
12	WDDTLWPRPMRH	1	117-184	WDDTLWPRPMRH
13	AMAVKLNYPLGY	2	117-184	AMAVKLNYPLGY
14	HLKMMVAPRTSL	2	117-184	HLKMMVAPRTSL
15	VISNHAESSRRL	1	117-184	VISNHAESSRRL
16	LMSPNNNTLRIS	1	117-184	LMSPNNNTLRIS
17	HYSIRLPASASL	1	117-184	HYSIRLPASASL
18	AXXXEMTPHLNX	1	117-184	EMTPHLNX
19	QTSSPTPLSHTQ	1	117-184	QTSSPTPLSHTQ
20	ALYKTSTATALL	5	117-256	ALYKTSTATALL
21	ASITHFKSGKSH	4	117-256	ASITHFKSGKSH
22	SVSLPYANLATH	1	117-256	SVSLPYANLATH
23	XXDGCSAYESWW	4	256-325	DGCSAYESWW
24	XXXXMVAPRTSL	3	256-325	MVAPRTSL

Figure 6.4: Table showing the sequence of the 24 different peptides selected as binding to domains of IRF-1. Peptides are numbered arbitrarily and these numbers are used to identify each peptide in subsequent assays (column 1). Where sequencing was incomplete, unknown amino acids are represented by an “X”. Ten peptides were sequenced per domain and the frequency with which any given sequence occurred out of these 10 is listed (column 3). The sequences of the biotinylated peptides generated from the phage displayed peptides are shown (column 5).

Following phage peptide display, the selected sequences required validation as domain specific binders. The recurrent selection of particular peptides against some domains (figure 6.4), such as DGCSAYESWW (peptide 23) against the C-terminal domain, suggests that enrichment of specific phage was successful, as does the selection of the same peptide by two different but overlapping domains for example, ALYKTSTATALL was selected by overlapping domains encompassing amino acids 60-124 (peptide 5) and 117-256 (peptide 20). Domain specificity was confirmed by testing peptide binding against immobilised and liquid phase domains (see figures 6.5 and 6.6). The 24 phage display peptides were synthesised carrying a biotinylated tag (Mimotopes Pepset) and were either immobilised on a streptavidin-coated 96-well microtitre plate (figure 6.5) or incubated with immobilised IRF-1 domains (figure 6.6). As in the initial phage display selection, the domains carried His tags, however, as the peptides bound differentially to each domain, tag-specific binding was regarded as negligible.

Overall, it was shown that peptides bound specifically to the domains they were selected with and occasionally to overlapping domains. For example, some peptides selected as binding to domain 60-124 (peptide 8), 117-184 (peptide 14) and 117-256 (peptide 22) also bound to the overlapping domain 1-140 (figure 6.5A and 6.6A). This provides further insight into the exact binding site of each of these peptides; for instance, peptide 22 would appear to bind between IRF-1 amino acids 117 and 140 (the region overlapped by domains 1-140 and 117-256). However, conformation as well as amino acid composition may be important for this interaction as this peptide does not bind domain 117-184, which also encompasses this region of IRF-1. Domain specificity can be seen most clearly for the two peptides selected against the extreme C-terminal domain. This domain does not overlap any of the others, and accordingly the peptides selected against it did not display any apparent affinity for the other domains.

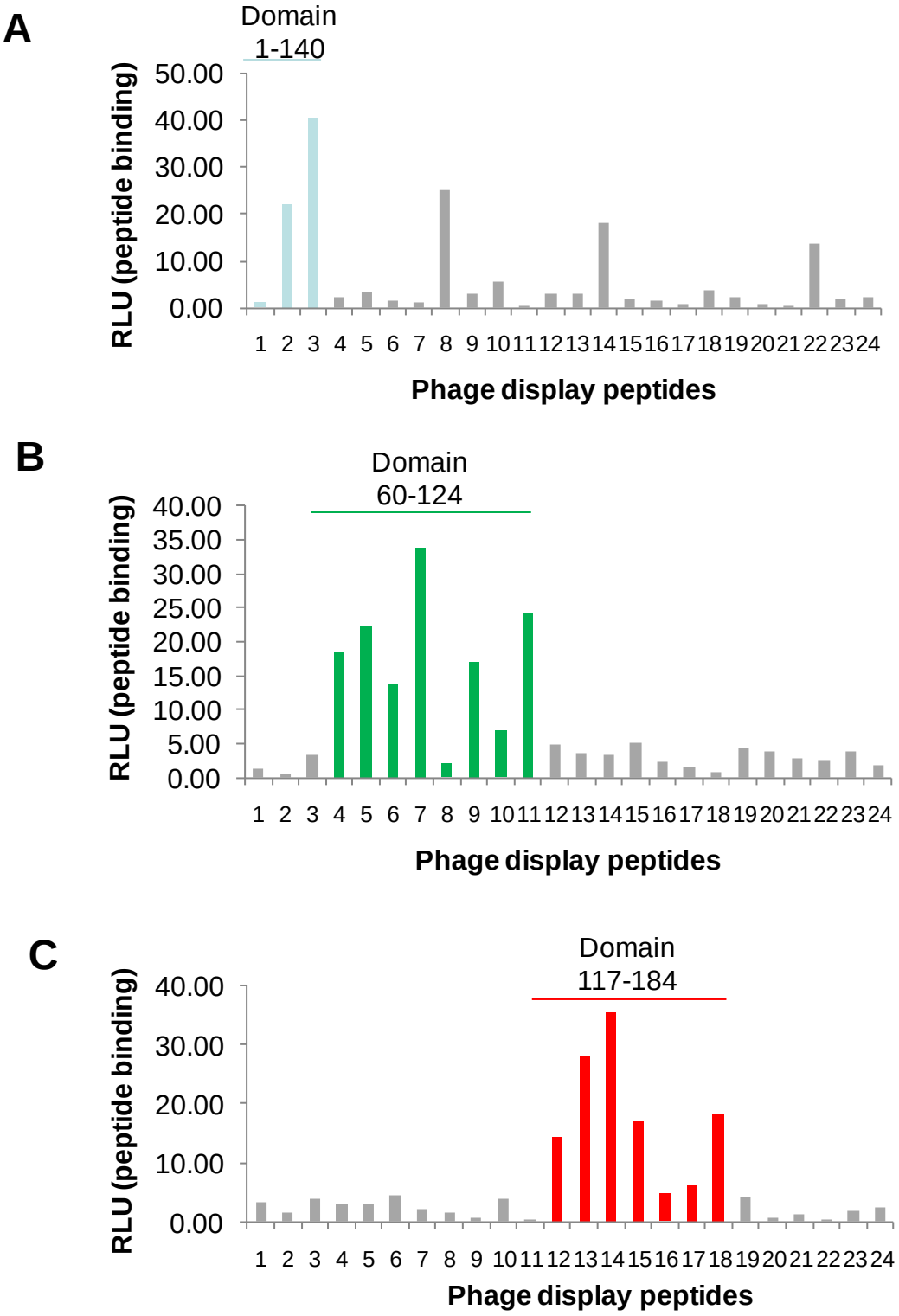

Figure 6.5: continued and described on next page

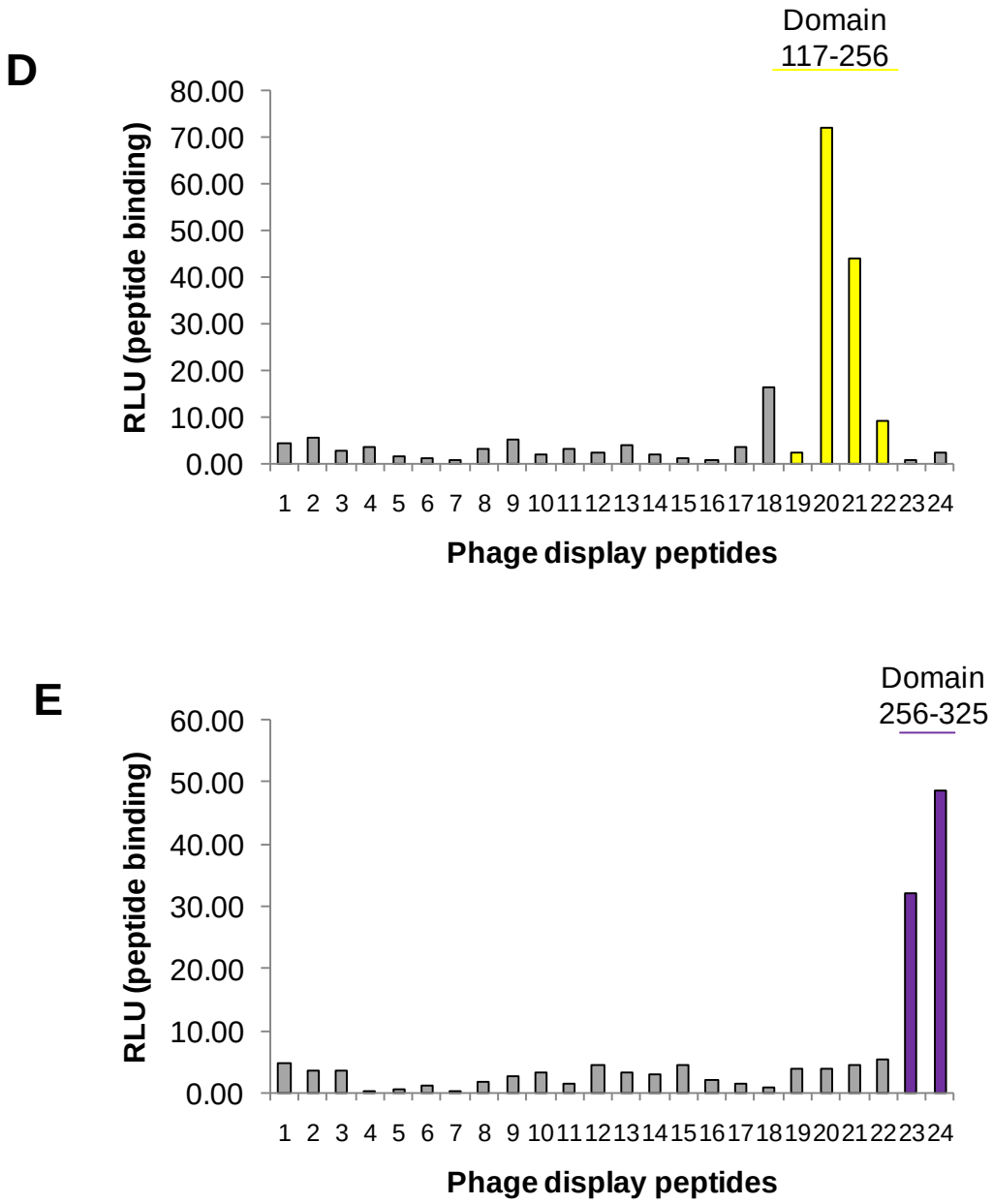

Figure 6.5: IRF-1 domain binding to phage display-derived peptides. Immobilised peptides (200 ng) were incubated with each IRF-1 domain (1 µg/ml). The graphs represent binding to the following domains, each named according to the IRF-1 amino acids they encompass: **(A)** 1-140, **(B)** 60-124, **(C)** 117-184, **(D)** 117-256 and **(E)** 265-325. The coloured columns indicate which of the 24 peptides were selected with the domain used in the assay. Following extensive washing, domain binding was detected with an anti-His antibody and enhanced chemiluminescence.

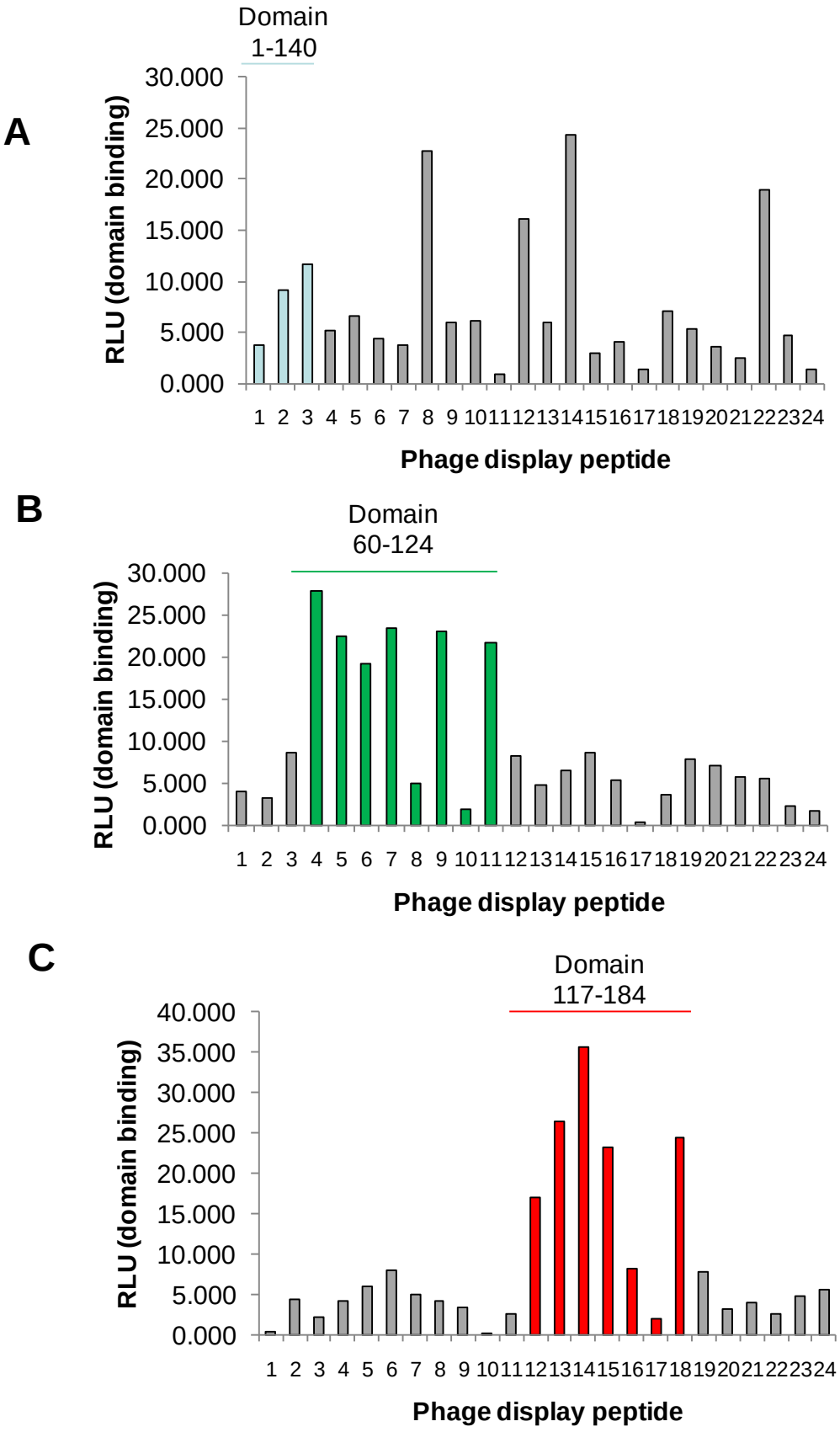

Figure 6.6: continued and described on next page

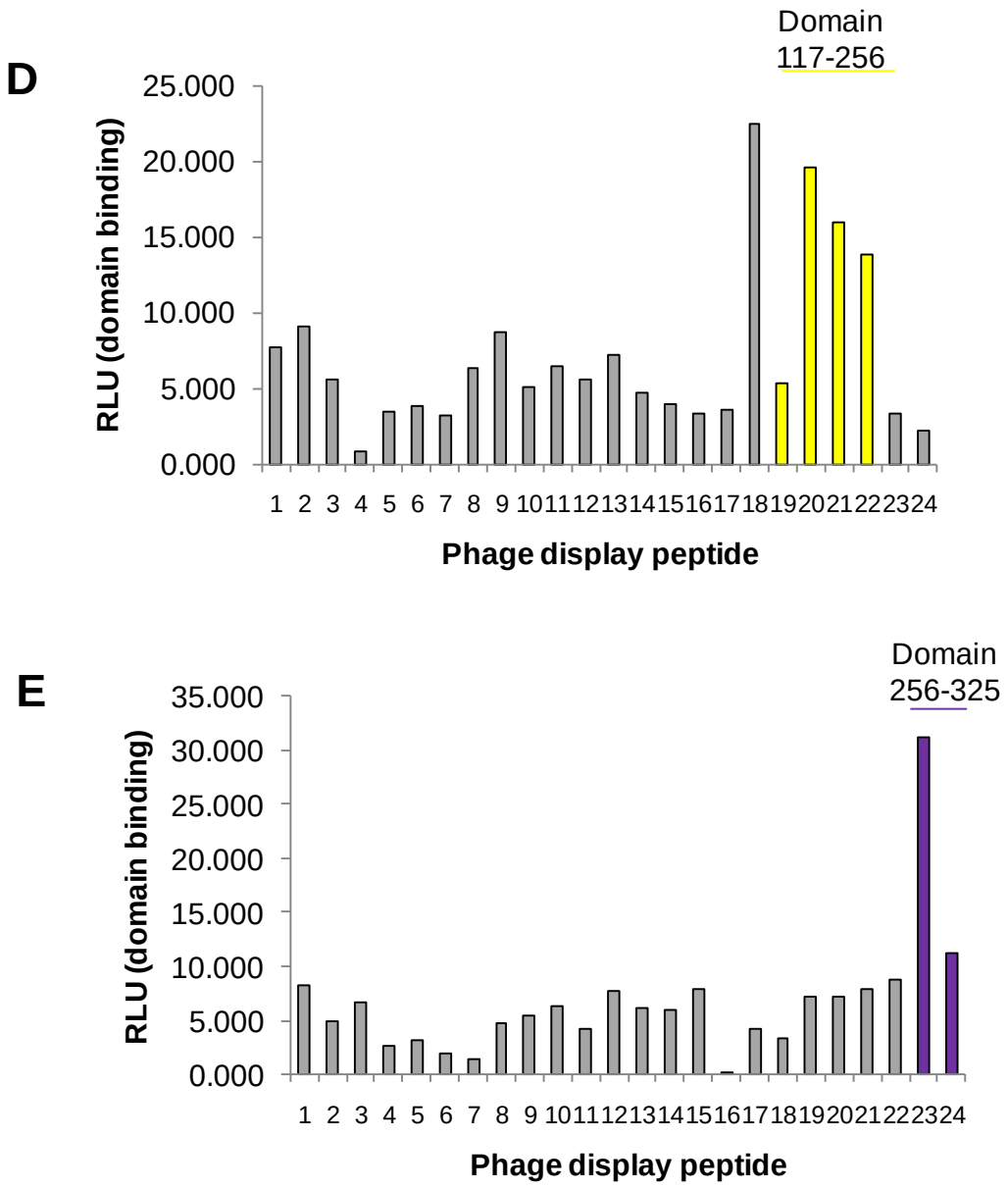

Figure 6.6: IRF-1 domain binding to phage display-derived peptides. Immobilised domains (200 ng) were incubated with each peptide (1 µg/ml). The graphs represent binding to the following domains, each named according to the IRF-1 amino acids they encompass: **(A)** 1-140, **(B)** 60-124, **(C)** 117-184, **(D)** 117-256 and **(E)** 265-325. The coloured columns indicate which of the 24 peptides were selected with the domain used in the assay. Following extensive washing, domain binding was detected with HRP-streptavidin and enhanced chemiluminescence.

Yet, there were still several peptides that did not bind to any of the domains, such as peptides 1, 16, 17 and 19 in figures 6.5 and 6.6, indicating that these peptides may need to be displayed as fusions to the minor phage coat protein or have their biotin tag removed before they show any binding activity.

As the aim of this study was to identify peptides/proteins capable of interacting with native IRF-1, it was essential to test for binding to the full-length IRF-1 protein. Therefore, binding assays were carried out using all 24 peptides selected by phage display, with either the peptides (figure 6.7A) or full-length IRF-1 (figure 6.7B) immobilised. Full-length IRF-1 was expressed with a GST-tag to enable purification; therefore the peptides were also tested for binding to purified GST. Non-specific binding to GST was seen for peptides 17 and 20 in figure 6.7A and peptides 4, 9, 12, 16, 17 and 19 in figure 6.7B. This supports earlier indications that peptides 16, 17 and 19 lost their IRF-1-specific binding capacity outwith the phage display system. This interaction may have previously been stabilised by the g3p coat protein or negatively affected by biotinylation. The data also indicates that peptides 4, 9 and 12 cannot bind their epitope within the context of full-length IRF-1, as these peptides displayed only a low relative affinity for IRF-1 binding in both figures 6.7A and B. The capacity to bind full length IRF-1 outside the phage display system is important for peptides used as IRF-1-specific reagents capable of detecting, purifying or even functionally modulating their target protein; even though such studies are not described in this thesis, the characterisation shown here highlights which peptides would be worthy of further development. Surprisingly, peptide 1, which did not bind to any of the IRF-1 domains (figures 6.5 and 6.6), was able to bind the full length protein with a relatively high affinity. The reason for this is not clear; however, it is possible that the availability of the peptide 1-epitope is different in the full-length protein and that this compensated for the peptide's decreased ability to interact stably outside the phage display system.

Figure 6.8 indicates which peptides were able to bind an IRF-1 domain or the full length protein with a relative affinity 50% higher than that shown by the 24 peptides on average. Peptides 3, 8, 14, 18 and 24 were able to bind both their target domains in isolation and full length IRF-1 with comparatively high affinities. Peptides 18 and

24 were of particular interest as they were able to bind both a domain and the full length protein regardless of which was immobilised, the peptide or the protein. The low affinity for GST and previously noted domain specificity all support the notion that phage display can be used to generate peptides which bind IRF-1 in a specific manner.

The amino acid sequence of phage-displayed peptides can be used to search protein databases for full-length proteins containing the same or similar sequence and which show the same affinity for a target protein [268, 279, 393]. This can be done by first searching for a consensus motif [279] using multiple sequence alignment tools such as CLUSTALW (EMBL-EBI) to identify residues conserved in the target protein-binding peptides. Such alignment tools can also generate motifs in which an amino acid's characteristic but not identity is conserved at a certain position, e.g. hydrophobicity. Additionally, flexible motifs can be created in which one or more amino acids are acceptable at a specific position. The quality of any binding motif obtained would depend on the number of sequences compared, which in this study is limited by inefficient sequencing. Initial CLUSTALW analysis revealed no strong consensus in the sequences selected against the domains of IRF-1; as a result, further motif searching has been postponed until a greater number of peptide sequences can be obtained for each round.

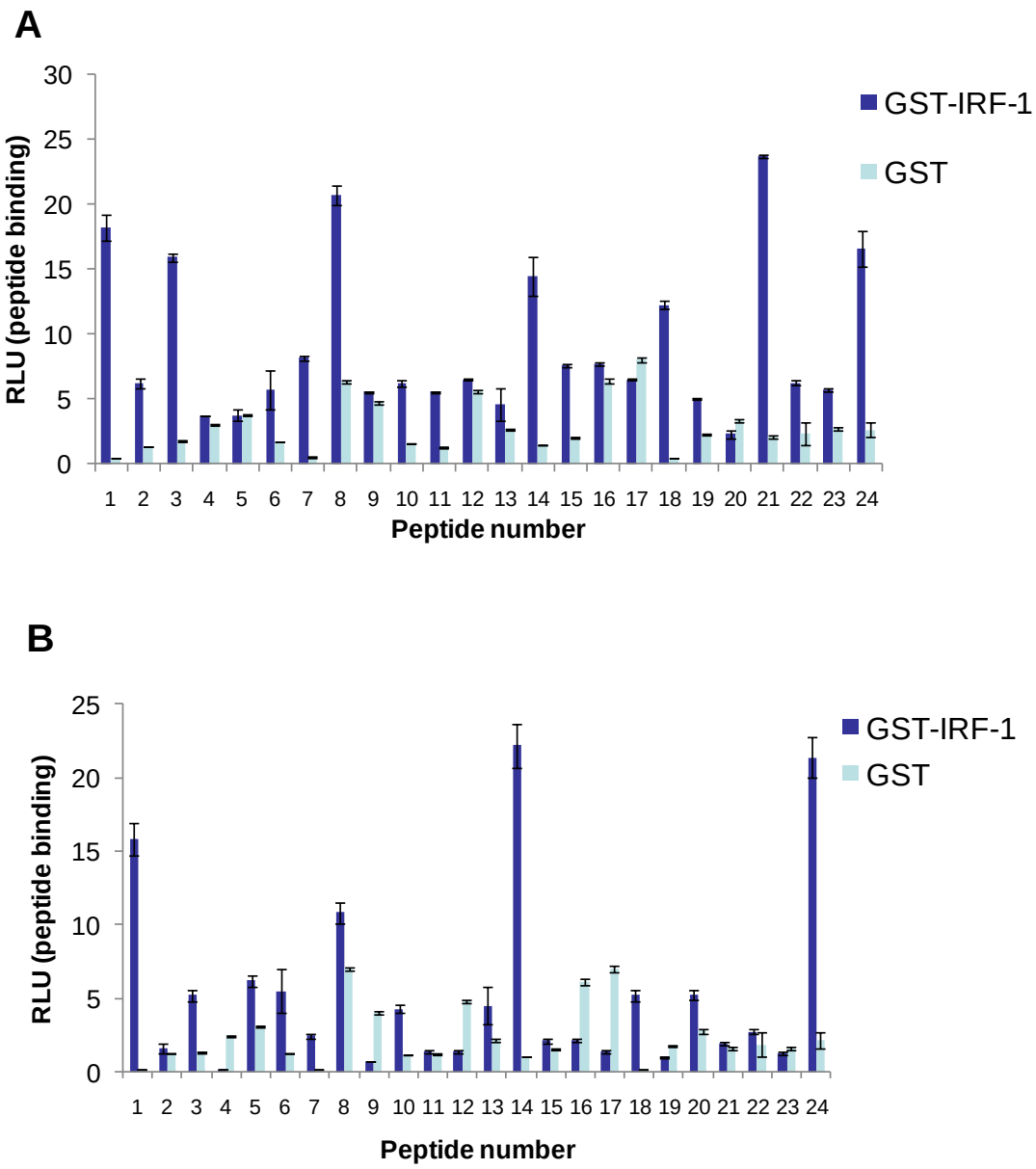

Figure 6.7: Peptide binding to full length IRF-1. (A) Immobilised-peptides (200 ng) derived from peptide phage display were incubated with free GST or GST-IRF-1 (1µg/ml). Following extensive washing, GST and GST-IRF-1 binding was detected with an anti-GST antibody and enhanced chemiluminescence. (B) As in A except that GST or GST-IRF-1 were immobilised (200 ng) and incubated with the biotinlyated phage display-derived peptides (1µg/ml). Peptide binding was detected with HRP-conjugated streptavidin and enhanced chemiluminescence.

Phage display peptide	1-140	60-124	117-184	117-256	256-325	Full length IRF-1
1						§*
2	*					
3	*					§
4	§	*				
5		§*				
6		§				
7		*				
8	*					§
9	§	*				
10		§				
11		*				
12		§	§*			
13	§		§*			
14	*		§*			§*
15	§		§*			
16						
17						
18			§*	§*		§*
19						
20				§*		
21				§*		
22	*			§		
23	§				§*	
24					§*	§*

Figure 6.8: Summary of phage display peptide-binding to IRF-1 domains or the full-length protein. The symbol § indicates that the peptide was immobilised to the microtitre plate in the binding assay, that the protein was in the mobile phase and that Relative Binding Affinity (RBA; measured in all peptide binding assays in relative light units (RLU)) was 50% higher than the mean. To calculate the mean RBA with which peptides bound full length GST-IRF-1, the values were first corrected for GST binding. The symbol * has the same meaning as §, except that the protein was immobilised in the binding assay and the peptide was in the mobile phase.

Instead a search for a homologous sequence within a protein database was carried out using the peptide sequences presented in figure 6.4. The BLAST, Basic Local Alignment Search Tool [98], was used to search non-redundant protein sequences in the *Homo sapiens* genome. This provided 100 BLAST "hits" ranked according to homology (bit score) with the associated E-value displayed (which gives a measure of the possibility the sequence occurred by chance). The E-values are unavoidably high for searches of several large databases with short peptides.

The BLAST online search tool provided a short description of each of the 100 hits and the GenBank accession number. Each description includes a short summary of the known function and/or interactions of the "hit" protein. 24 peptides produced 2400 BLAST hits. All 24 phage display-derived peptides were entered into the alignment tool to reduce the possibility of excluding low affinity but biologically significant motifs.

Based on the GenBank description for each of the hits, they were initially reduced to only those that were involved in post-translational regulation and/or processes in which IRF-1 has already been shown to play a role. Particular emphasis was given to hits involved in cancer biochemistry, in pathways already under investigation within the lab (e.g. TSC2), or detected in an earlier yeast-2-hybrid screen (data unpublished) e.g. ZNF350. This selection procedure was sufficiently stringent to limit the final number of homologous proteins to 30. This was deemed a manageable number for subsequent analysis. Thus, 30 biotinylated 12-mer peptides (henceforth referred to as BLAST peptides) were synthesised that encompassed the protein sequence homologous to the phage display peptide (see figure 6.9). If more than one region within a protein was found to be homologous to a selected peptide, then 2 peptides were generated to cover each of the homologous sequences; this was true for the KIAA0623 Kinase, SPEN homolog and Myc Binding protein 2 (PAM).

The selection of only 30 BLAST peptides meant that many proteins with the potential to interact with IRF-1 were excluded from this investigation. Their inclusion may have led to the discovery of new functions for IRF-1 or unexpected forms of post-translational regulation, but higher-throughput technologies than were available for this study would have been required.

The biotinylated peptides were screened first for binding to the IRF-1 domains, with either the BLAST peptide (figure 6.10) or IRF-1 domain (figure 6.11) immobilised on the microtitre plate. Overall, they retained the same domain specificity as their homologous phage display peptides. Of particular interest was BLAST peptide 30, which showed very stable binding to the extreme C-terminal domain (figures 6.10E and 6.11E), as had the phage display peptide upon which it was based (phage display peptide 24). The peptides were also screened against liquid phase (figure 6.12A) or immobilised (figure 6.12B) full length GST-tagged IRF-1. In this binding assay several peptides displayed a relative affinity for full length IRF-1 50% higher than the average (figure 6.13). This includes peptides 2, 3, 4, 6, 14, 18, 24, 25, 27 and 28. These peptides, and the full-length proteins they represent, could now be evaluated for their ability to bind intracellular IRF-1. The time constraints of this PhD have prevented more detailed study of these BLAST hits at this time, but the preliminary binding analysis shown here could act as a basis for future studies.

The IRF-1 specificity shown by BLAST peptide 30 in these ELISAs led to its further study. Although it was not one of the peptides with a very high relative affinity for full-length IRF-1 (figure 6.13), it did interact more stably with IRF-1 than with the GST control (figure 6.12). Additionally, figures 6.10 and 6.11 clearly show that peptide 30 was the only BLAST peptide that bound with a high relative affinity to this region and that it did not bind well to any of the other IRF-1 domains. As outlined in chapters seven and eight of this thesis, the extreme C-terminus of IRF-1 plays an important role in regulating transcription of IRF-1 target genes and degradation. This peptide contains amino acids 464-475 of the ZNF350 protein (Zinc finger 350, also known as ZBRK1). A potential interaction between ZNF350 and IRF-1 is further investigated in the next section.

Peptide no.	Homologous protein	Accession number	Phage display peptide			Blast peptide sequence
			Sequence	No.	Domain	
1	ubiquitin-conjugating enzyme E2, J2	CAI23259.1	HSKLNNRHHALL	2	1-140	QANRHHGLLGGA
2	A kinase (PRKA) anchor protein 8	EAW84474.1	HSKLNNRHHALL	2	1-140	SVLNNRHIVKML
3	DEAD box	AAH01238.1	HSKLNNRHHALL	2	1-140	GLNGRGHALLIL
4	receptor interacting protein kinase 5	NP_056190.1	HSKLNNRHHALL	2	1-140	EVTMHHALLQEV
5	bcr-abl1 e19a2 chimeric protein	CAM33013.1	ANPAWNADFSIF	3	1-140	TAEPNWNEEFEI
6	ABBA-1	NP_612392.1	SEWSYNSPPSLP	1	1-140	SWSYQTPPSVPS
7	SWI1-like	EAW47681.1	SEWSYNSPPSLP	1	1-140	QPSYQTPPSLPN
8	Metastasis suppressor 1	AAH23998	SEWSYNSPPSLP	1	1-140	YSQSYQTPPSSP
9	KIAA0623 Kinase	BAA86549.1	SEWSYNSPPSLP	1	1-140	PYGASPPSLEGL
10	KIAA0623 Kinase		SEWSYNSPPSLP	1	1-140	FASPPSLPDMQH
11	MAPKKK19	CAI23047.1	SEWSYNSPPSLP	1	1-140	ASSPPSLPLSSA
12	Peptidylprolyl isomerase (cyclophilin)-like 5	AAI07889.1	SEWSYNSPPSLP	1	1-140	SIWLSYHSIPSLP
13	SET domain, bifurcated 1	EAW53505.1	ALYKTSTATALL	5	60-124 & 117-256	FSMKTSSASALE
14	F-Box and WD repeat domain	NP_115677.2	ALYKTSTATALL	5	60-124 & 117-256	SVGALYTTSTDK
15	Ankhd1	AAH40231.1	ALYKTSTATALL	5	60-124 & 117-256	KTSTATSKTQTR
16	Ankhd1		ALYKTSTATALL	5	60-124 & 117-256	TSQATTLSTFQP
17	MAX gene-associated protein.	AAI36660.1	WDDTLWPRPMRH	12	117-184	STDTLWRPMPKL
18	Fanconi anemia, complementation group I	AAI44484.1	AMAVKLNYPLGY	13	117-184	VFAIDYELGR
19	Baculoviral IAP repeat-containing protein 6	NP_057336.3	HLKMMVAPRTSL	14	117-184	DQHLAMMVALQE
20	PRP8 protein	BAA22563.1	ASITHFKSGKSH	21	117-256	GITHFRSGMSHE
21	Transcription factor B1, mitochondrial	NP_057104.2	ASITHFKSGKSH	21	117-256	RQLSISHFKSLC
22	DNA repair protein XRCC4	NP_071801.1	ASITHFKSGKSH	21	117-256	VSEPSITHFKSLC
23	SPEN homolog	EAW51756.1	SVSLPYANLATH	22	117-256	PAGYANVATHST
24	SPEN homolog		SVSLPYANLATH	22	117-256	PAASSVGLPSRT
25	Tuberous sclerosis 2	EAW85559.1	SVSLPYANLATH	22	117-256	VFAISLPYTNPS
26	Myc binding protein 2	NP_055872.4	ASITHFKSGKSH	21	117-256	NSIGHFCGGWAG
27	Myc binding protein 2		ASITHFKSGKSH	21	117-256	PASTSGKSELLSS
28	NUF2	NP_113611.2	SVSLPYANLATH	22	117-256	GFLPFSNLVTHL
29	Similar to F-box only protein 2	EAW56867.1	MVAPRTSL	24	256-325	QHHVAPRTSGRG
30	Zinc finger protein 350	Q9GZX5.2	MVAPRTSL	24	256-325	VPSVAPQTSLNI

Figure 6.9: Table showing the 30 BLAST peptides (column 7), the proteins in which the BLAST peptide's sequence resides (column 2) and the phage display peptides to which they are homologous (column 4). Shared amino acids are shown in green. Peptides are numbered arbitrarily, and these numbers are used to identify each peptide in subsequent assays (column 1).

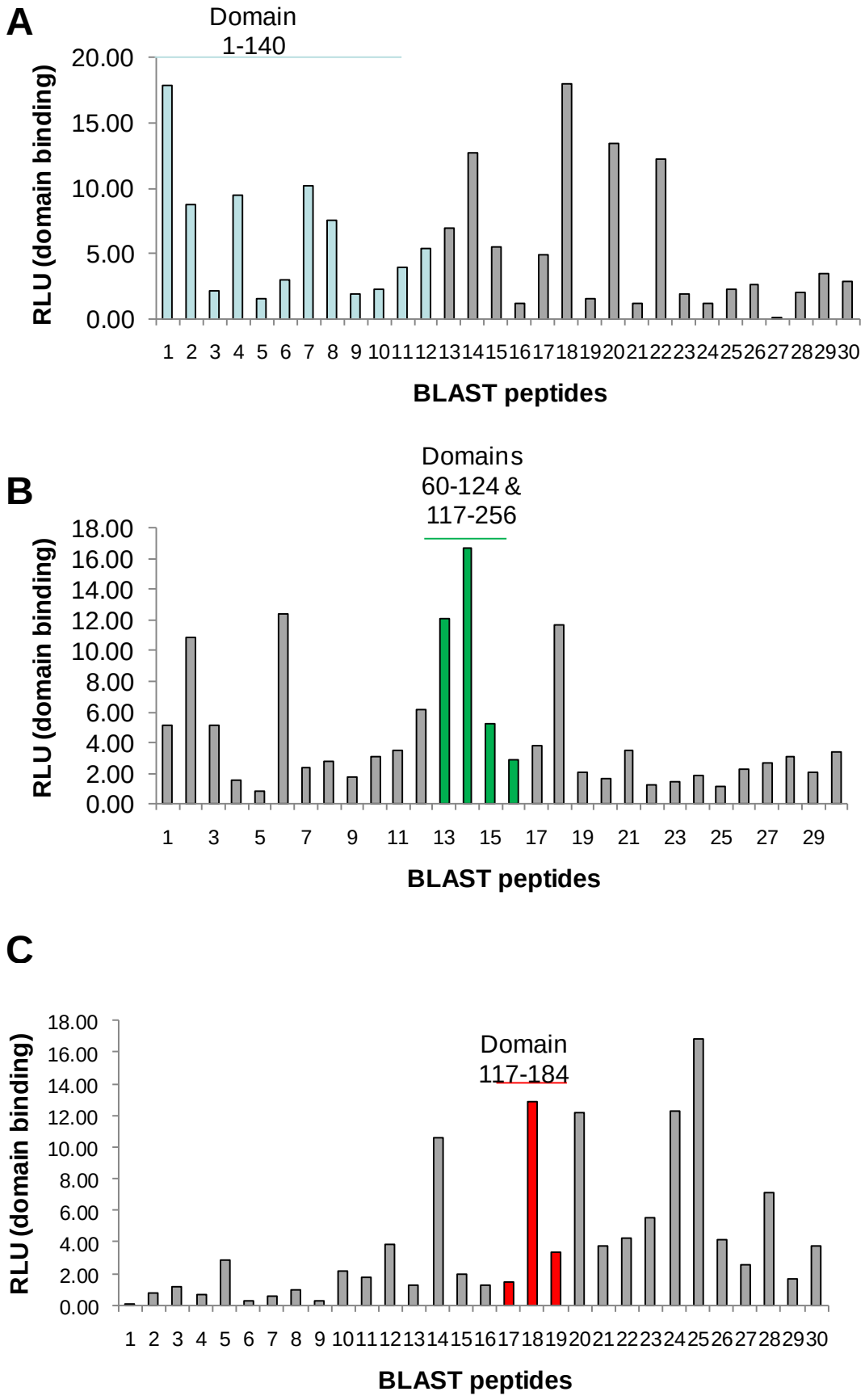

Figure 6.10: continued and described on next page

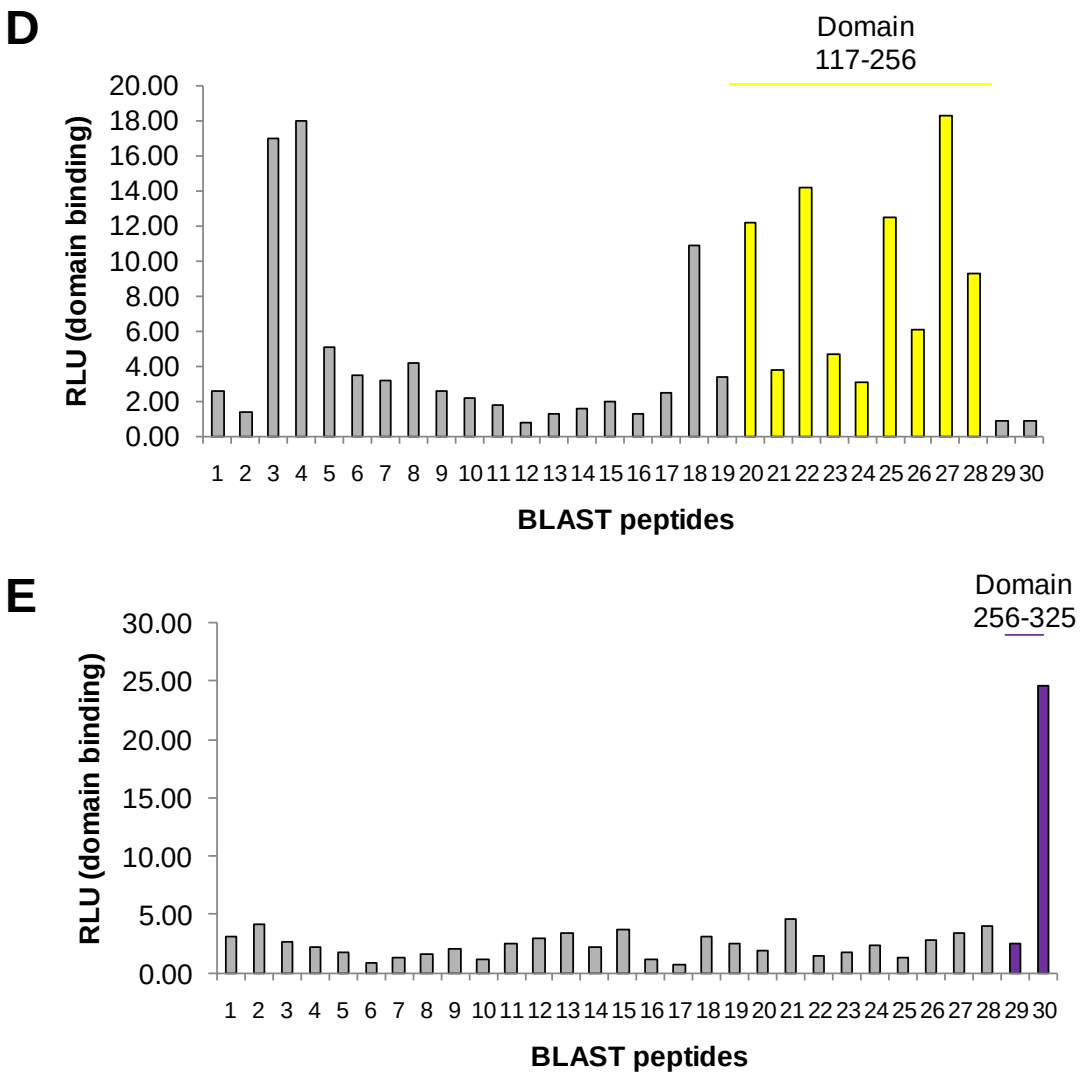

Figure 6.10: IRF-1 domain binding to BLAST peptides. Immobilised peptides (200 ng) were incubated with each IRF-1 domain (1 µg/ml). The graphs represent binding to the following domains, each named according to the IRF-1 amino acids they encompass: **(A)** 1-140, **(B)** 60-124, **(C)** 117-184, **(D)** 117-256 and **(E)** 265-325. The coloured columns indicate which of the 24 peptides were selected with the domain used in the assay. Following extensive washing, domain binding was detected with an anti-His antibody and enhanced chemiluminescence.

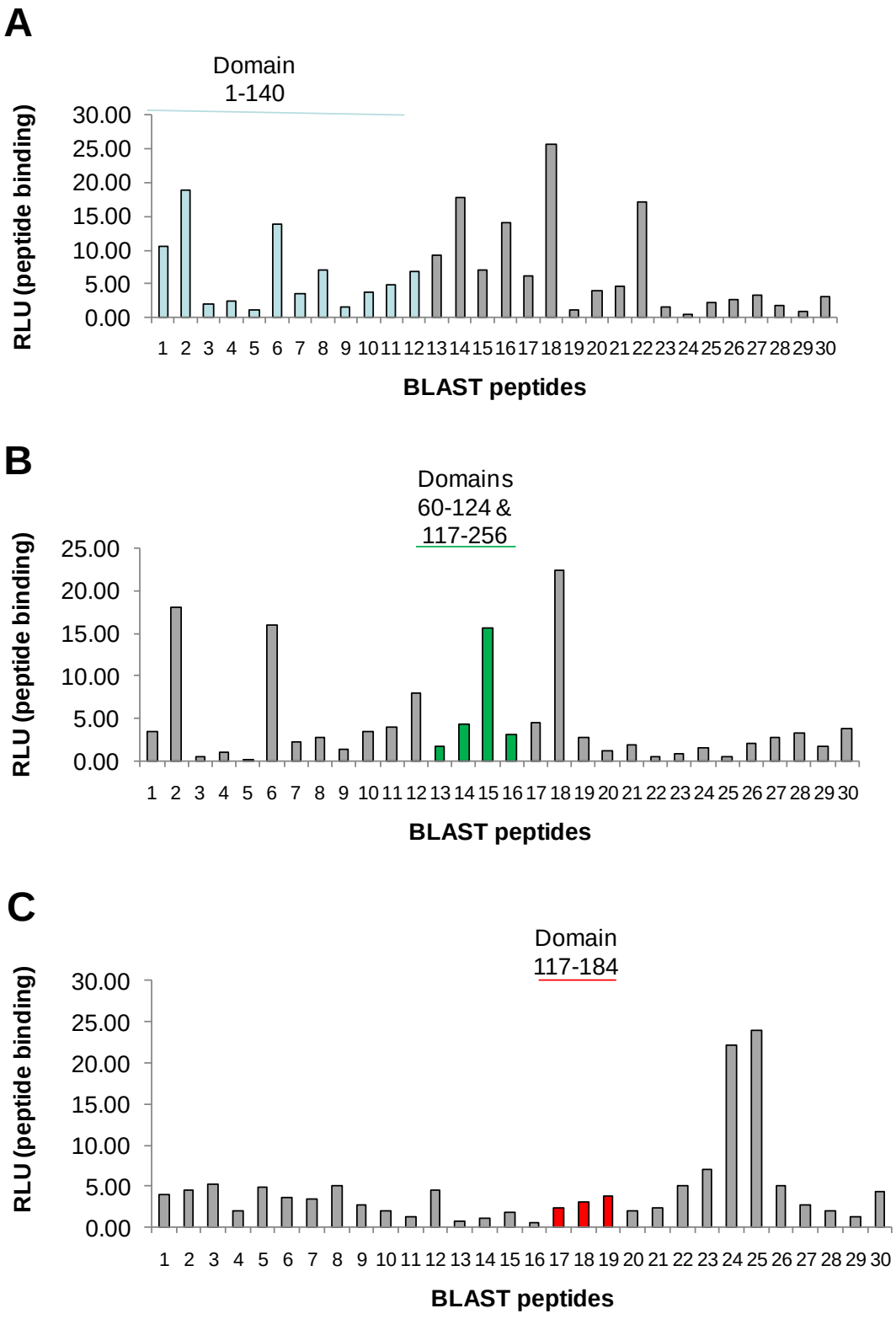

Figure 6.11: continued and described on next page

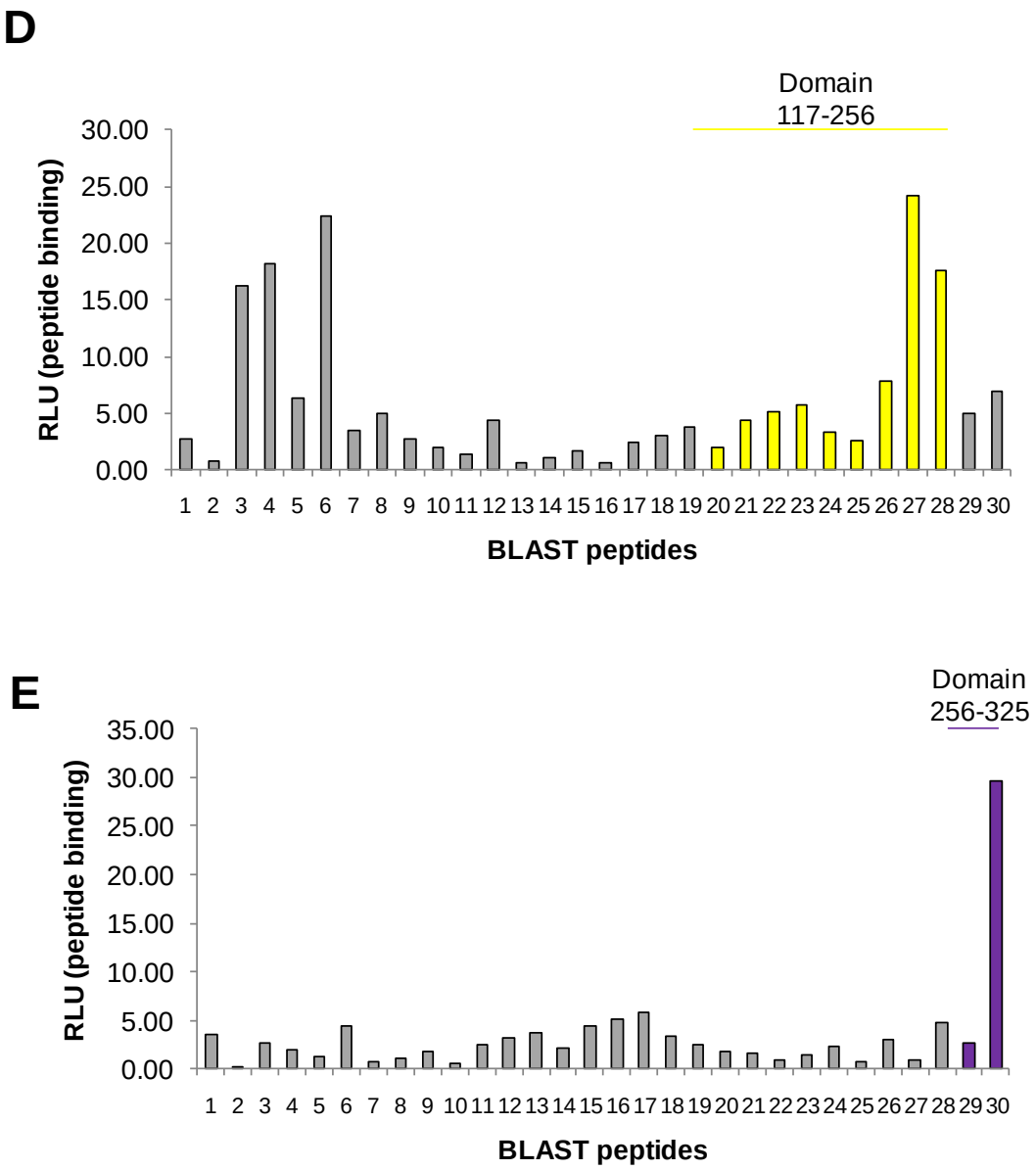

Figure 6.11: IRF-1 domain binding to BLAST peptides. Immobilised domains (200 ng) were incubated with each peptide (1 µg/ml). The graphs represent binding to the following domains, each named according to the IRF-1 amino acids they encompass: **(A)** 1-140, **(B)** 60-124, **(C)** 117-184, **(D)** 117-256 and **(E)** 265-325. The coloured columns indicate which of the 24 peptides were selected with the domain used in the assay. Following extensive washing, domain binding was detected with HRP-streptavidin and enhanced chemiluminescence.

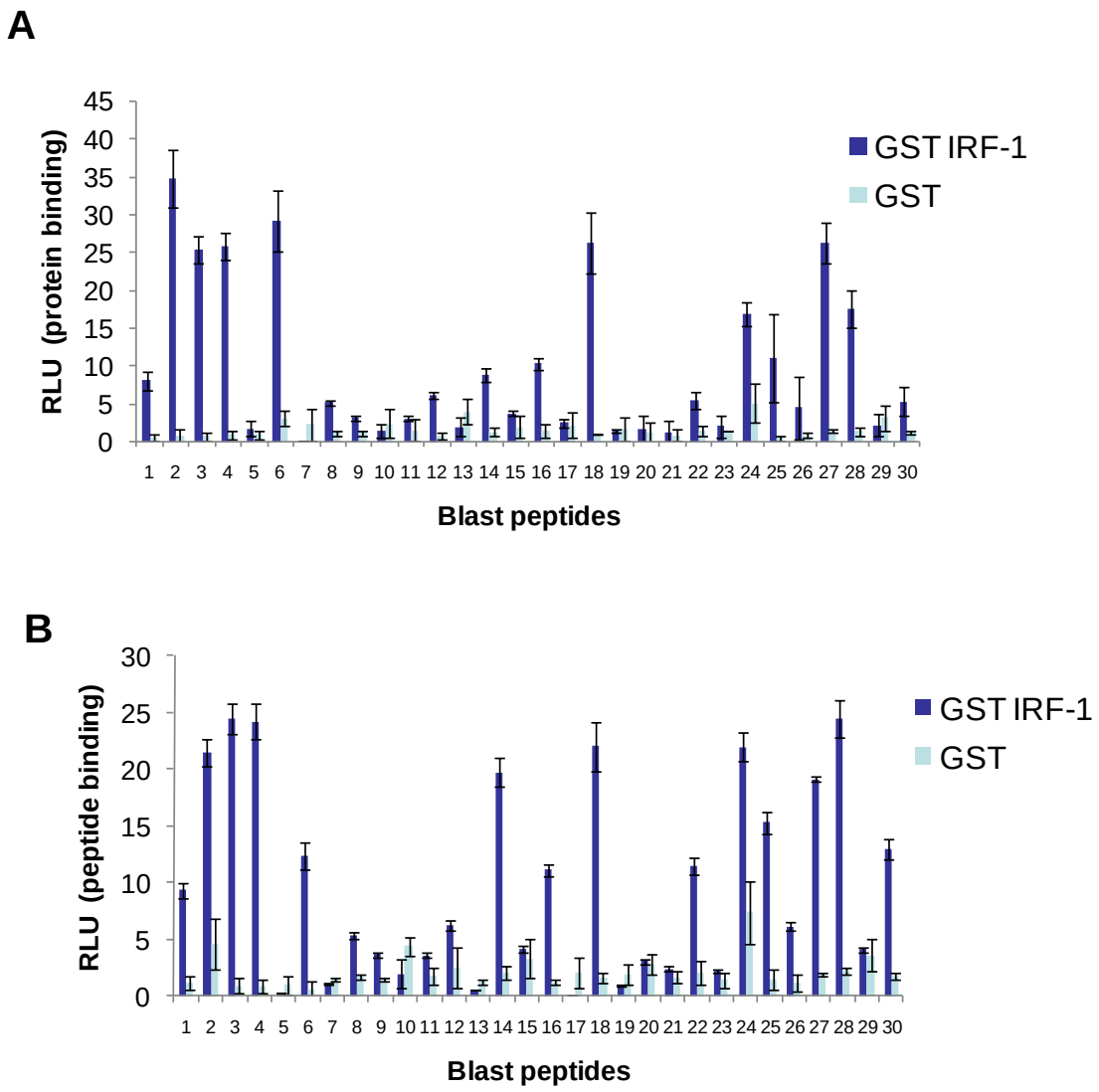

Figure 6.12: Peptide binding to full length IRF-1 **(A)** Immobilised BLAST peptides (200 ng) were incubated with free GST or GST-IRF-1 (1 µg/ml). Following extensive washing, GST and GST-IRF-1 binding was detected with an anti-GST antibody and enhanced chemiluminescence. **(B)** As in A except that GST or GST-IRF-1 (200 ng) were immobilised and incubated with the biotinlyated BLAST peptides (1 µg/ml). Peptide binding was detected with HRP-conjugated streptavidin and enhanced chemiluminescence.

Phage display peptide	1-140	60-124	117-184	117-256	256-325	Full length IRF-1
1	§*					
2	§*	§*				§*
3				§		§*
4	§			§		§*
5						
6	*	§*				§*
7	§					
8						
9						
10						
11						
12						
13		§				
14	§*	§	§			*
15		*				
16	*					
17						
18	§*	§*	§	§		§*
19						
20	§		§	§		
21						
22	§*			§		
23			*			
24			§*			*
25			§*	§		*
26						
27				§*		§*
28				§*		§*
29						
30					§*	

Figure 6.13: Summary of BLAST peptide binding to IRF-1 domains or the full-length protein. The symbol § indicates that the peptide was immobilised to the microtitre plate in the binding assay, that the protein was in the mobile phase and that relative binding affinity (measured in all peptide binding assays in relative light units (RLU)) was 50% higher than the mean. To calculate the mean RLU at which peptides bound full length GST-IRF-1, the values were first corrected for GST binding. The symbol * has the same meaning as §, except that the protein was immobilised in the binding assay and the peptide was in the mobile phase.

6.3 Preliminary validation of ZNF350 as an IRF-1-interacting protein

ZNF350 contains an N-terminal Kruppel-associated box (KRAB) repressor domain, a degradation signal, eight central C_2H_2 zinc fingers and a C-terminal repressor domain (CTRD) [398] (figure 6.14). BLAST peptide 30 lies within the CTRD. The first seven zinc fingers are required for DNA binding, whereas deletion of the eighth and the CTRD increases DNA-binding activity. The last nine amino acids of ZNF350 have been shown to be essential for oligomerisation, although the functional significance of ZNF350's ability to form tetramers is still unclear [399]. ZNF350 has been implicated in regulation of the DNA damage response [400, 401]. It has been shown to represses DNA damage response genes [400] and to be quickly degraded upon DNA damage, thus releasing target genes from repression [401]. The C-terminal repressor domain in which the IRF-1 binding element resides has been shown to function in a manner dependent on the breast and ovarian specific tumour suppressor BRCA-1 [398], whereas the N-terminal KRAB domain requires the co-repressor KAP-1 to repress target genes [402].

ZNF350 was also detected in a yeast-two-hybrid screen for IRF-1-interacting proteins using a human breast tumour epithelial cell library (mRNA from these cells was reverse-transcribed and used to generate a cDNA library that encoded over 124 million prey proteins: data unpublished). Additionally, our lab has recently shown that KAP-1 can be co-purified with an IRF-1 peptide (Narayan 2010, data unpublished). Each of the more than 220 KRAB domain zinc-finger proteins (ZFPs) encoded by the human genome contains an N-terminal 75-amino-acid KRAB box that binds directly to KAP-1 [403]. KAP-1 then recruits various silencing molecules, such as the NuRD histone deacetylase complex [404], the methyltransferase SET domain protein SETDB1 [405] and members of the heterochromatin protein 1 (HP1) family [406]. In this study, one of the peptides selected via phage display shows homology to a region of the SET domain. However the BLAST peptide that contained sequence from the SET domain (BLAST peptide 13) showed low relative binding affinities in ELISA assays against IRF-1 (figure 6.12A and B).

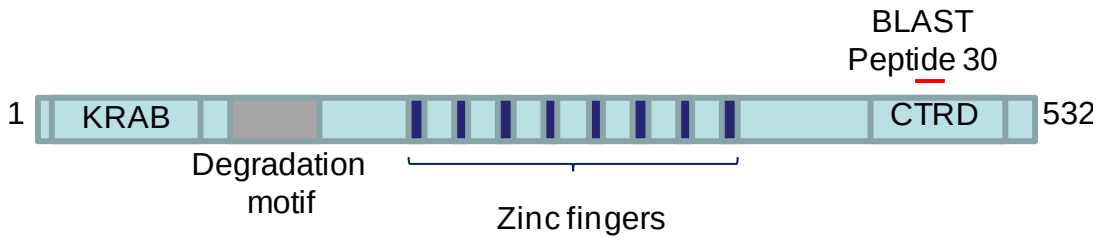

Figure 6.14: Structure of Zinc finger 350 protein. The region corresponding to IRF-1-binding BLAST peptide 30 is indicated. ZNF350 contains an N-terminal Kruppel-associated box (KRAB) repressor domain, a degradation signal, eight central C_2H_2 zinc fingers and a C-terminal repressor domain (CTRD).

To establish an intracellular interaction between endogenous IRF-1 and ZNF350, IRF-1 was immunoprecipitated using the single domain antibodies described in chapter 4. scFv3 and N, the single domain antibodies that showed the highest apparent affinity for IRF-1, were both able to co-immunoprecipitate endogenous IRF-1 and ZNF350 (figure 6.15). This indicates that neither scFv3 nor scFvN disrupt the IRF-1:ZNF350 interaction. A series of peptide-interaction assays were then used in an effort to map the ZNF350 binding site. A series of overlapping biotinylated peptides covering the full sequence of IRF-1 were immobilised onto streptavidin columns; next, untransfected lysate was added to each column and any bound protein was eluted after vigorous washing. Endogenous ZNF350 was found to bind specifically to a C-terminal IRF-1 peptide encompassing amino acids 300-320 (figure 6.16). This finding supports earlier peptide phage display evidence that ZNF350 binds within the extreme C-terminal domain of IRF-1 (figure 6.10E and 6.11E).

The peptide pull-down was validated in a separate experiment in which endogenous ZNF350 was co-precipitated using the C-terminal IRF-1 peptides spanning amino acids 300-320 and 305-325, but not with a control N-terminal IRF-1 peptide, or with a peptide containing sequence from the protein p21 which was also used as a negative control (figure 6.17). These two IRF-1 peptides contain an LXXLL motif previously shown to be important for interactions with co-factors [112]. However, an alanine scan of this motif was unable to abrogate ZNF350 binding (figure 6.17), suggesting that other residues are required for this interaction.

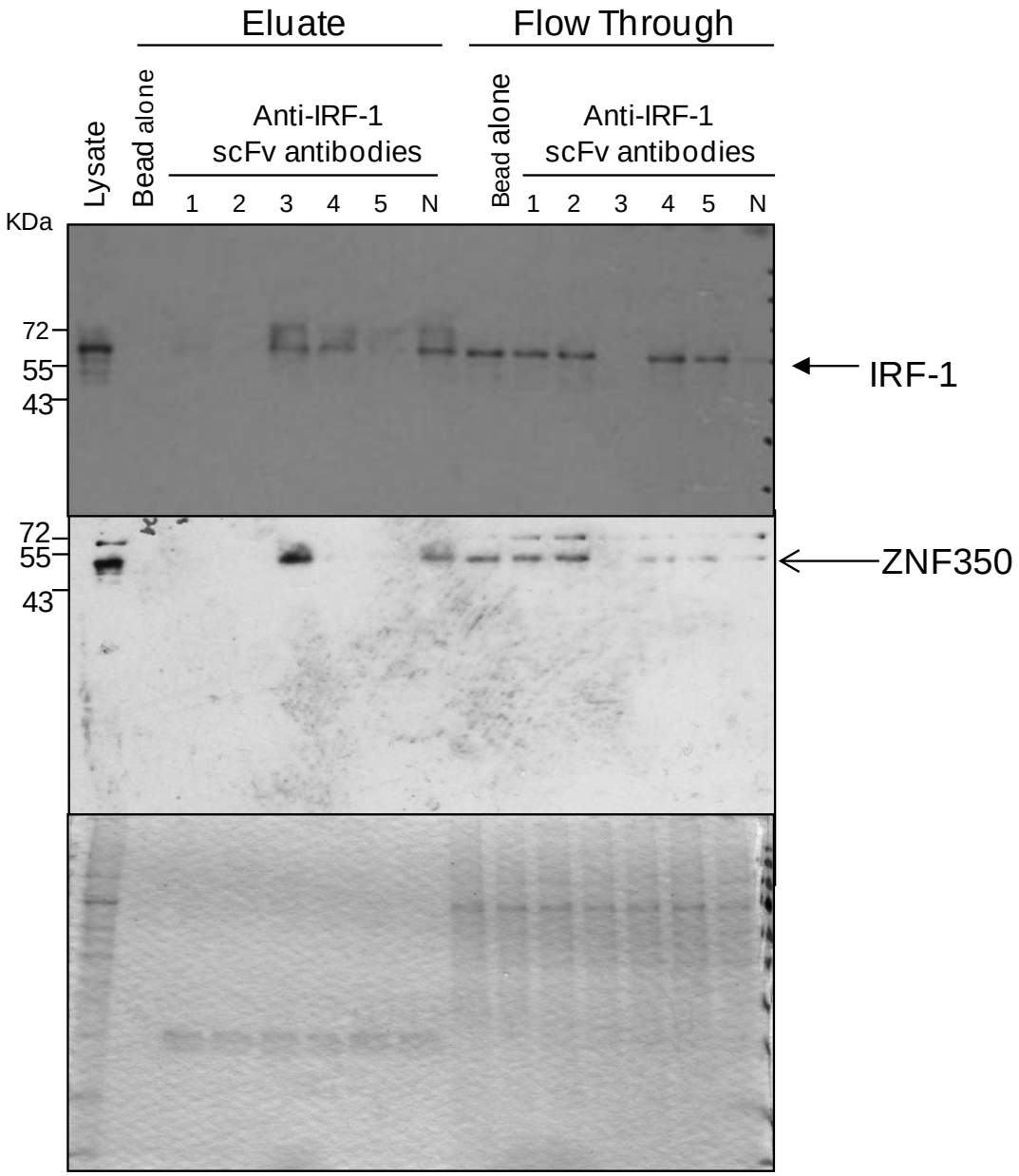

Figure 6.15: scFv antibodies immobilised on Ni^{2+}-NTA agarose beads were incubated with HeLa cell lysate (500 µg). Following extensive washing, bound proteins were eluted by in SDS-sample buffer and analysed by SDS-PAGE/immunoblot developed with anti-IRF-1 or anti-ZNF350 antibodies. Alternatively the gel was stained with colloidal blue (bottom panel). The results are representative of 2 independent experiments.

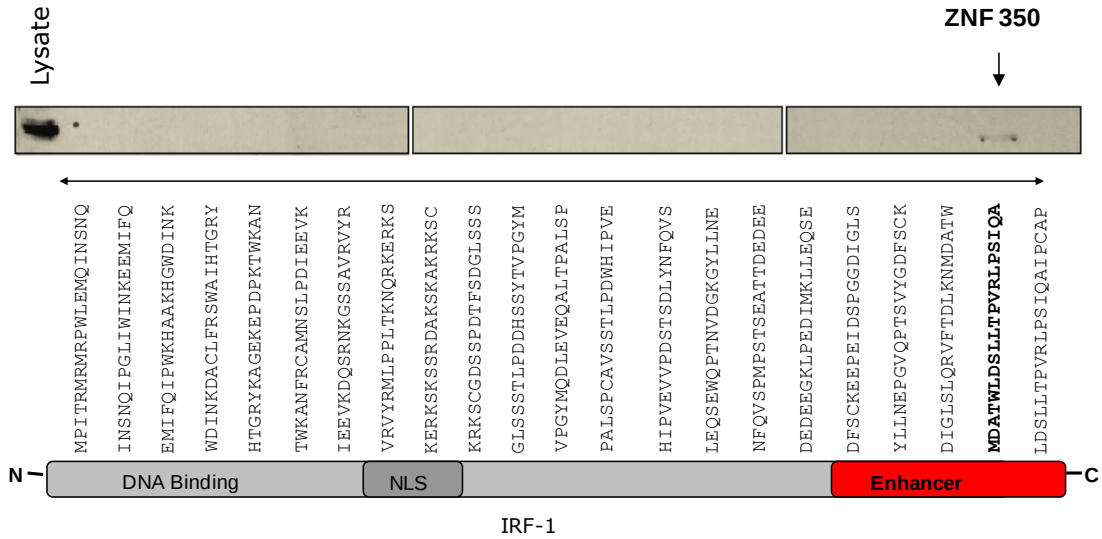

Figure 6.16: Overlapping IRF-1 peptides covering the entire length of the protein were used to generate affinity columns to which 0.5 mg of A375 cell lysate was added. Following rigorous washing, peptide-bound protein were eluted in SDS-PAGE sample buffer. The peptide pull-down was carried out in collaboration with Vikram Narayan. The eluates were then analysed through immunoblot with an anti-ZNF350 antibody.

A

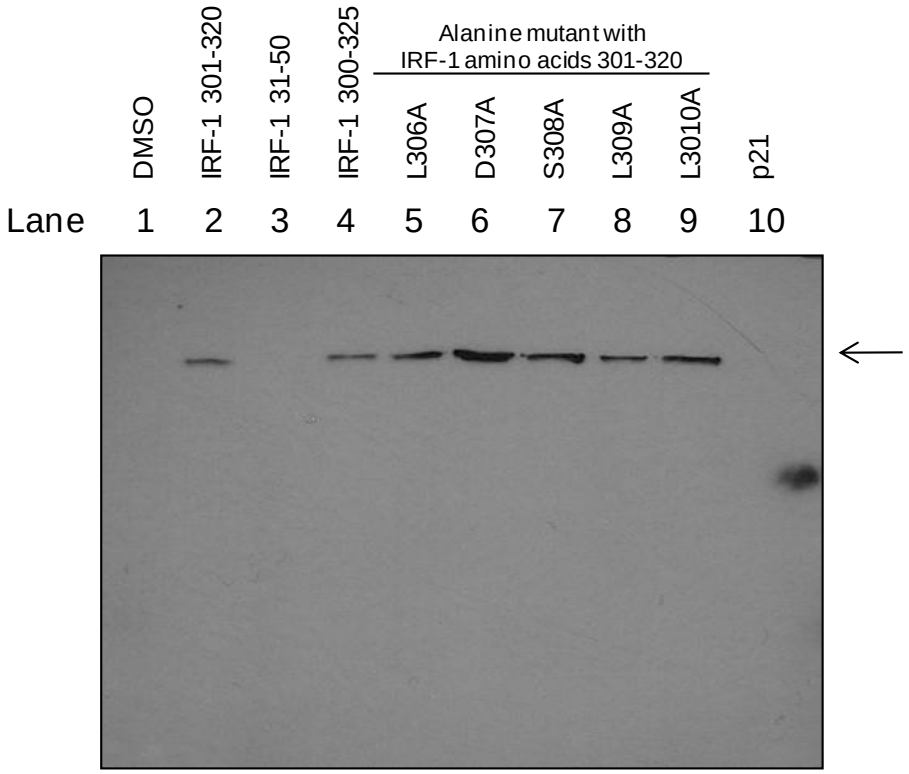

B Wild type peptide: 301- MDATWLDSLLTPVRLPSIQA - 320

Figure 6.17: (A) Biotinylated peptides were used to generate affinity columns to which 0.5 mg of A375 cell lysate was added. As the peptides were diluted in DMSO, lane 1 shows protein binding to DMSO alone. The IRF-1 peptides used were as follows: wild type amino acids 300-320 (lane 2), an N-terminal IRF-1 control peptide covering amino acids 31-50 (lane 3), an alanine scan within amino acids 301-320 of the LXXLL motif (lanes 5-9) and a control peptide containing sequence from the protein p21 (lanes 10). Following rigorous washing, peptide-bound proteins were eluted in SDS-PAGE sample buffer. The eluates were then analysed through immunoblot with an anti-ZNF350 antibody. This peptide pull-down was carried in collaboration with Vikram Narayan and Lucy Malin. **(B)** The sequence of the wild type peptide spanning IRF-1 amino acids 301-320 with the LXXLL motif underlined.

The importance of the C-terminus of IRF-1 for ZNF350 binding was further studied by attempting to co-precipitating endogenous ZNF350 with C-terminally truncated IRF-1 (figure 6.18A and B). One-STrEP-tagged wild type and ΔC25 IRF-1 were transiently transfected into mammalian cells and purified using a strep-tactin column (IBA GmbH) (figure 6.18A). Prior to lysis the transfected cells were treated with the chemical crosslinker DSP (Dithiobis[succinimidyl propionate]), which forms a covalent link between interacting proteins to aid co-purification of weakly interacting co-factors. In cells treated with DSP, endogenous ZNF350 was co-precipitated with transfected IRF-1 but not with the empty vector control. Unexpectedly, a smaller amount of ZNF350 also co-precipitated with ΔC25 IRF-1. This indicates that under the conditions of this experiment, ZNF350 can associate with transfected IRF-1 in a manner independent of the IRF-1 C-terminus. This may be through an intermediate protein or through a secondary binding site within IRF-1. To further examine the importance of the IRF-1 C-terminus in ZNF350 co-purification, the experiment was repeated with IRF-1 ΔC70 (figure 6.18B). In this instance no ZNF350 associated with the IRF-1 mutant.

These results indicate that the C-terminal 25 amino acids contain the primary ZNF350 interaction site, which is sufficient for co-precipitation of endogenous ZNF350 (figures 6.16 and 6.17). They also indicate that the C-terminal 70 amino acids house a second binding site that is required for a stable intracellular interaction between the two proteins (figure 6.18B), but is not sufficient for ZNF350 binding (figure 6.16). This model is represented in figure 6.19. As yet no direct interaction between full length IRF-1 and ZNF350 has been confirmed. A logical next step would be to clone ZNF350 into a bacterial expression vector so that further *in vitro* validation of this interaction can be attempted; however, neither this nor any further validation of this interaction is described in this thesis and such analysis is instead be left for future studies.

Figure 6.20 summarises the strategy used in this investigation and several of the steps that could be taken to expand it.

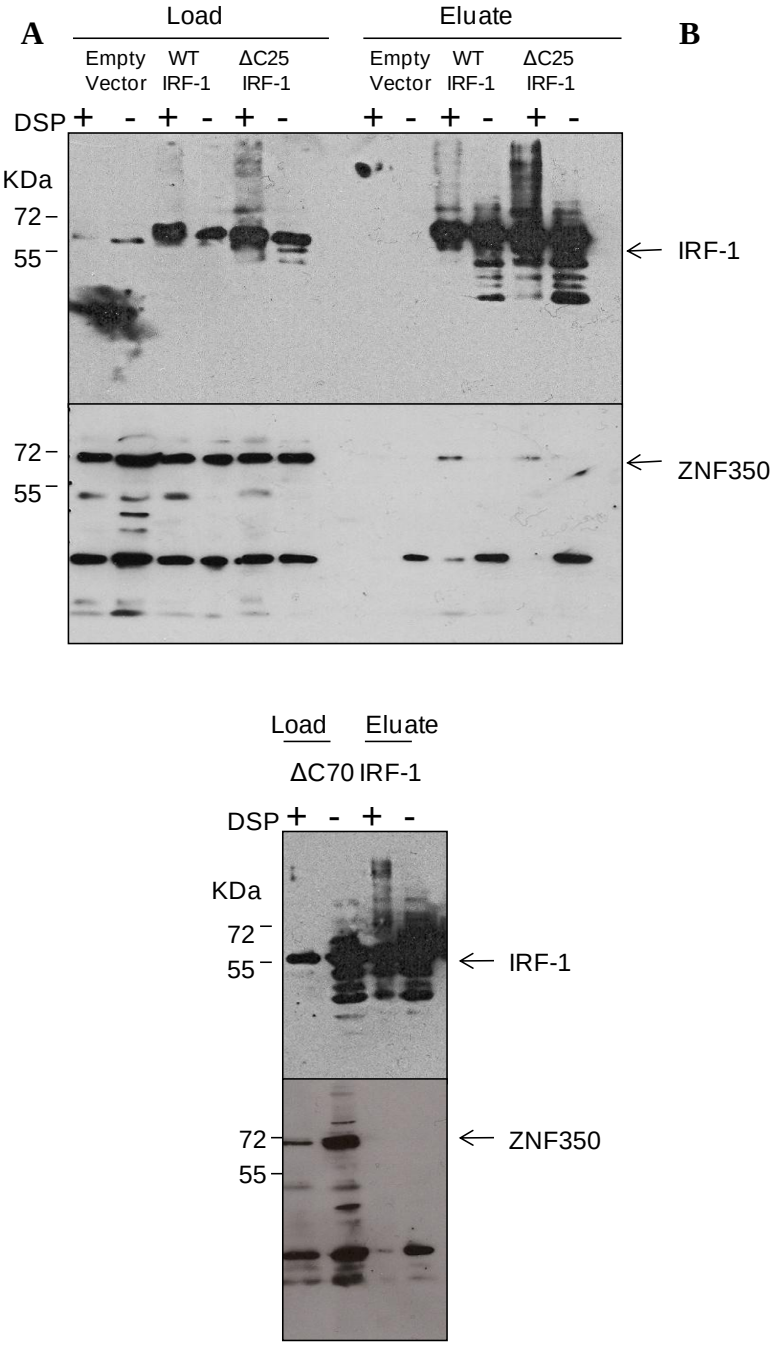

Figure 6.18: (A) One-STrEP-tagged wild type IRF-1, IRF-1 ΔC25 or empty vector were transiently transfected into A375 cells. Cells were then left untreated or exposed to 2 mM of the cross-linking agent DSP (Dithiobis[succinimidyl propionate]). One-STrEP-associated complexes were purified on Streptactin beads and analysed by SDS-PAGE and immunoblot with anti-IRF-1 (top panel) and anti-ZNF350 (bottom panel) antibodies. **(B)** One-STrEP-tagged ΔC70 IRF-1 was transiently transfected into A375 cells. Cells were then left untreated or exposed to 2 mM of the cross-linking agent DSP. One-STrEP-associated complexes were purified on Streptactin beads and analysed by SDS-PAGE and immunoblot with anti-IRF-1 (top panel) and anti-ZNF350 (bottom panel) antibodies. Performed by Lucy Mallin.

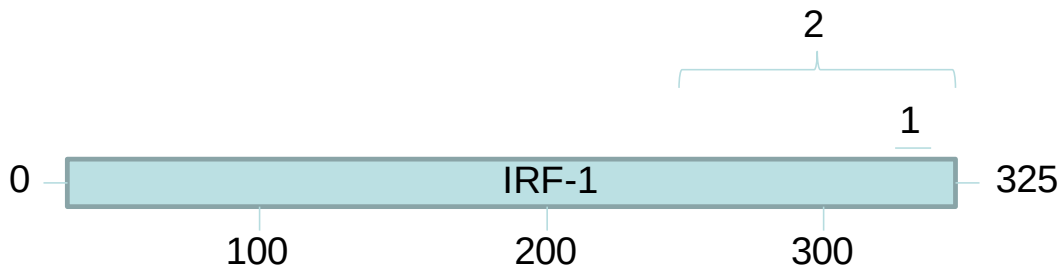

Figure 6.19: Modelling of ZNF350 interaction sites within IRF-1. **1:** primary binding site housed in last 25 amino acids of IRF-1, sufficient for interaction with ZNF350 **2:** secondary binding site in the last 70 amino acids of IRF-1, this site is required for stable binding to ZNF350, but not sufficient for this interaction.

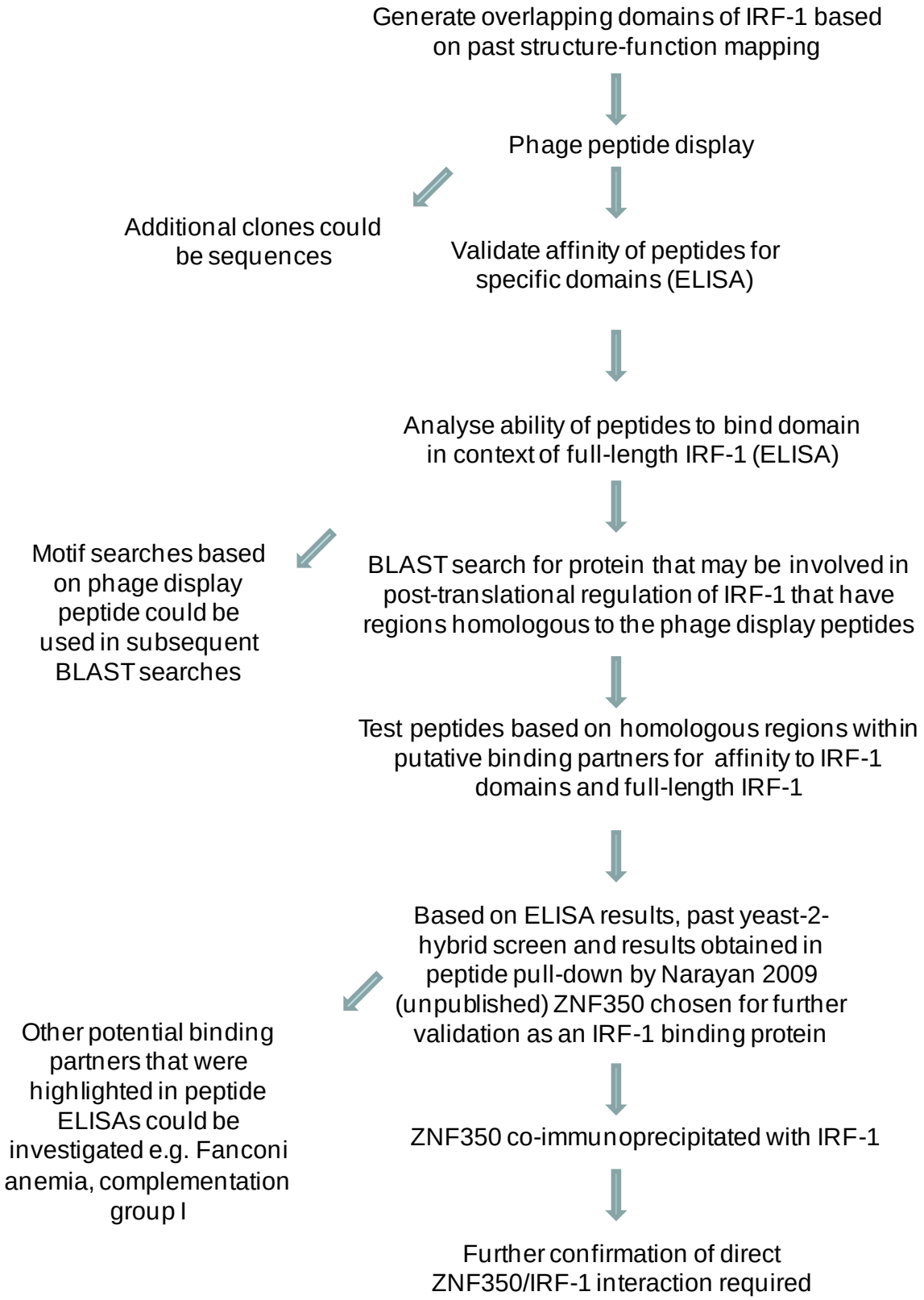

Figure 6.20: Flow diagram of the strategy used in this investigation. Possible additional avenues that could be taken to expand this study are indicated.

6.4 Results from new round of sequencing

The analysis described in section 6.2.1 was hampered by an inefficient sequencing service (all sequencing was necessarily out-sourced), which meant that only a limited number of phage display peptides could be sequenced. Following the trial of several alternative sequencing services, additional IRF-1-binding phage display peptides have now been successfully sequenced (figure 6.21). The time constraints of this PhD prevented these sequences from being tested for binding to IRF-1 or being used to define a novel IRF-1 binding motif. However, they have been included in this thesis in the hope that they could be used in future analysis.

The additional peptides included those selected for binding to IRF-1 domains spanning amino acids 1-124 and 256-300. The first of these encompasses the DNA binding and putative homodimerisation domain, and the second the enhancer domain minus the C-terminal 25 amino acids which have been shown to act in CDK2 repression and contain the LXXLL co-factor interaction motif [64, 72, 112]. The domains were subjected to the same peptide phage display screen as the other IRF-1 domains, but only four plaques were obtained following three selection rounds against domain 256-300; thus, only four sequences were obtained. To gain further insight into peptides able to bind this domain, the second round-pool of phage could be sequenced, or the third round of selection could be repeated. An additional ten phage-displayed peptides were also sequenced for each of the previously described IRF-1 domains (those encompassing amino acids: 1-140, 60-124, 117-184, 117-256 and 256-325).

The 12-mer phage display peptide 24 (figure 6.4), which was homologous to a region of ZNF350 (see figure 6.9), was sequenced in its entirety (figure 6.21): HSMVAPRTSLSP, and occurred with frequency (3/10) equal to that determined in the previous round of sequencing (figure 6.4). The newly identified residues did not increase its homology to BLAST peptide 30: VPS**VAP**Q**TSL**NI, which lies within ZNF350 (figure 6.14).

These newly acquired sequences should aid future validation of IRF-1 binding motifs and identification of novel binding partners.

Sequence	Frequency	Domain selected with
SEWSYNSPPSLP	4	1-140
HSKLNNRHHALL	2	1-140
ANPAWNADFSIF	2	1-140
SSTRVKSAPALL	2	1-140
HPKIIPHTLAAP	4	1-124
TFLSHSAGMLSL	1	1-124
SIIQMNLHRPTS	2	1-124
ALNWSPKLPVPP	2	1-124
LPGKPYMVEQLR	1	1-124
NYSHLRVKLPTP	1	60-124
ALYKTSTATALL	2	60-124
HFHYPKKAGLPP	2	60-124
SPFGMIAQQGLR	1	60-124
NFMPSLPRLGMH	1	60-124
SSYAPYVWQPIA	1	60-124
SDTTRPPSAGLP	1	60-124
TYHESQTSFTNT	1	60-124
WDDTLWPRPMRH	1	117-184
AMAVKLNYPLGY	2	117-184
HLKMMVAPRTSL	2	117-184
VISNHAESSRRL	1	117-184
LMSPNNNTLRIS	1	117-184
HYSIRLPASASL	1	117-184
RLEMTPHLNALL	1	117-184
QTSSPTPLSHTQ	1	117-184
ALYKTSTATALL	5	117-256
ASITHFKSGKSH	4	117-256
SVSLPYANLATH	1	117-256
HSMVAPRTSLSP	2	256-300
SAVPSSPALLTA	1	256-300
DDPTSATSWPAL	1	256-300

Figure 6.21: Sequence of 12-mer peptide selected as binding IRF-1 domains encompassing amino acids 1-140, 1-124, 60-124, 117-184, 117-256, 256-300 and 256-325. Newly identified sequence is shown in blue. Ten peptides sequenced per domain, except for domain 256-300 for which insufficient clones were obtained.

6.5 Discussion

The results detailed in this chapter show that IRF-1 binding peptides can be acquired through phage display and that the sequence of these peptides can be used to identify proteins that form intracellular complexes with IRF-1. Furthermore, these IRF-1-binding peptides provide reagents that could be developed in the future and used for the purification, detection or potentially even functional modulation of IRF-1 (bioactive peptides).

Peptide phage display can be used to quickly determine the amino acid sequence of target protein binding motifs, but systematic approaches are required to sift through this information and use it to gain new insight into biological pathways. In this study, peptides were tested for their ability to bind IRF-1 outside of the phage display system in an ELISA format. Of particular interest were phage display peptides 3, 8, 14, 18 and 24 which showed both domain specificity and high relative affinities for full length IRF-1 (figure 6.8). These peptides could be assessed in future studies for their ability to purify endogenous IRF-1 in peptide pull-down experiments or modulate IRF-1 expression following intracellular expression. For instance, it would be interesting to know if phage-display peptide 24 or BLAST peptide 30 could disrupt IRF-1's interaction with ZNF350 and if so what effect this had on the activity of both.

The use of isolated domains allows particular functions to be targeted and will aid future mapping of peptide binding sites. It also limits the possibility of peptides being selected against only one or two "hot-spots" (highly hydrophobic sites) within the protein [407, 408] which would reduce the number of functions studied. However, the technique has limitations in that several of the selected peptides show no affinity for IRF-1 outside the phage display system. Additionally, the experimental process relies on constant screening of the selected peptides as epitope availability may be different in the isolated domain compared to the full-length protein. Variation in epitope availability caused by immobilisation of target protein during phage display and ELISAs also affects peptide binding. It can be seen in figure 6 that when full length IRF-1 is immobilised (figure 6.12B), fewer peptides

are able to bind than when the peptides themselves are immobilised and IRF-1 is in the liquid phase (figure 6.12A).

In an effort to identify novel IRF-1 interacting proteins BLAST peptides were selected for their homology to proteins involved in pathways interesting to this research group. This is a deeply biased final selection; however, restricting the number proteins studied on the basis of function and known associations has been used successfully in the past as a strategy for identifying physiologically relevant co-factors [268, 279, 393, 396]. It is possible that IRF-1 may interact with more than one site within another protein. The ELISAs described here involve interactions with peptides and do not take account of avidity. Binding partners that require several weak interactions may not be identified. The One-STrEP co-purifications involving C-terminally truncated IRF-1 suggest that ZNF350 may also bind outside amino acids 301-320 of IRF-1, even through these residues were all that was needed to co-purify the endogenous protein. That no other IRF-1 peptide could pull-down endogenous ZNF350 suggests that this secondary interaction is weaker, an idea supported by the reduced amount of ZNF350 co-precipitated by IRF-1 ΔC25. Alternatively, as association with the mutant protein was seen in the context of total cell lysate, it is possible that ZNF350 interacts with truncated IRF-1 through an unidentified intermediate. KAP-1 was previously identified as an IRF-1 interacting protein (Narayan unpublished) in a pull-down using an IRF-1 20-mer peptide; therefore, the possible contribution of this protein to IRF-1/ZNF350 complex is worthy of further investigation. Another possible protein involved in this complex could be BRAC1, which also binds to the CTR domain of ZNF350 targeted by IRF-1 (the sequence of IRF-1-binding BLAST peptide 30 lies within this region). Cloning, expression and purification of full-length ZNF350 will allow a direct interaction with IRF-1 to be studied *in vitro* and is therefore the next logical step in characterising this interaction.

An interaction between ZNF350 and IRF-1 could have a number of consequences. Like IRF-1, ZNF350 has been shown to inhibit cell growth [409] and function as a transcription factor that can repress target gene expression [410]. Previously published experimental evidence indicates that the ZNF350/KAP-1 repressor

complex functions through association with other proteins; for example, ZNF-mediated repression has been shown to be modulated by interactions between KAP-1, histone methyltransferases and histone deacetylases [404, 405]. It has also been suggested that this complex has alternative functions as its association with the Epstein-Barr Virus replication protein BBLF2/3 stimulated DNA replication and deletion of a ZNF350 binding site at the origin of replication impaired replication [411]. ZNF350 has also been shown to complex with BRAC1 to repress transcription of GADD45 (Growth Arrest and DNA Damage 45) [400]. This study demonstrated that GADD45 repression required both the KAP-1 and BRCA1 binding domains in ZNF350 (also known as the KRAB and CTR domains), although the presence of KAP-1 within the repressor complex was not confirmed.

Few proteins have been shown to interact with the C-terminus of IRF-1 despite its many known functions [112]. ZNF350 may shed light on the mechanisms through which the IRF-1 C-terminus switches between mediation of transcriptional induction, repression and trans-activation of other transcription factors [64, 72, 101].

7 Final discussion

Previous studies have suggested that IRF-1 is primarily regulated through an increase in its expression in response to infection [2], cytokine stimulation [27] or DNA damage [29]; however it now seems possible that post-translational regulation could also play an important role. One of the most significant finding of this study is that IRF-1 can be activated through its C-terminal residues in a manner linked to its increased degradation. This ties in with the finding by Wantabe *et al* 1991 that, in cells transfected with IRF-1, transcription from an IRF-1-responsive reporter gene could be induced in the absence of *de novo* protein synthesis (i.e. in the presence of cycloheximide) through viral stimulation [67]. It was also shown that the kinase inhibitor staurosporine could block viral induction of the same reporter gene, suggesting that phosphorylation may be acting as an activating post-translational modification [67]. This idea was subsequently supported by a decrease in IRF-1 activity observed following mutation of potential phosphoaceptor sites in the transactivation domain: amino acids 219 to 231 [109], although it is possible this 12 residue deletion had other affects on IRF-1 besides preventing its phosphorylation. However, no link has been made between the extreme C-terminal residues of IRF-1 bound by scFv3 (amino acids 306-325) and phosphorylation; in fact the only IRF-1-targeting kinase identified to date, casein kinase II, has been described as binding within the N-terminal 120 amino acids and phosphorylating residues between amino acids l38-l50 and 219–231 [109]. The results given in chapter 5 indicate that post-translational regulation, mediated by the extreme C-terminus of IRF-1, is rate-limiting for the activity of the endogenous protein. This finding highlights a new avenue through which anti-cancer downstream targets of IRF-1 could be activated through the action of biologics similar to/or based on scFv3.

The data in chapter 5 also reveal that both intrabody-bound IRF-1 and P325A mutant exhibit an increased transactivation activity and rate of degradation. The co-localisation of these two characteristics suggests that they may be linked. Degradation is an obvious mechanism through which a signal could be “switched off”, but degradation coupled with *de novo* protein synthesis is an energy-expensive means of regulation. However, such a process would enable efficient cycling of

different transcription factor complexes on the same promoter. As detailed in the introduction to chapter 4 IRF-1 has a short half life of 20-40 minutes, is polyubiquitinated and degraded by the 26S proteosome [111]. Furthermore, fluctuations in IRF-1's half life have been linked to its role in DNA damage response [29]. It is therefore possible that tight control of IRF-1 turnover may be a mechanism through which its expression at specific points in the cell cycle and in response to stress are controlled.

Several studies have previously linked proteosomal degradation with transcriptional regulation. Some transcription factor co-activators have been shown to possess ubiquitin ligase activity. For example, E6-AP (E6-associated protein) is an E3 ligase that directly interacts with and activates the transcription factor PR (human progesterone receptor) [387]. Additionally, activation of the retinoic acid receptor by its ligand triggers both the receptor's transcription factor activity and its proteosomal degradation [248].

Proteosomal function has been more directly linked to the enhancement of some transcriptional activities. For instance ERα (estrogen receptor)-mediated transcription was seen to be lost following inhibition of the proteosome, whereas other transcription factors (Sp1, p53 and E2F) were moderately stimulated [412]. Several co-activators of ERα were shown to be subject to proteosomal degradation and, unlike ERα, show enhanced activity following inhibition of the proteosome. Although the exact mechanism through which the proteosome regulates ERα-mediated transcription is still not clear, it was suggested by the authors of this study that it may operate through co-factor turnover [412]. For instance, proteosomal inhibition may lead to the accumulation of an as yet unidentified repressor.

The Drosophila co-activator TAFI (TBP associated factor 1), the central subunit within the general transcription factor TBP (TATA box binding protein), was shown to mediate ubiquitination of histone H1 [413]. Point mutations in TAFI that abolished H1-specific ubiquitination reduced cellular levels of ubiquitinated histone H1 and also decreased the expression of genes targeted by the maternal transcription factor Dorsal [413]. Removal of histones would allow the DNA to decondense and transcription factors to gain access. In further support of transcriptional regulation

through degradation; RNA polymerase II has been shown to be ubiquitinated in response to DNA damage [414]. This may ensure transcription is halted so that the DNA repair machinery can function. These results indicate that co-activator-mediated ubiquitination of proteins within the transactivation pathway may contribute to activation of eukaryotic transcription. However, it should be noted that these two studies did not validate a link between ubiquitination and proteosomal degradation, and that ubiquitination has also be shown to mediate subcellular relocalisation and lysosomal degradation [115].

The shortened half life of scFv3 bound IRF-1 may have been caused by aggregation or misfolding, but this is not supported by the increased induction seen from IRF-1-specific reporter genes. As scFv3 affects on reporter gene activation were dependent on the IRF-1 binding site in these promoters. it is unlikely that scFv3 was stimulating the IFN-β or TLR3-luciferase genes in an IRF-1-independent manner. That CDK2 repression was unaffected by scFv3 co-transfection suggests only a sub-set of IRF-1 activities are regulated by the extreme C-terminal residues, although it is also possible that the scFv3 concentrations were not optimal for modulation of CDK2 repression. This may mean that the scFv3 epitope can act as a switch, allowing IRF-1 to mediate alternative responses to different stimuli. This possibility could be investigated by profiling changes in the transcriptome caused by scFv3 activation of IRF-1 in microarray assays. Such an experiment could be simplified by labelling scFv3 with a cell penetrating peptide [410] and adding it directly to the culture medium. This would also further test scFv3's ability to activate a more global IRF-1-mediated anti-tumour response. One key drawback of the study described in chapter 5 is the limited number of downstream IRF-1 targets investigated, which was affected by reagents available in the lab. As scFv3 has now been validated as an activating anti-IRF-1 intrabody, future studies should be able to increase the number of scFv3 affects investigated. In particular, it would be interesting to know if scFv3 can affect IRF-1 functions that are independent of DNA binding, such as its trans-activation of p53 through an association with p300 [72].

It is possible that the extreme C-terminus of IRF-1 acts as a co-factor docking site and thus modulates IRF-1 activity; i.e. that scFv3 binding mimicked a trans-activator

or dislodged a trans-repressor. To investigate this possibility, and as part of a long term strategy aimed at identifying binding partners of IRF-1, peptide phage display was used to isolate IRF-1-binding peptides (chapter 6). One of these peptides was homologous to a region in the C-terminal repressor domain of ZNF350. The immunoprecipitation of ZNF350 with endogenous IRF-1 by scFv3 further validates the usefulness of the scFv antibodies developed in chapter 4 and indicates ZNF350 may be a novel IRF-1 co-factor. It is possible that ZNF350 bound to scFv3 directly and non-specifically, although its ability to bind One-STrEP-tagged IRF-1 and the C-terminal IRF-1 peptide indicate that this is unlikely. Binding between full-length IRF-1 and full-length ZNF350 has not yet been shown to be direct, and hopefully this will be tackled in future studies. No previous link between ZNF350 and IRF-1 has been reported, although both are known to regulate the DNA damage response [71, 401, 415]. However, another member of my research group (Vikram Narayan: data unpublished) was able to purify Kap-1, a ZNF350 binding co-factor [402], from cell lysate with an IRF-1 20-mer peptide. It is also possible that BRCA-1, another ZNF350 co-factor [398], may be involved in a complex involving IRF-1, a possibility that could be tested in a future scFv immunoprecipitation experiment. Additionally, the effect of IRF-1co-transfection or knockout on a ZNF350 targeted reporter gene such as GADD45 could be investigated, as IRF-1 bound a peptide from the CTRD domain of ZNF350 required for GADD45 repression.

The possible impact of this association has already been discussed as part of chapter 3, but perhaps of greater interest for future research are the phage display peptides validated as having a high relative affinity for IRF-1. These peptides have been shown to bind IRF-1 *in vitro* (ELISA), and could next be used to co-purify endogenous IRF-1. Any peptide able to bind endogenous IRF-1 could then be tested for its ability to modify the activity of endogenous IRF-1 following intracellular expression. As these peptide would be smaller than scFv3 (20-mer compared to 183-mer) they may be better able to penetrate active sites within the folded protein. They would also have the advantage that they were selected to domains spanning the length of IRF-1, and could potentially therefore target a more diverse range of IRF-1 activities than the intrabodies. Although useful, a drawback of drugs like cycloheximide or staurosporine is that they globally affect protein synthesis and post-

translational modifications. For instance, the study by Wantabe *et al* 1991 indicated that the proteins responsible for post-translational activation of IRF-1 do not themselves need to be *de novo* synthesised, whereas the cycloheximide treatment may have in fact blocked the synthesis of physiologically important IRF-1 regulators. Studies limited by such all-inclusive drugs emphasise the need for more precise agents that target not only specific proteins, but even specific domains and activities. This study has demonstrated that phage display can be used to develop such reagents.

8 Bibliography

1. Fujita, T., et al., *Evidence for a nuclear factor(s), IRF-1, mediating induction and silencing properties to human IFN-beta gene regulatory elements.* Embo J, 1988. **7**(11): p. 3397-405.
2. Miyamoto, M., et al., *Regulated expression of a gene encoding a nuclear factor, IRF-1, that specifically binds to IFN-beta gene regulatory elements.* Cell, 1988. **54**(6): p. 903-13.
3. Latchman, D.S., *Transcription factors: an overview.* Int J Biochem Cell Biol, 1997. **29**(12): p. 1305-12.
4. Weake, V.M. and J.L. Workman, *Inducible gene expression: diverse regulatory mechanisms.* Nat Rev Genet, 2010. **11**(6): p. 426-37.
5. Harada, H., et al., *Structurally similar but functionally distinct factors, IRF-1 and IRF-2, bind to the same regulatory elements of IFN and IFN-inducible genes.* Cell, 1989. **58**(4): p. 729-39.
6. Willman, C.L., et al., *Deletion of IRF-1, mapping to chromosome 5q31.1, in human leukemia and preleukemic myelodysplasia.* Science, 1993. **259**(5097): p. 968-71.
7. Kessler, D.S., D.E. Levy, and J.E. Darnell, Jr., *Two interferon-induced nuclear factors bind a single promoter element in interferon-stimulated genes.* Proc Natl Acad Sci U S A, 1988. **85**(22): p. 8521-5.
8. Levy, D.E., et al., *Interferon-induced nuclear factors that bind a shared promoter element correlate with positive and negative transcriptional control.* Genes Dev, 1988. **2**(4): p. 383-93.
9. Foss, G.S. and H. Prydz, *Interferon regulatory factor 1 mediates the interferon-gamma induction of the human immunoproteasome subunit multicatalytic endopeptidase complex-like 1.* J Biol Chem, 1999. **274**(49): p. 35196-202.
10. Nguyen, H., et al., *Identification of the secretory leukocyte protease inhibitor (SLPI) as a target of IRF-1 regulation.* Oncogene, 1999. **18**(39): p. 5455-63.
11. Elser, B., et al., *IFN-gamma represses IL-4 expression via IRF-1 and IRF-2.* Immunity, 2002. **17**(6): p. 703-12.
12. Andersen, P., et al., *EGFR induces expression of IRF-1 via STAT1 and STAT3 activation leading to growth arrest of human cancer cells.* Int J Cancer, 2008. **122**(2): p. 342-9.
13. Okamoto, T., et al., *Optimal construction of non-immune scFv phage display libraries from mouse bone marrow and spleen established to select specific scFvs efficiently binding to antigen.* Biochem Biophys Res Commun, 2004. **323**(2): p. 583-91.
14. Bouker, K.B., et al., *Interferon regulatory factor-1 (IRF-1) exhibits tumor suppressor activities in breast cancer associated with caspase activation and induction of apoptosis.* Carcinogenesis, 2005. **26**(9): p. 1527-35.
15. Tanaka, N., M. Ishihara, and T. Taniguchi, *Suppression of c-myc or fosB-induced cell transformation by the transcription factor IRF-1.* Cancer Lett, 1994. **83**(1-2): p. 191-6.
16. Donehower, L.A., et al., *Mice deficient for p53 are developmentally normal but susceptible to spontaneous tumours.* Nature, 1992. **356**(6366): p. 215-21.
17. Tanaka, N., et al., *Cellular commitment to oncogene-induced transformation or apoptosis is dependent on the transcription factor IRF-1.* Cell, 1994. **77**(6): p. 829-39.

18. Harada, H., et al., *Accelerated exon skipping of IRF-1 mRNA in human myelodysplasia/leukemia; a possible mechanism of tumor suppressor inactivation.* Oncogene, 1994. **9**(11): p. 3313-20.
19. Boultwood, J., et al., *Allelic loss of IRF1 in myelodysplasia and acute myeloid leukemia: retention of IRF1 on the 5q- chromosome in some patients with the 5q- syndrome.* Blood, 1993. **82**(9): p. 2611-6.
20. Green, W.B., et al., *Lack of IRF-1 expression in acute promyelocytic leukemia and in a subset of acute myeloid leukemias with del(5)(q31).* Leukemia, 1999. **13**(12): p. 1960-71.
21. Moriyama, Y., et al., *Tumor-suppressor effect of interferon regulatory factor-1 in human hepatocellular carcinoma.* Clin Cancer Res, 2001. **7**(5): p. 1293-8.
22. Nozawa, H., et al., *Functionally inactivating point mutation in the tumor-suppressor IRF-1 gene identified in human gastric cancer.* Int J Cancer, 1998. **77**(4): p. 522-7.
23. Tzoanopoulos, D., et al., *Low expression of interferon regulatory factor-1 and identification of novel exons skipping in patients with chronic myeloid leukaemia.* Br J Haematol, 2002. **119**(1): p. 46-53.
24. Lee, E.J., et al., *Alternative splicing variants of IRF-1 lacking exons 7, 8, and 9 in cervical cancer.* Biochem Biophys Res Commun, 2006. **347**(4): p. 882-8.
25. Barber, S.A., et al., *Differential expression of interferon regulatory factor 1 (IRF-1), IRF-2, and interferon consensus sequence binding protein genes in lipopolysaccharide (LPS)-responsive and LPS-hyporesponsive macrophages.* Infect Immun, 1995. **63**(2): p. 601-8.
26. Kamijo, R., et al., *Requirement for transcription factor IRF-1 in NO synthase induction in macrophages.* Science, 1994. **263**(5153): p. 1612-5.
27. Galon, J., et al., *IL-12 induces IFN regulating factor-1 (IRF-1) gene expression in human NK and T cells.* J Immunol, 1999. **162**(12): p. 7256-62.
28. Coccia, E.M., et al., *IFN-gamma and IL-4 differently regulate inducible NO synthase gene expression through IRF-1 modulation.* Int Immunol, 2000. **12**(7): p. 977-85.
29. Pamment, J., et al., *Regulation of the IRF-1 tumour modifier during the response to genotoxic stress involves an ATM-dependent signalling pathway.* Oncogene, 2002. **21**(51): p. 7776-85.
30. Remoli, M.E., et al., *Selective expression of type I IFN genes in human dendritic cells infected with Mycobacterium tuberculosis.* J Immunol, 2002. **169**(1): p. 366-74.
31. Pine, R., A. Canova, and C. Schindler, *Tyrosine phosphorylated p91 binds to a single element in the ISGF2/IRF-1 promoter to mediate induction by IFN alpha and IFN gamma, and is likely to autoregulate the p91 gene.* Embo J, 1994. **13**(1): p. 158-67.
32. Darnell, J.E., Jr., I.M. Kerr, and G.R. Stark, *Jak-STAT pathways and transcriptional activation in response to IFNs and other extracellular signaling proteins.* Science, 1994. **264**(5164): p. 1415-21.
33. Pine, R., *Convergence of TNFalpha and IFNgamma signalling pathways through synergistic induction of IRF-1/ISGF-2 is mediated by a composite GAS/kappaB promoter element.* Nucleic Acids Res, 1997. **25**(21): p. 4346-54.
34. Moschonas, A., et al., *CD40 induces antigen transporter and immunoproteasome gene expression in carcinomas via the coordinated action of NF-kappaB and of NF-kappaB-mediated de novo synthesis of IRF-1.* Mol Cell Biol, 2008. **28**(20): p. 6208-22.
35. Burnet, M., *Cancer: a biological approach. III. Viruses associated with neoplastic conditions. IV. Practical applications.* Br Med J, 1957. **1**(5023): p. 841-7.
36. van den Broek, M.E., et al., *Decreased tumor surveillance in perforin-deficient mice.* J Exp Med, 1996. **184**(5): p. 1781-90.

37. Dighe, A.S., et al., *Enhanced in vivo growth and resistance to rejection of tumor cells expressing dominant negative IFN gamma receptors.* Immunity, 1994. **1**(6): p. 447-56.
38. Diefenbach, A., et al., *Ligands for the murine NKG2D receptor: expression by tumor cells and activation of NK cells and macrophages.* Nat Immunol, 2000. **1**(2): p. 119-26.
39. Diefenbach, A., et al., *Rae1 and H60 ligands of the NKG2D receptor stimulate tumour immunity.* Nature, 2001. **413**(6852): p. 165-71.
40. Gasser, S., et al., *The DNA damage pathway regulates innate immune system ligands of the NKG2D receptor.* Nature, 2005. **436**(7054): p. 1186-90.
41. Xiong, H., et al., *Complex formation of the interferon (IFN) consensus sequence-binding protein with IRF-1 is essential for murine macrophage IFN-gamma-induced iNOS gene expression.* J Biol Chem, 2003. **278**(4): p. 2271-7.
42. Lyons, C.R., G.J. Orloff, and J.M. Cunningham, *Molecular cloning and functional expression of an inducible nitric oxide synthase from a murine macrophage cell line.* J Biol Chem, 1992. **267**(9): p. 6370-4.
43. Liu, J., et al., *Differential regulation of interleukin (IL)-12 p35 and p40 gene expression and interferon (IFN)-gamma-primed IL-12 production by IFN regulatory factor 1.* J Exp Med, 2003. **198**(8): p. 1265-76.
44. Trinchieri, G., *Interleukin-12: a proinflammatory cytokine with immunoregulatory functions that bridge innate resistance and antigen-specific adaptive immunity.* Annu Rev Immunol, 1995. **13**: p. 251-76.
45. Zhou, F., *Expression of multiple granzymes by cytotoxic T lymphocyte implies that they activate diverse apoptotic pathways in target cells.* Int Rev Immunol, 2010. **29**(1): p. 38-55.
46. Raghavan, M., et al., *MHC class I assembly: out and about.* Trends Immunol, 2008. **29**(9): p. 436-43.
47. Min, W., J.S. Pober, and D.R. Johnson, *Kinetically coordinated induction of TAP1 and HLA class I by IFN-gamma: the rapid induction of TAP1 by IFN-gamma is mediated by Stat1 alpha.* J Immunol, 1996. **156**(9): p. 3174-83.
48. White, L.C., et al., *Regulation of LMP2 and TAP1 genes by IRF-1 explains the paucity of CD8+ T cells in IRF-1-/- mice.* Immunity, 1996. **5**(4): p. 365-76.
49. Ogasawara, K., et al., *Requirement for IRF-1 in the microenvironment supporting development of natural killer cells.* Nature, 1998. **391**(6668): p. 700-3.
50. Reis, L.F., et al., *Critical role of a common transcription factor, IRF-1, in the regulation of IFN-beta and IFN-inducible genes.* Embo J, 1992. **11**(1): p. 185-93.
51. Fujita, T., et al., *Induction of endogenous IFN-alpha and IFN-beta genes by a regulatory transcription factor, IRF-1.* Nature, 1989. **337**(6204): p. 270-2.
52. Tamura, T., et al., *The IRF family transcription factors in immunity and oncogenesis.* Annu Rev Immunol, 2008. **26**: p. 535-84.
53. Yarilina, A., et al., *TNF activates an IRF1-dependent autocrine loop leading to sustained expression of chemokines and STAT1-dependent type I interferon-response genes.* Nat Immunol, 2008. **9**(4): p. 378-87.
54. Au, W.C., et al., *Distinct activation of murine interferon-alpha promoter region by IRF-1/ISFG-2 and virus infection.* Nucleic Acids Res, 1992. **20**(11): p. 2877-84.
55. Matsuyama, T., et al., *Targeted disruption of IRF-1 or IRF-2 results in abnormal type I IFN gene induction and aberrant lymphocyte development.* Cell, 1993. **75**(1): p. 83-97.
56. Reis, L.F., et al., *Mice devoid of interferon regulatory factor 1 (IRF-1) show normal expression of type I interferon genes.* Embo J, 1994. **13**(20): p. 4798-806.

57. Fortier, M.E., et al., *The viral mimic, polyinosinic:polycytidylic acid, induces fever in rats via an interleukin-1-dependent mechanism.* Am J Physiol Regul Integr Comp Physiol, 2004. **287**(4): p. R759-66.
58. Ruffner, H., et al., *Induction of type I interferon genes and interferon-inducible genes in embryonal stem cells devoid of interferon regulatory factor 1.* Proc Natl Acad Sci U S A, 1993. **90**(24): p. 11503-7.
59. Kuo, T.C. and K.L. Calame, *B lymphocyte-induced maturation protein (Blimp)-1, IFN regulatory factor (IRF)-1, and IRF-2 can bind to the same regulatory sites.* J Immunol, 2004. **173**(9): p. 5556-63.
60. Wathelet, M.G., et al., *Virus infection induces the assembly of coordinately activated transcription factors on the IFN-beta enhancer in vivo.* Mol Cell, 1998. **1**(4): p. 507-18.
61. Sato, M., et al., *Distinct and essential roles of transcription factors IRF-3 and IRF-7 in response to viruses for IFN-alpha/beta gene induction.* Immunity, 2000. **13**(4): p. 539-48.
62. Xie, R.L., et al., *The tumor suppressor interferon regulatory factor 1 interferes with SP1 activation to repress the human CDK2 promoter.* J Biol Chem, 2003. **278**(29): p. 26589-96.
63. Wessely, R., et al., *A central role of interferon regulatory factor-1 for the limitation of neointimal hyperplasia.* Hum Mol Genet, 2003. **12**(2): p. 177-87.
64. Eckert, M., S.E. Meek, and K.L. Ball, *A novel repressor domain is required for maximal growth inhibition by the IRF-1 tumor suppressor.* J Biol Chem, 2006. **281**(32): p. 23092-102.
65. Sato, T., et al., *Inhibition of interferon regulatory factor-1 expression results in predominance of cell growth stimulatory effects of interferon-gamma due to phosphorylation of Stat1 and Stat3.* Blood, 1997. **90**(12): p. 4749-58.
66. Yim, J.H., et al., *The role of interferon regulatory factor-1 and interferon regulatory factor-2 in IFN-gamma growth inhibition of human breast carcinoma cell lines.* J Interferon Cytokine Res, 2003. **23**(9): p. 501-11.
67. Watanabe, N., et al., *Activation of IFN-beta element by IRF-1 requires a posttranslational event in addition to IRF-1 synthesis.* Nucleic Acids Res, 1991. **19**(16): p. 4421-8.
68. Masumi, A. and K. Ozato, *Coactivator p300 acetylates the interferon regulatory factor-2 in U937 cells following phorbol ester treatment.* J Biol Chem, 2001. **276**(24): p. 20973-80.
69. McGill, C.J. and G. Brooks, *Cell cycle control mechanisms and their role in cardiac growth.* Cardiovasc Res, 1995. **30**(4): p. 557-69.
70. Hengst, L. and S.I. Reed, *Inhibitors of the Cip/Kip family.* Curr Top Microbiol Immunol, 1998. **227**: p. 25-41.
71. Tanaka, N., et al., *Cooperation of the tumour suppressors IRF-1 and p53 in response to DNA damage.* Nature, 1996. **382**(6594): p. 816-8.
72. Dornan, D., et al., *Interferon regulatory factor 1 binding to p300 stimulates DNA-dependent acetylation of p53.* Mol Cell Biol, 2004. **24**(22): p. 10083-98.
73. Dulic, V., et al., *p53-dependent inhibition of cyclin-dependent kinase activities in human fibroblasts during radiation-induced G1 arrest.* Cell, 1994. **76**(6): p. 1013-23.
74. el-Deiry, W.S., et al., *WAF1, a potential mediator of p53 tumor suppression.* Cell, 1993. **75**(4): p. 817-25.
75. Lee, S.H., et al., *IFN-gamma/IRF-1-induced p27kip1 down-regulates telomerase activity and human telomerase reverse transcriptase expression in human cervical cancer.* FEBS Lett, 2005. **579**(5): p. 1027-33.

76. Toyoshima, H. and T. Hunter, *p27, a novel inhibitor of G1 cyclin-Cdk protein kinase activity, is related to p21.* Cell, 1994. **78**(1): p. 67-74.
77. Polyak, K., et al., *Cloning of p27Kip1, a cyclin-dependent kinase inhibitor and a potential mediator of extracellular antimitogenic signals.* Cell, 1994. **78**(1): p. 59-66.
78. Tashiro, E., A. Tsuchiya, and M. Imoto, *Functions of cyclin D1 as an oncogene and regulation of cyclin D1 expression.* Cancer Sci, 2007. **98**(5): p. 629-35.
79. Kroger, A., et al., *Tumor suppression by IFN regulatory factor-1 is mediated by transcriptional down-regulation of cyclin D1.* Cancer Res, 2007. **67**(7): p. 2972-81.
80. Xie, R., et al., *The cell cycle control element of histone H4 gene transcription is maximally responsive to interferon regulatory factor pairs IRF-1/IRF-3 and IRF-1/IRF-7.* J Biol Chem, 2001. **276**(21): p. 18624-32.
81. Nelson, D.M., et al., *Coupling of DNA synthesis and histone synthesis in S phase independent of cyclin/cdk2 activity.* Mol Cell Biol, 2002. **22**(21): p. 7459-72.
82. Testa, U. and R. Riccioni, *Deregulation of apoptosis in acute myeloid leukemia.* Haematologica, 2007. **92**(1): p. 81-94.
83. Aktas, O., T. Prozorovski, and F. Zipp, *Death ligands and autoimmune demyelination.* Neuroscientist, 2006. **12**(4): p. 305-16.
84. Kim, E.J., et al., *Interferon regulatory factor-1 mediates interferon-gamma-induced apoptosis in ovarian carcinoma cells.* J Cell Biochem, 2002. **85**(2): p. 369-80.
85. Vermeulen, K., D.R. Van Bockstaele, and Z.N. Berneman, *Apoptosis: mechanisms and relevance in cancer.* Ann Hematol, 2005. **84**(10): p. 627-39.
86. Iwase, S., et al., *Defective binding of IRFs to the initiator element of interleukin-1beta-converting enzyme (ICE) promoter in an interferon-resistant Daudi subline.* FEBS Lett, 1999. **450**(3): p. 263-7.
87. Jain, N., et al., *Role of p73 in regulating human caspase-1 gene transcription induced by interferon-{gamma} and cisplatin.* J Biol Chem, 2005. **280**(44): p. 36664-73.
88. Gao, J., et al., *IRF-1 transcriptionally upregulates PUMA, which mediates the mitochondrial apoptotic pathway in IRF-1-induced apoptosis in cancer cells.* Cell Death Differ, 2010. **17**(4): p. 699-709.
89. Yu, J. and L. Zhang, *PUMA, a potent killer with or without p53.* Oncogene, 2008. **27 Suppl 1**: p. S71-83.
90. Clarke, N., et al., *Tumor suppressor IRF-1 mediates retinoid and interferon anticancer signaling to death ligand TRAIL.* Embo J, 2004. **23**(15): p. 3051-60.
91. Kim, K., et al., *Molecular determinants of response to TRAIL in killing of normal and cancer cells.* Clin Cancer Res, 2000. **6**(2): p. 335-46.
92. Holoch, P.A. and T.S. Griffith, *TNF-related apoptosis-inducing ligand (TRAIL): a new path to anti-cancer therapies.* Eur J Pharmacol, 2009. **625**(1-3): p. 63-72.
93. Wang, J., et al., *c-Jun N-terminal kinase (JNK1) upregulates XIAP-associated factor 1 (XAF1) through interferon regulatory factor 1 (IRF-1) in gastrointestinal cancer.* Carcinogenesis, 2009. **30**(2): p. 222-9.
94. Wang, J., et al., *All-trans retinoic acid induces XAF1 expression through an interferon regulatory factor-1 element in colon cancer.* Gastroenterology, 2006. **130**(3): p. 747-58.
95. Liston, P., et al., *Identification of XAF1 as an antagonist of XIAP anti-Caspase activity.* Nat Cell Biol, 2001. **3**(2): p. 128-33.
96. Horiuchi, M., et al., *Interferon regulatory factor-1 up-regulates angiotensin II type 2 receptor and induces apoptosis.* J Biol Chem, 1997. **272**(18): p. 11952-8.

97. Horiuchi, M., et al., *The growth-dependent expression of angiotensin II type 2 receptor is regulated by transcription factors interferon regulatory factor-1 and -2.* J Biol Chem, 1995. **270**(34): p. 20225-30.
98. Altschul, S.F., et al., *Gapped BLAST and PSI-BLAST: a new generation of protein database search programs.* Nucleic Acids Res, 1997. **25**(17): p. 3389-402.
99. Upreti, M., S. Kumar, and P.C. Rath, *Replacement of 198MQMDII203 of mouse IRF-1 by 197IPVEVV202 of human IRF-1 abrogates induction of IFN-beta, iNOS, and COX-2 gene expression by IRF-1.* Biochem Biophys Res Commun, 2004. **314**(3): p. 737-44.
100. Escalante, C.R., et al., *Structure of IRF-1 with bound DNA reveals determinants of interferon regulation.* Nature, 1998. **391**(6662): p. 103-6.
101. Kirchhoff, S., et al., *Interplay between repressing and activating domains defines the transcriptional activity of IRF-1.* Eur J Biochem, 2000. **267**(23): p. 6753-61.
102. Barnes, B.J., P.A. Moore, and P.M. Pitha, *Virus-specific activation of a novel interferon regulatory factor, IRF-5, results in the induction of distinct interferon alpha genes.* J Biol Chem, 2001. **276**(26): p. 23382-90.
103. Kirchhoff, S., et al., *In vivo formation of IRF-1 homodimers.* Biochimie, 1998. **80**(8-9): p. 659-64.
104. Schaper, F., et al., *Functional domains of interferon regulatory factor I (IRF-1).* Biochem J, 1998. **335 (Pt 1)**: p. 147-57.
105. Kim, E.J., et al., *Functional dissection of the transactivation domain of interferon regulatory factor-1.* Biochem Biophys Res Commun, 2003. **304**(2): p. 253-9.
106. Dornan, D., et al., *DNA-dependent acetylation of p53 by the transcription coactivator p300.* J Biol Chem, 2003. **278**(15): p. 13431-41.
107. Lambert, P.F., et al., *Phosphorylation of p53 serine 15 increases interaction with CBP.* J Biol Chem, 1998. **273**(49): p. 33048-53.
108. Avantaggiati, M.L., et al., *Recruitment of p300/CBP in p53-dependent signal pathways.* Cell, 1997. **89**(7): p. 1175-84.
109. Lin, R. and J. Hiscott, *A role for casein kinase II phosphorylation in the regulation of IRF-1 transcriptional activity.* Mol Cell Biochem, 1999. **191**(1-2): p. 169-80.
110. Nakagawa, K. and H. Yokosawa, *Degradation of transcription factor IRF-1 by the ubiquitin-proteasome pathway. The C-terminal region governs the protein stability.* Eur J Biochem, 2000. **267**(6): p. 1680-6.
111. Pion, E., et al., *Role of the IRF-1 enhancer domain in signalling polyubiquitination and degradation.* Cell Signal, 2009. **21**(10): p. 1479-87.
112. Narayan, V., et al., *Cooperative regulation of the interferon regulatory factor-1 tumor suppressor protein by core components of the molecular chaperone machinery.* J Biol Chem, 2009. **284**(38): p. 25889-99.
113. Sharf, R., et al., *Phosphorylation events modulate the ability of interferon consensus sequence binding protein to interact with interferon regulatory factors and to bind DNA.* J Biol Chem, 1997. **272**(15): p. 9785-92.
114. Hong, H.Y., et al., *Phage Display Selection of Peptides that Home to Atherosclerotic Plaques: IL-4 Receptor as a Candidate Target in Atherosclerosis.* J Cell Mol Med, 2007.
115. d'Azzo, A., A. Bongiovanni, and T. Nastasi, *E3 ubiquitin ligases as regulators of membrane protein trafficking and degradation.* Traffic, 2005. **6**(6): p. 429-41.
116. Scheffner, M., U. Nuber, and J.M. Huibregtse, *Protein ubiquitination involving an E1-E2-E3 enzyme ubiquitin thioester cascade.* Nature, 1995. **373**(6509): p. 81-3.
117. Ulrich, H.D., *Mutual interactions between the SUMO and ubiquitin systems: a plea of no contest.* Trends Cell Biol, 2005. **15**(10): p. 525-32.

118. Kim, E.J., J.S. Park, and S.J. Um, *Ubc9-mediated sumoylation leads to transcriptional repression of IRF-1.* Biochem Biophys Res Commun, 2008. **377**(3): p. 952-6.
119. Park, S.M., et al., *SUMOylated IRF-1 shows oncogenic potential by mimicking IRF-2.* Biochem Biophys Res Commun, 2010. **391**(1): p. 926-30.
120. Steffan, J.S., et al., *SUMO modification of Huntingtin and Huntington's disease pathology.* Science, 2004. **304**(5667): p. 100-4.
121. Ross, S., et al., *SUMO-1 modification represses Sp3 transcriptional activation and modulates its subnuclear localization.* Mol Cell, 2002. **10**(4): p. 831-42.
122. Nakagawa, K. and H. Yokosawa, *PIAS3 induces SUMO-1 modification and transcriptional repression of IRF-1.* FEBS Lett, 2002. **530**(1-3): p. 204-8.
123. Sgarbanti, M., et al., *IRF-1 is required for full NF-kappaB transcriptional activity at the human immunodeficiency virus type 1 long terminal repeat enhancer.* J Virol, 2008. **82**(7): p. 3632-41.
124. Sanceau, J., et al., *Triggering of the human interleukin-6 gene by interferon-gamma and tumor necrosis factor-alpha in monocytic cells involves cooperation between interferon regulatory factor-1, NF kappa B, and Sp1 transcription factors.* J Biol Chem, 1995. **270**(46): p. 27920-31.
125. Saura, M., et al., *Interaction of interferon regulatory factor-1 and nuclear factor kappaB during activation of inducible nitric oxide synthase transcription.* J Mol Biol, 1999. **289**(3): p. 459-71.
126. Bidlingmaier, S., et al., *Identification of MCAM/CD146 as the target antigen of a human monoclonal antibody that recognizes both epithelioid and sarcomatoid types of mesothelioma.* Cancer Res, 2009. **69**(4): p. 1570-7.
127. Neish, A.S., et al., *Endothelial interferon regulatory factor 1 cooperates with NF-kappa B as a transcriptional activator of vascular cell adhesion molecule 1.* Mol Cell Biol, 1995. **15**(5): p. 2558-69.
128. Reeves, R. and L. Beckerbauer, *HMGI/Y proteins: flexible regulators of transcription and chromatin structure.* Biochim Biophys Acta, 2001. **1519**(1-2): p. 13-29.
129. Thanos, D. and T. Maniatis, *Virus induction of human IFN beta gene expression requires the assembly of an enhanceosome.* Cell, 1995. **83**(7): p. 1091-100.
130. Merika, M., et al., *Recruitment of CBP/p300 by the IFN beta enhanceosome is required for synergistic activation of transcription.* Mol Cell, 1998. **1**(2): p. 277-87.
131. Shi, D., et al., *CBP and p300 are cytoplasmic E4 polyubiquitin ligases for p53.* Proc Natl Acad Sci U S A, 2009. **106**(38): p. 16275-80.
132. Grossman, S.R., et al., *Polyubiquitination of p53 by a ubiquitin ligase activity of p300.* Science, 2003. **300**(5617): p. 342-4.
133. Ford, E. and D. Thanos, *The transcriptional code of human IFN-beta gene expression.* Biochim Biophys Acta, 2010. **1799**(3-4): p. 328-36.
134. Chatterjee-Kishore, M., F. van Den Akker, and G.R. Stark, *Adenovirus E1A down-regulates LMP2 transcription by interfering with the binding of stat1 to IRF1.* J Biol Chem, 2000. **275**(27): p. 20406-11.
135. Weisz, A., S. Kirchhoff, and B.Z. Levi, *IFN consensus sequence binding protein (ICSBP) is a conditional repressor of IFN inducible promoters.* Int Immunol, 1994. **6**(8): p. 1125-31.
136. Sgarbanti, M., et al., *Modulation of human immunodeficiency virus 1 replication by interferon regulatory factors.* J Exp Med, 2002. **195**(10): p. 1359-70.
137. Bovolenta, C., et al., *Molecular interactions between interferon consensus sequence binding protein and members of the interferon regulatory factor family.* Proc Natl Acad Sci U S A, 1994. **91**(11): p. 5046-50.

138. Liu, J., et al., *Synergistic activation of interleukin-12 p35 gene transcription by interferon regulatory factor-1 and interferon consensus sequence-binding protein.* J Biol Chem, 2004. **279**(53): p. 55609-17.
139. Liang, S., et al., *Screening and identification of vascular-endothelial-cell-specific binding peptide in gastric cancer.* J Mol Med, 2006. **84**(9): p. 764-73.
140. Zhang, J., et al., *Activation of IL-27 p28 gene transcription by interferon regulatory factor 8 in cooperation with interferon regulatory factor 1.* J Biol Chem, 2010. **285**(28): p. 21269-81.
141. Masumi, A., et al., *IRF-8/ICSBP and IRF-1 cooperatively stimulate mouse IL-12 promoter activity in macrophages.* FEBS Lett, 2002. **531**(2): p. 348-53.
142. Blanco, J.C., et al., *The histone acetylase PCAF is a nuclear receptor coactivator.* Genes Dev, 1998. **12**(11): p. 1638-51.
143. Korzus, E., et al., *Transcription factor-specific requirements for coactivators and their acetyltransferase functions.* Science, 1998. **279**(5351): p. 703-7.
144. Kondo, T., et al., *Identification and characterization of nucleophosmin/B23/numatrin which binds the anti-oncogenic transcription factor IRF-1 and manifests oncogenic activity.* Oncogene, 1997. **15**(11): p. 1275-81.
145. Tazi, J. and A. Bird, *Alternative chromatin structure at CpG islands.* Cell, 1990. **60**(6): p. 909-20.
146. Mizzen, C.A., et al., *The TAF(II)250 subunit of TFIID has histone acetyltransferase activity.* Cell, 1996. **87**(7): p. 1261-70.
147. Winkler, C.J., A. Ponce, and A.J. Courey, *Groucho-mediated repression may result from a histone deacetylase-dependent increase in nucleosome density.* PLoS One, 2010. **5**(4): p. e10166.
148. Coward, W.R., et al., *Repression of IP-10 by Interactions between Histone Deacetylation and Hypermethylation in Idiopathic Pulmonary Fibrosis.* Mol Cell Biol, 2010. **30**(12): p. 2874-86.
149. Yoo, J.Y., et al., *Histone deacetylase 3 is selectively involved in L3MBTL2-mediated transcriptional repression.* FEBS Lett, 2010. **584**(11): p. 2225-30.
150. Masumi, A., et al., *The histone acetylase PCAF is a phorbol-ester-inducible coactivator of the IRF family that confers enhanced interferon responsiveness.* Mol Cell Biol, 1999. **19**(3): p. 1810-20.
151. Park, J.S., et al., *Inactivation of interferon regulatory factor-1 tumor suppressor protein by HPV E7 oncoprotein. Implication for the E7-mediated immune evasion mechanism in cervical carcinogenesis.* J Biol Chem, 2000. **275**(10): p. 6764-9.
152. Maggi, L.B., Jr., et al., *Nucleophosmin serves as a rate-limiting nuclear export chaperone for the Mammalian ribosome.* Mol Cell Biol, 2008. **28**(23): p. 7050-65.
153. Bertwistle, D., M. Sugimoto, and C.J. Sherr, *Physical and functional interactions of the Arf tumor suppressor protein with nucleophosmin/B23.* Mol Cell Biol, 2004. **24**(3): p. 985-96.
154. Colombo, E., et al., *Nucleophosmin regulates the stability and transcriptional activity of p53.* Nat Cell Biol, 2002. **4**(7): p. 529-33.
155. Bhandare, R., et al., *Glucocorticoid receptor interacting protein-1 restores glucocorticoid responsiveness in steroid-resistant airway structural cells.* Am J Respir Cell Mol Biol, 2010. **42**(1): p. 9-15.
156. Honda, K., et al., *Role of a transductional-transcriptional processor complex involving MyD88 and IRF-7 in Toll-like receptor signaling.* Proc Natl Acad Sci U S A, 2004. **101**(43): p. 15416-21.
157. Takaoka, A., et al., *Integral role of IRF-5 in the gene induction programme activated by Toll-like receptors.* Nature, 2005. **434**(7030): p. 243-9.

158. Negishi, H., et al., *Evidence for licensing of IFN-gamma-induced IFN regulatory factor 1 transcription factor by MyD88 in Toll-like receptor-dependent gene induction program.* Proc Natl Acad Sci U S A, 2006. **103**(41): p. 15136-41.
159. Whiteside, S.T. and S. Goodbourn, *Signal transduction and nuclear targeting: regulation of transcription factor activity by subcellular localisation.* J Cell Sci, 1993. **104 (Pt 4)**: p. 949-55.
160. Umegaki, N., et al., *Differential regulation of karyopherin alpha 2 expression by TGF-beta1 and IFN-gamma in normal human epidermal keratinocytes: evident contribution of KPNA2 for nuclear translocation of IRF-1.* J Invest Dermatol, 2007. **127**(6): p. 1456-64.
161. Goldfarb, D.S., et al., *Importin alpha: a multipurpose nuclear-transport receptor.* Trends Cell Biol, 2004. **14**(9): p. 505-14.
162. Hyman, P. and S.T. Abedon, *Bacteriophage host range and bacterial resistance.* Adv Appl Microbiol, 2010. **70**: p. 217-48.
163. Marks, J.D., et al., *Molecular evolution of proteins on filamentous phage. Mimicking the strategy of the immune system.* J Biol Chem, 1992. **267**(23): p. 16007-10.
164. Clackson, T., et al., *Making antibody fragments using phage display libraries.* Nature, 1991. **352**(6336): p. 624-8.
165. Kurzepa, A., et al., *Molecular modification of T4 bacteriophage proteins and its potential application - review.* Folia Microbiol (Praha), 2009. **54**(1): p. 5-15.
166. Sharma, S.C., et al., *T7 phage display as a method of peptide ligand discovery for PDZ domain proteins.* Biopolymers, 2009. **92**(3): p. 183-93.
167. Garufi, G., et al., *Display libraries on bacteriophage lambda capsid.* Biotechnol Annu Rev, 2005. **11**: p. 153-90.
168. Cen, X., Q. Bi, and S. Zhu, *Construction of a large phage display antibody library by in vitro package and in vivo recombination.* Appl Microbiol Biotechnol, 2006. **71**(5): p. 767-72.
169. Smith, G.P., *Filamentous fusion phage: novel expression vectors that display cloned antigens on the virion surface.* Science, 1985. **228**(4705): p. 1315-7.
170. Jespers, L.S., et al., *Surface expression and ligand-based selection of cDNAs fused to filamentous phage gene VI.* Biotechnology (N Y), 1995. **13**(4): p. 378-82.
171. Krumpe, L.R., et al., *T7 lytic phage-displayed peptide libraries exhibit less sequence bias than M13 filamentous phage-displayed peptide libraries.* Proteomics, 2006. **6**(15): p. 4210-22.
172. Sambrook J., R.D.W., *Molecular Cloning: A laboratory manual*. Third ed. 1989: Cold Spring Harbour Laboratory Press.
173. Marvin, D.A., *Filamentous phage structure, infection and assembly.* Curr Opin Struct Biol, 1998. **8**(2): p. 150-8.
174. Barbas, C.F., 3rd, et al., *Assembly of combinatorial antibody libraries on phage surfaces: the gene III site.* Proc Natl Acad Sci U S A, 1991. **88**(18): p. 7978-82.
175. O'Connell, D., et al., *Phage versus phagemid libraries for generation of human monoclonal antibodies.* J Mol Biol, 2002. **321**(1): p. 49-56.
176. Sidhu, S.S., *Engineering M13 for phage display.* Biomol Eng, 2001. **18**(2): p. 57-63.
177. Li, M., *Applications of display technology in protein analysis.* Nat Biotechnol, 2000. **18**(12): p. 1251-6.
178. Griffiths, A.D. and A.R. Duncan, *Strategies for selection of antibodies by phage display.* Curr Opin Biotechnol, 1998. **9**(1): p. 102-8.
179. Winter, G., et al., *Making antibodies by phage display technology.* Annu Rev Immunol, 1994. **12**: p. 433-55.

180. Gram, H., et al., *In vitro selection and affinity maturation of antibodies from a naive combinatorial immunoglobulin library.* Proc Natl Acad Sci U S A, 1992. **89**(8): p. 3576-80.
181. Carmen, S. and L. Jermutus, *Concepts in antibody phage display.* Brief Funct Genomic Proteomic, 2002. **1**(2): p. 189-203.
182. Soltes, G., et al., *On the influence of vector design on antibody phage display.* J Biotechnol, 2007. **127**(4): p. 626-37.
183. Reichert, J.M., et al., *Monoclonal antibody successes in the clinic.* Nat Biotechnol, 2005. **23**(9): p. 1073-8.
184. Schroeder, H.W., Jr. and L. Cavacini, *Structure and function of immunoglobulins.* J Allergy Clin Immunol, 2010. **125**(2 Suppl 2): p. S41-52.
185. Hagemeyer, C.E., et al., *Single-chain antibodies as diagnostic tools and therapeutic agents.* Thromb Haemost, 2009. **101**(6): p. 1012-9.
186. Holliger, P. and P.J. Hudson, *Engineered antibody fragments and the rise of single domains.* Nat Biotechnol, 2005. **23**(9): p. 1126-36.
187. Putnam, F.W., Y.S. Liu, and T.L. Low, *Primary structure of a human IgA1 immunoglobulin. IV. Streptococcal IgA1 protease, digestion, Fab and Fc fragments, and the complete amino acid sequence of the alpha 1 heavy chain.* J Biol Chem, 1979. **254**(8): p. 2865-74.
188. de Wildt, R.M., et al., *Antibody arrays for high-throughput screening of antibody-antigen interactions.* Nat Biotechnol, 2000. **18**(9): p. 989-94.
189. Silacci, M., et al., *Design, construction, and characterization of a large synthetic human antibody phage display library.* Proteomics, 2005. **5**(9): p. 2340-50.
190. Bird, R.E., et al., *Single-chain antigen-binding proteins.* Science, 1988. **242**(4877): p. 423-6.
191. Huston, J.S., et al., *Protein engineering of antibody binding sites: recovery of specific activity in an anti-digoxin single-chain Fv analogue produced in Escherichia coli.* Proc Natl Acad Sci U S A, 1988. **85**(16): p. 5879-83.
192. Harmsen, M.M., et al., *Llama heavy-chain V regions consist of at least four distinct subfamilies revealing novel sequence features.* Mol Immunol, 2000. **37**(10): p. 579-90.
193. Stanfield, R.L., et al., *Maturation of shark single-domain (IgNAR) antibodies: evidence for induced-fit binding.* J Mol Biol, 2007. **367**(2): p. 358-72.
194. Desmyter, A., et al., *Three camelid VHH domains in complex with porcine pancreatic alpha-amylase. Inhibition and versatility of binding topology.* J Biol Chem, 2002. **277**(26): p. 23645-50.
195. Stanfield, R.L., et al., *Crystal structure of a shark single-domain antibody V region in complex with lysozyme.* Science, 2004. **305**(5691): p. 1770-3.
196. Ward, E.S., et al., *Binding activities of a repertoire of single immunoglobulin variable domains secreted from Escherichia coli.* Nature, 1989. **341**(6242): p. 544-6.
197. Jespers, L., et al., *Crystal structure of HEL4, a soluble, refoldable human V(H) single domain with a germ-line scaffold.* J Mol Biol, 2004. **337**(4): p. 893-903.
198. Colby, D.W., et al., *Development of a human light chain variable domain (V(L)) intracellular antibody specific for the amino terminus of huntingtin via yeast surface display.* J Mol Biol, 2004. **342**(3): p. 901-12.
199. Stijlemans, B., et al., *Efficient targeting of conserved cryptic epitopes of infectious agents by single domain antibodies. African trypanosomes as paradigm.* J Biol Chem, 2004. **279**(2): p. 1256-61.
200. Casey, J.L., et al., *Tumour targeting of humanised cross-linked divalent-Fab' antibody fragments: a clinical phase I/II study.* Br J Cancer, 2002. **86**(9): p. 1401-10.

201. Weir, A.N., et al., *Formatting antibody fragments to mediate specific therapeutic functions.* Biochem Soc Trans, 2002. **30**(4): p. 512-6.
202. Holliger, P., T. Prospero, and G. Winter, *"Diabodies": small bivalent and bispecific antibody fragments.* Proc Natl Acad Sci U S A, 1993. **90**(14): p. 6444-8.
203. Perisic, O., et al., *Crystal structure of a diabody, a bivalent antibody fragment.* Structure, 1994. **2**(12): p. 1217-26.
204. Iliades, P., A.A. Kortt, and P.J. Hudson, *Triabodies: single chain Fv fragments without a linker form trivalent trimers.* FEBS Lett, 1997. **409**(3): p. 437-41.
205. Atwell, J.L., et al., *scFv multimers of the anti-neuraminidase antibody NC10: length of the linker between VH and VL domains dictates precisely the transition between diabodies and triabodies.* Protein Eng, 1999. **12**(7): p. 597-604.
206. Dolezal, O., et al., *ScFv multimers of the anti-neuraminidase antibody NC10: shortening of the linker in single-chain Fv fragment assembled in V(L) to V(H) orientation drives the formation of dimers, trimers, tetramers and higher molecular mass multimers.* Protein Eng, 2000. **13**(8): p. 565-74.
207. Hoffmann, P., et al., *Serial killing of tumor cells by cytotoxic T cells redirected with a CD19-/CD3-bispecific single-chain antibody construct.* Int J Cancer, 2005. **115**(1): p. 98-104.
208. Schlereth, B., et al., *Eradication of tumors from a human colon cancer cell line and from ovarian cancer metastases in immunodeficient mice by a single-chain Ep-CAM-/CD3-bispecific antibody construct.* Cancer Res, 2005. **65**(7): p. 2882-9.
209. Vallera, D.A., et al., *Molecular modification of a recombinant, bivalent anti-human CD3 immunotoxin (Bic3) results in reduced in vivo toxicity in mice.* Leuk Res, 2005. **29**(3): p. 331-41.
210. Bang, S., et al., *HA22 (R490A) is a recombinant immunotoxin with increased antitumor activity without an increase in animal toxicity.* Clin Cancer Res, 2005. **11**(4): p. 1545-50.
211. Zhang, M., et al., *Pretargeting radioimmunotherapy of a murine model of adult T-cell leukemia with the alpha-emitting radionuclide, bismuth 213.* Blood, 2002. **100**(1): p. 208-16.
212. Cheng, W.W. and T.M. Allen, *The use of single chain Fv as targeting agents for immunoliposomes: an update on immunoliposomal drugs for cancer treatment.* Expert Opin Drug Deliv, 2010. **7**(4): p. 461-78.
213. Cheng, W.W. and T.M. Allen, *Targeted delivery of anti-CD19 liposomal doxorubicin in B-cell lymphoma: a comparison of whole monoclonal antibody, Fab' fragments and single chain Fv.* J Control Release, 2008. **126**(1): p. 50-8.
214. Sheets, M.D., et al., *Efficient construction of a large nonimmune phage antibody library: the production of high-affinity human single-chain antibodies to protein antigens.* Proc Natl Acad Sci U S A, 1998. **95**(11): p. 6157-62.
215. Tanha, J., et al., *Selection by phage display of llama conventional V(H) fragments with heavy chain antibody V(H)H properties.* J Immunol Methods, 2002. **263**(1-2): p. 97-109.
216. van Koningsbruggen, S., et al., *Llama-derived phage display antibodies in the dissection of the human disease oculopharyngeal muscular dystrophy.* J Immunol Methods, 2003. **279**(1-2): p. 149-61.
217. Liu, J.L., et al., *Selection of cholera toxin specific IgNAR single-domain antibodies from a naive shark library.* Mol Immunol, 2007. **44**(7): p. 1775-83.
218. Pilkington, G.R., et al., *Recombinant human Fab antibody fragments to HIV-1 Rev and Tat regulatory proteins: direct selection from a combinatorial phage display library.* Mol Immunol, 1996. **33**(4-5): p. 439-50.

219. Hoogenboom, H.R., et al., *Multi-subunit proteins on the surface of filamentous phage: methodologies for displaying antibody (Fab) heavy and light chains.* Nucleic Acids Res, 1991. **19**(15): p. 4133-7.
220. Jupin, I. and B. Gronenborn, *Abundant, easy and reproducible production of single-stranded DNA from phagemids using helper phage-infected competent cells.* Nucleic Acids Res, 1995. **23**(3): p. 535-6.
221. Palmer, D.B., A.J. George, and M.A. Ritter, *Selection of antibodies to cell surface determinants on mouse thymic epithelial cells using a phage display library.* Immunology, 1997. **91**(3): p. 473-8.
222. Pereira, S., et al., *A model system for detection and isolation of a tumor cell surface antigen using antibody phage display.* J Immunol Methods, 1997. **203**(1): p. 11-24.
223. Edwards, B.M., et al., *Isolation and tissue profiles of a large panel of phage antibodies binding to the human adipocyte cell surface.* J Immunol Methods, 2000. **245**(1-2): p. 67-78.
224. Ravn, P., et al., *Identification of phage antibodies toward the Werner protein by selection on Western blots.* Electrophoresis, 2000. **21**(3): p. 509-16.
225. Liu, B. and J.D. Marks, *Applying phage antibodies to proteomics: selecting single chain Fv antibodies to antigens blotted on nitrocellulose.* Anal Biochem, 2000. **286**(1): p. 119-28.
226. Meli, G., et al., *Direct in vivo intracellular selection of conformation-sensitive antibody domains targeting Alzheimer's amyloid-beta oligomers.* J Mol Biol, 2009. **387**(3): p. 584-606.
227. Visintin, M., et al., *In vivo selection of intrabodies specifically targeting protein-protein interactions: a general platform for an "undruggable" class of disease targets.* J Biotechnol, 2008. **135**(1): p. 1-15.
228. Pizzoferrato, E., et al., *Ectopic expression of interferon regulatory factor-1 promotes human breast cancer cell death and results in reduced expression of survivin.* Cancer Res, 2004. **64**(22): p. 8381-8.
229. An, F., et al., *Targeted drug delivery to mesothelioma cells using functionally selected internalizing human single-chain antibodies.* Mol Cancer Ther, 2008. **7**(3): p. 569-78.
230. Paz, K., et al., *Human single-domain neutralizing intrabodies directed against Etk kinase: a novel approach to impair cellular transformation.* Mol Cancer Ther, 2005. **4**(11): p. 1801-9.
231. Tellez, C., D. Jean, and M. Bar-Eli, *Construction and expression of intracellular anti-ATF-1 single chain Fv fragment: a modality to inhibit melanoma tumor growth and metastasis.* Methods, 2004. **34**(2): p. 233-9.
232. Biocca, S., et al., *Redox state of single chain Fv fragments targeted to the endoplasmic reticulum, cytosol and mitochondria.* Biotechnology (N Y), 1995. **13**(10): p. 1110-5.
233. Cattaneo, A. and S. Biocca, *The selection of intracellular antibodies.* Trends Biotechnol, 1999. **17**(3): p. 115-21.
234. Worn, A. and A. Pluckthun, *Stability engineering of antibody single-chain Fv fragments.* J Mol Biol, 2001. **305**(5): p. 989-1010.
235. Beerli, R.R., W. Wels, and N.E. Hynes, *Intracellular expression of single chain antibodies reverts ErbB-2 transformation.* J Biol Chem, 1994. **269**(39): p. 23931-6.
236. Zhou, P., et al., *Cells transfected with a non-neutralizing antibody gene are resistant to HIV infection: targeting the endoplasmic reticulum and trans-Golgi network.* J Immunol, 1998. **160**(3): p. 1489-96.

237. Li, L., et al., *Transfection with anti-p65 intrabody suppresses invasion and angiogenesis in glioma cells by blocking nuclear factor-kappaB transcriptional activity.* Clin Cancer Res, 2007. **13**(7): p. 2178-90.
238. Melchionna, T. and A. Cattaneo, *A protein silencing switch by ligand-induced proteasome-targeting intrabodies.* J Mol Biol, 2007. **374**(3): p. 641-54.
239. Caron de Fromentel, C., et al., *Restoration of transcriptional activity of p53 mutants in human tumour cells by intracellular expression of anti-p53 single chain Fv fragments.* Oncogene, 1999. **18**(2): p. 551-7.
240. Cohen, P.A., J.C. Mani, and D.P. Lane, *Characterization of a new intrabody directed against the N-terminal region of human p53.* Oncogene, 1998. **17**(19): p. 2445-56.
241. Riley, C.J., et al., *Design and activity of a murine and humanized anti-CEACAM6 single-chain variable fragment in the treatment of pancreatic cancer.* Cancer Res, 2009. **69**(5): p. 1933-40.
242. Bai, J., et al., *Inhibition of Tat-mediated transactivation and HIV-1 replication by human anti-hCyclinT1 intrabodies.* J Biol Chem, 2003. **278**(3): p. 1433-42.
243. Peng, J.L., et al., *Downregulation of transferrin receptor surface expression by intracellular antibody.* Biochem Biophys Res Commun, 2007. **354**(4): p. 864-71.
244. Deshane, J., et al., *Transductional efficacy and safety of an intraperitoneally delivered adenovirus encoding an anti-erbB-2 intracellular single-chain antibody for ovarian cancer gene therapy.* Gynecol Oncol, 1997. **64**(3): p. 378-85.
245. Alvarez, R.D., et al., *A cancer gene therapy approach utilizing an anti-erbB-2 single-chain antibody-encoding adenovirus (AD21): a phase I trial.* Clin Cancer Res, 2000. **6**(8): p. 3081-7.
246. Orten, D.J., et al., *Differential effects of monoclonal antibodies on activating transcription factor-1 and cAMP response element binding protein interactions with DNA.* J Biol Chem, 1994. **269**(51): p. 32254-63.
247. Jean, D., et al., *Inhibition of tumor growth and metastasis of human melanoma by intracellular anti-ATF-1 single chain Fv fragment.* Oncogene, 2000. **19**(22): p. 2721-30.
248. Zhu, Q., et al., *Extended half-life and elevated steady-state level of a single-chain Fv intrabody are critical for specific intracellular retargeting of its antigen, caspase-7.* J Immunol Methods, 1999. **231**(1-2): p. 207-22.
249. Richardson, J.H., et al., *Phenotypic knockout of the high-affinity human interleukin 2 receptor by intracellular single-chain antibodies against the alpha subunit of the receptor.* Proc Natl Acad Sci U S A, 1995. **92**(8): p. 3137-41.
250. Mary, M.N., et al., *A tumor specific single chain antibody dependent gene expression system.* Oncogene, 1999. **18**(2): p. 559-64.
251. Sparks, A.B., et al., *Identification and characterization of Src SH3 ligands from phage-displayed random peptide libraries.* J Biol Chem, 1994. **269**(39): p. 23853-6.
252. Li, W., *Foreign peptides displayed on the major coat protein of filamentous bacteriophage.* Chinese Science Bulletin, 1998. **43**(14): p. 1158-1162.
253. Hirosue, S. and T. Weber, *pH-Dependent lytic peptides discovered by phage display.* Biochemistry, 2006. **45**(20): p. 6476-87.
254. Giebel, L.B., et al., *Screening of cyclic peptide phage libraries identifies ligands that bind streptavidin with high affinities.* Biochemistry, 1995. **34**(47): p. 15430-5.
255. Wu, P., et al., *Identification of novel peptide inhibitors for human trypsins.* Biol Chem, 2010. **391**(2-3): p. 283-93.
256. Smith, G.P. and V.A. Petrenko, *Phage Display.* Chem Rev, 1997. **97**(2): p. 391-410.
257. Cain, S.A., A. Higginbottom, and P.N. Monk, *Characterisation of C5a receptor agonists from phage display libraries.* Biochem Pharmacol, 2003. **66**(9): p. 1833-40.

258. Shimizu, A., et al., *Identification of an oligopeptide binding to hepatocellular carcinoma.* Oncology, 2006. **71**(1-2): p. 136-45.
259. Hou, S.T., et al., *Identification of polypeptides with selective affinity to intact mouse cerebellar granule neurons from a random peptide-presenting phage library.* J Neurosci Methods, 2004. **138**(1-2): p. 39-44.
260. Sun, Y., et al., *Phage-display selection on tumor histological specimens with laser capture microdissection.* J Immunol Methods, 2009. **347**(1-2): p. 46-53.
261. Akita, N., et al., *Identification of oligopeptides binding to peritoneal tumors of gastric cancer.* Cancer Sci, 2006. **97**(10): p. 1075-81.
262. Arap, W., et al., *Steps toward mapping the human vasculature by phage display.* Nat Med, 2002. **8**(2): p. 121-7.
263. Witt, H., et al., *Identification of a rhabdomyosarcoma targeting peptide by phage display with sequence similarities to the tumour lymphatic-homing peptide LyP-1.* Int J Cancer, 2009. **124**(9): p. 2026-32.
264. Holig, P., et al., *Novel RGD lipopeptides for the targeting of liposomes to integrin-expressing endothelial and melanoma cells.* Protein Eng Des Sel, 2004. **17**(5): p. 433-41.
265. Ulises, H.C., et al., *Peptide sequences identified by phage display are immunodominant functional motifs of Pet and Pic serine proteases secreted by Escherichia coli and Shigella flexneri.* Peptides, 2009. **30**(12): p. 2127-35.
266. Binder, M., et al., *The epitope recognized by rituximab.* Blood, 2006. **108**(6): p. 1975-8.
267. Binder, M., et al., *Identification of their epitope reveals the structural basis for the mechanism of action of the immunosuppressive antibodies basiliximab and daclizumab.* Cancer Res, 2007. **67**(8): p. 3518-23.
268. Hills, R., et al., *Identification of an ADAMTS-4 cleavage motif using phage display leads to the development of fluorogenic peptide substrates and reveals matrilin-3 as a novel substrate.* J Biol Chem, 2007. **282**(15): p. 11101-9.
269. White, S.J., et al., *Efficient isolation of peptide ligands for the endothelial cell protein C receptor (EPCR) using candidate receptor phage display biopanning.* Peptides, 2005. **26**(7): p. 1264-9.
270. Gordon, N.C., et al., *Multiple novel classes of APRIL-specific receptor-blocking peptides isolated by phage display.* J Mol Biol, 2010. **396**(1): p. 166-77.
271. Hessling, J., M.J. Lohse, and K.N. Klotz, *Peptide G protein agonists from a phage display library.* Biochem Pharmacol, 2003. **65**(6): p. 961-7.
272. Cheng, X., B.K. Kay, and R.L. Juliano, *Identification of a biologically significant DNA-binding peptide motif by use of a random phage display library.* Gene, 1996. **171**(1): p. 1-8.
273. Kim, Y.G., et al., *Screening of LPS-specific peptides from a phage display library using epoxy beads.* Biochem Biophys Res Commun, 2005. **329**(1): p. 312-7.
274. Whaley, S.R., et al., *Selection of peptides with semiconductor binding specificity for directed nanocrystal assembly.* Nature, 2000. **405**(6787): p. 665-8.
275. Zuo, R., D. Ornek, and T.K. Wood, *Aluminum- and mild steel-binding peptides from phage display.* Appl Microbiol Biotechnol, 2005. **68**(4): p. 505-9.
276. Qin, X., et al., *Identification of a novel peptide ligand of human vascular endothelia growth factor receptor 3 for targeted tumour diagnosis and therapy.* J Biochem, 2007. **142**(1): p. 79-85.
277. Dietz, J., et al., *Inhibition of HIV-1 by a peptide ligand of the genomic RNA packaging signal Psi.* ChemMedChem, 2008. **3**(5): p. 749-55.

278. Goenaga, A.L., et al., *Identification and characterization of tumor antigens by using antibody phage display and intrabody strategies.* Mol Immunol, 2007. **44**(15): p. 3777-88.
279. Deng, Q., et al., *Identification and characterization of peptides that interact with hepatitis B virus via the putative receptor binding site.* J Virol, 2007. **81**(8): p. 4244-54.
280. Perschinka, H., et al., *Identification of atherosclerosis-associated conformational heat shock protein 60 epitopes by phage display and structural alignment.* Atherosclerosis, 2007. **194**(1): p. 79-87.
281. Lunder, M., et al., *Peptide inhibitor of pancreatic lipase selected by phage display using different elution strategies.* J Lipid Res, 2005. **46**(7): p. 1512-6.
282. De, J., et al., *Isolation of a mycoplasma-specific binding peptide from an unbiased phage-displayed peptide library.* Mol Biosyst, 2005. **1**(2): p. 149-57.
283. Pini, A., et al., *Antimicrobial activity of novel dendrimeric peptides obtained by phage display selection and rational modification.* Antimicrob Agents Chemother, 2005. **49**(7): p. 2665-72.
284. Eda, K., S. Eda, and I.W. Sherman, *Identification of peptides targeting the surface of Plasmodium falciparum-infected erythrocytes using a phage display peptide library.* Am J Trop Med Hyg, 2004. **71**(2): p. 190-5.
285. Perosa, F., et al., *CD20 mimicry by a mAb rituximab-specific linear peptide: a potential tool for active immunotherapy of autoimmune diseases.* Ann N Y Acad Sci, 2005. **1051**: p. 672-83.
286. Amemiya, K., et al., *Hyaluronan-binding motif identified by panning a random peptide display library.* Biochim Biophys Acta, 2005. **1724**(1-2): p. 94-9.
287. Nagai, Y., et al., *Inhibition of polyglutamine protein aggregation and cell death by novel peptides identified by phage display screening.* J Biol Chem, 2000. **275**(14): p. 10437-42.
288. Wang, H., et al., *Identification and immunogenicity of an immunodominant mimotope of Avibacterium paragallinarum from a phage display peptide library.* Vet Microbiol, 2007. **119**(2-4): p. 231-9.
289. Tarnovitski, N., et al., *Mapping a neutralizing epitope on the SARS coronavirus spike protein: computational prediction based on affinity-selected peptides.* J Mol Biol, 2006. **359**(1): p. 190-201.
290. Wu, P., et al., *Identification of novel peptide inhibitors for human trypsins.* Biol Chem, 2010. **391**(2-3): p. 283-93.
291. Piotukh, K., et al., *Cyclophilin A binds to linear peptide motifs containing a consensus that is present in many human proteins.* J Biol Chem, 2005. **280**(25): p. 23668-74.
292. Mettu, N.B., et al., *The nuclear receptor-coactivator interaction surface as a target for peptide antagonists of the peroxisome proliferator-activated receptors.* Mol Endocrinol, 2007. **21**(10): p. 2361-77.
293. Cheong, J.Y., et al., *Genetic polymorphism of interferon-gamma, interferon-gamma receptor, and interferon regulatory factor-1 genes in patients with hepatitis B virus infection.* Biochem Genet, 2006. **44**(5-6): p. 246-55.
294. Frick, C., et al., *Interaction of ICAM-1 with beta 2-integrin CD11c/CD18: characterization of a peptide ligand that mimics a putative binding site on domain D4 of ICAM-1.* Eur J Immunol, 2005. **35**(12): p. 3610-21.
295. Giordano, R.J., et al., *Structural basis for the interaction of a vascular endothelial growth factor mimic peptide motif and its corresponding receptors.* Chem Biol, 2005. **12**(10): p. 1075-83.

296. Ono, K., et al., *Production of anti-prion scFv-Fc fusion proteins by recombinant animal cells.* J Biosci Bioeng, 2003. **95**(3): p. 231-8.
297. Oshima, S., et al., *Interferon regulatory factor 1 (IRF-1) and IRF-2 distinctively up-regulate gene expression and production of interleukin-7 in human intestinal epithelial cells.* Mol Cell Biol, 2004. **24**(14): p. 6298-310.
298. Bradbury, A.R. and J.D. Marks, *Antibodies from phage antibody libraries.* J Immunol Methods, 2004. **290**(1-2): p. 29-49.
299. McCafferty, J., et al., *Phage antibodies: filamentous phage displaying antibody variable domains.* Nature, 1990. **348**(6301): p. 552-4.
300. Sastry, L., et al., *Cloning of the immunological repertoire in Escherichia coli for generation of monoclonal catalytic antibodies: construction of a heavy chain variable region-specific cDNA library.* Proc Natl Acad Sci U S A, 1989. **86**(15): p. 5728-32.
301. Huse, W.D., et al., *Generation of a large combinatorial library of the immunoglobulin repertoire in phage lambda.* Science, 1989. **246**(4935): p. 1275-81.
302. Harada, H., et al., *Anti-oncogenic and oncogenic potentials of interferon regulatory factors-1 and -2.* Science, 1993. **259**(5097): p. 971-4.
303. Eckert, M.J., *Transciptional and post-transcriptional regulation of the IRF-1 tumour suppressor protein*. 2005, University of Dundee. p. 190.
304. Kristensen, P. and G. Winter, *Proteolytic selection for protein folding using filamentous bacteriophages.* Fold Des, 1998. **3**(5): p. 321-8.
305. Jensen, K.B., et al., *Functional improvement of antibody fragments using a novel phage coat protein III fusion system.* Biochem Biophys Res Commun, 2002. **298**(4): p. 566-73.
306. Goffinet, M., et al., *Identification of a GTP-bound Rho specific scFv molecular sensor by phage display selection.* BMC Biotechnol, 2008. **8**: p. 34.
307. Goodyear, C.S. and G.J. Silverman, *Death by a B cell superantigen: In vivo VH-targeted apoptotic supraclonal B cell deletion by a Staphylococcal Toxin.* J Exp Med, 2003. **197**(9): p. 1125-39.
308. Geneservice. ***Tomlinson I and J library: Phage Display Questions & Answers***. [cited; Available from: http://www.mrc-cpe.cam.ac.uk/index.php?module=pagemaster&PAGE_user_op=view_page&PAGE_id=12&MMN_position=26:5:23.
309. Chang, H.W., et al., *Phage display antibodies to allelic determinants of canine blood cells.* J Immunol Methods, 2006. **311**(1-2): p. 1-11.
310. Boulter-Bitzer, J.I., H. Lee, and J.T. Trevors, *Single-chain variable fragment antibodies selected by phage display against the sporozoite surface antigen P23 Of Cryptosporidium parvum.* J Parasitol, 2009. **95**(1): p. 75-81.
311. Sanchez, L., et al., *High cytoplasmic expression in E. coli, purification, and in vitro refolding of a single chain Fv antibody fragment against the hepatitis B surface antigen.* J Biotechnol, 1999. **72**(1-2): p. 13-20.
312. Proba, K., et al., *Antibody scFv fragments without disulfide bonds made by molecular evolution.* J Mol Biol, 1998. **275**(2): p. 245-53.
313. Philibert, P., et al., *A focused antibody library for selecting scFvs expressed at high levels in the cytoplasm.* BMC Biotechnol, 2007. **7**: p. 81.
314. Laden, J.C., et al., *Expression and folding of an antibody fragment selected in vivo for high expression levels in Escherichia coli cytoplasm.* Res Microbiol, 2002. **153**(7): p. 469-74.

315. Lecerf, J.M., et al., *Human single-chain Fv intrabodies counteract in situ huntingtin aggregation in cellular models of Huntington's disease.* Proc Natl Acad Sci U S A, 2001. **98**(8): p. 4764-9.
316. Gennari, F., et al., *Direct phage to intrabody screening (DPIS): demonstration by isolation of cytosolic intrabodies against the TES1 site of Epstein Barr virus latent membrane protein 1 (LMP1) that block NF-kappaB transactivation.* J Mol Biol, 2004. **335**(1): p. 193-207.
317. Mitani, N. and R. Matsumoto, *Expression of a single-chain antibody against indole-3-acetic acid in Escherichia coli.* Biosci Biotechnol Biochem, 2004. **68**(7): p. 1565-8.
318. Goel, A., et al., *Relative position of the hexahistidine tag effects binding properties of a tumor-associated single-chain Fv construct.* Biochim Biophys Acta, 2000. **1523**(1): p. 13-20.
319. Butler, J.E., *Solid supports in enzyme-linked immunosorbent assay and other solid-phase immunoassays.* Methods, 2000. **22**(1): p. 4-23.
320. Stein, A., et al., *Dynamic interactions of proteins in complex networks: a more structured view.* Febs J, 2009. **276**(19): p. 5390-405.
321. Ward, J.J., et al., *The DISOPRED server for the prediction of protein disorder.* Bioinformatics, 2004. **20**(13): p. 2138-9.
322. Ay, J., et al., *Crystal structure of a phage library-derived single-chain Fv fragment complexed with turkey egg-white lysozyme at 2.0 A resolution.* J Mol Biol, 2000. **301**(2): p. 239-46.
323. Wesolowski, J., et al., *Single domain antibodies: promising experimental and therapeutic tools in infection and immunity.* Med Microbiol Immunol, 2009. **198**(3): p. 157-74.
324. Saerens, D., G.H. Ghassabeh, and S. Muyldermans, *Single-domain antibodies as building blocks for novel therapeutics.* Curr Opin Pharmacol, 2008. **8**(5): p. 600-8.
325. Cossins, A.J., et al., *Recombinant production of a VL single domain antibody in Escherichia coli and analysis of its interaction with peptostreptococcal protein L.* Protein Expr Purif, 2007. **51**(2): p. 253-9.
326. Kraneveld, A.D., et al., *Elicitation of allergic asthma by immunoglobulin free light chains.* Proc Natl Acad Sci U S A, 2005. **102**(5): p. 1578-83.
327. Redegeld, F.A., et al., *Immunoglobulin-free light chains elicit immediate hypersensitivity-like responses.* Nat Med, 2002. **8**(7): p. 694-701.
328. Redegeld, F.A., et al., *Functional role for Ig free light chains in immediate and delayed hypersensitivity responses.* Inflamm Res, 2004. **53 Suppl 1**: p. S6-8.
329. Gottenberg, J.E., et al., *Serum immunoglobulin free light chain assessment in rheumatoid arthritis and primary Sjogren's syndrome.* Ann Rheum Dis, 2007. **66**(1): p. 23-7.
330. Painter, R.G., H.J. Sage, and C. Tanford, *Contributions of heavy and light chains of rabbit immunoglobulin G to antibody activity. I. Binding studies on isolated heavy and light chains.* Biochemistry, 1972. **11**(8): p. 1327-37.
331. Sun, M., et al., *Antigen recognition by an antibody light chain.* J Biol Chem, 1994. **269**(1): p. 734-8.
332. Yoo, T.J., O.A. Roholt, and D. Pressman, *Specific binding activity of isolated light chains of antibodies.* Science, 1967. **157**(789): p. 707-9.
333. Olsen, R.J., et al., *Minimal structural elements of an inhibitory anti-ATF1/CREB single-chain antibody fragment (scFv41.4).* Hybrid Hybridomics, 2003. **22**(2): p. 65-77.

334. Lipinski, R.J. and W. Bushman, *Identification of Hedgehog Signaling Inhibitors with Relevant Human Exposure by Small Molecule Screening.* Toxicol In Vitro, 2010. **24**(5):1404-9.
335. Tada, S., et al., *Interferon regulatory factor-1 gene abnormality and loss of growth inhibitory effect of interferon-alpha in human hepatoma cell lines.* Int J Oncol, 1998. **13**(6): p. 1207-16.
336. Ireson, C.R. and L.R. Kelland, *Discovery and development of anticancer aptamers.* Mol Cancer Ther, 2006. **5**(12): p. 2957-62.
337. Worn, A., et al., *Correlation between in vitro stability and in vivo performance of anti-GCN4 intrabodies as cytoplasmic inhibitors.* J Biol Chem, 2000. **275**(4): p. 2795-803.
338. Marasco, W.A., W.A. Haseltine, and S.Y. Chen, *Design, intracellular expression, and activity of a human anti-human immunodeficiency virus type 1 gp120 single-chain antibody.* Proc Natl Acad Sci U S A, 1993. **90**(16): p. 7889-93.
339. Wu, Y., et al., *Binding of intracellular anti-Rev single chain variable fragments to different epitopes of human immunodeficiency virus type 1 rev: variations in viral inhibition.* J Virol, 1996. **70**(5): p. 3290-7.
340. Visintin, M., et al., *Selection of antibodies for intracellular function using a two-hybrid in vivo system.* Proc Natl Acad Sci U S A, 1999. **96**(21): p. 11723-8.
341. Brockmann, E.C., et al., *Selecting for antibody scFv fragments with improved stability using phage display with denaturation under reducing conditions.* J Immunol Methods, 2005. **296**(1-2): p. 159-70.
342. Nakada, E., et al., *Toll-like receptor-3 stimulation upregulates sFLT-1 production by trophoblast cells.* Placenta, 2009. **30**(9): p. 774-9.
343. Matsumoto, M., et al., *Establishment of a monoclonal antibody against human Toll-like receptor 3 that blocks double-stranded RNA-mediated signaling.* Biochem Biophys Res Commun, 2002. **293**(5): p. 1364-9.
344. Heinz, S., et al., *Species-specific regulation of Toll-like receptor 3 genes in men and mice.* J Biol Chem, 2003. **278**(24): p. 21502-9.
345. Ohtsubo, M., et al., *Human cyclin E, a nuclear protein essential for the G1-to-S phase transition.* Mol Cell Biol, 1995. **15**(5): p. 2612-24.
346. Devoto, S.H., et al., *A cyclin A-protein kinase complex possesses sequence-specific DNA binding activity: p33cdk2 is a component of the E2F-cyclin A complex.* Cell, 1992. **68**(1): p. 167-76.
347. Montagnoli, A., et al., *Ubiquitination of p27 is regulated by Cdk-dependent phosphorylation and trimeric complex formation.* Genes Dev, 1999. **13**(9): p. 1181-9.
348. Okuda, M., et al., *Nucleophosmin/B23 is a target of CDK2/cyclin E in centrosome duplication.* Cell, 2000. **103**(1): p. 127-40.
349. Merino, D., et al., *Differential inhibition of TRAIL-mediated DR5-DISC formation by decoy receptors 1 and 2.* Mol Cell Biol, 2006. **26**(19): p. 7046-55.
350. Pan, G., et al., *The receptor for the cytotoxic ligand TRAIL.* Science, 1997. **276**(5309): p. 111-3.
351. Pan, G., et al., *An antagonist decoy receptor and a death domain-containing receptor for TRAIL.* Science, 1997. **277**(5327): p. 815-8.
352. Marsters, S.A., et al., *A novel receptor for Apo2L/TRAIL contains a truncated death domain.* Curr Biol, 1997. **7**(12): p. 1003-6.
353. Kischkel, F.C., et al., *Apo2L/TRAIL-dependent recruitment of endogenous FADD and caspase-8 to death receptors 4 and 5.* Immunity, 2000. **12**(6): p. 611-20.

354. Papageorgiou, A., C.P. Dinney, and D.J. McConkey, *Interferon-alpha induces TRAIL expression and cell death via an IRF-1-dependent mechanism in human bladder cancer cells.* Cancer Biol Ther, 2007. **6**(6): p. 872-9.
355. Moore, T.A., et al., *Inhibition of gamma delta T cell development and early thymocyte maturation in IL-7 -/- mice.* J Immunol, 1996. **157**(6): p. 2366-73.
356. Peschon, J.J., et al., *Early lymphocyte expansion is severely impaired in interleukin 7 receptor-deficient mice.* J Exp Med, 1994. **180**(5): p. 1955-60.
357. Armant, M., G. Delespesse, and M. Sarfati, *IL-2 and IL-7 but not IL-12 protect natural killer cells from death by apoptosis and up-regulate bcl-2 expression.* Immunology, 1995. **85**(2): p. 331-7.
358. Sudo, T., et al., *Expression and function of the interleukin 7 receptor in murine lymphocytes.* Proc Natl Acad Sci U S A, 1993. **90**(19): p. 9125-9.
359. Komschlies, K.L., et al., *Administration of recombinant human IL-7 to mice alters the composition of B-lineage cells and T cell subsets, enhances T cell function, and induces regression of established metastases.* J Immunol, 1994. **152**(12): p. 5776-84.
360. Silva, M.R., et al., *Generation of human natural killer cells from immature progenitors does not require marrow stromal cells.* Blood, 1994. **84**(3): p. 841-6.
361. Barata, J.T., et al., *Interleukin-7 promotes survival and cell cycle progression of T-cell acute lymphoblastic leukemia cells by down-regulating the cyclin-dependent kinase inhibitor p27(kip1).* Blood, 2001. **98**(5): p. 1524-31.
362. Nguyen, L.H., et al., *The human interferon- and estrogen-regulated ISG20/HEM45 gene product degrades single-stranded RNA and DNA in vitro.* Biochemistry, 2001. **40**(24): p. 7174-9.
363. Espert, L., et al., *ISG20, a new interferon-induced RNase specific for single-stranded RNA, defines an alternative antiviral pathway against RNA genomic viruses.* J Biol Chem, 2003. **278**(18): p. 16151-8.
364. Espert, L., et al., *Interferon-induced exonuclease ISG20 exhibits an antiviral activity against human immunodeficiency virus type 1.* J Gen Virol, 2005. **86**(Pt 8): p. 2221-9.
365. Gongora, C., et al., *A unique ISRE, in the TATA-less human Isg20 promoter, confers IRF-1-mediated responsiveness to both interferon type I and type II.* Nucleic Acids Res, 2000. **28**(12): p. 2333-41.
366. Espert, L., et al., *The exonuclease ISG20 is directly induced by synthetic dsRNA via NF-kappaB and IRF1 activation.* Oncogene, 2004. **23**(26): p. 4636-40.
367. Galabru, J. and A. Hovanessian, *Autophosphorylation of the protein kinase dependent on double-stranded RNA.* J Biol Chem, 1987. **262**(32): p. 15538-44.
368. Lemaire, P.A., et al., *Mechanism of PKR Activation by dsRNA.* J Mol Biol, 2008. **381**(2): p. 351-60.
369. Lee, S.B., et al., *The interferon-induced double-stranded RNA-activated human p68 protein kinase potently inhibits protein synthesis in cultured cells.* Virology, 1993. **192**(1): p. 380-5.
370. Majumdar, R. and U. Maitra, *Regulation of GTP hydrolysis prior to ribosomal AUG selection during eukaryotic translation initiation.* Embo J, 2005. **24**(21): p. 3737-46.
371. Sudhakar, A., et al., *Phosphorylation of serine 51 in initiation factor 2 alpha (eIF2 alpha) promotes complex formation between eIF2 alpha(P) and eIF2B and causes inhibition in the guanine nucleotide exchange activity of eIF2B.* Biochemistry, 2000. **39**(42): p. 12929-38.
372. Ward, S.V. and C.E. Samuel, *The PKR kinase promoter binds both Sp1 and Sp3, but only Sp3 functions as part of the interferon-inducible complex with ISGF-3 proteins.* Virology, 2003. **313**(2): p. 553-66.

373. Beretta, L., et al., *Expression of the protein kinase PKR in modulated by IRF-1 and is reduced in 5q- associated leukemias.* Oncogene, 1996. **12**(7): p. 1593-6.
374. Polymenidou, M., et al., *The POM monoclonals: a comprehensive set of antibodies to non-overlapping prion protein epitopes.* PLoS One, 2008. **3**(12): p. e3872.
375. Hupp, T.R., et al., *Regulation of the specific DNA binding function of p53.* Cell, 1992. **71**(5): p. 875-86.
376. Skrabana, R., et al., *Monoclonal antibody MN423 as a stable mold facilitates structure determination of disordered tau protein.* J Struct Biol, 2010. **171** (1) p. 74-81
377. Muratani, M. and W.P. Tansey, *How the ubiquitin-proteasome system controls transcription.* Nat Rev Mol Cell Biol, 2003. **4**(3): p. 192-201.
378. Lipford, J.R. and R.J. Deshaies, *Diverse roles for ubiquitin-dependent proteolysis in transcriptional activation.* Nat Cell Biol, 2003. **5**(10): p. 845-50.
379. Reid, J. and J.Q. Svejstrup, *DNA damage-induced Def1-RNA polymerase II interaction and Def1 requirement for polymerase ubiquitylation in vitro.* J Biol Chem, 2004. **279**(29): p. 29875-8.
380. Somesh, B.P., et al., *Multiple mechanisms confining RNA polymerase II ubiquitylation to polymerases undergoing transcriptional arrest.* Cell, 2005. **121**(6): p. 913-23.
381. Dhananjayan, S.C., A. Ismail, and Z. Nawaz, *Ubiquitin and control of transcription.* Essays Biochem, 2005. **41**: p. 69-80.
382. Ransom, M., et al., *FACT and the proteasome promote promoter chromatin disassembly and transcriptional initiation.* J Biol Chem, 2009. **284**(35): p. 23461-71.
383. Gillette, T.G., et al., *Physical and functional association of RNA polymerase II and the proteasome.* Proc Natl Acad Sci U S A, 2004. **101**(16): p. 5904-9.
384. Collins, G.A. and W.P. Tansey, *The proteasome: a utility tool for transcription?* Curr Opin Genet Dev, 2006. **16**(2): p. 197-202.
385. Saccani, S., et al., *Degradation of promoter-bound p65/RelA is essential for the prompt termination of the nuclear factor kappaB response.* J Exp Med, 2004. **200**(1): p. 107-13.
386. Ostendorff, H.P., et al., *Ubiquitination-dependent cofactor exchange on LIM homeodomain transcription factors.* Nature, 2002. **416**(6876): p. 99-103.
387. Nawaz, Z., et al., *The Angelman syndrome-associated protein, E6-AP, is a coactivator for the nuclear hormone receptor superfamily.* Mol Cell Biol, 1999. **19**(2): p. 1182-9.
388. Romeo, G., et al., *IRF-1 as a negative regulator of cell proliferation.* J Interferon Cytokine Res, 2002. **22**(1): p. 39-47.
389. Kirkwood, J.M., et al., *Mechanisms and management of toxicities associated with high-dose interferon alfa-2b therapy.* J Clin Oncol, 2002. **20**(17): p. 3703-18.
390. Sleijfer, S., et al., *Side effects of interferon-alpha therapy.* Pharm World Sci, 2005. **27**(6): p. 423-31.
391. Pan, W., et al., *Identification of peptide substrates for human MMP-11 (stromelysin-3) using phage display.* J Biol Chem, 2003. **278**(30): p. 27820-7.
392. Cloutier, S.M., et al., *Substrate specificity of human kallikrein 2 (hK2) as determined by phage display technology.* Eur J Biochem, 2002. **269**(11): p. 2747-54.
393. Kofler, M., K. Motzny, and C. Freund, *GYF domain proteomics reveals interaction sites in known and novel target proteins.* Mol Cell Proteomics, 2005. **4**(11): p. 1797-811.
394. Neduva, V. and R.B. Russell, *Linear motifs: evolutionary interaction switches.* FEBS Lett, 2005. **579**(15): p. 3342-5.

395. Neurath, A.R., et al., *Identification and chemical synthesis of a host cell receptor binding site on hepatitis B virus.* Cell, 1986. **46**(3): p. 429-36.
396. Kofler, M., et al., *Novel interaction partners of the CD2BP2-GYF domain.* J Biol Chem, 2005. **280**(39): p. 33397-402.
397. Huang, B., et al., *Global characterization of interferon regulatory factor (IRF) genes in vertebrates: glimpse of the diversification in evolution.* BMC Immunol, 2010. **11**: p. 22.
398. Tan, W., et al., *Functional dissection of transcription factor ZBRK1 reveals zinc fingers with dual roles in DNA-binding and BRCA1-dependent transcriptional repression.* J Biol Chem, 2004. **279**(8): p. 6576-87.
399. Tan, W., S. Kim, and T.G. Boyer, *Tetrameric oligomerization mediates transcriptional repression by the BRCA1-dependent Kruppel-associated box-zinc finger protein ZBRK1.* J Biol Chem, 2004. **279**(53): p. 55153-60.
400. Zheng, L., et al., *Sequence-specific transcriptional corepressor function for BRCA1 through a novel zinc finger protein, ZBRK1.* Mol Cell, 2000. **6**(4): p. 757-68.
401. Yun, J. and W.H. Lee, *Degradation of transcription repressor ZBRK1 through the ubiquitin-proteasome pathway relieves repression of Gadd45a upon DNA damage.* Mol Cell Biol, 2003. **23**(20): p. 7305-14.
402. Friedman, J.R., et al., *KAP-1, a novel corepressor for the highly conserved KRAB repression domain.* Genes Dev, 1996. **10**(16): p. 2067-78.
403. Mark, C., M. Abrink, and L. Hellman, *Comparative analysis of KRAB zinc finger proteins in rodents and man: evidence for several evolutionarily distinct subfamilies of KRAB zinc finger genes.* DNA Cell Biol, 1999. **18**(5): p. 381-96.
404. Schultz, D.C., J.R. Friedman, and F.J. Rauscher, 3rd, *Targeting histone deacetylase complexes via KRAB-zinc finger proteins: the PHD and bromodomains of KAP-1 form a cooperative unit that recruits a novel isoform of the Mi-2alpha subunit of NuRD.* Genes Dev, 2001. **15**(4): p. 428-43.
405. Schultz, D.C., et al., *SETDB1: a novel KAP-1-associated histone H3, lysine 9-specific methyltransferase that contributes to HP1-mediated silencing of euchromatic genes by KRAB zinc-finger proteins.* Genes Dev, 2002. **16**(8): p. 919-32.
406. Lechner, M.S., et al., *Molecular determinants for targeting heterochromatin protein 1-mediated gene silencing: direct chromoshadow domain-KAP-1 corepressor interaction is essential.* Mol Cell Biol, 2000. **20**(17): p. 6449-65.
407. Hsiao, K.C., et al., *Peptides identify multiple hotspots within the ligand binding domain of the TNF receptor 2.* Proteome Sci, 2003. **1**(1): p. 1.
408. Pillutla, R.C., et al., *Peptides identify the critical hotspots involved in the biological activation of the insulin receptor.* J Biol Chem, 2002. **277**(25): p. 22590-4.
409. Lin, L.F., et al., *ZBRK1 acts as a metastatic suppressor by directly regulating MMP9 in cervical cancer.* Cancer Res, 2010. **70**(1): p. 192-201.
410. Sawant, R. and V. Torchilin, *Intracellular transduction using cell-penetrating peptides.* Mol Biosyst, 2010. **6**(4): p. 628-40.
411. Liao, G., et al., *The Epstein-Barr virus replication protein BBLF2/3 provides an origin-tethering function through interaction with the zinc finger DNA binding protein ZBRK1 and the KAP-1 corepressor.* J Virol, 2005. **79**(1): p. 245-56.
412. Lonard, D.M., et al., *The 26S proteasome is required for estrogen receptor-alpha and coactivator turnover and for efficient estrogen receptor-alpha transactivation.* Mol Cell, 2000. **5**(6): p. 939-48.
413. Pham, A.D. and F. Sauer, *Ubiquitin-activating/conjugating activity of TAFII250, a mediator of activation of gene expression in Drosophila.* Science, 2000. **289**(5488): p. 2357-60.

414. Beaudenon, S.L., et al., *Rsp5 ubiquitin-protein ligase mediates DNA damage-induced degradation of the large subunit of RNA polymerase II in Saccharomyces cerevisiae.* Mol Cell Biol, 1999. **19**(10): p. 6972-9.
415. Frontini, M., et al., *A ChIP-chip approach reveals a novel role for transcription factor IRF1 in the DNA damage response.* Nucleic Acids Res, 2009. **37**(4): p. 1073-85.